STRUCTURE ADAPTIVE MULTIPLE TESTING WITH APPLICATIONS TO BIOINFORMATICS

A Dissertation

by

HUIJUAN ZHOU

Submitted to the Office of Graduate and Professional Studies of
Texas A&M University
in partial fulfillment of the requirements for the degree of

DOCTOR OF PHILOSOPHY

Chair of Committee,	Xianyang Zhang
Committee Members,	Raymond J. Carroll
	Raymond Ka Wai Wong
	Ke Kurt Zhang
Head of Department,	Brani Vidakovic

May 2021

Major Subject: Statistics

ABSTRACT

In many scientific studies and real life scenes, one of the essential questions is “Are there any signals in the datasets?”. For example in genetics, scientists are interested in genes that are differentially expressed with respected to certain diseases. In fund investment, we want to identify funds administered by skilled instead of just “lucky" managers. These and many other applications could be formulated as a multiple hypothesis testing problem, where we consider a set of statistical inferences simultaneously. Motivated by those real world applications, many research problems arise in multiple testing and remain to be addressed.

This dissertation contains two projects addressing different challenges arising from bioinformatics.

The first project considers a covariate adaptive family-wise error rate (FWER)-controlling procedure for genome-wide association studies. With the increasing availability of functional genomics data, it is possible to increase the detection power by leveraging these genomic functional annotations in genome-wide association studies. Previous efforts to accommodate covariates in multiple testing focus on the false discovery rate control while covariate-adaptive FWER-controlling procedures remain under-developed. Here we propose a novel covariate-adaptive FWER-controlling procedure that incorporates external covariates which are potentially informative of either the statistical power or the prior null probability. An efficient algorithm is developed to implement the proposed method. We prove its asymptotic validity and obtain the rate of convergence through a perturbation-type argument. Our numerical studies show that the new procedure is more powerful than competing methods and maintains robustness across different settings. We apply the proposed approach to the UK Biobank data and analyze 27 traits with 9 million single-nucleotide polymorphisms tested for associations. Seventy-five genomic annotations are used as covariates. Our approach detects more genome-wide significant loci than other methods in 21 out of the 27 traits.

One fundamental statistical task in microbiome data analysis is differential abundance analysis,

which aims to identify microbial taxa whose abundance covaries with a variable of interest. Although the main interest is on the change in the absolute abundance, i.e., the number of microbial cells per unit area/volume at the ecological site such as the human gut, the data from a sequencing experiment reflects only the taxa relative abundances in a sample. Thus, microbiome data are compositional in nature. Analysis of such compositional data is challenging since the change in the absolute abundance of one taxon will lead to changes in the relative abundances of other taxa, making false positive control difficult. In the second project, we present a simple, yet robust and highly scalable approach to tackle the compositional effects in differential abundance analysis. The method only requires the application of established statistical tools. It fits linear regression models on the centered log-ratio transformed data, identifies a bias term due to the transformation and compositional effect, and corrects the bias using the mode of the regression coefficients. Due to the algorithmic simplicity, our method is 100-1000 times faster than the state-of-the-art method ANCOM-BC. Under mild assumptions, we prove its asymptotic FDR control property, making it the first differential abundance method that enjoys a theoretical FDR control guarantee. The proposed method is very flexible and can be extended to mixed-effect models for the analysis of correlated microbiome data. Using comprehensive simulations and real data applications, we demonstrate that our method has overall the best performance in terms of FDR control and power among the competitors. We implemented the proposed method in the R package `LinDA` (`https://github.com/zhouhj1994/LinDA`).

ACKNOWLEDGMENTS

The graduate study at Texas A&M University is one of the most important experiences in my life, where I met my advisor, Professor Xianyang Zhang. He made great efforts to guide me on thinking, researching, writing and presenting, from details to big pictures. He showed me what enthusiastic researchers and noble mentors are. Words cannot express how grateful I am. I will always cherish those earnest helps.

Thanks to all my committee members, Professor Raymond J. Carroll, Professor Raymond Ka Wai Wong and Professor Ke Kurt Zhang. I deeply appreciate their consistent support and invaluable comments. A special thanks to Professor Ke Kurt Zhang. It has been a pleasure working with him. He and Professor Linglin Xie have made the lab a loving family. Moreover, I am thankful for the wonderful collaborations with Professor Jun Chen and Professor Kejun He. Their contributions to the research work of this dissertation are marvelous and they have taught me a lot in doing research.

I would also like to thank the department and everyone who generously offered help during the whole journey of my Ph.D. program.

I thank my parents for raising and loving me. Thanks to my sisters, cousins and friends for their encouragement and company all the time. Without them, I would never have accomplished as much as I have.

CONTRIBUTORS AND FUNDING SOURCES

Contributors

This work was supported by a dissertation committee consisting of Professor Xianyang Zhang (advisor), Professor Raymond J. Carroll and Professor Raymond Ka Wai Wong of the Department of Statistics and Professor Ke Kurt Zhang of the Department of Nutrition and Food Science.

The work of Chapter 2 was conducted with Professor Xianyang Zhang and Professor Jun Chen of the Division of Biomedical Statistics and Informatics at Mayo Clinic. The work of Chapter 3 is a collaborative product with Professor Xianyang Zhang, Professor Jun Chen and Professor Kejun He of the Institute of Statistics and Big Data at Renmin University of China. All the research work of the dissertation was completed by the student as the first author.

Funding Sources

In this dissertation, the research work of the student is supported by NSF DMS-1830392 and NSF DMS-1811747, and a grant from the College of Science Strategic Transformative Research Program at Texas A&M University.

TABLE OF CONTENTS

Page

LIST OF FIGURES

FIGURE Page

LIST OF TABLES

TABLE Page

1. INTRODUCTION

1.1 Multiple hypothesis testing[1]

Multiple testing arises when we face a large number of hypotheses and aim to discover signals while controlling specific error measures. Table 1.1 lists the possible outcomes when testing multiple hypotheses. For a single hypothesis test, we usually control the type I error rate, i.e., the probability of rejecting a true null hypothesis. When the number of hypotheses is large, controlling the type I error rate for each hypothesis at the usual nominal level (say 5%) could lead to a large number of false positives. For example, if there are 10000 true null hypotheses, then around 500 p-values will be smaller than 0.05 according to the law of large numbers. Therefore, we need more stringent error measures. The family-wise error rate (FWER) and the false discovery rate (FDR) are two commonly used error measures employed in a wide range of scientific studies. The FWER is the probability of making one false discovery, while the FDR is the expected proportion of false positives:

$$\text{FWER: } \mathbb{P}(V \geq 1) \quad \text{FDR: } \mathbb{E}\{V/(R \vee 1)\}.$$

The FWER provides stringent control of type I errors and is preferable if (i) the overall conclusion from various individual inferences is likely to be erroneous when at least one of them is, or (ii) the existence of a single false claim would cause significant loss. In contrast, the FDR control procedure provides less stringent control of type I errors, and it generally delivers higher power at the cost of an increased number of type I errors. Consider the problem of simultaneously testing m hypotheses. We reject the hypotheses whose p-values are less than a cutoff t^*. For many FWER and FDR controlling procedures, the t^* that controls either one of them at level α is obtained by

[1]Reprinted with permission from "Covariate Adaptive Family-wise Error Rate Control for Genome-Wide Association Studies" by Huijuan Zhou, et al., 2020. Biometrika forthcoming, Copyright 2020 by Oxford University Press.

Table 1.1: Possible outcomes when testing multiple hypotheses.

	Not rejected	Rejected	Total
True nulls	U	V	m_0
True alternatives	T	S	m_1
Total	$m - R$	R	m

solving the following constraint optimization problem

$$\text{maximize}_{t\in[0,1]} R(t) \quad \text{s.t.} \quad M(t) \leq \alpha, \tag{1.1}$$

where $R(t)$ denotes the total number of rejections given the threshold t and $M(t)$ is a (conservative) estimate of the FWER or FDR. The most fundamental procedure for controlling the FWER is the Bonferroni method. It corresponds to the choice of $M(t) = mt$, which is the union bound on the FWER under the assumption that the null p-values are uniformly distributed (or super-uniform) on $[0, 1]$:

$$\mathbb{P}(V \geq 1) = \mathbb{P}\{\cup_{i=1}^{m_0}(p_i \leq t)\} \leq \sum_{i=1}^{m_0} t \leq mt,$$
$$t^* = \max\{t : mt \leq \alpha\} = \alpha/m,$$

where without loss of generality, we assume the first m_0 null hypotheses are true. The classical Benjamini–Hochberg (BH) procedure for controlling the FDR can also be formulated using (1.1) with $M(t) = mt/R(t)$ being a conservative estimate of the FDR (Benjamini and Hochberg, 1995):

$$\mathbb{E}\left\{\sum_{i=1}^{m_0}\mathbb{I}(p_i \leq t)\right\} \leq \sum_{i=1}^{m_0} t \leq mt,$$
$$t^* = \max\left\{t : \frac{mt}{\sum_{i=1}^{m}\mathbb{I}(p_i \leq t)} \leq \alpha\right\} \equiv \max\left\{p_{(i)}, i \in \{1, ..., m\} : \frac{mp_{(i)}}{i} \leq \alpha\right\},$$

where $p_{(1)} \leq ... \leq p_{(m)}$ are the order statistics of $p_1, ..., p_m$.

Formulation (1.1) assumes that the hypotheses for different features are exchangeable. How-

ever, in many scientific applications, there are informative covariates for each hypothesis that could provide information on prior null probabilities or distributional characteristics of signals. In Chapter 2, we will introduce a novel covariate adaptive FWER controlling procedure which could incorporate multi-dimensional covariates so as to improve the statistical power.

1.2 Real world applications of multiple testing

Multiple testing plays an important role in many scientific studies and real world problems. For example in finance, we want to identify skilled fund managers by testing alphas of all funds in the population (Barras et al., 2010; Lan and Du, 2019). In brain imaging studies, we want to find areas of the brain that differ between two groups of subjects with respect to a special characteristic of interest such as the diffusion of water molecules (Schwartzman et al., 2008; Leek and Storey, 2008). In astronomy, a recurrent statistical problem is to decide whether the observed astrophysical data (e.g., an observed power spectrum of of galaxies or clusters) are consistent with the predictions of a theoretical model (Miller et al., 2001). Similar example can be found in climatology (Ventura et al., 2004).

In genomic studies, a central and persistent problem is identifying genomic features associated with clinical outcomes, which was discussed in great many multiple testing literatures (Reiner et al., 2003; Roeder and Wasserman, 2009; Fan et al., 2012; Zhang and Chen, 2020). It often involves simultaneously testing a large number of hypotheses, each associated with a particular genomic feature. Examples include testing the association between single-nucleotide polymorphisms (SNPs) and heritable diseases in genome-wide association studies (GWASs), examining the association between epigenetic variations and phenotypes in epigenome-wide association studies, detecting the relationship between human microbiome abundances and diseases in microbiome-wide association studies. In these applications, the number of genomic features often ranges from hundreds to tens of thousands, which calls for multiple testing procedures to account for the multiplicity. The two projects discussed in this dissertation were motivated by two specific applications arising in bioinformatics. The first project is about adaptive multiple testing with side information, which focuses on leveraging different types of covariates (prior) information to improve statisti-

cal power in GWASs while controlling the FWER. The second project addresses a fundamental statistical problem for microbiome data analysis: differential abundance analysis of compositional data. The difficulty lies in that the observed data reflects only the relative abundances thus careful treatments for the data are needed to avoid type I error inflation.

1.3 Overall structure

We developed a novel multiple hypothesis testing method for each of the two projects. Chapter 2 and 3 are devoted to the detailed discussions on the two methods respectively and both include the descriptions of the asymptotic properties, simulations and real data analyses. Chapter 4 summarizes the two projects. Lemmas and proofs of the theorems, and additional results of simulations and real data applications are provided in the appendices.

2. COVARIATE ADAPTIVE FAMILY-WISE ERROR RATE CONTROL FOR GENOME-WIDE ASSOCIATION STUDIES

2.1 Introduction

As mentioned in Section 1.1 , the classical multiple testing procedures, such as BH procedure and Bonferroni procedure, assume that the hypotheses for different features are exchangeable. However, in many scientific applications, there are informative covariates for each hypothesis that could reflect the group structure among the hypotheses, or provide information on prior null probabilities or distributional characteristics of signals. These covariates can be roughly divided into two classes: statistical covariates and external covariates (Ignatiadis et al., 2016). Statistical covariates are derived from the data itself and could reflect the power or null probability. For example, in meta-analyses where samples are pooled across studies, the loci-specific sample sizes and population-level frequency can be informative for association analyses by influencing the sampling variability (Boca and Leek, 2018). External covariates are derived from external sources and are usually informative of the prior null probability. For example in GWASs, the SNPs in active chromatin state are more likely to be significantly associated with the phenotype (GTEx Consortium, 2017). P-values from previous or related studies is also considered useful prior information. It is thus promising to incorporate these covariates to improve the detection power in GWAS.

Multiple testing procedures that leverage different types of covariates (prior) information have received considerable attention in the literature especially for the FDR control. Genovese et al. (2006) pioneered multiple testing procedures with prior information using weighted p-values and demonstrated that their weighted procedure controls the FWER and FDR while improving power. Roeder and Wasserman (2009) further explored their p-value weighting procedure by introducing an optimal weighting scheme for the FWER control. Inspired by the above works, Hu et al. (2010) developed a group BH procedure by estimating the proportions of null hypotheses for each group separately. Bourgon et al. (2010) developed a particular weighting method called independent

filtering, which first filters hypotheses by a criterion independent of the p-values and only tests hypotheses passing the filter. Ignatiadis et al. (2016) proposed the independent hypothesis weighting for multiple testing with covariate information. The idea is to bin the covariate into several groups and then apply the weighted BH procedure with piecewise constant weights. A similar idea has been used in the structure-adaptive BH algorithm introduced in Li and Barber (2019), where the weight assigned for each p-value is the reciprocal of the estimated null probability of the corresponding hypothesis. The null probabilities were estimated by utilizing censored p-values and structural information believed to be present among the hypotheses. Boca and Leek (2018) employed a similar approach by using the censored p-values and a regression approach to estimate null probabilities based on informative covariates. The above procedures can all be viewed to some extent as different variants of the weighted BH or Bonferroni procedure. On the other hand, there are FDR-controlling procedures designed to find an optimal decision threshold by taking into account the p-value distribution under the alternatives, mostly based on the local FDR framework. For example, Sun et al. (2015) developed an local-FDR-based procedure to incorporate spatial information. Scott et al. (2015) and Tansey et al. (2018) proposed EM-type algorithms to estimate the local FDR by taking into account covariate and spatial information, respectively. Lei and Fithian (2018) proposed the AdaPT procedure, which iteratively estimates the p-value thresholds based on a two-group mixture model using the partially masked p-values together with the covariates. Zhang and Chen (2020) proposed a more computationally efficient procedure to assign each p-value a covariate-adaptive threshold. Another related method AdaFDR addressed the local "bump" and global "slope" structures delivered through the covariates in what they called "enrichment" pattern by modeling a mixture of the generalized linear model and Gaussian mixture for a threshold function (Zhang et al., 2019). Other relevant works include Ferkingstad et al. (2008), Zablocki et al. (2014), Dobriban et al. (2015), Wen (2016), Stephens (2017), Xiao et al. (2017), Lei et al. (2017) and Li and Barber (2017).

Recent developments on covariate-adaptive multiple testing focus on the FDR control, while methods for the FWER control lag behind. Existing FWER-controlling methods can all be thought

to be variants of the weighted Bonferroni method, with the weights reflecting only the prior null probabilities. It has been demonstrated clearly in the FDR literature that incorporating the alternative p-value distribution leads to the optimal rejection region in theory and more power in practice, see, e.g., Efron (2010). Given the popularity of the FWER control in GWAS, we introduce a new covariate-adaptive FWER-controlling procedure, which takes into account the prior null probabilities as well as the alternative p-value distribution, making it distinct from the existing FWER-controlling procedures. To illustrate the idea, suppose we are given a set of p-values p_i together with the external covariates x_i. Our method is motivated by the two-group mixture model

$$p_i \mid x_i \sim \pi(x_i) f_0(\cdot) + \{1 - \pi(x_i)\} f_1(\cdot)$$

with $\pi(x_i)$ and $f_1(\cdot)$ reflecting the heterogeneity of the probabilities of being null and the distributional characteristics of signals. We construct an objective function to control a conservative estimate of FWER while maximizing the expected number of true rejections. Specifically, we formulate the following constrained optimization problem

$$\max_{t_i} \sum_{i=1}^{m} \{1 - \pi(x_i)\} F_1(t_i) \;\; \text{s.t.} \;\; \sum_{i=1}^{m} \pi(x_i) F_0(t_i) \leq \alpha,$$

where F_0 and F_1 are the cumulative distribution functions of f_0 and f_1 respectively. To establish the asymptotic FWER control, and the rate of convergence, new theoretical developments are needed. Existing theoretical analysis techniques developed for the FDR-controlling procedures are not applicable to the FWER-controlling procedure, since we aim to control a sum instead of a proportion encountered in the FDR control. The arguments based on the Rademacher complexity in Li and Barber (2019) do not provide a meaningful bound on the FWER. Employing a perturbation-type argument, we develop a more delicate analysis for each of the summands, which leads to a useful bound on the sum and thus the FWER. The main contributions of this project are two-fold:

- We propose a powerful covariate-adaptive FWER-controlling procedure that can incorporate multi-dimensional covariates and exploit the information from both the null probability and

the alternative distribution. We prove the asymptotic FWER control of the proposed procedure when the pairs of covariate and p-value across different hypotheses are independent and derive the exact rate of convergence based on a novel perturbation technique. We emphasize that our proofs do not rely on the correct specification of the two-group mixture model.

- We develop an efficient algorithm to implement the proposed method and demonstrate its usefulness in handling big datasets arising from GWAS. In the application to the GWAS of about 9 million SNPs and 75 covariates, we could complete the analysis in hours. The proposed method is implemented in the R package `CAMT`.

The rest of this chapter is organized as follows. Section 2.2 derives the optimal rejection rule based on the two-group mixture model and introduces a feasible procedure to implement the proposed method, while Section 2.3 discusses the theoretical results on the asymptotic FWER control of the new method. In Sections 2.4, we evaluate the finite-sample performance of the proposed method via simulation studies. In Section 2.5, we apply the proposed procedure to the GWAS of the UK Biobank data. Section 2.6 points out a few future research directions. Technical details including intermediate lemmas and proofs of the theorems, and additional results of simulations and real data applications are presented in Appendix A.

2.2 Methodology

2.2.1 The setup

Denote by $\|v\|$ the Euclidean norm of a vector v. With some abuse of notation, let $\|A\|$ be the spectral norm of a matrix A. For two symmetric matrices A and B, $A \preceq B$ means that $B - A$ is positive semidefinite. For $a, b \in \mathbb{R}$, write $a \vee b = \max(a, b)$ and $a \wedge b = \min(a, b)$. Throughout the chapter, we use c to denote a positive constant which can be different from line to line. The notations in this chapter are consistent with the notations in Appendix A.

We consider the problem of covariate-adaptive multiple testing to control the FWER. Suppose we are given m hypotheses, among which m_0 are true nulls. For each hypothesis, we observe a p-value p_i as well as a covariate x_i lying in some space $\mathcal{X} \subseteq \mathbb{R}^d$ which encodes potentially useful

external information concerning the presence of a signal. Let $H_i = 0$ if the ith null hypothesis is true and $H_i = 1$ otherwise. Denote by $\mathcal{M}_0$ the set of all true null hypotheses. We transform the ith p-value based on a map $T_i : [0, 1] \to \mathbb{R}_+$ that will be estimated from the covariates and p-values. The larger $T_i(p_i)$ is, the more likely the ith hypothesis is from the alternative. The motivation for such a transformation will be discussed in the next section. In a nutshell, the optimal T_i is the likelihood ratio between the ith p-value distributions under the alternative and the null.

2.2.2 Optimal rejection rule

Let $f_0(\cdot)$ be the null p-value distribution and $f_1(\cdot)$ denote the alternative p-value distribution. Denote by $F_0(\cdot)$ and $F_1(\cdot)$ the corresponding cumulative distribution functions. Suppose we reject the ith hypothesis if $p_i \leq t_i$ for some cutoff t_i. Before presenting the procedure that inspires the choice of T_i, it is worth clarifying the definition of the FWER from both the frequentist and Bayesian perspectives. The key difference between these two viewpoints lies on whether we treat the indicators $\{H_i\}$ as fixed or random quantities. From the frequentist perspective, the indicators $\{H_i\}$ are deterministic and we have by the union bound,

$$\text{FWER}_{\text{Freq}} = \mathbb{P}(p_i \leq t_i \text{ for some } i \in \mathcal{M}_0) \leq \sum_{i=1}^{m} \mathbb{I}(H_i = 0) F_0(t_i).$$

From a Bayesian's point of view, it is natural to posit the two-group mixture model

$$p_i \mid x_i \sim \pi(x_i) f_0(\cdot) + \{1 - \pi(x_i)\} f_1(\cdot).$$

In this case, conditional on x_i, H_i is assumed to be a Bernoulli random variable with the success probability $1 - \pi(x_i)$. The Bayesian FWER can be bounded as follows

$$\text{FWER}_{\text{Bay}} = \mathbb{P}(p_i \leq t_i \text{ for some } i \in \mathcal{M}_0) \leq \sum_{i=1}^{m} \mathbb{P}(p_i \leq t_i, H_i = 0) = \sum_{i=1}^{m} \mathbb{E}\left\{\pi(x_i)\right\} F_0(t_i). \tag{2.1}$$

To motivate our procedure, it is more convenient to adopt the Bayesian viewpoint. But we emphasize that the proposed procedure indeed provides asymptotic FWER control in the usual frequentist sense, as shown in Section 2.3.

We aim to find $\{t_i\}$ to maximize the expected number of true rejections given by

$$\mathbb{E}\left\{\sum_{i=1}^{m}\mathbb{I}(H_i=1,p_i\le t_i)\right\}=\sum_{i=1}^{m}\mathbb{E}[\{1-\pi(x_i)\}]F_1(t_i)$$

while controlling the FWER at a desired level α. To achieve both goals, we formulate the following constraint optimization problem

$$\max_{t_i}\sum_{i=1}^{m}\{1-\pi(x_i)\}F_1(t_i)\ \text{ s.t. }\sum_{i=1}^{m}\pi(x_i)F_0(t_i)\le\alpha, \tag{2.2}$$

where $\sum_{i=1}^{m}\pi(x_i)F_0(t_i)$ serves as a conservative estimate of the Bayesian FWER based on the derivations in (2.1). The Lagrangian for problem (2.2) is

$$L(t_1,\ldots,t_m;\lambda)=\sum_{i=1}^{m}\{1-\pi(x_i)\}F_1(t_i)-\lambda\left\{\sum_{i=1}^{m}\pi(x_i)F_0(t_i)-\alpha\right\}$$

with $\lambda>0$. Differentiating the Lagrangian with respect to t_i and setting the derivative to be zero (at the optimal value t_i^*), we obtain

$$\frac{\{1-\pi(x_i)\}f_1(t_i^*)}{\pi(x_i)f_0(t_i^*)}=\lambda.$$

Motivated by the above observation, we set

$$T_i(p)=\frac{\{1-\pi(x_i)\}f_1(p)}{\pi(x_i)f_0(p)}.$$

We note that $T_i(p)$ is related to the local FDR as follows

$$\frac{1}{T_i(p)+1} = \frac{\pi(x_i)f_0(p)}{\pi(x_i)f_0(p) + \{1-\pi(x_i)\}f_1(p)} = \mathbb{P}(H_i = 0 \mid p, x_i).$$

In the following discussions, we suppose f_0 is the uniform distribution on $[0,1]$ and f_1 is strictly decreasing, which is a common assumption in the literature, e.g., Sun and Cai (2007) and Cao et al. (2013). As T_i is strictly decreasing in this case, we may reduce our attention to the rejection rule $p_i \le t_i^*$ as $T_i(p_i) \ge T_i(t_i^*) := \tau^*$. The cutoff can then be expressed as

$$t_i^* = f_1^{-1}\left\{\frac{\pi(x_i)\tau^*}{1-\pi(x_i)}\right\},$$

where f_1^{-1} denotes the inversion of f_1. Notice that the expected number of true rejections and the conservative estimate of the Bayesian FWER in (2.1) are both monotonically decreasing in τ. Therefore, the solution to (2.2) satisfies that

$$\tau^* = \min\left\{\tau > 0 : \sum_{i=1}^{m} \pi(x_i) f_1^{-1}\left\{\frac{\pi(x_i)\tau}{1-\pi(x_i)}\right\} \le \alpha\right\}. \tag{2.3}$$

In practice, both π and f_1 are unknown and need to be replaced by estimates from the data. We provide detailed discussions about estimating the unknowns in the next section.

2.2.3 A feasible procedure

We describe a feasible procedure based on suitable estimates of π and f_1. To avoid overfitting and facilitate the theoretical analysis, we adopt the idea of censoring p-values as in Storey (2002), Li and Barber (2019) and Boca and Leek (2018). Under the two-group mixture model, for a prespecified $0 < \gamma < 1$, we have

$$\mathbb{I}(p_i > \gamma) \mid x_i \sim \pi(x_i)\text{Bern}(1-\gamma) + \{1-\pi(x_i)\}\text{Bern}\{1-F_1(\gamma)\},$$

where Bern$(1-\gamma)$ denotes the Bernoulli distribution with success probability $1-\gamma$. We model f_1 using the beta distribution $f_1(p) = kp^{k-1}$ for $0 < k < 1$ as it provides reasonably well approximation to a wide range of alternative distributions as demonstrated in Zhang and Chen (2020). Here we treat k as fixed and will discuss the choice of data-driven k in Section 2.2.4.

Before presenting our method, it is worth clarifying the rationale behind our procedure. Notice that $\pi(x_i)$ appears both inside and outside the function f_1^{-1} in (2.3). To achieve asymptotic FWER control, we need a conservative estimate for $\pi(x_i)$ outside the function f_1^{-1}, while for the one inside f_1^{-1}, we require it to depend on the covariates to reflect the heterogeneity among signals while retaining certain form of stability (see more details in Section 2.3). The reason will become clear by inspecting the proof of Proposition 1. We first observe that

$$\mathbb{E}\left\{\frac{\mathbb{I}(p_i > \gamma)}{1-\gamma} \mid x_i\right\} = \pi(x_i) + \{1-\pi(x_i)\}\frac{1-F_1(\gamma)}{1-\gamma} \geq \pi(x_i).$$

Therefore, we suggest replacing the $\pi(x_i)$ outside f_1^{-1} by $\mathbb{I}(p_i > \gamma)/(1-\gamma)$. To estimate $\pi(x_i)$ inside f_1^{-1}, we consider the logistic model

$$\log\left\{\frac{\pi(x_i)}{1-\pi(x_i)}\right\} = x_i^{\mathrm{T}}\beta.$$

The quasi log-likelihood function is then

$$L_m(\beta) = \sum_{i=1}^{m} \log\left[\pi(x_i)(1-\gamma)^{y_i}\gamma^{1-y_i} + \{1-\pi(x_i)\}(1-\gamma^k)^{y_i}\gamma^{k(1-y_i)}\right],$$

where $\pi(x_i) = (1+e^{-x_i^{\mathrm{T}}\beta})^{-1}$ and $y_i = \mathbb{I}(p_i > \gamma)$. Define the corresponding quasi-maximum likelihood estimator (MLE) as

$$\hat{\beta} = \arg\max_{\beta\in\mathcal{B}} L_m(\beta), \tag{2.4}$$

where $\mathcal{B}$ is some compact subset of $\mathbb{R}^d$. Let

$$\hat{\pi}(x_i) = \{\tilde{\pi}(x_i) \vee \varepsilon_1\} \wedge \varepsilon_2,$$

where $\tilde{\pi}(x_i) = (1 + e^{-x_i^{\mathrm{T}}\hat{\beta}})^{-1}$ and $0 < \varepsilon_1 < \varepsilon_2 < 1$. We have used winsorization to prevent $\hat{\pi}(x_i)$ from being too close to zero and one. Further denote

$$\hat{\tau} = \min\left\{\tau \geq \varepsilon : \sum_{i=1}^{m} \frac{\mathbb{I}(p_i > \gamma)}{1-\gamma} f_1^{-1}\left\{\frac{\hat{\pi}(x_i)\tau}{1-\hat{\pi}(x_i)}\right\} \leq \alpha\right\}$$

for some $\varepsilon > 0$. It is straightforward to show that $\hat{\tau} = \tilde{\tau} \vee \varepsilon$ with

$$\tilde{\tau} = k\left[\sum_{i=1}^{m} \frac{\mathbb{I}(p_i > \gamma)}{\alpha(1-\gamma)}\left\{\frac{1-\hat{\pi}(x_i)}{\hat{\pi}(x_i)}\right\}^{1/(1-k)}\right]^{1-k}.$$

Finally, we set

$$\hat{t}_i = \left[\frac{\{1-\hat{\pi}(x_i)\}k}{\hat{\pi}(x_i)\hat{\tau}}\right]^{1/(1-k)},$$

and reject the ith hypothesis if

$$p_i \leq \hat{t}_i \wedge \gamma.$$

Remark 1 (Connection to the weighted Bonferroni procedure)**.** Suppose $\varepsilon_1 = \varepsilon = 0$ and $\varepsilon_2 = 1$. Then we have

$$\hat{t}_i = \left[\frac{\{1-\tilde{\pi}(x_i)\}k}{\tilde{\pi}(x_i)\tilde{\tau}}\right]^{1/(1-k)} = \alpha w_i,$$

where

$$w_i = e^{-\frac{x_i^{\mathrm{T}}\hat{\beta}}{1-k}}\left\{\sum_{i=1}^{m} \frac{\mathbb{I}(p_i > \gamma)}{1-\gamma} e^{-\frac{x_i^{\mathrm{T}}\hat{\beta}}{1-k}}\right\}^{-1}.$$

We reject the ith hypothesis if

$$p_i \leq \alpha w_i \wedge \gamma.$$

In this sense, our procedure can be viewed as a particular type of weighted Bonferroni procedure. However, different from existing methods, our weight incorporates the information regarding the alternative p-value distribution, which often leads to more rejections and thus higher power, as observed in our numerical studies.

2.2.4 EM algorithm

Algorithm 1 below provides the details of our iterative algorithm to solve problem (2.4).

Algorithm 1. *EM algorithm for problem (2.4).*

Input: $\{x_i, y_i\}_{i=1}^m, \gamma, k$*; initializer:* $\beta^{(0)}$.

Output: $\hat{\beta}$.

Notation: $b_{0i} = (1-\gamma)^{y_i}\gamma^{1-y_i}$*;* $b_{1i} = (1-\gamma^k)^{y_i}\gamma^{k(1-y_i)}$*; tol: tolerance level.*

Iteration:

E step:

$Q_i^{(t)} = \mathbb{E}\{\mathbb{I}(H_i = 0) \mid y_i, x_i, \beta^{(t)}\} = \pi_i^{(t)} b_{0i} / \{\pi_i^{(t)} b_{0i} + (1-\pi_i^{(t)}) b_{1i}\}$,

where $\pi_i^{(t)} = (1 + e^{-x_i^{\mathrm{T}}\beta^{(t)}})^{-1}$.

M step:

$\beta^{(t+1)} = \arg\max_{\beta \in \mathcal{B}} \sum_{i=1}^m \{Q_i^{(t)} \log(\pi_i) + (1 - Q_i^{(t)}) \log(1-\pi_i)\}$,

where $\pi_i = (1 + e^{-x_i^{\mathrm{T}}\beta})^{-1}$.

Until: $|L_m(\beta^{(t+1)}) - L_m(\beta^{(t)})| / |L_m(\beta^{(t)})| <$ *tol.*

Return: $\beta^{(t+1)}$ *after a sufficient number of iterations.*

The theory in Section 2.3 below shows that our procedure controls FWER asymptotically for any fixed k. However, a suitable choice of k, which produces a beta-distribution closer to the true f_1 (especially on the small p-value region), will improve the statistical power. In practice, an EM algorithm can be used to estimate the k and β jointly. To be precise, we define the quasi log-likelihood function,

$$L_m(\beta, k) = \sum_{i=1}^m \log\left[\pi(x_i)(1-\gamma)^{y_i}\gamma^{1-y_i} + \{1-\pi(x_i)\}(1-\gamma^k)^{y_i}\gamma^{k(1-y_i)}\right].$$

Then we estimate (β, k) jointly by the quasi-MLE defined as

$$(\hat{\beta}, \hat{k}) = \arg \max_{\beta \in \mathcal{B}, k \in (0,1)} L_m(\beta, k). \tag{2.5}$$

We summarize the algorithm for solving problem (2.5) in Algorithm 2.

Algorithm 2. *EM algorithm for problem (2.5).*

Input: $\{x_i, y_i\}_{i=1}^m, \gamma$*; initializer:* $\beta^{(0)}, k^{(0)}$.

Output: $\hat{\beta}, \hat{k}$.

Notation: $b_{0i} = (1-\gamma)^{y_i}\gamma^{1-y_i}$*; tol: tolerance level.*

Iteration:

E step:

$Q_i^{(t)} = \mathbb{E}\{\mathbb{I}(H_i = 0) \mid y_i, x_i, \beta^{(t)}, k^{(t)}\} = \pi_i^{(t)} b_{0i} / \{\pi_i^{(t)} b_{0i} + (1-\pi_i^{(t)}) b_{1i}^{(t)}\}$,

where $\pi_i^{(t)} = (1 + e^{-x_i^{\mathrm{T}} \beta^{(t)}})^{-1}$, $b_{1i}^{(t)} = (1-\gamma^{k^{(t)}})^{y_i} \gamma^{k^{(t)}(1-y_i)}$.

M step:

$\beta^{(t+1)} = \arg\max_{\beta \in \mathcal{B}} \sum_{i=1}^m \{Q_i^{(t)} \log(\pi_i) + (1 - Q_i^{(t)}) \log(1-\pi_i)\}$,

where $\pi_i = (1 + e^{-x_i^{\mathrm{T}} \beta})^{-1}$*;*

$k^{(t+1)} = \arg\max_{k \in (0,1)} \sum_{i=1}^m (1 - Q_i^{(t)}) \{y_i \log(1-\gamma^k) + k(1-y_i)\log(\gamma)\}$.

Until: $|L_m(\beta^{(t+1)}, k^{(t+1)}) - L_m(\beta^{(t)}, k^{(t)})| / |L_m(\beta^{(t)}, k^{(t)})| <$ *tol.*

Return: $\beta^{(t+1)}, k^{(t+1)}$ *after a sufficient number of iterations.*

2.3 Asymptotic FWER control

In this section, we prove the asymptotic FWER control for the procedure proposed in Section 2.2.3. Throughout this section, we shall adopt the frequentist viewpoint, i.e., we view the indicators $\{H_i\}$ as a deterministic sequence.

Let $p_{j \to a} = (p_1, \ldots, p_{j-1}, a, p_{j+1}, \ldots, p_m)^{\mathrm{T}} \in \mathbb{R}^m$ for $a = 0, 1$. We define $\hat{\beta}(p_{j \to a})$ and $\hat{t}_i(p_{j \to a})$ by setting the jth p-value to be equal to a when estimating the corresponding quantities. We make the following assumption.

Assumption 1. *Denote by F_{0i} the cumulative distribution function for p_i with $H_i = 0$. Suppose that $\{p_i\}_{i\in\mathcal{M}_0}$ are super-uniform, i.e., $F_{0i}(t) \le t$ for all $t \in [0,1]$ and $i \in \mathcal{M}_0$.*

Assumption 1 is standard in the literature, see e.g., Benjamini and Yekutieli (2001).

Proposition 1. *If $\{p_i\} \in \mathcal{M}_0$ are mutually independent and are independent with the non-null p-values, then under Assumption 1, we have*

$$\textit{FWER} \le J_m + \alpha \le c(J_{m,1} + J_{m,2}) + \alpha,$$

where

$$\begin{aligned}
J_m &= \sum_{j=1}^{m} \mathbb{E}\left\{\left|\hat{t}_j(p_{j\to 0}) - \hat{t}_j(p_{j\to 1})\right|\right\}, \\
J_{m,1} &= \sum_{j=1}^{m} \mathbb{E}\left[\frac{|x_j^{\mathrm{T}}\{\hat{\beta}(p_{j\to 0}) - \hat{\beta}(p_{j\to 1})\}|}{\left\{c\alpha^{-1}\sum_{i\neq j}\mathbb{I}(p_i > \gamma)\right\} \vee \varepsilon^{1/(1-k)}}\right], \\
J_{m,2} &= \sum_{j=1}^{m} \mathbb{E}\left(\frac{\alpha^{-1}\sum_{i\neq j}\mathbb{I}(p_i > \gamma)|x_i^{\mathrm{T}}\{\hat{\beta}(p_{j\to 0}) - \hat{\beta}(p_{j\to 1})\}| + \alpha^{-1}}{\left[\left\{c\alpha^{-1}\sum_{i\neq j}\mathbb{I}(p_i > \gamma)\right\} \vee \varepsilon^{1/(1-k)}\right]^2}\right),
\end{aligned}$$

and ε has been defined in Section 2.2.3.

The above proposition shows that the validity of the asymptotic FWER control relies on the stability of $\hat{t}_j$, i.e., the smallness of $|\hat{t}_j(p_{j\to 0}) - \hat{t}_j(p_{j\to 1})|$ which in turn depends on $\|\hat{\beta}(p_{j\to 0}) - \hat{\beta}(p_{j\to 1})\|$. Set $z_i = (x_i, y_i)$, where $y_i = \mathbb{I}\{p_i > \gamma\}$. Define

$$l(\beta; z_i) = \log\left\{\frac{1}{1+e^{-x_i^{\mathrm{T}}\beta}}(1-\gamma)^{y_i}\gamma^{1-y_i} + \frac{e^{-x_i^{\mathrm{T}}\beta}}{1+e^{-x_i^{\mathrm{T}}\beta}}(1-\gamma^k)^{y_i}\gamma^{k(1-y_i)}\right\},$$

and $\mathbb{P}_m l(\beta) = m^{-1}\sum_{i=1}^{m} l(\beta; z_i)$. To ensure $\|\hat{\beta}(p_{j\to 0}) - \hat{\beta}(p_{j\to 1})\|$ to be small, we impose the following assumptions.

Assumption 2. *Suppose $z_i \in \mathbb{R}^{d+1}$ are independent and possibly non-identically distributed.*

Assumption 2 is not uncommon in the multiple testing literature, see e.g., Ignatiadis et al. (2016). We suspect that the results still hold when z_i is a sequence of weakly dependent variables although a rigorous proof is left for future investigation.

Assumption 3. *There exists a continuous function of β, denoted by $\mathcal{L}(\beta)$, such that*

$$\lim_{m\to+\infty} \sup_{\beta\in\mathcal{B}} |\mathbb{E}\{\mathbb{P}_m l(\beta)\} - \mathcal{L}(\beta)| = 0.$$

Assumption 4. *Suppose $\mathcal{L}(\beta)$ has a unique global maximizer β^* over the compact space $\mathcal{B}$.*

Assumption 4 is needed in our perturbation argument. If the maximizer is not unique, there seems no guarantee that the difference between $\hat{\beta}(p_{j\to 0})$ and $\hat{\beta}(p_{j\to 1})$ will be small.

Proposition 2. *Suppose Assumptions 2–4 are satisfied and further assume $\sup_{1\le i\le m}\mathbb{E}(\|x_i\|^8) < \infty$. Then we have*

$$\hat{\beta}(p_{j\to 0}) - \hat{\beta}(p_{j\to 1}) = (S_j^* + \Delta_j)^{-1}(U_j^* + \Pi_j),$$

where S_j^* and U_j^* are the leading terms such that $S_j^* = -\sum_{i\neq j}\nabla^2 l(\beta^*; z_i)$ and $\sup_{1\le j\le m}\|U_j^*\| = O_{\mathbb{P}}(1)$, and Δ_j and Π_j are the remainder terms satisfying that

$$\sup_{1\le j\le m}\|\Delta_j\| = o_{\mathbb{P}}(m) \text{ and } \sup_{1\le j\le m}\|\Pi_j\| = o_{\mathbb{P}}(1).$$

Given Propositions 1 and 2, we have the following theorem of asymptotic FWER control.

Theorem 1. *Suppose the following conditions are satisfied:*

(i) Assumptions 1–4 hold;

(ii) for some $q \ge 2$ and $\epsilon > 0$, we have $\sup_{1\le i\le m}\mathbb{E}(\|x_i\|^{4q+\epsilon}) < \infty$;

(iii) we have $\sup_{\beta\in\mathcal{B}}|\mathbb{E}\{\mathbb{P}_m l(\beta)\} - \mathcal{L}(\beta)| = O(m^{-1/2})$;

(iv) the function $\mathcal{L}(\beta)$ is twice continuously differentiable;

(v) the global maximizer β^* is not on the boundary of $\mathcal{B}$;

(vi) for some $c > 0$, we have $\nabla^2 \mathcal{L}(\beta^*) \preceq -cI$, where I denotes the identity matrix;

(vii) for large enough m and some $c > 0$, we have $\mathbb{E}\{\nabla^2 \mathbb{P}_m l(\beta^*)\} \preceq -cI$; and

(viii) the number of true null hypotheses m_0 satisfies that $\liminf m_0/m > 0$.

Then

$$\textit{FWER} \leq J_m + \alpha = \begin{cases} o(\alpha m^{\frac{1-q}{4}}) + \alpha, & \textit{if } 2 \leq q \leq 2 + \sqrt{5}, \\ O(\alpha m^{\frac{-q}{1+q}}) + \alpha, & \textit{if } q > 2 + \sqrt{5}. \end{cases}$$

Theorem 1 derives the bound and its exact order on the FWER. Interestingly, the order of the bound depends crucially on the tail behavior of the covariates. And it shows an interesting phase transition depending on the value of q. We briefly explain this result as follows. From Proposition 1, we can see that the FWER is upper bounded by an expression of the form $\alpha + \sum_{i=1}^{m} r_i$ with $r_i \geq 0$. Our argument optimizes the summation $\sum_{i=1}^{m} r_i$ in the upper bound. Depending on the value of q, the dominant term in this summation will change, which eventually leads to different convergence rates. When the covariates have exponential tails, the rate of convergence can be as close to m^{-1} as possible. The details of the proof are provided in the appendices. As we discussed earlier, Assumptions 1–4 enable us to show that the upper bound on the FWER relies on the smallness of $\|\hat{\beta}(p_{j\to 0}) - \hat{\beta}(p_{j\to 1})\|$ and to get the expression for $\hat{\beta}(p_{j\to 0}) - \hat{\beta}(p_{j\to 1})$. As our goal is to quantify the exact rate of convergence of the FWER upper bound to the nominal level α, we further need to quantify the exact difference between $\hat{\beta}(p_{j\to 0})$ and $\hat{\beta}(p_{j\to 1})$. Through Conditions (iii)–(v) and the strong-concavity Condition (vi), we obtain the concentration inequality for $\|\hat{\beta}(p_{j\to a}) - \beta^*\|$. Conditions (ii) and (vii) are used for controlling the inverse $(S_j^* + \Delta_j)^{-1}$ in the expression of $\hat{\beta}(p_{j\to 0}) - \hat{\beta}(p_{j\to 1})$. Condition (viii) requires the number of true null hypotheses to be at least some positive proportion of all hypotheses, which is fairly mild. We give one toy example where all the conditions are satisfied.

Example 1. *Suppose all hypotheses are true nulls and (x_i, p_i) are i.i.d.with x_i being 1-dimensional, $x_i \perp\!\!\!\perp p_i$ and $p_i \sim$ Unif$([0,1])$, i.e., the uniform distribution on $[0,1]$. Then $\mathcal{L}(\beta) = \mathbb{E}\{\mathbb{P}_m l(\beta)\} =$*

$\mathbb{E}\{l(\beta; z_1)\}$. *If* x_i *follows a distribution symmetric about zero and* $\mathbb{P}(x_i \neq 0) > 0$*, it can be shown that* $\mathcal{L}'(\beta) = 0$ *if* $\beta = 0$*,* $\mathcal{L}'(\beta) > 0$ *if* $\beta < 0$*,* $\mathcal{L}'(\beta) < 0$ *if* $\beta > 0$*, and* $\mathcal{L}'(\beta) = -\mathcal{L}'(-\beta)$*. Thus* $\beta^* = 0$ *is the unique maximizer. We can further prove that* $\mathcal{L}''(0) \leq -c$ *as long as* $\mathbb{E}(x_i^2) > c'$ *for some* $c' > 0$*. Other conditions are naturally satisfied. When* x_i *follows a non-symmetric distribution, we also illustrate its obedience to these conditions. One mandatory requirement for the distribution of* x_i *is that* $\mathbb{P}(x_i > 0) > 0$ *and* $\mathbb{P}(x_i < 0) > 0$*. In practice, we could always achieve this by shifting the covariate via subtracting the median (or by standardizing the covariate). See more details in the appendices.*

2.4 Numerical studies

2.4.1 Simulation setups

We conduct comprehensive simulations to evaluate the finite-sample performance of the proposed method and compare it to competing methods. For genome-scale multiple testing, the numbers of hypotheses could range from thousands to millions. For demonstration purpose, we start with $m = 10,000$ hypotheses. To study the impact of signal density and strength, we simulate three levels of signal density (sparse, medium and dense signals) and six levels of signal strength (from very weak to very strong). To demonstrate the power improvement by using external covariates, we simulate covariates of varying informativeness (non-informative, moderately informative and strongly informative). For simplicity, we simulate one covariate $x_i \sim N(0, 1)$ for $i = 1, \cdots, m$. Given x_i, we denote $\pi(x_i)$ by π_i and let

$$\pi_i = \frac{\exp(\eta_i)}{1 + \exp(\eta_i)}, \quad \eta_i = \eta_0 + k_d x_i,$$

where η_0 and k_d determine the baseline signal density and the informativeness of the covariate, respectively. We set $\eta_0 = 3.5, 2.5$ and 1.5, which achieves a signal density of around 3%, 8%, and 18% respectively at the baseline (i.e., no covariate effect), representing sparse, medium and dense signals. Here k_d is set to be 0, 1 and 1.5, representing a non-informative, moderately informative

and strongly informative covariate. Based on π_i, the underlying truth H_i is simulated from

$$H_i \sim \text{Bern}(1 - \pi_i).$$

Finally, we simulate independent z-scores using

$$z_i \sim N(k_s H_i, 1),$$

where k_s controls the signal strength (effect size), and we use six values equally spaced on [2, 2.8] and we label them as $\{1, 2, ..., 6\}$. Z- scores are converted into p-values using the one-sided formula $1 - \Phi(z_i)$. P-values together with x_i are used as the input for the proposed method.

In addition to the basic setting (denoted as S0), we investigate other settings to study the robustness of the proposed method. Specifically, we study

- Setup S1. *Additional f_1 distribution*. Instead of simulating normal z-scores under f_1, we simulate z-scores from a non-central gamma distribution with the shape parameter 2. The scale/non-centrality parameters of the non-central gamma distribution are chosen to match the variance and mean of the normal distribution under S0.

- Setup S2. *Correlated hypotheses*. We further investigate the effect of dependency among hypotheses by simulating correlated multivariate normal z-scores. Four correlation structures, including two block correlation structures and two AR(1) correlation structures, are investigated. For the block correlation structure, we divide the 10,000 hypotheses into 500 equal-sized blocks. Within each block, we simulate equal positive correlations ($\rho = 0.5$) (S2.1). On top of S2.1, we divide the block into 2 by 2 sub-blocks, and simulate negative correlations ($\rho = -0.5$) between the two sub-blocks (S2.2). For AR(1) structure, we investigate both $\rho = 0.75^{|i-j|}$ (S2.3) and $\rho = (-0.75)^{|i-j|}$ (S2.4).

We present the simulation result for the Setup S0 in the main text and the results for the Setups S1 and S2 in the appendices.

2.4.2 Competing methods

We compared the proposed covariate-adaptive FWER-controlling procedure (denoted by CAMT.fwer) to IHW-Bonferroni, weighted Bonferroni and Holm's step-down methods (Holm, 1979). The covariate-adaptive FWER-controlling procedure, implemented using the CAMT.fwer function in the R package `CAMT`, used the model $\log[\pi(x_i)/\{1-\pi(x_i)\}] = x_i^{\mathrm{T}}\beta$, set $f_1(p) = kp^{k-1}$ and estimated β and k jointly using Algorithm 2. The weighted Bonferroni method rejected the ith hypothesis if $p_i < \alpha/(m\pi_i)$, where π_i's were estimated from CAMT.fwer. The IHW-Bonferroni method was implemented using the R package `IHW`, and Holm's step-down method using the holm function from the R package `mutoss`. We also implemented an oracle procedure based on the proposed optimal rejection rule, where π_i's and f_1 were the true null probabilities and alternative density that generated the data.

Storey et al. (2004) proposed the bootstrap method to estimate the overall null probability π, which is implemented in the R package `qvalue`. The method uses censored p-values $\mathbb{I}\{p_i > \lambda\}$ with $\lambda = 0.05, 0.1, ..., 0.95$ to obtain the corresponding estimates of the null probability, π_λ, and returns the best $\pi_{\hat{\lambda}}$. We set $\gamma = \hat{\lambda}$. We evaluated the performance based on the FWER control (probability of making at least one false positive) and power (true positive rate) with a target FWER level of 5%. Results were averaged over 1000 simulation runs. In addition, we investigated the FWER control across different target levels, $\alpha = 0.01, 0.05, 0.1, 0.15, 0.2$, for cases where there are no signals and under the Setup S0 with moderate signal density ($\eta_0 = 2.5$), signal strength ($k_s = 2.4$) and covariate informativeness ($k_d = 1$).

2.4.3 Simulation results

We showcase the simulation results of Setup S0 in Figure 2.1 and Setups S1–S2 in the appendices as well as the FWER control across different target levels (see Figures A.4–A.11 in the appendices). All methods control the FWER around the 5% target level (Figure 2.1A). We additionally draw the 95% confidence intervals (CIs) of the proposed method CAMT.fwer and observe that almost all the intervals cover the 5% target level (dashed line) (Figure 2.1A), which sug-

gests adequate FWER control of CAMT.fwer under finite samples. In terms of power (Figure 2.1B), generally, the five competing methods from the best to the worst are oracle, CAMT.fwer, IHW-Bonferroni and weighted Bonferroni (the performance of these two methods depends on the cases), Holm's step-down methods. The oracle procedure represents the performance upper bound and dominates other methods.

We now study the impact of the external (prior) information , signal density and strength (Figure 2.1B). First, we note that the power increases with the signal strength (effect size) for all methods as expected. Second, as the prior informativeness increases, the performance difference between methods widens. CAMT.fwer is close to the oracle procedure: it is as powerful as other methods when the prior is not informative and is substantially more powerful when the prior is highly informative. Both IHW-Bonferroni and weighted Bonferroni methods improve over Holm's step-down method when the prior is informative. Third, the proposed method maintains high power across different signal densities. In contrast, IHW-Bonferroni method performs better than weighted Bonferroni method when the signal is sparse and performs worse when the signal is dense.

Figures A.4–A.5 show the weak and strong FWER control of the competing methods across different target levels. All the methods including CAMT.fwer control the FWER at the target level. Figure A.6 compares the power across different target levels at moderate signal density, signal strength and prior informativeness. CAMT.fwer remains more powerful than other methods. In fact, as the target level increases, the power difference becomes larger.

We next study the robustness of the proposed method under the Setup S1 (additional f_1 distribution, Figure A.7) and Setup S2 (correlated hypotheses, Figures A.8–A.11). The general trend remains similar to Setup S0, indicating that CAMT.fwer is robust to different f_1 distributions and various correlation structures. Interestingly, as we generate z-scores from non-central gamma distribution for the alternative in Setup S1, the power of CAMT.fwer is even closer to that of the oracle procedure (Figure A.7), indicating that the beta distribution can model the alternative p-value distribution very accurately in this case.

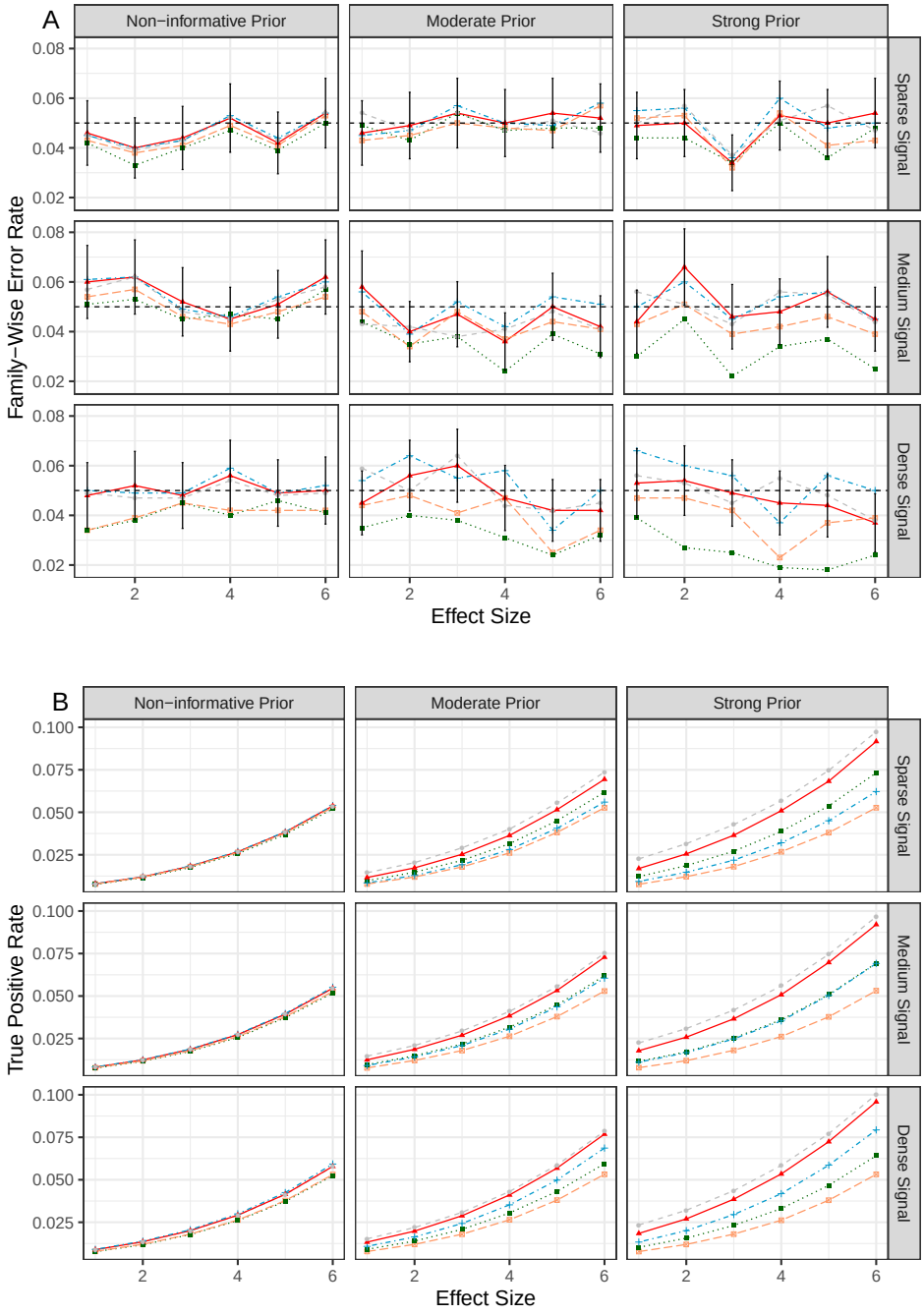

Figure 2.1: Performance comparison under the basic setting (S0). Family-wise error rates (A) and true positive rates (B) were averaged over 1000 simulation runs. The dashed gray, solid red, dotted green, dot-dashed blue and long-dashed orange lines represent the oracle, CAMT.fwer, IHW-Bonferroni, weighted Bonferroni and Holm's step-down methods respectively. The error bars (A) represent the 95% CIs of the method CAMT.fwer and the dashed horizontal line indicates the target FWER level of 0.05.

2.5 Application to GWAS of UK Biobank data

To demonstrate the use of the proposed procedure in real world applications, we applied CAMT.fwer to UK Biobank data (Kichaev et al., 2019). We downloaded the data (p-values and functional annotations) from `https://data.broadinstitute.org/alkesgroup/UKBB/` and `https://data.broadinstitute.org/alkesgroup/FINDOR/`. The genome-wide association p-values for 9 million SNPs and 27 traits were calculated using BOLT-LMM (Loh et al., 2018) based on 459K samples. The annotation data consists of 75 coding, conserved, regulatory, and linkage-disequilibrium-related annotations that have previously been shown to be enriched for the disease heritability (Kichaev et al., 2019). We compared our method with IHW-Bonferroni, weighted Bonferroni and Holm's step-down methods. For the IHW-Bonferroni method, as it can only deal with one-dimensional covariate, we chose the covariate that had the maximum Spearman correlation with the p-values out of the 75 covariates for the 27 traits separately. For the weighted Bonferroni method, we rejected the ith hypothesis if $p_i < \alpha/(m\pi_i)$, where π_i's were estimated from CAMT.fwer. The details of the use of CAMT.fwer are given below.

Appropriate initial values of (β, k) are important for the algorithm to reach convergence in less iterations and reduce the computation time significantly. To achieve this end, we estimate those initial values based on small p-values (so the initial beta distribution fits the small p-value region more accurately). Let π^s be the estimate of the proportion of the true null hypotheses based on Storey's procedure (R package `qvalue`). We define the "small p-values" as the first $m(1-\pi^s)$ smallest p-values and let u be the maximum value of those small p-values. Note that

$$f(p \mid p < u) = \frac{\pi + (1-\pi)kp^{k-1}}{\pi u + (1-\pi)u^k},$$

is the conditional density of the mixture model $f(p) = \pi + (1-\pi)kp^{k-1}$ given that the value is less than u. We estimate π and k by maximizing the (conditional) log-likelihood function,

$$(\tilde{\pi}, \tilde{k}) = \arg \max_{\pi \in (0,1), k \in (0,1)} \sum_{i: p_i < u} \log\left\{\pi + (1-\pi)kp_i^{k-1}\right\} - n \log\{\pi u + (1-\pi)u^k\},$$

where n is the number of p-values that are smaller than u. Let $\tilde{\beta} = (\log\{\tilde{\pi}/(1-\tilde{\pi})\}, 0)^{\mathrm{T}}$. Then we set $(\tilde{\beta}, \tilde{k})$ as the initializer in Algorithm 2.

Due to the linkage disequilibrium between SNPs, after getting the rejected SNPs, we used PLINK's linkage-disequilibrium-based clumping algorithm with a 5 Mb window and an r^2 threshold of 0.01 to form clumps of SNPs. The British population in the 1000 genomes data (1000 Genomes Project Consortium, 2015) was used to calculate the linkage disequilibrium. The rejected SNPs belonging to the same clump count for only one significant locus. The numbers of significant loci at the 5% FWER level detected by the four competing methods are presented in Table 2.1. We present the numbers of rejections before clumping in the appendices. CAMT.fwer detected more loci than other methods in 21 out of the 27 traits. Averaged across the traits, our approach attained 4.20% increase in significant loci detected compared with the Holm's step-down method.

2.6 Discussions

To conclude, we point out a few future research directions. First, in the two-group mixture model, we assume that the success probabilities $\pi(x_i)$ vary with x_i while f_1 is independent of x_i. This assumption is reasonable in some applications but it can be restrictive when the covariates also affect the effect sizes. It is thus of interest to develop a procedure by allowing f_1 to be dependent on x_i in such scenarios. Second, modeling f_1 and π using nonparametric procedures would give us the flexibility to capture more complicated signal patterns. Finally, extending the method to accommodate more general structural information such as the phylogenetic tree structure (Xiao et al., 2017) is an interesting direction.

Table 2.1: Significant loci detected at the FWER level of 0.05. Improve=(CAMT.fwer $-$ Holm)/Holm $\times$ 100%. The numbers with subscript $*$ are the maximum numbers of rejections among the four competing methods for the corresponding traits.

	Holm	IHW	weighted Bonferroni	CAMT.fwer	Improve
Balding Type I	836_*	836_*	836_*	833	-0.4%
BMI	1287	1287	1347	1364_*	6%
Heel T Score	2104	2104	2144	2146_*	2%
Height	3463	3460	3555_*	3550	2.5%
Waist-hip Ratio	909	909	937	952_*	4.7%
Eosinophil Count	1750	1750	1817_*	1797	2.7%
Mean Corpular Hemoglobin	1913	1913	1953_*	1925	0.6%
Red Blood Cell Count	1570	1570	1609	1633_*	4%
Red Blood Cell Distribution Width	1470	1470	1493_*	1470	0%
White Blood Cell Count	1393	1393	1430	1462_*	5%
Auto Immune Traits	179	179	180_*	138	-22.9%
Cardiovascular Diseases	512	512	529	540_*	5.5%
Eczema	423	423	426	431_*	1.9%
Hypothyroidism	373	373	377	424_*	13.7%
Respiratory and Ear-nose-throat Diseases	228	228	231	236_*	3.5%
Type 2 Diabetes	156	156	158	160_*	2.6%
Age at Menarche	634	634	648	652_*	2.8%
Age at Menopause	200	200	201	203_*	1.5%
FEV1-FVC Ratio	1537	1537	1575	1599_*	4%
Forced Vital Capacity (FVC)	867	867	924	947_*	9.2%
Hair Color	1606	1606	1616	1629_*	1.4%
Morning Person	204	204	217	229_*	12.3%
Neuroticism	176	115	189	198_*	12.5%
Smoking Status	221	159	232	254_*	14.9%
Sunburn Occasion	232	232	232	237_*	2.2%
Systolic Blood Pressure	1108	1108	1148	1157_*	4.4%
Years of Education	383	383	416	447_*	16.7%

3. LinDA: LINEAR MODELS FOR DIFFERENTIAL ABUNDANCE ANALYSIS OF MICROBIOME COMPOSITIONAL DATA

3.1 Introduction

The role of the human microbiome in health and disease has been intensively studied over the past few years, see, e.g., Fan and Pedersen (2021) and Valdes et al. (2018), for several reviews. Potentially pathogenic or probiotic microorganisms can be identified by analyzing their abundances in a microbial ecosystem (e.g., the human gut) with respect to some variable of interest such as disease status. Current prevailing technologies for studying the human microbiome use metagenomic sequencing, where either the DNA of a taxonomically informative gene (e.g. 16S rRNA) or all the genomic DNA in the microbial genome is sequenced. After obtaining the raw sequencing reads, the reads can be clustered into operational taxonomic units (OTUs), denoised into amplicon sequence variants (ASVs), or mapped to a microbial reference database (taxa) using existing bioinformatics pipelines such as UPARSE, DADA2, and MetaPhlAn (Edgar, 2013; Callahan et al., 2016; Segata et al., 2012). For simplicity, we use the term taxon (pl. taxa) to represent any taxonomic unit (OTU/ASV/taxon) from a bioinformatics pipeline. Therefore, after bioinformatics processing, we have an abundance table recording the frequencies of detected taxa in the samples, together with a meta data table capturing the sample-level information. Differential abundance analysis is then carried out based on the abundance and meta data table.

Ideally, we want to measure the absolute abundance of the microorganisms, i.e., the number of microorganisms per unit area/volume at the microbial ecosystem, and differential abundance analysis is performed on the absolute abundance data. In practice, the data from a sequencing experiment only captures the relative abundance (compositional) information since the total sequence read count, also known as sequencing depth or library size, does not reflect the total microbial load in the specimen due to the complex chemistry involved in sequencing (Gloor et al., 2017; Tsilimigras and Fodor, 2016). Drawing inferences about the changes on the unknown absolute abundance

based on the measured relative abundance data is challenging due to missing the total microbial load information. The increase or decrease in the abundance of some taxa with respect to a variable of interest automatically results in changes in the relative abundances of all other taxa, a statistical phenomenon known as compositional effects. Therefore, using the standard statistical techniques such as two-sample t-test, Wilcoxon rank sum test, and linear regression analysis ignoring the compositional nature of the data could lead to a large number of false discoveries. We consider an artificial example for illustration. Suppose we have two samples with three detected taxa. The absolute taxa abundances for the two samples are $(10, 20, 70)$ and $(30, 20, 70)$. Thus, only the first taxon is differentially abundant. Now suppose, after sequencing (ignoring the sampling variability), the read counts for the two samples are $(100, 200, 700)$ and $(3, 2, 7)$, where the first sample is more deeply sequenced. Since the total read sum is an experimental artifact, we normalize the data into relative abundances by dividing by the library size, and the corresponding relative abundances for the two samples become $(0.1, 0.2, 0.7)$ and $(0.25, 0.167, 0.583)$. Hence, all three taxa appear differentially abundant while the truth is that only the first is differential.

Based on the relative abundance data alone, it is impossible to tell whether it is the first taxon that is differential or all the taxa are differential for the previous example. For the problem to be well defined, one has to make assumptions. One assumption is that the differential signal is sparse, i.e., only a small proportion of taxa are associated with the variable of interest. This is the assumption the proposed method is based on. However, we acknowledge that, although many studies have supported the sparse signal assumption, there are also studies support dense signal hypotheses, where a large number of taxa are differential with small effect sizes (Xiao et al., 2018)(Xiao et al., 2018). Therefore, the validity of a method and the definition of true or false positive depends on the specific assumption one is willing to accept. Here we do not claim that our method is “correct": all we want to achieve is to provide a statistical tool that could be potentially useful for pinpointing top candidate taxa for further biological validation.

To address compositional effects in differential analysis, one popular approach is robust normalization. It involves calculating a normalizing factor (scale factor), which is robust to a small

number of differential taxa and could well capture the sequencing effort for the non-differential part. Therefore, dividing by such a normalizing factor will bring the abundance of the non-differential taxa to the same scale while retaining the differences for those differential ones. In contrast, the naive total sum scaling (TSS) normalization, which divides the counts by the library size, is not robust as illustrated in the previous example. An ideal normalizing factor for the previous example would be 900 and 9, which are the sum of the counts of the two non-differentially abundant taxa. The corresponding normalized data are then $(100/900, 200/900, 700/900)$ and $(3/9, 2/9, 7/9)$. Thus, only the first taxon is differentially abundant. In reality, however, we do not know which taxa are non-differential in advance. Assuming the number of differential taxa is small, different strategies have been used to calculate a robust normalizing factor including TMM, RLE, CSS, and GMPR (Robinson and Oshlack, 2010; Anders and Huber, 2010; Paulson et al., 2013; Chen et al., 2018). We list these methods in the Appendix Table B.1.

These normalization techniques can be combined with different statistical procedures in differential abundance analysis. For example, we can divide the counts by the normalizing factor from the normalization techniques in Appendix Table B.1 and then apply standard statistical tools based on the normalized data. The normalizing factor could also be included as an offset in regression models such as EdgeR (Robinson et al., 2010), DESeq2 (Love et al., 2014), MicrobiomeDDA (Chen et al., 2018), and MetagenomeSeq (Paulson et al., 2013), where the TMM, RLE, GMPR, and CSS normalization are the accompanying normalization methods. A variant to the robust normalization approach is to find a reference taxon or a set of reference taxa, which are assumed to be non-differential with respect to the variable of interest. The data are then normalized by the count of the reference taxon (or the sum of the counts of the reference taxa). This strategy was used in RAIDA (Sohn et al., 2015) and DACOMP (Brill et al., 2020).

Another line of methods to tackle the compositional effect uses (log) ratio approach since only ratios are well defined for compositional data (Aitchison, 1986). The ALDEx2 method by Fernandes et al. (2014) uses the centered log-ratio (CLR) transformation, where the counts of a sample are divided by their geometric mean before taking logarithms. Differential abundance analysis is

then performed using Wilcoxon rank sum test or t-test based on the CLR transformed data. In the CLR approach, the geometric mean can also be regarded as a robust normalizing factor. The ANCOM proposed by Mandal et al. (2015) computes the pairwise ratios of the relative abundances and identifies the taxa with the most differential ratios. This is based on the observation that the abundance ratios for those differential taxa to other taxa are all differential assuming distinct effect sizes while the ratios for those non-differential taxa are mostly non-differential. Therefore, by analyzing the pattern of the pairwise ratios, one could distinguish the differential taxa from a background of non-differential taxa with high accuracy. Recently, Lin and Peddada (2020) proposed a bias-corrected version of ANCOM (called ANCOM-BC), which uses a linear regression framework based on log-transformed taxa count and estimates the unknown bias term due to the compositional effect through an EM algorithm.

Weiss et al. (2017) and Hawinkel et al. (2019) evaluated several popular methods in differential abundance analysis (ANCOM-BC not included) and showed that the inflation of the FDR is a ubiquitous problem, and no method is satisfactory in all aspects. A method that is computationally efficient, relatively robust and powerful, and flexible enough to allow covariate adjustment and application to correlated microbiome data is still lacking in the field. In this project, we propose a linear regression framework for differential abundance analysis (LinDA) to fill the methodological gap. LinDA involves three simple steps that can be carried out efficiently. First, it runs linear regressions using the CLR transformed taxa data as the response. Then it identifies a bias term due to the compositional effect and corrects for the bias using the mode of the regression coefficients across different taxa. Finally, it computes the p-values based on the bias-corrected regression coefficients and applies the BH procedure to control the FDR. We rigorously prove the asymptotic FDR control of the proposed method, making it the first procedure that enjoys a theoretical FDR control guarantee. Our approach is related to ANCOM-BC but differs in several aspects. (i) Our derivation provides a clear interpretation of the bias term and suggests a simple way to correct it. (ii) Our procedure does not involve the EM-algorithm and can be 100–1000 times faster than ANCOM-BC in our numerical studies. (iii) Our method can be directly extended to the mixed-effect models.

Longitudinal and repeated measurement-based microbiome studies have been increasingly common (Faust et al., 2015; Lewis et al., 2015) but statistical tools for correlated microbiome data analysis remain scarce. LinDA can analyze the correlated microbiome data using the classic linear mixed effects models. Through extensive simulation studies and real data analyses, we show that the new method outperforms the state-of-the-art approaches in terms of FDR control and power.

The rest of this chapter is organized as follows. Section 3.2 introduces the proposed method, including the log linear model for differential abundance analysis, its estimation method, and the testing procedure. The main theoretical result on the asymptotic FDR control of the proposed method is presented in Section 3.3. The practical performance of the proposed method illustrated via simulation studies and real data applications can be respectively found in Sections 3.4 and 3.5. The main contributions of this project are summarized in Section 3.6 with some concluding remarks. Technical details, as well as additional results of simulation and real data applications, are provided in Appendix B.

3.2 Methodology

3.2.1 Setup

Throughout this chapter, we use C, C_1, and C_2 to denote positive constants, which can be different from line to line. The notations in this chapter are consistent with the notations in Appendix B.

As summarized in the introduction, there are two ways to tackle the compositional effects in differential abundance analysis, namely normalization and log-ratio transformation. In this project, we adopt the CLR transformation and develop a bias-correction procedure to address the compositional effects. Denote the absolute abundance and the observed read count of the ith taxon in the sth sample by X_{is} and Y_{is}, respectively. For the sth sample, the total read count of all taxa, $N_s = \sum_{i=1}^{m} Y_{is}$, is determined by the sequencing depth and DNA materials. Given N_s, it is natural

to model the stratified count data over m taxa through a multinomial distribution as

$$P(Y_{1s} = y_{1s}, \ldots, Y_{ms} = y_{ms}) = \frac{N_s!}{\prod_{i=1}^{m} y_{is}!} \prod_{j=1}^{m} \left(\frac{X_{js}}{\sum_{i=1}^{m} X_{is}} \right)^{y_{js}} \tag{3.1}$$

Under (3.1), we have

$$\log \left(\frac{Y_{is}}{\sum_{j=1}^{m} Y_{js}} \right) = \log \left(\frac{X_{is}}{\sum_{j=1}^{m} X_{js}} \right) + e_{is}, \tag{3.2}$$

where e_{is} denotes the estimation error, which is expected to diminish as N_s gets large.

3.2.2 OLS estimation

We consider the log linear model on the absolute abundance

$$\log (X_{is}) = u_s \alpha_i + (1, \mathbf{c}_s^\top) \boldsymbol{\beta}_i + \epsilon_{is}, \tag{3.3}$$

where $\mathbf{c}_s = (c_{s1}, ..., c_{sd})^\top$ is the d-dimensional covariates to be adjusted, u_s is the variable of interest, and ϵ_{is} is the error term. Our goal is to discover taxa that are differentially abundant with respect to u_s. Statistically, we want to simultaneously test the following m hypotheses

$$H_{0,i} : \alpha_i = 0 \text{ versus } H_{a,i} : \alpha_i \neq 0.$$

Set $\varepsilon_{is} = \epsilon_{is} + e_{is}$. Under (3.2) and (3.3), the CLR-transformed data satisfies the following linear model

$$\begin{aligned} W_{is} :&= \log \left\{ \frac{Y_{is}}{(\prod_{j=1}^{m} Y_{js})^{1/m}} \right\} = \log \left(\frac{Y_{is}}{\sum_{k=1}^{m} Y_{ks}} \right) - \frac{1}{m} \sum_{j=1}^{m} \log \left(\frac{Y_{js}}{\sum_{k=1}^{m} Y_{ks}} \right) \\ &= \log(X_{is}) - \frac{1}{m} \sum_{j=1}^{m} \log(X_{js}) + e_{is} - \frac{1}{m} \sum_{j=1}^{m} e_{js} \\ &= u_s (\alpha_i - \bar{\alpha}) + (1, \mathbf{c}_s^\top) \left(\boldsymbol{\beta}_i - \bar{\boldsymbol{\beta}} \right) + \varepsilon_{is} - \bar{\varepsilon}_s, \end{aligned} \tag{3.4}$$

where $\bar{\alpha} = m^{-1}\sum_{i=1}^{m}\alpha_i$, $\bar{\boldsymbol{\beta}} = m^{-1}\sum_{i=1}^{m}\boldsymbol{\beta}_i$, and $\bar{\varepsilon}_s = m^{-1}\sum_{i=1}^{m}\varepsilon_{is}$. From (3.4), we can see that the OLS estimator for α based on the CLR transformed data is biased with the bias term being $\bar{\alpha}$. Let $\bar{\alpha}_i = \alpha_i - \bar{\alpha}$, $\bar{\boldsymbol{\beta}}_i = \boldsymbol{\beta}_i - \bar{\boldsymbol{\beta}}$, $\bar{\varepsilon}_{is} = \varepsilon_{is} - \bar{\varepsilon}_s$, and $\bar{\sigma}_i^2 = \text{var}(\bar{\varepsilon}_{is})$. Denote by $\tilde{\alpha}_i$, $\tilde{\boldsymbol{\beta}}_i$, and $\hat{\sigma}_i^2$ the OLS estimators of $\bar{\alpha}_i$, $\bar{\boldsymbol{\beta}}_i$, and $\bar{\sigma}_i^2$, respectively. We then have

$$(\tilde{\alpha}_i, \tilde{\boldsymbol{\beta}}_i^\top)^\top = \left(\sum_{s=1}^{n}\mathbf{z}_s\mathbf{z}_s^\top\right)^{-1}\left(\sum_{s=1}^{n}\mathbf{z}_s W_{is}\right), \quad \hat{\sigma}_i^2 = \frac{1}{n-d-2}\sum_{s=1}^{n}\left\{W_{is} - \left(\tilde{\alpha}_i, \tilde{\boldsymbol{\beta}}_i^\top\right)\mathbf{z}_s\right\}^2, \tag{3.5}$$

where $\mathbf{z}_s = (u_s, 1, \mathbf{c}_s^\top)^\top$. We respectively let $\text{var}_{\mathbf{z}}(\cdot)$ and $\text{cov}_{\mathbf{z}}(\cdot,\cdot)$ denote the variance and covariance computed conditional on $\mathbf{z}_1, ..., \mathbf{z}_n$ respectively. It can be shown that

$$\begin{aligned}
\text{var}_{\mathbf{z}}(\tilde{\alpha}_i) &= \hat{\rho}n^{-1}\bar{\sigma}_i^2 = \hat{\rho}n^{-1}m^{-1}\left\{(m-2)\sigma_i^2 + m^{-1}\sum_{i=1}^{m}\sigma_i^2\right\}, \\
\text{cov}_{\mathbf{z}}(\tilde{\alpha}_i, \tilde{\alpha}_j) &= \hat{\rho}n^{-1}m^{-1}\left\{-(\sigma_i^2 + \sigma_j^2) + m^{-1}\sum_{i=1}^{m}\sigma_i^2\right\}, \quad \text{for } i \neq j,
\end{aligned}$$

where $\hat{\rho}$ is the $(1,1)$th element of $(n^{-1}\sum_{s=1}^{n}\mathbf{z}_s\mathbf{z}_s^\top)^{-1}$.

3.2.3 Bias correction

In many applications, it is reasonable to assume that there is only a small portion of differential taxa, i.e., most α_i's are equal to 0. Under this assumption, as $\tilde{\alpha}_i$ is an unbiased estimator for $\bar{\alpha}_i = \alpha_i - \bar{\alpha}$, the mode of $\tilde{\alpha}_i$ is expected to be close to $-\bar{\alpha}$. This observation motivates us to estimate $-\bar{\alpha}$ by

$$-\tilde{\alpha} = \frac{\widehat{\text{mode}}(\{\sqrt{n}\tilde{\alpha}_i\}_{i=1}^m)}{\sqrt{n}}, \quad \text{where} \quad \widehat{\text{mode}}(\{\sqrt{n}\tilde{\alpha}_i\}_{i=1}^m) = \arg\max_{x\in\mathbb{R}}\frac{1}{mh}\sum_{i=1}^{m}K\left(\frac{x-\sqrt{n}\tilde{\alpha}_i}{h}\right). \tag{3.6}$$

In (3.6), K is a non-negative even function with $\int_{-\infty}^{\infty} K(y)dy = 1$, and h is the bandwidth parameter. Under some regular conditions, we have

$$\sqrt{n}(\tilde{\alpha} - \bar{\alpha}) = o_{\mathbb{P}}(1)$$

as $m, n \to \infty$ (see the appendices for the proof). Therefore, one can estimate α_i by the bias-corrected estimator $\hat{\alpha}_i = \tilde{\alpha}_i + \tilde{\alpha}$.

3.2.4 Testing procedure

To construct a statistic for testing $H_{0,i}$, we need to find a proper estimator for the variance of $\hat{\alpha}_i$. To this end, we note that

$$\text{var}_{\mathbf{z}}(\hat{\alpha}_i) = \text{var}_{\mathbf{z}}(\tilde{\alpha}_i) + \text{var}_{\mathbf{z}}(\tilde{\alpha}) + 2\text{cov}_{\mathbf{z}}(\tilde{\alpha}_i, \tilde{\alpha}).$$

Since $\text{var}_{\mathbf{z}}(\tilde{\alpha}_i) = \hat{\rho}\bar{\sigma}_i^2/n$, it dominates $\text{var}_{\mathbf{z}}(\tilde{\alpha})$ and $\text{cov}_{\mathbf{z}}(\tilde{\alpha}_i, \tilde{\alpha})$ as $n, m \to \infty$ under mild conditions. Thus, we estimate the variance of $\hat{\alpha}_i$ by $\hat{\rho}\hat{\sigma}_i^2/n$. As shown in the next section, the studentized statistic $T_i := \sqrt{n}\hat{\alpha}_i/\sqrt{\hat{\rho}\hat{\sigma}_i^2}$ is asymptotically normal. However, for small sample, we found that t distribution provides a better approximation to the sampling distribution of T_i. We define the p-value for testing $H_{0,i}$ as

$$p_i = 2F_{n-d-2}\left(-|T_i|\right), \tag{3.7}$$

where $F_{n-d-2}(\cdot)$ denotes the cumulative distribution function of t distribution with $n-d-2$ degrees of freedom. Based on the above p-values, we can use the BH procedure to control the FDR. Our algorithm is summarized as the following Algorithm 3.

Algorithm 3. *Linear model for differential abundance analysis (LinDA).*

1. *Step 1: Run OLS based on the CLR transformed observations and calculate $\tilde{\alpha}_i$ and $\hat{\sigma}_i^2$ as in (3.5).*

2. *Step 2: Compute the bias-corrected estimates $\hat{\alpha}_i = \tilde{\alpha}_i + \tilde{\alpha}$ with $\tilde{\alpha}$ defined in (3.6).*

3. *Step 3: Calculate the p-values as in (3.7) and run the BH procedure.*

Remark 2. Built upon the linear regression framework, our method could be easily extended to the mixed-effect model:

$$\log(X_{is}) = u_s\alpha_i + (1, \mathbf{c}_s^\top)\boldsymbol{\beta}_i + \mathbf{r}_s^\top\boldsymbol{\gamma}_i + \varepsilon_{is},$$

where $\boldsymbol{\gamma}_i$ is the random effect and $\mathbf{r}_s$ is the corresponding design. Mixed effects can be used to analyze correlated microbiome data from studies involving replicates or spatial sampling as well as family-based and longitudinal microbiome studies. We suggest using the R function `lmer` to estimate the parameters for the CLR-transformed data. Denote by $\tilde{\alpha}_{i,\text{lmer}}$, $\hat{\sigma}^2_{i,\text{lmer}}$, and $\text{df}_{i,\text{lmer}}$ the estimations for $\bar{\alpha}_i$, the variance of $\tilde{\alpha}_{i,\text{lmer}}$, and the degrees of freedom of $\tilde{\alpha}_{i,\text{lmer}}$ from the `lmer` function. We compute the bias-corrected estimates $\hat{\alpha}_{i,\text{lmer}} = \tilde{\alpha}_{i,\text{lmer}} + \tilde{\alpha}_{\text{lmer}}$, where $\tilde{\alpha}_{\text{lmer}}$ is obtained as the same procedure used in (3.6). Similarly, we let $T_{i,\text{lmer}} = \hat{\alpha}_{i,\text{lmer}}/\hat{\sigma}_{i,\text{lmer}}$ and $p_{i,\text{lmer}} = 2F_{\text{df}_{i,\text{lmer}}}(-|T_{i,\text{lmer}}|)$. The BH procedure on $p_{i,\text{lmer}}$ is finally used to control the FDR.

Remark 3. Compared to the existing methods based on either normalization or CLR transformation, our method is computationally much more efficient and can be easily scaled to problems with tens of thousands of taxa. Table 3.1 compares the computation time of LinDA and ANCOM-BC based on simulated datasets. We observe that our method is 100–1000 times faster than ANCOM-BC. We also tested on a massive dataset of the similar scale of the AmericanGut project (McDonald et al., 2018) ($m = 5000$ and $n = 10000$). ANCOM-BC completed the analysis in 85 minutes compared to 28 seconds for our method (see the column of S0C0 in Table 3.1). Large-scale microbiome studies have been increasingly common to overcome the large inter-subject variability, making our method practically useful for the analysis of big microbiome datasets.

3.3 Asymptotic FDR control

Suppose the target FDR controlling level is q. The BH procedure is equivalent to finding the smallest t^* such that $\widehat{\text{FDP}}(t^*) \leq q$, where

$$\widehat{\text{FDP}}(t) = \frac{2mF_{n-d-2}(-t)}{\sum_{i=1}^{m} \mathbb{I}\left(\sqrt{n}|\hat{\alpha}_i|/\sqrt{\hat{\rho}\hat{\sigma}_i^2} > t\right)}.$$

To show the asymptotic FDR control as $m, n \to \infty$, we take a Bayesian perspective by assuming that the parameters α_i's are independently generated from a common distribution. The key result is summarized in the following theorem.

Theorem 2. *Let ρ be the $(1,1)$th element of $\{\mathbb{E}(\mathbf{z}_s\mathbf{z}_s^\top)\}^{-1}$. Suppose the following conditions are satisfied:*

(i) $\mathbf{z}_s$'s are i.i.d.; u_s and $c_{sa}, a = 1, ..., d$, are sub-Gaussian; $\sigma_{min}\{\mathbb{E}(\mathbf{z}_s\mathbf{z}_s^\top)\} > C$, where $\sigma_{min}(\mathbf{A})$ represents the minimum eigenvalue of a matrix $\mathbf{A}$.

(ii) σ_i's are i.i.d. and $\mathbb{P}(C_1 < \sigma_i < C_2) = 1$.

(iii) $\varepsilon_{is}/\sigma_i \sim^{i.i.d.} \mathcal{E} =^d N(0,1)$ for $i = 1, ..., m$ and $s = 1, ..., n$.

(iv) α_i's are i.i.d.

(v) $\mathbf{z}_s, \sigma_i, \varepsilon_{is}/\sigma_i$, and α_i for $i = 1, ..., m$ and $s = 1, ..., n$ are mutually independent.

(vi) Denote by $f_n(\cdot; a)$ the density function of $\sqrt{n}\alpha_i + \sqrt{a}\varepsilon_{is}$ for any $a > 0$. For large enough n, the density $f_n(\cdot; \rho)$ has a unique mode at 0, i.e., $\arg\max_{x\in\mathbb{R}} f_n(x; \rho) = 0$; for any $\epsilon > 0$, there exists a $\delta > 0$ such that $\min_n \inf_{|x|>\epsilon} |f_n(x; \rho) - f_n(0; \rho)| > \delta$.

(vii) The Fourier transform $k(u) = \int_{-\infty}^{\infty} e^{-\imath uy} K(y)dy$ is absolutely integrable, where $\imath = \sqrt{-1}$ is the imaginary unit.

(viii) $h = o(1)$ and $1/(mh^2) = o(1)$.

(ix) $m = o(e^{Cn})$.

(x) Let $S_{\infty,n}(t) = \mathbb{P}(|\mathcal{E} + \sqrt{n}\alpha_i/\sqrt{\rho\sigma_i^2}| > t)$. There exists t_0 such that for large enough n, $2F_{n-d-2}(-t_0)/S_{\infty,n}(t_0) \leq q$.

Let

$$\textit{FDR}_{m,n}(t) = \mathbb{E}\left\{ \frac{\sum_{i:\alpha_i=0} \mathbb{I}\left(|\sqrt{n}\hat{\alpha}_i|/\sqrt{\hat{\rho}\hat{\sigma}_i^2} > t\right)}{1 \vee \sum_{i=1}^{m} \mathbb{I}\left(|\sqrt{n}\hat{\alpha}_i|/\sqrt{\hat{\rho}\hat{\sigma}_i^2} > t\right)} \right\}.$$

Under the above conditions, we have

$$\limsup_{m\to\infty, n\to\infty} \textit{FDR}_{m,n}(t^*) \leq q.$$

Conditions (i)–(v) help prove the consistency of the variance estimators and the mode of the regression coefficients. By assuming that the errors follow the normal distributions (Condition (iii)), we can integrate all the relevant covariate information in a single parameter $\hat{\rho}$, which facilitates the establishment of the consistency of the kernel density estimation and hence the estimator of mode. In the simulation studies, we also investigated the scenario of non-normal distribution. We use an example to illustrate Condition (vi). In particular, we assume that $\sqrt{n}\alpha_i$ follows a discrete distribution with $\mathbb{P}\{\sqrt{n}\alpha_i = a_{n,l}\} = \pi_l$ for $l = 0, 1$, where $a_{n,0} = 0$, $a_{n,1} \neq 0$, $\pi_l > 0$, and $\pi_0 + \pi_1 = 1$. To reflect the sparsity, π_0 is set to be 0.8. We choose $a_{n,1} = 2$ and 5 representing weak and strong signals, respectively. We consider two cases for the error variance: (i) $\sigma_i = 1$; (ii) $\sigma_i \sim \text{IG}(a, b)$, i.e., σ_i follows the inverse-gamma distribution with the shape parameter a and scale parameter b. As seen from Figure 3.1, when the signal strength is weak, the mode of $\sqrt{n}\alpha_i + \sqrt{\rho}\varepsilon_{is}$ slightly deviates from 0 as the blue curve in the left panel indicates. For strong signals, the mode is exactly equal to zero. As shown in Parzen (1962), Condition (vii) is fulfilled by many commonly used kernels such as the Gaussian kernel and the uniform kernel on $[-1, 1]$. Condition (ix) allows the number of taxa to be exponentially larger than the sample size. Condition (x) ensures the existence of a cut-off value to control the FDR at level q. A similar assumption was imposed in Theorem 4 of Storey et al. (2004).

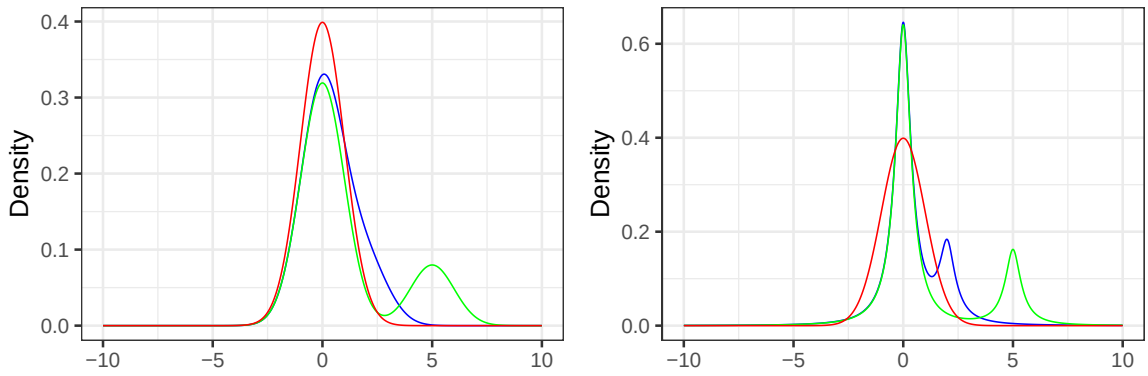

Figure 3.1: Density of $\sqrt{n}\alpha_i + \varepsilon_{is}$. The panels on the left and right correspond to $\sigma_i = 1$ and $\sigma_i \sim \text{IG}(2, 1)$ respectively, where IG denotes the inverse-gamma distribution. The red curve is the density of the standard normal distribution. The blue and green curves are the densities of $\sqrt{n}\alpha_i + \varepsilon_{is}$ with $\mathbb{P}(\sqrt{n}\alpha_i = 0) = 0.8$ and $\mathbb{P}(\sqrt{n}\alpha_i = 2) = 0.2$, and $\mathbb{P}(\sqrt{n}\alpha_i = 0) = 0.8$ and $\mathbb{P}(\sqrt{n}\alpha_i = 5) = 0.2$, respectively.

3.4 Numerical studies

3.4.1 Setups

We conducted comprehensive simulations to evaluate the performance of the proposed method under different setups. We set $m = 500$ as the baseline for the number of taxa, which is similar to the number of tests at the species level for a typical microbiome study. We investigated the sample size $n = 50,\ 200$ representing small and large sample size, respectively. More combinations of m and n were also studied as the variational settings. We simulated two levels of signal density (i.e., percentage of differential taxa) γ = 5%, 20%, roughly corresponding to sparse and dense signals. These differential taxa were randomly drawn from the entire set. Let $H_i = 0$ if the ith taxon is differentially abundant and $H_i = 1$ otherwise. The underlying truth H_i was simulated from

$$H_i \sim^{\text{i.i.d.}} \text{Bernoulli}(\gamma).$$

We assume that the baseline absolute abundance $X_{is}^{(0)}$ follows

$$\log\left(X_{is}^{(0)}\right) \sim^{\text{i.i.d.}} N\left(\beta_i^{(0)}, \sigma_i^2\right),$$

and generate the absolute abundance X_{is} based on

$$\log(X_{is}) \sim^{\text{i.i.d.}} N\left(\beta_i^{(0)} + u_s\alpha_i + \mathbf{c}_s^\top \boldsymbol{\beta}_i^{-(0)}, \sigma_i^2\right),$$

where $\boldsymbol{\beta}_i^{-(0)}$ represents the coefficients of the confounders. Let

$$\pi_{is} = \frac{X_{is}}{\sum_{j=1}^m X_{js}}.$$

The observed OTUs data were simulated by

$$(Y_{1s}, \ldots, Y_{ms}) \sim^{\text{i.i.d.}} \text{Multinomial}(N_s, \pi_{1s}, \ldots, \pi_{ms}).$$

To create a power curve, we included six effect sizes labeled as $\{1, 2, ..., 6\}$ in the figures. We make the effect sizes have the same signs for differential taxa (i.e., the differential taxa have the same direction of change), creating a relatively strong compositional effect. Since low-abundance taxa have much less statistical power, we up-weighted their effects so that the power will not be dominated by those abundant ones. Specifically, for a randomly drawn differential taxon i, we set

$$\alpha_i = \log(2\mu)\mathbb{I}\left(\bar{\pi}_i^{(0)} > 0.005\right) + \log\left\{2\mu\left(0.005/\bar{\pi}_i^{(0)}\right)^{\frac{1}{3}}\right\}\mathbb{I}\left(\bar{\pi}_i^{(0)} \leq 0.005\right) \text{ for } n = 50,$$
$$\alpha_i = \log(\mu)\mathbb{I}\left(\bar{\pi}_i^{(0)} > 0.005\right) + \log\left\{\mu\left(0.005/\bar{\pi}_i^{(0)}\right)^{\frac{1}{3}}\right\}\mathbb{I}\left(\bar{\pi}_i^{(0)} \leq 0.005\right) \text{ for } n = 200,$$

where μ is equally spaced on $[1.05, 2]$, $\bar{\pi}_i^{(0)} = \sum_{s=1}^n \pi_{is}^{(0)}/n$ and $\pi_{is}^{(0)} = X_{is}^{(0)}/(\sum_{j=1}^m X_{js}^{(0)})$. We considered three cases for the covariate and confounders:

C0. $u_s \sim^{\text{i.i.d.}} \text{Bernoulli}(1/2)$ and no confounder.

C1. $u_s \sim^{\text{i.i.d.}} N(0,1)$ and no confounder.

C2. $u_s \sim$ Bernoulli$(\{1+\exp(-0.5c_{s1}-0.5c_{s2})\}^{-1})$ independently, where c_{s1} and c_{s2} are confounders ($\mathbf{c}_s = (c_{s1}, c_{s2})^\top$), c_{s1} independently and identically follows the Rademacher distribution and $c_{s2} \sim^{\text{i.i.d.}} N(0,1)$. Let $\boldsymbol{\beta}^{(1)} \sim N(\mathbf{1}, \mathbf{I}_m)$ and $\boldsymbol{\beta}^{(2)} \sim N(\mathbf{2}, \mathbf{I}_m)$, then $\boldsymbol{\beta}_i^{-(0)} = (\beta_i^{(1)}, \beta_i^{(2)})^\top$, where $\beta_i^{(1)}$ and $\beta_i^{(2)}$ are the ith elements of $\boldsymbol{\beta}^{(1)}$ and $\boldsymbol{\beta}^{(2)}$ respectively.

The parameters $\beta_i^{(0)}$, σ_i^2 and N_s were estimated based on a real dataset (COMBO) from the study of the gut microbiota in a general population (Wu et al., 2011), which consists of 98 samples and 6674 taxa. We only used its 500 most abundant taxa. Since $\beta_i^{(0)}$ and σ_i^2 were not directly estimable using the relative abundance data, we estimated $\beta_i^{(0)} - \beta_j^{(0)}$ and $\sigma_i^2 + \sigma_j^2$ based on the pairwise log ratios, forced some $\beta_i^{(0)}$'s to be zeros to obtain the estimations of $\beta_1^{(0)}, ..., \beta_m^{(0)}$, and derived σ_i^2 from the values of $\{\sigma_i^2 + \sigma_j^2\}_{i,j}$. We assume that the library size for each sample follows the negative binomial distribution

$$N_s \sim^{\text{i.i.d.}} \text{NB}(7645, 5.3),$$

where the mean and dispersion parameters were estimated based on the combo data. The resulting sparsity (percent of zeros) of the count matrix is around 65%–75%.

In addition to the basic setting (denoted as S0), we investigated other settings to study the robustness of the proposed method. Specifically, on top of S0 and C0, we studied

S1. *Zero inflated absolute abundances.* The microbiome data contains excessive zeros and most of the zeros in the microbiome data can be explained by insufficient sampling (Silverman et al., 2020) since majority of the taxa are of low-abundance. However, it is also possible that zeros are due to physical absence of the taxa (Kaul et al., 2017). To study the effect of zero inflation on differential abundance analysis, we randomly forced 30% of the absolute abundance data to be 0.

S2. *Correlated absolute abundances.* Existing differential abundance analysis methods assume independence among taxa. However, in practice, taxa are interconnected forming networks

(Kurtz et al., 2015). It is interesting to see if the methods compared are robust to the correlations among the taxa. We simulated block-correlation structure by dividing the 500 taxa into 25 equal-sized blocks. Within each block, we further divided the block into 2 by 2 sub-blocks and simulated equal positive correlations (0.5) within each sub-block and equal negative correlations (-0.5) between the two sub-blocks. This mimics the scenario that there are mutualistic relationships within the group and competitive relationships between groups.

S3. *Gamma abundance distribution.* Although the log normal distribution has been widely used for modeling species abundance data, other models such as gamma distribution are also possible (Connolly et al., 2014). We thus did additional simulation studies using the gamma distribution. Let $X_{is}^{(0)} \sim^{\text{i.i.d.}} \text{Gamma}(\eta_i^{(0)}, 1)$ and $X_{is} \sim^{\text{i.i.d.}} \text{Gamma}(\eta_i^{(0)} \exp(u_s\alpha_i + \mathbf{c}_s^\top \boldsymbol{\beta}_i^{-(0)}), 1)$. Similarly, we estimated $\eta_i^{(0)}$ from the COMBO data, where we first estimated the baseline proportion $\pi_i^{(0)}$ based on the Dirichlet-multinomial distribution using the R function `dirmult` and set the over-dispersion parameter $\theta^{(0)}$ to be 0.003, then let $\eta_i^{(0)} = \pi_i^{(0)}(1/\theta^{(0)} - 1)$.

S4. *Smaller m.* In microbiome data, each taxon can be assigned a taxonomic lineage and taxa abundances can be aggregated at different taxonomic ranks. Differential abundance analysis at higher ranks such as family and genus is also routinely performed. At the higher ranks, the number of taxa is much smaller. We thus studied a small number of taxa ($m = 50$) to see if the proposed method is robust to a small m. We randomly chose 50 elements from $\boldsymbol{\beta}^{(0)} = (\beta_1^{(0)}, ..., \beta_{500}^{(0)})^\top$ and $\boldsymbol{\sigma}^2 = (\sigma_1^2, ..., \sigma_{500}^2)^\top$ in each simulation run. We set $N_s \sim \text{NB}(1500, 5.3)$.

S5. *Smaller n.* In pilot microbiome studies, the sample sizes are usually small. It is interesting to study the performance of the methods at a much smaller sample size. We studied $n = 20,\ 30$ and used the same effect size as $n = 50$.

S6. *10-fold difference in library size.* When the microbiome samples are not fully randomized in sequencing, it is likely that samples of the two groups end up in two separate sequencing

runs leading to very different library sizes for the two groups. Since the presence/absence of a taxon strongly depends on the library size, the differential library size will confound the two-sample comparison, especially for those rare taxa (Weiss et al., 2017). To create differential library sizes, we generated the library size from $N_s \sim \text{NB}(5000, 5.3)$ and $N_s \sim \text{NB}(50000, 5.3)$ for the two groups, respectively.

S7. *Mixed-effect model.* We considered two scenarios: *Pre-treatment and post-treatment comparison* (S7.1) and *Replicate sampling* (S7.2). Under S7.1, for $n = 50\ (200)$, we simulate $25\ (100)$ subjects and each has paired pre-treatment and post-treatment samples. The aim is to detect taxa affected by treatment. Under S7.2, each subject is subject to multiple measurements. For $n = 50\ (200)$, we simulate 25 (50) subjects with each having 2 (4) replicates. Specifically, we let

$$\log(X_{is}) \sim \mathbf{r}_s^\top \boldsymbol{\gamma}_i + N(\beta_i^{(0)} + u_s \alpha_i + \mathbf{c}_s^\top \boldsymbol{\beta}_i^{-(0)}, \sigma_i^2),$$

where $\mathbf{r}_s$ has one element equal to 1 and all other elements equal to 0 indicating the subject ID of sample s and the elements of $\boldsymbol{\gamma}_i$ follow $N(0, \tau_i^2)$ independently, where we let $\tau_i^2 = a_i \sigma_i^2$ with $a_i \sim \text{Unif}([0, 1])$.

3.4.2 Competing methods

We compared our method with ANCOM-BC, ALDEx2, DESeq2, EdgeR, and MetagenomeSeq. For DESeq2 and EdgeR, we replaced their native normalization methods with GMPR normalization, which was shown to improve the power and false positive control in differential abundance analysis (Chen et al., 2018). For MetagenomeSeq, there are two implementations, `fitZig` and `fitFeatureModel`, in the R Bioconductor package `metagenomeSeq`. Currently, `fitFeatureModel` is only applicable to binary covariate case (C0). We use MetagenomeSeq and MetagenomeSeq-2 to denote the `fitFeatureModel` and `fitZig` procedures, respectively. We also compared to the standard non-parametric methods: Wilcoxon rank sum test for case C0 and Spearman correlation test for case C1, both with the GMPR normalized data.

For the proposed method, we considered two zero-handling approaches. The first approach adds a pseudo count of 0.5 to all the counts, which is widely used in microbiome data analysis on the log scale. However, it has been shown to be problematic under certain situations (Brill et al., 2020). We thus designed a new imputation-based approach, where we imputed the zeros by $N_s/(\max_{k:Y_{ik}=0} N_k)(i = 1, \cdots, m)$. In other words, zeros were treated differently according to the library size of the sample and zeros in the sample with a larger library size were replaced with larger fractions. The purpose of the imputation approach is to reduce false positives when the library size is correlated with the variable of interest. As shown in the simulation studies, the pseudo-count approach worked sufficiently well in most settings except the setting S6, where the library size between the groups differed by 10 folds. In contrast, the imputation approach reduced the false positive rate extensively for the setting S6 (Appendix Figure B.1). However, it was slightly less powerful than the pseudo-count approach when the library size was a not confounder (Appendix Figure B.2). Thus, in the implementation, we used an adaptive approach: we first test the association between the variable of interest and the library size. If the p-value is smaller than 0.1, we use the imputation approach conservatively; otherwise, we use the pseudo-count approach. Appendix Figures B.1 and B.2 show that the adaptive method controls the false positives when the library sizes are very different among groups while retaining the power when the library sizes are similar.

The proposed LinDA method can be viewed as a three-step procedure: CLR+OLS+BC (BC stands for bias correction), which can be easily extended to the linear mixed effects model setting using CLR+LMM+BC (LMM stands for linear mixed-effect model). In the setting S7 (correlated microbiome data), we compared CLR+LMM+BC to CLR+OLS+BC, CLR+OLS and CLR+LMM to demonstrate the utility of LinDA for correlated microbiome data analysis.

3.4.3 Simulation results

First, we found that DESeq2, EdgeR and MetagenomeSeq-2 had severe FDR inflation under most settings (Appendix Figure B.3). We thus did not include them in the main comparison and focused on the comparison between LinDA, ANCOM-BC, ALDEx2, MetagenomeSeq and

Wilcoxon. Full results of all methods are available at `https://github.com/zhouhj1994/LinDA-manuscript-result`. We use S0C0 to denote the setting S0 with covariate design C0 and likewise for other setups.

Figure 3.2 and Appendix Figures B.4 and B.5 show the results of the competing methods under the log-normal distribution with three covariate designs: binary covariate (S0C0), continuous covariate (S0C1), and binary covariate with confounders (S0C2), respectively. Generally speaking, LinDA and ANCOM-BC outperform other methods in both the FDR control and power. Under C0 and C2 (binary covariate), both methods control the FDR around the target level, and ANCOM-BC is slightly more powerful than LinDA when the sample size is small. However, under C1 (continuous covariate, Appendix Figure B.4), LinDA controls FDR at the target level at both sample sizes while ANCOM-BC has slight FDR inflation when the sample size is small. LinDA is also slightly more powerful than ANCOM-BC at a small sample size. The Wilcoxon rank sum test based on GMPR normalized data performs well under C0 with slightly inflated FDR at larger effect sizes and reasonable power across settings. In contrast, for a continuous covariate (C1, Appendix Figure B.4), Spearman rank correlation test has a large FDR inflation when the signal is dense. When there are confounders (C2, Appendix Figure B.5), Wilcoxon has severe FDR inflation when the sample size is large due to its inability to adjust for confounders. ALDEx2 is a conservative method, which offers the strongest FDR control but is much less powerful. MetagenomeSeq performs well when the signal is sparse but fails to control the FDR when the signal is dense. We also studied the effect of zero inflation and the correlations among taxa (S1C0 and S2C0, Appendix Figures B.6 and B.7), we observed similar patterns and LinDA and ANCOM-BC had overall the best performance.

Since LinDA assumes a log normal distribution of the absolute abundance, it is interesting to evaluate its performance when the log normal assumption is violated. We thus simulated the absolute abundance data using a gamma distribution (S3C0). Figure 3.3 shows the results. LinDA controls the FDR close to the target level and has the highest power. When the signal is dense (20%), ANCOM-BC has a noticeable FDR inflation while ALDEx2, MetagenomeSeq and Wilcoxon have severe FDR inflation when the signal is dense.

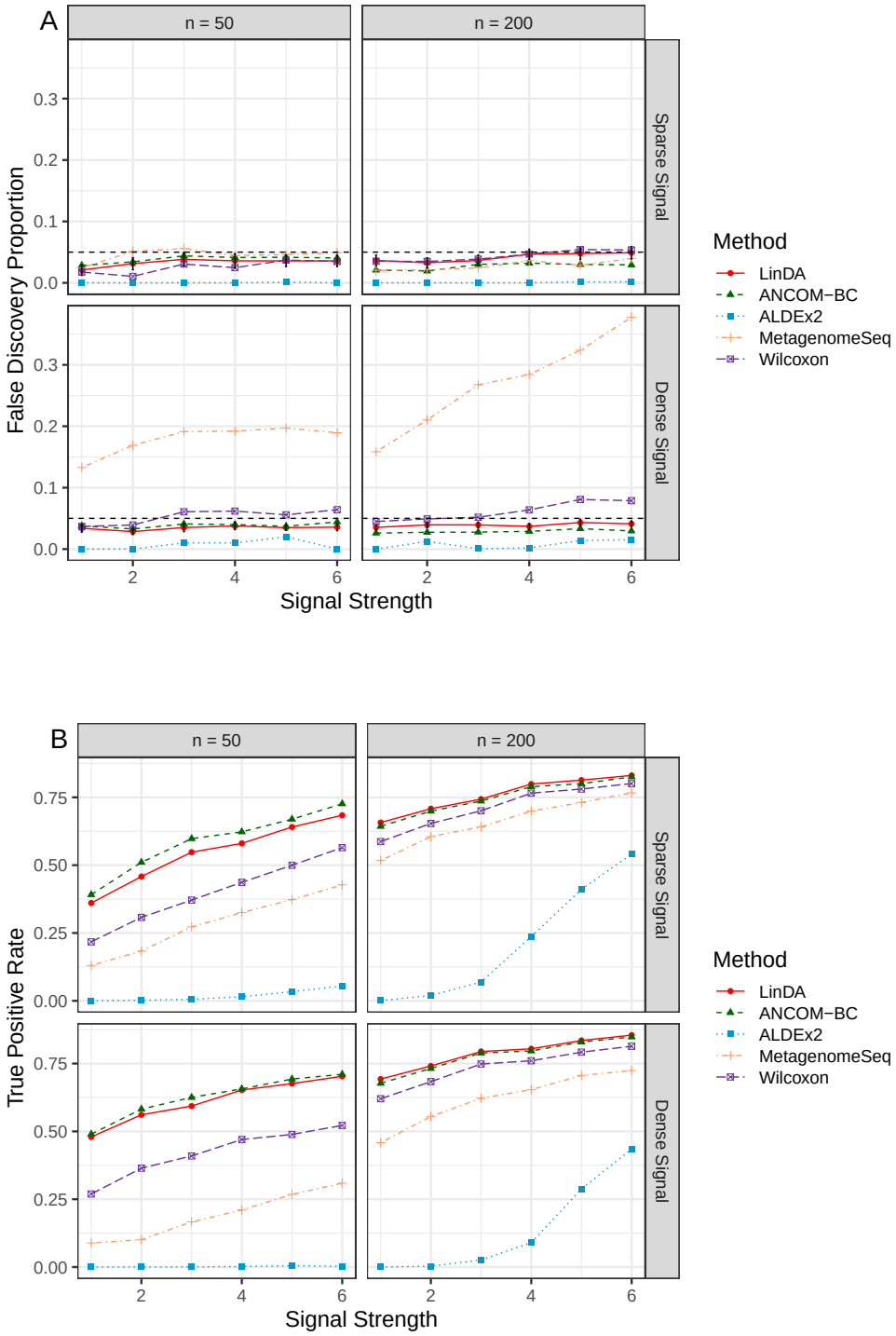

Figure 3.2: Performance comparison (S0C0, log normal distribution for absolute abundances with a binary covariate). False discovery proportions (A) and true positive rates (B) were averaged over 100 simulation runs. Error bars (A) represent the 95% confidence intervals (CIs) of the method LinDA and the dashed horizontal line indicates the target FDR level of 0.05.

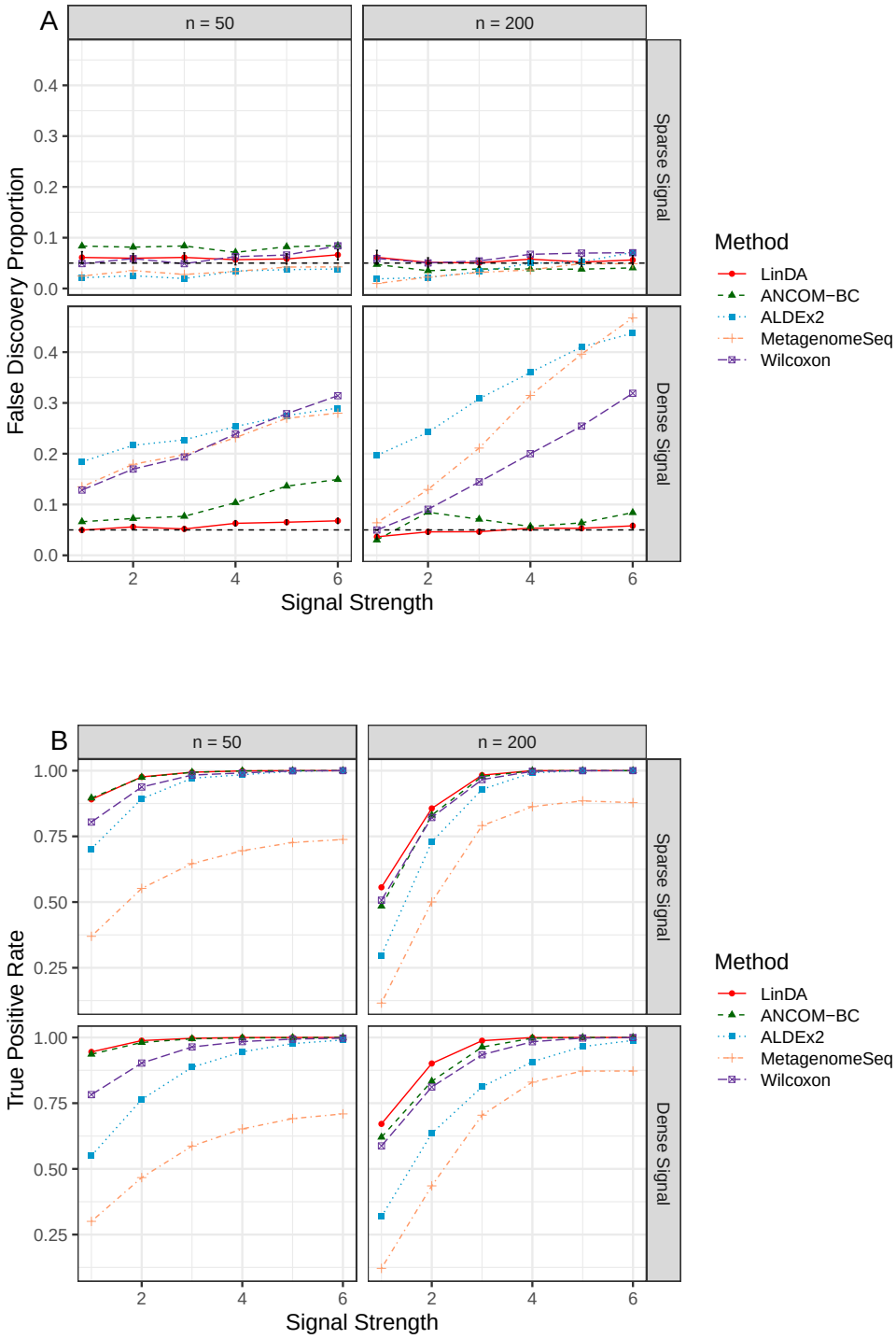

Figure 3.3: Performance comparison (S3C0, gamma distribution for absolute abundances with a binary covariate). False discovery proportions (A) and true positive rates (B) were averaged over 100 simulation runs. Error bars (A) represent the 95% CIs of the method LinDA and the dashed horizontal line indicates the target FDR level of 0.05.

With a smaller number of taxa ($m = 50$, S4C0, Appendix Figure B.8), ANCOM-BC shows the best FDR and power trade-off. LinDA is the most powerful but it has slight FDR inflation. MetagenomeSeq and Wilcoxon controls the FDR when the signal is sparse but are less powerful. When the signal is dense, they could not control the FDR properly. When the sample size is very small ($n = 20,\ 30$, S5C0), LinDA stands out among its competitors: it controls the FDR around the target level and maintains high power (Appendix Figure B.9). ANCOM-BC and MetagenomeSeq have large FDR inflation and the inflation seems to increase with a decreasing sample size. Wilcoxon is much less powerful at small sample sizes and ALDEx2 has virtually no power. Under the setting S6, where the sequencing depth differs by 10 folds, all methods, except our method with adaptive zero-handling approach, fail to control the FDR (Appendix Figure B.10). We point out here that when we implemented ANCOM-BC, we disabled its zero treatment. To further investigate whether its zero treatment option improves its performance, we also run the procedure enabling its zero treatment (zero_cut = 0.9, lib_cut = 1000, struc_zero = TRUE), and found the results were very similar (S6, Appendix Figure B.11).

Finally, we applied LinDA to correlated microbiome data (S7C0), where the competing methods are not applicable to correlated data. Appendix Figures B.12 and B.13 compare the methods CLR+LMM+BC (LinDA-LMM), CLR+OLS+BC (LinDA-OLS), CLR+LMM and CLR+OLS for correlated data. In the setting comparing the pre-treatment and post-treatment samples (S7.1, Appendix Figure B.12), we could clearly see that ignoring the bias tremendously increases the FDR level especially under dense signals (LinDA-LMM vs CLR+LMM). In addition, LinDA-LMM is more powerful than LinDA-OLS due to its ability to exploit the correlation between pre- and post-treatment samples. Under the replicate sampling setting (S7.2, Appendix Figure B.13), we see that the LinDA-OLS has significant FDR inflation by treating the replicate samples as independent. In contrast, LinDA-LMM controls the FDR at the target level.

We summarize the performance comparison in Table 3.2. We can see that LinDA and ANCOM-BC have overall the best performance among the methods evaluated. However, ANCOM-BC is computationally more intensive. As shown in Table 3.1, LinDA could be 100-1000 times faster

Table 3.1: Runtime (in second) comparison under different settings (R version 4.0.3 (2020-10-10); Platform: x86_64-pc-linux-gnu (64-bit); CPU: E5-2670 v2 @ 2.50GHz; Memory: 67.7 GB). The result is based on a one time run. The"elapsed" from the R command `system.time()` was used.

		S0C0		S0C1		S0C2	
		LinDA	ANCOM-BC	LinDA	ANCOM-BC	LinDA	ANCOM-BC
$m = 500$	$n = 200$	0.454	21.835	0.218	22.057	0.206	64.519
	$n = 10000$	6.844	162.218	4.043	163.552	5.073	216.564
$m = 5000$	$n = 200$	1.598	184.972	1.607	162.611	1.615	599.985
	$n = 10000$	28.253	5,135.393	15.314	5,157.148	15.494	5,506.353

Table 3.2: Performance comparison. Three $\star$ represents that the FDR is controlled; two $\star$ represents that the FDR is slightly inflated; one $\star$ represents large FDR inflation and no $\star$ represents severe FDR inflation. Three $\circ$ represents the highest power and no $\circ$ represents very low or no power.

	LinDA	ANCOM-BC	ALDEx2	MetagenomeSeq	Wilcoxon
S0C0	⋆⋆⋆○○○	⋆⋆⋆○○○	⋆⋆⋆○	⋆○○	⋆⋆○○
S0C1	⋆⋆⋆○○○	⋆⋆○○○	⋆⋆⋆○	NA	⋆○○○
S0C2	⋆⋆⋆○○○	⋆⋆⋆○○○	⋆⋆⋆	NA	○○
S1C0	⋆⋆⋆○○○	⋆⋆⋆○○○	⋆⋆⋆○	⋆○○	⋆⋆⋆○○
S2C0	⋆⋆⋆○○○	⋆⋆⋆○○○	⋆⋆⋆○	⋆○○	⋆⋆○○
S3C0	⋆⋆⋆○○○	⋆⋆○○○	⋆○○	⋆○	⋆○○
S4C0	⋆⋆○○○	⋆⋆⋆○○○	⋆⋆⋆○	⋆⋆⋆○○	⋆⋆⋆○○
S5C0	⋆⋆⋆○○○	⋆○○○	⋆⋆⋆	○○	⋆⋆⋆○
S6C0	⋆⋆○○	○○○	⋆○○	○	○○○

	LinDA-LMM	LinDA-OLS	CLR+LMM	CLR+OLS
S7.1C0	⋆⋆⋆○○○	⋆⋆⋆○○	○	⋆○
S7.2C0	⋆⋆⋆○○	⋆○○○	⋆○	○○○

than ANCOM-BC, making LinDA a highly scalable method.

3.5 Real data applications

3.5.1 Datasets

We applied LinDA and the competing methods to three real datasets with independent samples from the studies of C. difficile infection (CDI) (Schubert et al., 2014), inflammatory bowel disease (IBD) (Morgan et al., 2012) and rheumatoid arthritis (RA) (Scher et al., 2013). To demonstrate the use of LinDA to correlated microbiome samples, we applied LinDA to a dataset from the study of the smoking effect on the human upper respiratory tract (SMOKE) (Charlson et al., 2010). We

Table 3.3: Characteristics for four real microbiome datasets. NORA represents new-onset untreated rheumatoid arthritis. The second and the third columns list the number of taxa and sample size of each filtered dataset (prevalence $\geq 10\%$, library size ≥ 1000).

	m	n	u	$\mathbf{c}$
CDI	123	183	CDI/Diarrhea control (94 v.s. 89)	
IBD	579	81	Crohn's disease/Healthy (62 v.s. 19)	Antibiotic use (n/y, 48 + 19 v.s. 14 + 0)
RA	438	72	NORA/Healthy (44 v.s. 28)	
SMOKE	209	132	Smoke (n/y, 67 v.s. 65)	Female/Male (31 + 16 v.s. 36 + 49)

used the microbiome samples from the throat for illustration, where each subject has two samples from the left and right side of the throat. The CDI and RA datasets were provided by the authors while the IBD and the SMOKE datasets were downloaded from the Qiita database (Gonzalez et al., 2018) with the study ID 1460 and 524. All the datasets have binary phenotypes. Antibiotics use is the confounder for the IBD dataset ($p = 0.03$ and OR = 0) while sex is the confounder for the SMOKE dataset ($p = 0.02$ and OR= 2.26). They will be adjusted in methods that are capable of covariate adjustment. We excluded samples with less than 1000 read counts, and taxa which appear in less than 10% samples. The basic characteristics for the four filtered datasets are summarized in Table 3.3. We compared the detection power as well as their overlap patterns for LinDA, ANCOM-BC, Aldex2, MetagenomeSeq and Wilcoxon. Specifically, we compared the number of discoveries at different FDR levels (0.01–0.25) and used Venn diagram to show the overlap at the target FDR of 0.1. We used winsorization at quantile 0.97 to reduce the impact of potential outliers as recommended in Chen et al. (2018).

3.5.2 Results

For the CDI dataset, LinDA made the most discoveries at different FDR levels (Figure 3.4). At 10% FDR, LinDA discovered eight taxa associated with CDI while ANCOM-BC, Aldex2 and Wilcoxon discovered three and MetagenomeSeq discovered two. As discussed in Schubert et al. (2014), subjects with CDI were more likely to have the bacterial family Lachnospiraceae and Erysipelotrichaceae. LinDA found one more taxon belonging to Lachnospiraceae than other methods. Besides, LinDA and Wilcoxon found one differential taxon belonging to Erysipelotrichaceae

while the other three methods did not identify any. For the IBD dataset, LinDA detected a similar number of taxa as ANCOM-BC and more taxa than MetagenomeSeq and Aldex2 at different FDR levels. Wilcoxon rank sum test detected a large number of taxa associated with the disease status, but this could be due to the confounding effects of antibiotics use since it could not adjust for covariates. From Figure 3.5, we observe that most discoveries by LinDA are shared by ANCOM-BC or Wilcoxon. For the RA dataset, LinDA detected a similar number of taxa as ANCOM-BC and more taxa than Wilcoxon, MetegenomeSeq and Aldex2. The differential taxa detected by LinDA and ANCOM-BC are mostly overlapped. Overall, the results are consistent with the simulation studies, where LinDA and ANCOM-BC generally performed the best.

Finally, we applied LinDA-LMM to the SMOKE dataset, where each subject has two replicate samples from the throat. The aim is to identify smoking-associated taxa adjusting for the sex. To account for the correlation between the replicate samples, we included a subject-level random intercept in LinDA-LMM. As a comparison, we also applied LinDA-OLS to the right and left throat samples separately, since LinDA-OLS could not analyze correlated samples. LinDA-OLS based on the left or right throat samples alone discovered 12 and 15 differential taxa at 10% FDR. When both left and right samples were used in LinDA-LMM, 21 differential taxa were identified, covering the majority of the taxa identified based on the left or right throat samples alone (Figure 3.5). In addition, LinDA-LMM detected five taxa, which were missed by analyzing the left or right samples. Therefore, LinDA-LMM provides a convenient way to analyze correlated microbiome datasets and enjoys the power improvement by analyzing all samples together.

Our package `LinDA` provides a function to generate the effect size plot for differential taxa and volcano plot. Appendix Figures B.15–B.18 display the effect size plots and volcano plots for the four datasets. At FDR level of 0.1, we observe that, compared to the diarrheal control group, the C. difficile infection group has two less abundant taxa and six more abundant taxa, while comparing the Crohn's disease group with healthy group, and NORA group with healthy group, we find that most differential taxa are less abundant in the disease group than the healthy group. For SMOKE dataset, around half differential taxa are less abundant and half are more abundannt in the smkoer

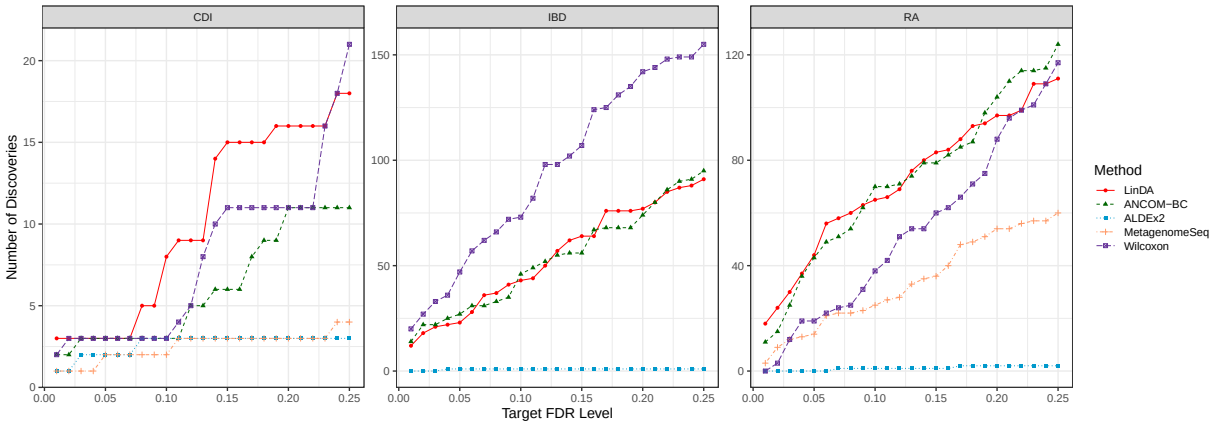

Figure 3.4: Number of discoveries v.s. target FDR level (0.01–0.25)

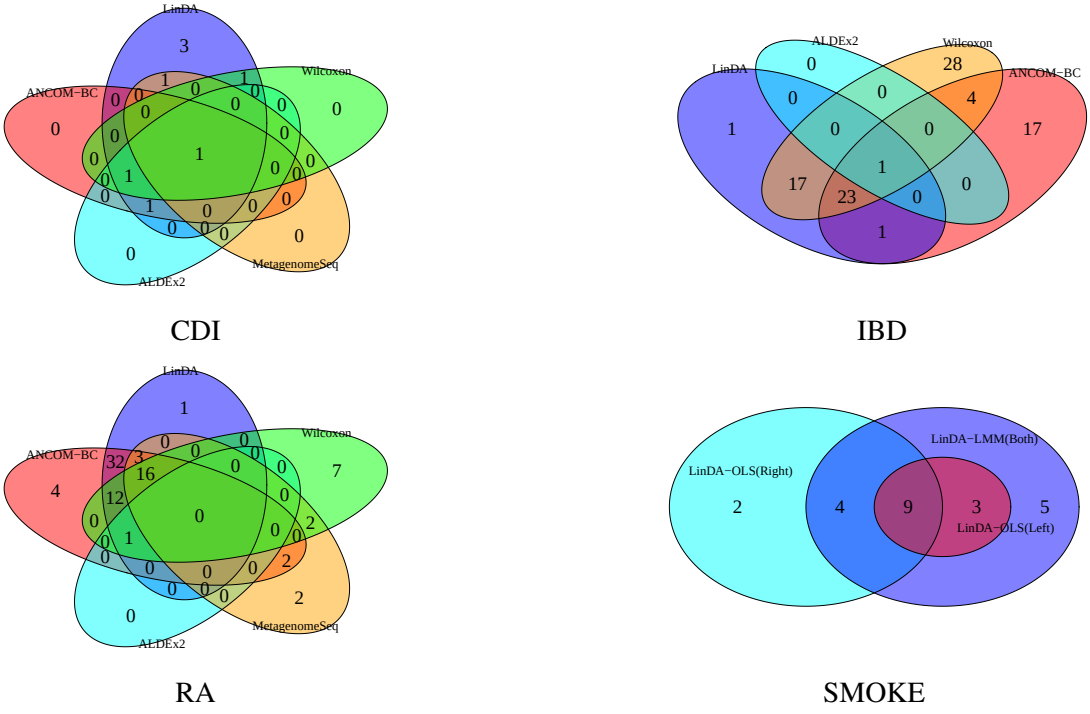

CDI IBD

RA SMOKE

Figure 3.5: Overlap of differential taxa with target FDR level of 0.1.

group compared to the non-smoker group. Therefore, we expect IBD, CDI and RA datasets to have stronger compositional effects than the SMOKE dataset since the changes are more unbalanced. Indeed, the effect size plots, where we plot both the debiased and un-debiased coefficients, revealed larger biases for the IBD, CDI and RA datasets.

3.6 Discussion

Differential abundance analysis is at the core of the statistical analysis of microbiome data. Microbiome data are compositional in nature and all we know are the relative abundances, making the identification of differentially abundant taxa at the ecological site particularly challenging (Gloor et al., 2017; Tsilimigras and Fodor, 2016). Numerous differential abundance analysis methods have been proposed focusing on addressing the compositional effects (Robinson et al., 2010; Love et al., 2014; Chen et al., 2018; Paulson et al., 2013; Sohn et al., 2015; Brill et al., 2020; Fernandes et al., 2014; Mandal et al., 2015; Lin and Peddada, 2020) through either robust normalization or using ratio approaches. Among all the competing methods, ANCOM-BC is the state-of-the-art method, it has been demonstrated to be more robust and powerful than the competing methods. However, there are two drawbacks of ANCOM-BC. First, it is computationally intensive for large-scale microbiome datasets such as the AmericanGut dataset. Due to the huge inter-subject variation, large-scale microbiome studies have been increasingly popular, resulting in larger sample sizes. On the other hand, metagenomic sequencing has become increasingly deeper to have a high resolution view of the microbiome, leading to an unprecedented number of new microbial features. To meet the analysis need for such large-scale datasets, a computationally efficient tool is much needed. Secondly, ANCOM-BC is not applicable to correlated/clustered microbiome datasets such as those from family/longitudinal microbiome studies or studies with paired and repeated measurements (Faust et al., 2015; Lewis et al., 2015). Longitudinal microbiome studies, which enable the study of the trajectory of the microbiome as well as control for potential confounders, has been increasingly employed in human microbiome studies. Unfortunately, statistical tools for longitudinal microbiome studies are scarce. In contrast, LinDA is computationally efficient since it only involves fitting regular linear regression models and could be easily scaled to

hundreds of thousands of taxa. Moreover, the extension of LinDA to linear mixed effects models (LMM) is straightforward and we have highly efficient tools such as the R `lme4` package (Bates et al., 2015) for fitting LMM. Therefore, differential abundance analysis of correlated/clustered microbiome datasets could be easily performed using LinDA. Our framework also gives more insights into the CLR-based approach, which has been widely used in compositional data analysis (Aitchison, 1986). However, the bias of CLR regression models has not been formally recognized to our best knowledge. Our framework justifies the use of CLR regression and provides a solution to correct the bias associated with CLR regression.

In the simulation, we found that Wilcoxon rank sum test on GMPR normalized data performed fairly well and the power was reasonable in most settings. However, Wilcoxon rank sum test has limited ability to adjust covariates and it does not provide interpretable effect size estimates. It also did not perform well when the abundance data followed a gamma distribution (FDR inflation) or the sample size was small (very low power). When we simulated even stronger compostional effect by drawing the differential taxa from the top 25% most abundant taxa, we found Wilcoxon rank sum test began to break down (Appendix Figure B.14). ANCOM-BC was overall robust and powerful but it had inflated type I error at small sample sizes. MetagenomeSeq did not perform well when the signal was dense and was generally less powerful than ANCOM-BC and LinDA. Interestingly, its FDR control was better when compositional effect was very strong (Appendix Figure B.14). ALDEx2 was generally the most conservative and less powerful than the other methods. Type I error inflation was also noted when the abundance data had a gamma distribution. LinDA was as competitive as ANCOM-BC in most settings. It showed better FDR control than ANCOM-BC when the sample size was small or the variable of interest was continuous or the absolute abundances followed gamma distribution. It had slight FDR inflation while ANCOM-BC controlled the FDR when the number of taxa was small. Under strong compostional effect (Appendix Figure B.14), LinDA showed some FDR inflation but overall achieved the best performance.

When the library size was associated with the variable of interest, all existing methods had severe type I error inflation. Fortunately, such association is detectable and if we see a significant

association, rarefaction should be used for those methods. Although rarefaction controls the effect of uneven library sizes, it discards a significant portion of the read counts and thus loses a lot of information in the data. When there are samples with very small sample sizes, the users have to make a decision as whether to retain more reads or more samples. In LinDA, we implemented a heuristic imputation method, where the imputed values are proportional to the library sizes. This procedure makes the imputed data after CLR transformation independent of the library size and substantially reduces the inflated type I error due to library size confounding.

Our method uses the log linear model, where the coefficients can be interpreted as the log fold change in response to the one unit change of the covariate. In analysis of biological data, interpretation is one key factor in selecting relevant tools. As for all model-based approaches, LinDA has several assumptions. First, LinDA relies on the assumption that there is a mode at 0 for the regression coefficients (Condition (vi) in Theorem 2). This assumption is easy to be met if the signal is sparse. In the simulation, we show that when the signal density is around 20%, LinDA is still very robust. However, when the signal is extremely dense, LinDA could fail. Second, LinDA assumes a log linear model on the absolute abundance. Although this is a reasonable assumption, which has been widely adopted in the analysis of abundance data, the interaction between the host and the microbiome could be more complex than the simple log linear relationship. Analysis of the residuals from the CLR regression could provide evidence about whether the assumption is reasonable. If the model assumption is violated, permutation test or transformation of the variables may be performed. Finally, although LinDA provides asymptotic FDR control, its finite-sample FDR control is not guaranteed. Based on numerical simulations, we demonstrate that LinDA performs well under small sample and feature sizes with slight inflation under certain settings.

LinDA uses the relative abundance data and does not model the sampling variability of the read counts. This could reduce the statistical power especially for those less abundant taxa, whose sampling variability is larger than those abundant taxa. To remedy the power loss, another multinomial sampling layer could be imposed on top of LinDA. However, the computational complexity will be increased significantly and breaking the simplicity of LinDA. Another approach is to perform

posterior inference of the underlying proportions based on a Bayes approach. Once we obtain the posterior samples, LinDA can be applied to the posterior samples and results are then aggregated, similar in the spirit to the multiple imputation method (Carpenter and Kenward, 2012).

Finally, we comment that, besides microbiome data, LinDA could be applied to other sequencing data such as RNA-Seq data. In fact, there are arguments for treating RNA-Seq data as compositional (Quinn et al., 2018). Thus, LinDA could be an alternative for differential expression analysis if there is strong compositional effect for example, when the highly abundant genes are differential with the same direction of change.

4. SUMMARY

Large-scale multiple testing is a fundamental statistical problem in modern biomedical sciences. A powerful multiple testing procedure could tremendously reduce the experimental cost in the discovery stage. This dissertation has introduced two new multiple testing procedures focusing on two application areas in bioinformatics.

In Chapter 2, we have discussed a covariate adaptive FWER-controlling procedure, which takes into account the alternative p-value distribution as well as prior null probabilities simultaneously to capture as much information from the p-values and covariates as possible. We derive the exact rate of convergence of the FWER of the proposed method through a novel perturbation-type argument. Numerical studies show that our procedure controls the FWER in the strong sense and is more powerful than the competing methods. It maintains the robustness across different settings, including scenarios of model misspecification and correlated hypotheses. The method is highly scalable and can be applied to a problem with millions of hypotheses in GWASs.

There are still numbers of open questions in integrating auxiliary data in genomic data analysis. In our method, we provide a parametric method for incorporating covariates, and a natural extension is to use more flexible non-parametric models. In addition, we could accommodate more general structural information such as the phylogenetic tree structure, group structure, order structure for improving the statistical power.

In Chapter 3, we have presented a new differential abundance analysis method, named LinDA, as a short for "linear models for differential abundance analysis", which is surprisingly simple and only needs to fit regular linear models and linear mixed effects models for independent and correlated microbiome data, respectively. With our method, analysis of compositional data becomes straightforward and highly interpretable. Analysis of independent and correlated microbiome data are unified in a single framework. Moreover, it is 100-1000 faster than the state-of-the-art method. We also rigorously prove the asymptotical FDR control of the proposed method, making it the first method that enjoys theoretical guarantee under some mild assumptions in differential abundance

analysis. We conduct comprehensive simulations and real data applications to show that LinDA is powerful, robust, flexible and scalable.

Continuing this work, we plan to further develop statistical tools for microbiome data focusing on imputation for zeros that are widely existing in count tables. Zeros are problematic for microbiome data analysis since log transformation is usually applied for taxa abundance data. We shall propose a Bayesian approach to infer the underlying true composition, upon which LinDA could be performed.

REFERENCES

1000 Genomes Project Consortium (2015). A global reference for human genetic variation. *Nature* **526,** 68–74.

Aitchison, J. (1986). *The statistical analysis of compositional data*. Chapman and Hall.

Anders, S. and Huber, W. (2010). Differential expression analysis for sequence count data. *Genome Biology* **11,** R106.

Barras, L., Scaillet, O., and Wermers, R. (2010). False discoveries in mutual fund performance: Measuring luck in estimated alphas. *The journal of finance* **65,** 179–216.

Bates, D., Mächler, M., Bolker, B., and Walker, S. (2015). Fitting linear mixed-effects models using lme4. *Journal of Statistical Software* **67,**.

Benjamini, Y. and Hochberg, Y. (1995). Controlling the false discovery rate: a practical and powerful approach to multiple testing. *Journal of the Royal Statistical Society, Series B* **57,** 289–300.

Benjamini, Y. and Yekutieli, D. (2001). The control of the false discovery rate in multiple testing under dependency. *Annals of statistics* pages 1165–1188.

Boca, S. M. and Leek, J. T. (2018). A direct approach to estimating false discovery rates conditional on covariates. *PeerJ* **6,** e6035.

Bourgon, R., Gentleman, R., and Huber, W. (2010). Independent filtering increases detection power for high-throughput experiments. *PNAS* **107,** 9546–9551.

Brill, B., Amir, A., and Heller, R. (2020). Testing for differential abundance in compositional counts data, with application to microbiome studies. *arXiv preprint arXiv:1904.08937* .

Callahan, B. J., McMurdie, P. J., Rosen, M. J., Han, A. W., Johnson, A. J. A., and Holmes, S. P. (2016). Dada2: high-resolution sample inference from illumina amplicon data. *Nature methods* **13,** 581–583.

Cao, H., Sun, W., and Kosorok, M. R. (2013). The optimal power puzzle: scrutiny of the monotone likelihood ratio assumption in multiple testing. *Biometrika* **100,** 495–502.

Carpenter, J. and Kenward, M. (2012). *Multiple imputation and its application*. John Wiley & Sons.

Charlson, E. S., Chen, J., Custers-Allen, R., Bittinger, K., Li, H., Sinha, R., Hwang, J., Bushman, F. D., and Collman, R. G. (2010). Disordered microbial communities in the upper respiratory tract of cigarette smokers. *PloS one* **5,** e15216.

Chen, J., King, E., Deek, R., Wei, Z., Yu, Y., Grill, D., and Ballman, K. (2018). An omnibus test for differential distribution analysis of microbiome sequencing data. *Bioinformatics* **34,** 643–651.

Chen, L., Reeve, J., Zhang, L., Huang, S., Wang, X., and Chen, J. (2018). Gmpr: A robust normalization method for zero-inflated count data with application to microbiome sequencing data. *PeerJ* **6,** e4600.

Connolly, S. R., MacNeil, M. A., Caley, M. J., Knowlton, N., Cripps, E., Hisano, M., Thibaut, L. M., Bhattacharya, B. D., Benedetti-Cecchi, L., Brainard, R. E., et al. (2014). Commonness and rarity in the marine biosphere. *Proceedings of the National Academy of Sciences* **111,** 8524–8529.

Dobriban, E., Fortney, K., Kim, S. K., and Owen, A. B. (2015). Optimal multiple testing under a gaussian prior on the effect sizes. *Biometrika* **102,** 753–766.

Edgar, R. C. (2013). Uparse: highly accurate otu sequences from microbial amplicon reads. *Nature methods* **10,** 996–998.

Efron, B. (2010). *Large-scale inference: empirical Bayes methods for estimation, testing, and prediction*, volume 1. Cambridge University Press.

Fan, J., Han, X., and Gu, W. (2012). Estimating false discovery proportion under arbitrary covariance dependence. *Journal of the American Statistical Association* **107,** 1019–1035.

Fan, Y. and Pedersen, O. (2021). Gut microbiota in human metabolic health and disease. *Nature Reviews Microbiology* **19,** 55–71.

Faust, K., Lahti, L., Gonze, D., De Vos, W. M., and Raes, J. (2015). Metagenomics meets time series analysis: unraveling microbial community dynamics. *Current opinion in microbiology* **25,** 56–66.

Ferkingstad, E., Frigessi, A., Rue, H., Thorleifsson, G., Kong, A., et al. (2008). Unsupervised empirical bayesian multiple testing with external covariates. *The Annals of Applied Statistics* **2,** 714–735.

Fernandes, A. D., Reid, J. N., Macklaim, J. M., McMurrough, T. A., Edgell, D. R., and Gloor, G. B. (2014). Unifying the analysis of high-throughput sequencing datasets: characterizing rna-seq, 16s rrna gene sequencing and selective growth experiments by compositional data analysis. *Microbiome* **2,** 15.

Genovese, C. R., Roeder, K., and Wasserman, L. (2006). False discovery control with p-value weighting. *Biometrika* **93,** 509–524.

Gloor, G. B., Macklaim, J. M., Pawlowsky-Glahn, V., and Egozcue, J. J. (2017). Microbiome datasets are compositional: and this is not optional. *Frontiers in microbiology* **8,** 2224.

Gonzalez, A., Navas-Molina, J. A., Kosciolek, T., McDonald, D., Vázquez-Baeza, Y., Ackermann, G., DeReus, J., Janssen, S., Swafford, A. D., Orchanian, S. B., et al. (2018). Qiita: rapid, web-enabled microbiome meta-analysis. *Nature methods* **15,** 796–798.

GTEx Consortium (2017). Genetic effects on gene expression across human tissues. *Nature* **550,** 204–213.

Hawinkel, S., Mattiello, F., Bijnens, L., and Thas, O. (2019). A broken promise: microbiome differential abundance methods do not control the false discovery rate. *Briefings in bioinformatics* **20,** 210–221.

Holm, S. (1979). A simple sequentially rejective multiple test procedure. *Scandinavian journal of statistics* pages 65–70.

Hu, J. X., Zhao, H., and Zhou, H. H. (2010). False discovery rate control with groups. *Journal of the American Statistical Association* **105,** 1215–1227.

Ignatiadis, N., Klaus, B., Zaugg, J. B., and Huber, W. (2016). Data-driven hypothesis weighting increases detection power in genome-scale multiple testing. *Nature methods* **13,** 577–580.

Kaul, A., Mandal, S., Davidov, O., and Peddada, S. D. (2017). Analysis of microbiome data in the presence of excess zeros. *Frontiers in microbiology* **8,** 2114.

Kichaev, G., Bhatia, G., Loh, P.-R., Gazal, S., Burch, K., Freund, M. K., Schoech, A., Pasaniuc, B., and Price, A. L. (2019). Leveraging polygenic functional enrichment to improve gwas power. *The American Journal of Human Genetics* **104,** 65–75.

Kurtz, Z. D., Müller, C. L., Miraldi, E. R., Littman, D. R., Blaser, M. J., and Bonneau, R. A. (2015). Sparse and compositionally robust inference of microbial ecological networks. *PLoS Computational Biology* **11,** e1004226.

Lan, W. and Du, L. (2019). A factor-adjusted multiple testing procedure with application to mutual fund selection. *Journal of Business & Economic Statistics* **37,** 147–157.

Leek, J. T. and Storey, J. D. (2008). A general framework for multiple testing dependence. *PNAS* **105,** 18718–18723.

Lei, L. and Fithian, W. (2018). Adapt: an interactive procedure for multiple testing with side information. *Journal of the Royal Statistical Society, Series B* **80,** 649–679.

Lei, L., Ramdas, A., and Fithian, W. (2017). Star: A general interactive framework for fdr control under structural constraints. *Biometrika* to appear.

Lewis, J. D., Chen, E. Z., Baldassano, R. N., Otley, A. R., Griffiths, A. M., Lee, D., Bittinger, K., Bailey, A., Friedman, E. S., Hoffmann, C., et al. (2015). Inflammation, antibiotics, and diet as environmental stressors of the gut microbiome in pediatric crohn's disease. *Cell host & microbe* **18,** 489–500.

Li, A. and Barber, R. F. (2017). Accumulation tests for fdr control in ordered hypothesis testing. *Journal of the American Statistical Association* **112,** 837–849.

Li, A. and Barber, R. F. (2019). Multiple testing with the structure-adaptive benjamini–hochberg algorithm. *Journal of the Royal Statistical Society, Series B* **81,** 45–74.

Lin, H. and Peddada, S. D. (2020). Analysis of compositions of microbiomes with bias correction. *Nature communications* **11,** 3514.

Loh, P.-R., Kichaev, G., Gazal, S., Schoech, A. P., and Price, A. L. (2018). Mixed-model association for biobank-scale datasets. *Nature genetics* **50,** 906–908.

Love, M. I., Huber, W., and Anders, S. (2014). Moderated estimation of fold change and dispersion

for rna-seq data with deseq2. *Genome biology* **15,** 550.

Mandal, S., Van Treuren, W., White, R. A., Eggesbø, M., Knight, R., and Peddada, S. D. (2015). Analysis of composition of microbiomes: a novel method for studying microbial composition. *Microbial ecology in health and disease* **26,** 27663.

McDonald, D., Hyde, E., Debelius, J. W., Morton, J. T., Gonzalez, A., Ackermann, G., Aksenov, A. A., Behsaz, B., Brennan, C., Chen, Y., et al. (2018). American gut: an open platform for citizen science microbiome research. *Msystems* **3,** e00031–18.

Miller, C. J., Genovese, C., Nichol, R. C., Wasserman, L., Connolly, A., Reichart, D., Hopkins, A., Schneider, J., and Moore, A. (2001). Controlling the false-discovery rate in astrophysical data analysis. *The Astronomical Journal* **122,** 3492.

Morgan, X. C., Tickle, T. L., Sokol, H., Gevers, D., Devaney, K. L., Ward, D. V., Reyes, J. A., Shah, S. A., LeLeiko, N., Snapper, S. B., et al. (2012). Dysfunction of the intestinal microbiome in inflammatory bowel disease and treatment. *Genome biology* **13,** R79.

Parzen, E. (1962). On estimation of a probability density function and mode. *The annals of mathematical statistics* **33,** 1065–1076.

Paulson, J. N., Stine, O. C., Bravo, H. C., and Pop, M. (2013). Differential abundance analysis for microbial marker-gene surveys. *Nature methods* **10,** 1200–1202.

Quinn, T. P., Erb, I., Richardson, M. F., and Crowley, T. M. (2018). Understanding sequencing data as compositions: an outlook and review. *Bioinformatics* **34,** 2870–2878.

Reiner, A., Yekutieli, D., and Benjamini, Y. (2003). Identifying differentially expressed genes using false discovery rate controlling procedures. *Bioinformatics* **19,** 368–375.

Robinson, M. D., McCarthy, D. J., and Smyth, G. K. (2010). edger: a bioconductor package for differential expression analysis of digital gene expression data. *Bioinformatics* **26,** 139–140.

Robinson, M. D. and Oshlack, A. (2010). A scaling normalization method for differential expression analysis of rna-seq data. *Genome biology* **11,** 1–9.

Roeder, K. and Wasserman, L. (2009). Genome-wide significance levels and weighted hypothesis testing. *Statistical science: a review journal of the Institute of Mathematical Statistics* **24,** 398–

413.

Scher, J. U., Sczesnak, A., Longman, R. S., Segata, N., Ubeda, C., Bielski, C., Rostron, T., Cerundolo, V., Pamer, E. G., Abramson, S. B., et al. (2013). Expansion of intestinal prevotella copri correlates with enhanced susceptibility to arthritis. *elife* **2,** e01202.

Schubert, A. M., Rogers, M. A., Ring, C., Mogle, J., Petrosino, J. P., Young, V. B., Aronoff, D. M., and Schloss, P. D. (2014). Microbiome data distinguish patients with clostridium difficile infection and non-c. difficile-associated diarrhea from healthy controls. *MBio* **5,** e01021–14.

Schwartzman, A., Dougherty, R. F., Taylor, J. E., et al. (2008). False discovery rate analysis of brain diffusion direction maps. *Annals of Applied Statistics* **2,** 153–175.

Scott, J. G., Kelly, R. C., Smith, M. A., Zhou, P., and Kass, R. E. (2015). False discovery rate regression: an application to neural synchrony detection in primary visual cortex. *Journal of the American Statistical Association* **110,** 459–471.

Segata, N., Waldron, L., Ballarini, A., Narasimhan, V., Jousson, O., and Huttenhower, C. (2012). Metagenomic microbial community profiling using unique clade-specific marker genes. *Nature methods* **9,** 811–814.

Silverman, J. D., Roche, K., Mukherjee, S., and David, L. A. (2020). Naught all zeros in sequence count data are the same. *Computational and structural biotechnology journal* **18,** 2789–2798.

Sohn, M. B., Du, R., and An, L. (2015). A robust approach for identifying differentially abundant features in metagenomic samples. *Bioinformatics* **31,** 2269–2275.

Stephens, M. (2017). False discovery rates: a new deal. *Biostatistics* **18,** 275–294.

Storey, J. D. (2002). A direct approach to false discovery rates. *Journal of the Royal Statistical Society: Series B (Statistical Methodology)* **64,** 479–498.

Storey, J. D., Taylor, J. E., and Siegmund, D. (2004). Strong control, conservative point estimation and simultaneous conservative consistency of false discovery rates: a unified approach. *Journal of the Royal Statistical Society, Series B* **66,** 187–205.

Sun, W. and Cai, T. T. (2007). Oracle and adaptive compound decision rules for false discovery rate control. *Journal of the American Statistical Association* **102,** 901–912.

Sun, W., Reich, B. J., Cai, T. T., Guindani, M., and Schwartzman, A. (2015). False discovery control in large-scale spatial multiple testing. *Journal of the Royal Statistical Society, Series B* **77,** 59–83.

Tansey, W., Koyejo, O., Poldrack, R. A., and Scott, J. G. (2018). False discovery rate smoothing. *Journal of the American Statistical Association* **113,** 1156–1171.

Tsilimigras, M. C. and Fodor, A. A. (2016). Compositional data analysis of the microbiome: fundamentals, tools, and challenges. *Annals of epidemiology* **26,** 330–335.

Valdes, A. M., Walter, J., Segal, E., and Spector, T. D. (2018). Role of the gut microbiota in nutrition and health. *Bmj* **361,** k2179.

Ventura, V., Paciorek, C. J., and Risbey, J. S. (2004). Controlling the proportion of falsely rejected hypotheses when conducting multiple tests with climatological data. *Journal of Climate* **17,** 4343–4356.

Weiss, S., Xu, Z. Z., Peddada, S., Amir, A., Bittinger, K., Gonzalez, A., Lozupone, C., Zaneveld, J. R., Vázquez-Baeza, Y., Birmingham, A., et al. (2017). Normalization and microbial differential abundance strategies depend upon data characteristics. *Microbiome* **5,** 27.

Wen, X. (2016). Molecular qtl discovery incorporating genomic annotations using bayesian false discovery rate control. *Annals of Applied Statistics* **10,** 1619–1638.

Wu, G. D., Chen, J., Hoffmann, C., Bittinger, K., Chen, Y.-Y., Keilbaugh, S. A., Bewtra, M., Knights, D., Walters, W. A., Knight, R., et al. (2011). Linking long-term dietary patterns with gut microbial enterotypes. *Science* **334,** 105–108.

Xiao, J., Cao, H., and Chen, J. (2017). False discovery rate control incorporating phylogenetic tree increases detection power in microbiome-wide multiple testing. *Bioinformatics* **33,** 2873–2881.

Xiao, J., Chen, L., Johnson, S., Yu, Y., Zhang, X., and Chen, J. (2018). Predictive modeling of microbiome data using a phylogeny-regularized generalized linear mixed model. *Frontiers in microbiology* **9,** 1391.

Xiao, J., Chen, L., Yu, Y., Zhang, X., and Chen, J. (2018). A phylogeny-regularized sparse regression model for predictive modeling of microbial community data. *Frontiers in microbiology* **9,**

3112.

Zablocki, R. W., Schork, A. J., Levine, R. A., Andreassen, O. A., Dale, A. M., and Thompson, W. K. (2014). Covariate-modulated local false discovery rate for genome-wide association studies. *Bioinformatics* **30,** 2098–2104.

Zhang, M. J., Xia, F., and Zou, J. (2019). Fast and covariate-adaptive method amplifies detection power in large-scale multiple hypothesis testing. *Nature communications* **10,** 3433.

Zhang, X. and Chen, J. (2020). Covariate adaptive false discovery rate control with applications to omics-wide multiple testing. *Journal of the American Statistical Association* forthcoming.

APPENDIX A

APPENDIX FOR CHAPTER 2

The appendix is organized as follows. In Section A.1, we provide more technical details for Example 1. Section A.2 presents Lemmas 1–2 and their proofs that are useful in the proof of Proposition 2. Section A.3 presents the proofs of Propositions 1–2. In Section A.4, we provide other intermediate results for the proof of Theorem 1 together with their proofs. In Section A.5, we prove Theorem 1. Sections A.6 and A.7 present the additional simulation results and the numbers of rejections before clumping mentioned in Section 2.5 of the main text, respectively.

A.1 More about Example 1

Suppose all hypotheses are true nulls and (x_i, p_i) are i.i.d.with x_i being 1-dimensional, $x_i \perp\!\!\!\perp p_i$ and $p_i \sim \text{Unif}([0,1])$. Then

$$\begin{aligned}&\mathcal{L}(\beta) = \mathbb{E}\{\mathbb{P}_m l(\beta)\} = \mathbb{E}\left\{l(\beta; z_i)\right\}\\ =&\mathbb{E}\left[(1-\gamma)\log\left\{1-\gamma+(\gamma-\gamma^k)\frac{e^{-x_i\beta}}{1+e^{-x_i\beta}}\right\}+\gamma\log\left\{\gamma-(\gamma-\gamma^k)\frac{e^{-x_i\beta}}{1+e^{-x_i\beta}}\right\}\right]\end{aligned}$$

and $\mathcal{L}'(\beta) = (\gamma-\gamma^k)^2\mathbb{E}\left\{g(x_i;\beta)\right\}$, where

$$g(x;\beta) = \frac{xe^{-x\beta}}{(1+e^{-x\beta})^2}\frac{\frac{e^{-x\beta}}{1+e^{-x\beta}}}{\left\{1-\gamma+(\gamma-\gamma^k)\frac{e^{-x\beta}}{1+e^{-x\beta}}\right\}\left\{\gamma-(\gamma-\gamma^k)\frac{e^{-x\beta}}{1+e^{-x\beta}}\right\}}.$$

We observe that $\gamma - \gamma^k < 0$,

$$\begin{aligned}1-\gamma^k <&1-\gamma+(\gamma-\gamma^k)\frac{e^{-x\beta}}{1+e^{-x\beta}} < 1-\gamma,\\ \gamma <&\gamma-(\gamma-\gamma^k)\frac{e^{-x\beta}}{1+e^{-x\beta}} < \gamma^k,\end{aligned} \tag{A.1}$$

and

$$
\begin{aligned}
g(x;\beta)+g(-x;\beta) =& \frac{xe^{-x\beta}}{(1+e^{-x\beta})^2}\frac{\frac{e^{-x\beta}}{1+e^{-x\beta}}}{\left\{1-\gamma+(\gamma-\gamma^k)\frac{e^{-x\beta}}{1+e^{-x\beta}}\right\}\left\{\gamma-(\gamma-\gamma^k)\frac{e^{-x\beta}}{1+e^{-x\beta}}\right\}} \\
& - \frac{xe^{x\beta}}{(1+e^{x\beta})^2}\frac{\frac{e^{x\beta}}{1+e^{x\beta}}}{\left\{1-\gamma+(\gamma-\gamma^k)\frac{e^{x\beta}}{1+e^{x\beta}}\right\}\left\{\gamma-(\gamma-\gamma^k)\frac{e^{x\beta}}{1+e^{x\beta}}\right\}} \\
=& \frac{xe^{x\beta}}{(1+e^{x\beta})^2}\left[\frac{\frac{1}{1+e^{x\beta}}}{\left\{1-\gamma+(\gamma-\gamma^k)\frac{1}{1+e^{x\beta}}\right\}\left\{\gamma-(\gamma-\gamma^k)\frac{1}{1+e^{x\beta}}\right\}}\right. \\
& \qquad \left. - \frac{\frac{e^{x\beta}}{1+e^{x\beta}}}{\left\{1-\gamma+(\gamma-\gamma^k)\frac{e^{x\beta}}{1+e^{x\beta}}\right\}\left\{\gamma-(\gamma-\gamma^k)\frac{e^{x\beta}}{1+e^{x\beta}}\right\}}\right] \\
=& \frac{xe^{x\beta}}{(1+e^{x\beta})^2}\left[\frac{\frac{e^{x\beta}}{1+e^{x\beta}}}{\left\{1-\gamma+(\gamma-\gamma^k)\frac{1}{1+e^{x\beta}}\right\}\left\{\gamma e^{x\beta}-(\gamma-\gamma^k)\frac{e^{x\beta}}{1+e^{x\beta}}\right\}}\right. \\
& \qquad \left. - \frac{\frac{e^{x\beta}}{1+e^{x\beta}}}{\left\{1-\gamma+(\gamma-\gamma^k)\frac{e^{x\beta}}{1+e^{x\beta}}\right\}\left\{\gamma-(\gamma-\gamma^k)\frac{e^{x\beta}}{1+e^{x\beta}}\right\}}\right].
\end{aligned}
$$

Thus if $\beta = 0$ then $g(x;\beta)+g(-x;\beta) = 0$, if $\beta > 0$ then $g(x;\beta)+g(-x;\beta) < 0$ (as long as $x \neq 0$), and if $\beta < 0$ then $g(x;\beta)+g(-x;\beta) > 0$ (as long as $x \neq 0$). Note also that $g(0;\beta) = 0$ and $g(x;\beta)+g(-x;\beta) = -\{g(x;-\beta)+g(-x;-\beta)\}$. Therefore, if x_i follows a distribution that is symmetric about zero and $\mathbb{P}(x_i \neq 0) > 0$, then we have

$$
\begin{aligned}
\mathcal{L}'(\beta) =& (\gamma-\gamma^k)^2\mathbb{E}\{g(x_i;\beta)\mathbb{I}(x_i>0)+g(x_i;\beta)\mathbb{I}(x_i\leq 0)\} \\
=& (\gamma-\gamma^k)^2\mathbb{E}\{g(x_i;\beta)\mathbb{I}(x_i>0)+g(-x_i;\beta)\mathbb{I}(x_i>0)\} \\
=& (\gamma-\gamma^k)^2\mathbb{E}[\{g(x_i;\beta)+g(-x_i;\beta)\}\mathbb{I}(x_i>0)]
\end{aligned}
$$

and hence $\mathcal{L}'(\beta) = -\mathcal{L}'(-\beta)$, and $\mathcal{L}'(\beta) = 0$ if $\beta = 0$, $\mathcal{L}'(\beta) > 0$ if $\beta < 0$ and $\mathcal{L}'(\beta) < 0$ if $\beta > 0$. Thus $\beta^* = 0$. Let $h(x;\beta) = e^{-x\beta}/(1+e^{-x\beta})$ and $h'(x;\beta) = -xe^{-x\beta}/(1+e^{-x\beta})^2$. Then

$$g(x;\beta) = \frac{x\left\{h(x;\beta)\right\}^3 e^{x\beta}}{\left\{1-\gamma+(\gamma-\gamma^k)h(x;\beta)\right\}\left\{\gamma-(\gamma-\gamma^k)h(x;\beta)\right\}},$$

$$\begin{aligned} & g'(x;\beta) \\ =& \frac{\left[3x\left\{h(x;\beta)\right\}^2 h'(x;\beta)e^{x\beta} + x^2\left\{h(x;\beta)\right\}^3 e^{x\beta}\right]\left\{1-\gamma+(\gamma-\gamma^k)h(x;\beta)\right\}\left\{\gamma-(\gamma-\gamma^k)h(x;\beta)\right\}}{\left\{1-\gamma+(\gamma-\gamma^k)h(x;\beta)\right\}^2\left\{\gamma-(\gamma-\gamma^k)h(x;\beta)\right\}^2} \\ & - \frac{x\left\{h(x;\beta)\right\}^3 e^{x\beta}\left[(\gamma-\gamma^k)h'(x;\beta)\left\{2\gamma-1-2(\gamma-\gamma^k)h(x;\beta)\right\}\right]}{\left\{1-\gamma+(\gamma-\gamma^k)h(x;\beta)\right\}^2\left\{\gamma-(\gamma-\gamma^k)h(x;\beta)\right\}^2}, \end{aligned}$$

and

$$\begin{aligned} g'(x;0) =& \frac{-\frac{x^2}{16}\left\{1-\gamma+(\gamma-\gamma^k)/2\right\}\left\{\gamma-(\gamma-\gamma^k)/2\right\} + \frac{x^2}{32}(\gamma-\gamma^k)(\gamma+\gamma^k-1)}{\left\{1-\gamma+(\gamma-\gamma^k)/2\right\}^2\left\{\gamma-(\gamma-\gamma^k)/2\right\}^2} \\ =& -\frac{x^2}{32}u(\gamma,k), \end{aligned}$$

where

$$u(\gamma,k) = \frac{2\left\{1-\gamma+(\gamma-\gamma^k)/2\right\}\left\{\gamma-(\gamma-\gamma^k)/2\right\} - (\gamma-\gamma^k)(\gamma+\gamma^k-1)}{\left\{1-\gamma+(\gamma-\gamma^k)/2\right\}^2\left\{\gamma-(\gamma-\gamma^k)/2\right\}^2}.$$

We study $u(\gamma,k)$ numerically. Let γ range from 0.05 to 0.95. Then the values of $\min\{u(\gamma,k); k \in [0,1]\}$ are shown in Figure A.1. We point out that the left most point in Figure A.1 is $\min\{u(0.05,k) : k \in [0,1]\} = u(0.05, 0.23) = 4.94$. Therefore

$$\mathcal{L}''(0) = \frac{\mathrm{d}}{\mathrm{d}\beta}(\gamma-\gamma^k)^2\mathbb{E}\{g(x_i,\beta)\}\Big|_{\beta=0} = -\frac{(\gamma-\gamma^k)^2 u(\gamma,k)}{32}\mathbb{E}(x_i^2) \le -c$$

as long as $\mathbb{E}(x_i^2) > c'$ for some $c' > 0$. Next, we illustrate the behavior of $\mathcal{L}'(\beta)$ by considering four cases: (i) $x_i \sim N(0,1)$; (ii) $x_i \sim$ Gamma$(1, 0.5)$, i.e., Gamma distribution with shape 1 and rate 0.5; (iii) $x_i = w_i -$ median$(w_1, ..., w_m)$, where $w_i \sim$ Gamma$(1, 0.5)$; (iv) $x_i = w_i -$ median$(w_1, ..., w_m)$, where $w_i \sim$ Pois(2), i.e., Poisson distribution with parameter 2. Let $\gamma = 0.5$,

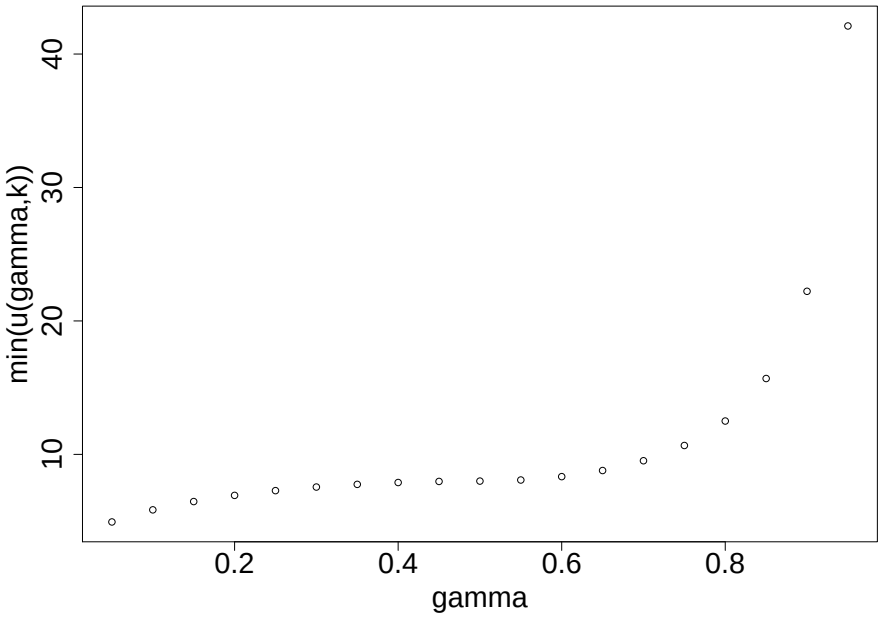

Figure A.1: Values of $\min\{u(\gamma, k); k \in [0, 1]\}$ with γ ranging from 0.05 to 0.95.

$k = 0.25$. When x_i follows the standard normal distribution which is symmetric about zero, the behavior of $\mathcal{L}'(\beta)$ as observed in (i) of Figure A.2 is consistent with our theory. As illustrated by (ii) of Figure A.2, Condition (v) is violated if $\mathbb{P}(X \geq 0) = 1$ (or $\mathbb{P}(X \leq 0) = 1$). Nevertheless, we can resolve this issue by simply subtracting the observations by the sample median. As we can see from (iii)–(iv) of Figure A.2, the pattern of the curve of $\mathcal{L}'(\beta)$ is similar to that of the standard normal distribution. In addition, by standardizing the observations, we can obtain the similar curves as (iii)–(iv) of Figure A.2.

A.2 Intermediate results for Proposition 2

Lemma 1. *Assume that* $\sup_{1 \leq i \leq m} \mathbb{E}(\|x_i\|^2) < \infty$. *Then under Assumptions 2 and 3, we have*

$$\sup_{\beta \in \mathcal{B}} |\mathbb{P}_m l(\beta) - \mathcal{L}(\beta)| \to 0, \quad \textit{in probability.}$$

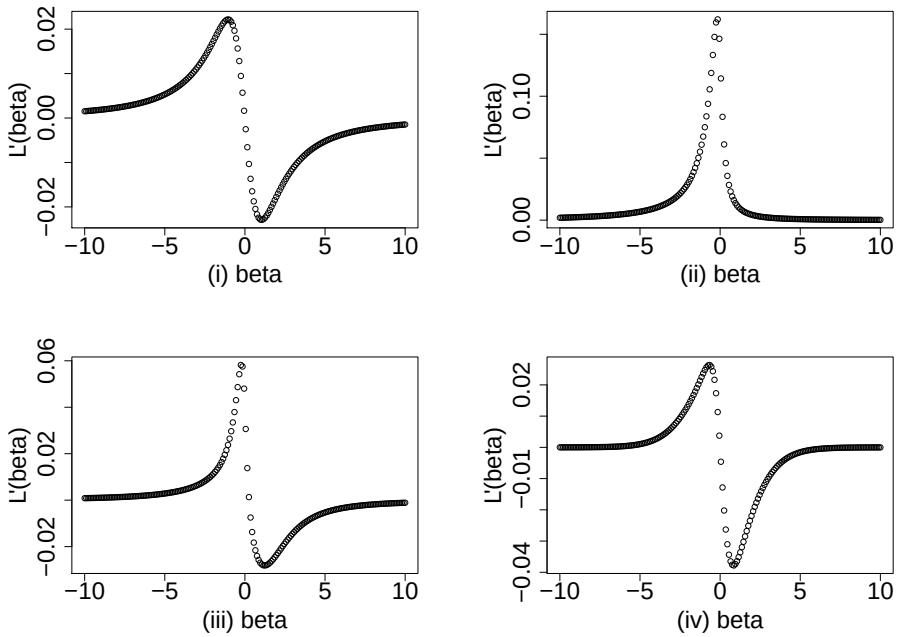

Figure A.2: Curves of $\mathcal{L}'(\beta)$ with $\gamma = 0.5$ and $k = 0.25$ under four different cases. (i) $x_i \sim N(0,1)$; (ii) $x_i \sim$ Gamma(shape $= 1$, rate $= 0.5$); (iii) $x_i = w_i -$ median$(w_1, ..., w_m)$, where $w_i \sim$ Gamma(shape $= 1$, rate $= 0.5$); (iv) $x_i = w_i -$ median$(w_1, ..., w_m)$, where $w_i \sim$ Pois(2).

Proof. Note that

$$
\begin{aligned}
l\{\beta;(x,1)\} =& \log\left[(1+e^{-x^{\mathrm{T}}\beta})^{-1}(1-\gamma) + \left\{1-(1+e^{x^{\mathrm{T}}\beta})^{-1}\right\}(1-\gamma^k)\right], \\
l\{\beta;(x,0)\} =& \log\left[(1+e^{-x^{\mathrm{T}}\beta})^{-1}\gamma + \left\{1-(1+e^{x^{\mathrm{T}}\beta})^{-1}\right\}\gamma^k\right].
\end{aligned}
$$

Thus $l(\beta;z)$ is bounded uniformly over β and z according to (A.1), that is, $L_1 \le l(\beta;z) \le L_2$, where $L_1 = \log(1-\gamma^k) \wedge \log(\gamma)$ and $L_2 = \log(1-\gamma) \vee \log(\gamma^k)$. Note also that for $0 < \gamma < 1$,

$$
\begin{aligned}
\|\nabla l\{\beta;(x,1)\}\| &= \left\| \frac{(\gamma^k-\gamma)(1+e^{-x^{\mathrm{T}}\beta})^{-2}e^{-x^{\mathrm{T}}\beta}x}{(\gamma^k-\gamma)(1+e^{-x^{\mathrm{T}}\beta})^{-1} + (1-\gamma^k)} \right\| \le \frac{\gamma^k-\gamma}{1-\gamma^k}\|x\|, \\
\|\nabla l\{\beta;(x,0)\}\| &= \left\| \frac{(\gamma-\gamma^k)(1+e^{-x^{\mathrm{T}}\beta})^{-2}e^{-x^{\mathrm{T}}\beta}x}{(\gamma-\gamma^k)(1+e^{-x^{\mathrm{T}}\beta})^{-1} + \gamma^k} \right\| \le \frac{\gamma^k-\gamma}{\gamma}\|x\|.
\end{aligned}
$$

Thus for any $\beta_1, \beta_2 \in \mathcal{B}$, we have

$$|l(\beta_1; z) - l(\beta_2; z)| \leq c\|x\|\|\beta_1 - \beta_2\|,$$

which implies that $l(\beta; z)$ is $c\|x\|$-Lipschitz continuous in β. Let $\{\beta_n\}_{n=1}^N$ be an $\epsilon/(2c)$ covering of $\mathcal{B}$, that is, for any $\beta \in \mathcal{B}$, there exists n, such that $\|\beta - \beta_n\| \leq \epsilon/(2c)$. Then for $i = 1, ..., m$, we have

$$|l(\beta; z_i) - l(\beta_n; z_i)| \leq c\|x_i\|\|\beta - \beta_n\| \leq \frac{\epsilon}{2}\|x_i\|,$$

and hence

$$l(\beta_n; z_i) - \frac{\epsilon}{2}\|x_i\| \leq l(\beta; z_i) \leq l(\beta_n; z_i) + \frac{\epsilon}{2}\|x_i\|,$$

and

$$\begin{aligned}
\mathbb{P}_m l(\beta) - \mathbb{E}\left\{\mathbb{P}_m l(\beta)\right\} \leq & \mathbb{P}_m l(\beta_n) + \frac{\epsilon}{2m}\sum_{i=1}^m \|x_i\| - \left[\mathbb{E}\left\{\mathbb{P}_m l(\beta_n)\right\} - \frac{\epsilon}{2m}\sum_{i=1}^m \mathbb{E}\left(\|x_i\|\right)\right] \\
= & \mathbb{P}_m l(\beta_n) - \mathbb{E}\left\{\mathbb{P}_m l(\beta_n)\right\} + \frac{\epsilon}{2m}\sum_{i=1}^m \left\{\|x_i\| + \mathbb{E}\left(\|x_i\|\right)\right\}, \\
\mathbb{E}\left[\mathbb{P}_m l(\beta)\right] - \mathbb{P}_m l(\beta) \leq & \mathbb{E}\left\{\mathbb{P}_m l(\beta_n)\right\} + \frac{\epsilon}{2m}\sum_{i=1}^m \mathbb{E}(\|x_i\|) - \left(\mathbb{P}_m l(\beta_n) - \frac{\epsilon}{2m}\sum_{i=1}^m \|x_i\|\right) \\
= & \mathbb{E}\left\{\mathbb{P}_m l(\beta_n)\right\} - \mathbb{P}_m l(\beta_n) + \frac{\epsilon}{2m}\sum_{i=1}^m \left\{\|x_i\| + \mathbb{E}\left(\|x_i\|\right)\right\}.
\end{aligned}$$

Then we have

$$
\begin{aligned}
&\sup_{\beta\in\mathcal{B}} |\mathbb{P}_m l(\beta) - \mathbb{E}\{\mathbb{P}_m l(\beta)\}| \\
&\leq \max_{1\leq n\leq N} |\mathbb{P}_m l(\beta_n) - \mathbb{E}\{\mathbb{P}_m l(\beta_n)\}| + \frac{\epsilon}{2m}\sum_{i=1}^{m}\{\|x_i\| + \mathbb{E}(\|x_i\|)\} \\
&= \max_{1\leq n\leq N} |\mathbb{P}_m l(\beta_n) - \mathbb{E}\{\mathbb{P}_m l(\beta_n)\}| + \frac{\epsilon}{2m}\sum_{i=1}^{m}\{\|x_i\| - \mathbb{E}(\|x_i\|)\} + \frac{\epsilon}{m}\sum_{i=1}^{m}\mathbb{E}(\|x_i\|) = o_{\mathbb{P}}(1) + O(\epsilon),
\end{aligned}
$$

where we have used the fact that $l(\beta; z)$ is bounded, Assumption 2 (which ensures that x_i's are independent), the assumption that $\sup_{1\leq i\leq m}\mathbb{E}(\|x_i\|^2) < \infty$ and the Chebyshev's inequality. As ϵ can be arbitrarily small, under Assumption 3, we have

$$
\sup_{\beta\in\mathcal{B}} |\mathbb{P}_m l(\beta) - \mathcal{L}(\beta)| \leq \sup_{\beta\in\mathcal{B}} |\mathbb{P}_m l(\beta) - \mathbb{E}\{\mathbb{P}_m l(\beta)\}| + \sup_{\beta\in\mathcal{B}} |\mathbb{E}\{\mathbb{P}_m l(\beta)\} - \mathcal{L}(\beta)| = o_{\mathbb{P}}(1).
$$

□

Lemma 2. *Under Assumptions 2–4 and the assumption that* $\sup_{1\leq i\leq m}\mathbb{E}(\|x_i\|^2) < \infty$*, we have* $\hat{\beta} \to \beta^*$ *in probability. Moreover, for* $a = 0, 1$*,*

$$
\sup_{1\leq j\leq m} \left|\hat{\beta}(p_{j\to a}) - \beta^*\right| \to 0, \quad \textit{in probability.}
$$

Proof. By Assumptions 3 and 4, for every $\epsilon > 0$, we know that there exists a $\delta > 0$ such that $\mathcal{L}(\beta) < \mathcal{L}(\beta^*) - \delta$ for $\|\beta - \beta^*\| > \epsilon$. Therefore

$$
\mathbb{P}\left(\|\hat{\beta} - \beta^*\| > \epsilon\right) \leq \mathbb{P}\left\{\mathcal{L}(\beta^*) - \mathcal{L}(\hat{\beta}) > \delta\right\}.
$$

To prove $\hat{\beta} \to \beta^*$ in probability, it suffices to show that $\mathcal{L}(\beta^*) - \mathcal{L}(\hat{\beta}) = o_{\mathbb{P}}(1)$. To this end, we

note that $\mathcal{L}(\beta^*) \geq \mathcal{L}(\hat{\beta})$ and

$$\begin{aligned}\mathcal{L}(\beta^*) - \mathcal{L}(\hat{\beta}) &= \mathcal{L}(\beta^*) - \mathbb{P}_m l(\beta^*) + \mathbb{P}_m l(\beta^*) - \mathbb{P}_m l(\hat{\beta}) + \mathbb{P}_m l(\hat{\beta}) - \mathcal{L}(\hat{\beta}) \\ &\leq \mathcal{L}(\beta^*) - \mathbb{P}_m l(\beta^*) + \sup_{\beta \in \mathcal{B}} |\mathbb{P}_m l(\beta) - \mathcal{L}(\beta)| = o_{\mathbb{P}}(1),\end{aligned}$$

where the inequality follows from the fact that $\hat{\beta}$ is the maximizer of $\mathbb{P}_m l(\beta)$ and hence $\mathbb{P}_m l(\beta^*) - \mathbb{P}_m l(\hat{\beta}) \leq 0$ and the last equality follows from Lemma 1. To prove the uniform convergence of $\hat{\beta}(p_{j\to a})$, let

$$\mathbb{P}_m^{j\to a} l(\beta) = \frac{1}{m}\sum_{i\neq j} l(\beta; z_i) + \frac{1}{m} l\{\beta; (x_j, a)\} = \mathbb{P}_m l(\beta) + \frac{1}{m}\left[l\{\beta; (x_j, a)\} - l(\beta; z_j)\right],$$

and $L = L_2 - L_1$ with L_1 and L_2 defined in the proof of Lemma 1. We have

$$\sup_{1\leq j\leq m} \sup_{\beta\in\mathcal{B}} \left|\mathbb{P}_m^{j\to a} l(\beta) - \mathbb{P}_m l(\beta)\right| \leq \frac{L}{m}.$$

Note that

$$\begin{aligned}\mathbb{P}\left\{\sup_{1\leq j\leq m}\left|\hat{\beta}(p_{j\to a}) - \beta^*\right| > \epsilon\right\} \leq& \mathbb{P}\left[\inf_{1\leq j\leq m} \mathcal{L}\{\hat{\beta}(p_{j\to a})\} < \mathcal{L}(\beta^*) - \delta\right] \\ =& \mathbb{P}\left(\sup_{1\leq j\leq m}\left[\mathcal{L}(\beta^*) - \mathcal{L}\{\hat{\beta}(p_{j\to a})\}\right] > \delta\right).\end{aligned}$$

Then we only need to prove that $\sup_{1\leq j\leq m}[\mathcal{L}(\beta^*) - \mathcal{L}\{\hat{\beta}(p_{j\to a})\}] = o_{\mathbb{P}}(1)$. The proof is completed

by noting that $\sup_{1\le j\le m}[\mathcal{L}(\beta^*) - \mathcal{L}\{\hat{\beta}(p_{j\to a})\}] \ge 0$ and

$$
\begin{aligned}
&\sup_{1\le j\le m}\left[\mathcal{L}(\beta^*) - \mathcal{L}\{\hat{\beta}(p_{j\to a})\}\right] \\
=&\sup_{1\le j\le m}\Big[\mathcal{L}(\beta^*) - \mathbb{P}_m l(\beta^*) + \mathbb{P}_m l(\beta^*) - \mathbb{P}_m^{j\to a} l(\beta^*) + \mathbb{P}_m^{j\to a} l(\beta^*) - \mathbb{P}_m^{j\to a} l\{\hat{\beta}(p_{j\to a})\} \\
&\qquad + \mathbb{P}_m^{j\to a} l\{\hat{\beta}(p_{j\to a})\} - \mathbb{P}_m l\{\hat{\beta}(p_{j\to a})\} + \mathbb{P}_m l\{\hat{\beta}(p_{j\to a})\} - \mathcal{L}\{\hat{\beta}(p_{j\to a})\}\Big] \\
\le&\mathcal{L}(\beta^*) - \mathbb{P}_m l(\beta^*) + \frac{2L}{m} + \sup_{\beta\in\mathcal{B}} |\mathbb{P}_m l(\beta) - \mathcal{L}(\beta)| = o_{\mathbb{P}}(1),
\end{aligned}
$$

where we have used the fact that $\hat{\beta}(p_{j\to a})$ is the maximizer of $\mathbb{P}_m^{j\to a} l(\beta)$ and hence $\sup_{1\le j\le m}[\mathbb{P}_m^{j\to a} l(\beta^*) - \mathbb{P}_m^{j\to a} l\{\hat{\beta}(p_{j\to a})\}] \le 0$ and the result from Lemma 1. □

A.3 Proofs of Propositions 1 and 2

Proof of Proposition 1. We recall some notations defined in the main text and give some new definitions. Let $p_{j\to a} = (p_1, \ldots, p_{j-1}, a, p_{j+1}, \ldots, p_m) \in \mathbb{R}^m$ for $a = 0, 1$, and $p_{-j} = (p_1, ..., p_{j-1}, p_{j+1}, ..., p_m) \in \mathbb{R}^{m-1}$. We define $\hat{\beta}(p_{j\to a}), \hat{\pi}(x_i; p_{j\to a}), \tilde{\tau}(p_{j\to a}), \hat{\tau}(p_{j\to a})$ and $\hat{t}_i(p_{j\to a})$ by setting the jth p-value to be equal to a when estimating the corresponding quantities. First, we prove the first inequality. Observe that

$$
\begin{aligned}
\text{FWER} &\le \sum_{j\in\mathcal{M}_0} \mathbb{P}\left(p_j \le \hat{t}_j \wedge \gamma\right) \\
&\le \sum_{j\in\mathcal{M}_0} \mathbb{E}\left\{\mathbb{I}\left(p_j \le \hat{t}_j \wedge \gamma\right) - \frac{\mathbb{I}(p_j > \gamma)}{1-\gamma}\hat{t}_j\right\} + \sum_{i=1}^{m} \mathbb{E}\left\{\frac{\mathbb{I}(p_i > \gamma)}{1-\gamma}\hat{t}_i\right\} \\
&\le \sum_{j\in\mathcal{M}_0} \mathbb{E}\left\{\mathbb{I}\left(p_j \le \hat{t}_j \wedge \gamma\right) - \frac{\mathbb{I}(p_j > \gamma)}{1-\gamma}\hat{t}_j\right\} + \alpha,
\end{aligned}
$$

where we have used the fact that $\sum_{i=1}^{m} \mathbb{I}(p_i > \gamma)\hat{t}_i/(1-\gamma) \le \alpha$. Denote by $\mathbb{E}_0$ and $\mathbb{P}_0$ the expectation and probability under the null. If $\{p_i\} \in \mathcal{M}_0$ are mutually independent and are independent

with the non-null p-values, then under Assumption 1, we have

$$
\begin{aligned}
&\mathbb{E}_0\left\{\mathbb{I}\left(p_j \le \hat{t}_j \wedge \gamma\right) - \frac{\mathbb{I}(p_j > \gamma)}{1-\gamma}\hat{t}_j \mid p_{-j}\right\} \\
=&\mathbb{E}_0\left\{\mathbb{I}\left(p_j \le \hat{t}_j \wedge \gamma\right) - \frac{\mathbb{I}(p_j > \gamma)}{1-\gamma}\hat{t}_j \mid p_{-j}, p_j > \gamma\right\}\mathbb{P}_0(p_j > \gamma) \\
&+ \mathbb{E}_0\left\{\mathbb{I}\left(p_j \le \hat{t}_j \wedge \gamma\right) - \frac{\mathbb{I}(p_j > \gamma)}{1-\gamma}\hat{t}_j \mid p_{-j}, p_j \le \gamma\right\}\mathbb{P}_0(p_j \le \gamma) \\
=&\left\{0 - \frac{1}{1-\gamma}\hat{t}_j(p_{j\to 1})\right\}\{1 - F_{0j}(\gamma)\} + \left[\frac{F_{0j}\{\hat{t}_j(p_{j\to 0}) \wedge \gamma\}}{F_{0j}(\gamma)} - 0\right]F_{0j}(\gamma) \\
=&F_{0j}\{\hat{t}_j(p_{j\to 0}) \wedge \gamma\} - \frac{1 - F_{0j}(\gamma)}{1-\gamma}\hat{t}_j(p_{j\to 1}) \\
\le&\hat{t}_j(p_{j\to 0}) \wedge \gamma - \hat{t}_j(p_{j\to 1}) \le \hat{t}_j(p_{j\to 0}) - \hat{t}_j(p_{j\to 1}),
\end{aligned}
$$

where the first inequality is due to the assumption that $F_{0j}(t) \le t$. Thus, we have

$$
\text{FWER} \le \sum_{j\in\mathcal{M}_0}\mathbb{E}\left[\mathbb{E}_0\left\{\mathbb{I}\left(p_j \le \hat{t}_j \wedge \gamma\right) - \frac{\mathbb{I}(p_j > \gamma)}{1-\gamma}\hat{t}_j \mid p_{-j}\right\}\right] + \alpha \le J_m + \alpha,
$$

where

$$
J_m = \sum_{j=1}^{m}\mathbb{E}\left\{\left|\hat{t}_j(p_{j\to 0}) - \hat{t}_j(p_{j\to 1})\right|\right\}.
$$

For the second inequality, note that

$$
\begin{aligned}
\left|\frac{\hat{t}_j(p_{j\to 0}) - \hat{t}_j(p_{j\to 1})}{k^{1/(1-k)}}\right| &= \left|\left\{\frac{1-\hat{\pi}(x_j; p_{j\to 0})}{\hat{\pi}(x_j; p_{j\to 0})\hat{\tau}(p_{j\to 0})}\right\}^{1/(1-k)} - \left\{\frac{1-\hat{\pi}(x_j; p_{j\to 1})}{\hat{\pi}(x_j; p_{j\to 1})\hat{\tau}(p_{j\to 1})}\right\}^{1/(1-k)}\right| \\
&\le \left|\left\{\frac{1-\hat{\pi}(x_j; p_{j\to 0})}{\hat{\pi}(x_j; p_{j\to 0})\hat{\tau}(p_{j\to 0})}\right\}^{1/(1-k)} - \left\{\frac{1-\hat{\pi}(x_j; p_{j\to 1})}{\hat{\pi}(x_j; p_{j\to 1})\hat{\tau}(p_{j\to 0})}\right\}^{1/(1-k)}\right| \\
&\quad + \left|\left\{\frac{1-\hat{\pi}(x_j; p_{j\to 1})}{\hat{\pi}(x_j; p_{j\to 1})\hat{\tau}(p_{j\to 0})}\right\}^{1/(1-k)} - \left\{\frac{1-\hat{\pi}(x_j; p_{j\to 1})}{\hat{\pi}(x_j; p_{j\to 1})\hat{\tau}(p_{j\to 1})}\right\}^{1/(1-k)}\right| \\
&\le \frac{c|\hat{\pi}(x_j; p_{j\to 0}) - \hat{\pi}(x_j; p_{j\to 1})|}{\hat{\tau}(p_{j\to 0})^{1/(1-k)}} + c\left|\frac{1}{\hat{\tau}(p_{j\to 0})^{1/(1-k)}} - \frac{1}{\hat{\tau}(p_{j\to 1})^{1/(1-k)}}\right|,
\end{aligned}
$$

where the last inequality follows by using the mean-value theorem for the function $f(x) = (1/x - 1)^{1/(1-k)}$ and the fact that $\hat{\pi}$ is bounded from below by ε_1. Thus we have

$$J_m \leq c(I_{m,1} + I_{m,2}),$$

where

$$I_{m,1} = \mathbb{E}\left\{\sum_{j=1}^{m} \frac{|\hat{\pi}(x_j; p_{j\to 0}) - \hat{\pi}(x_j; p_{j\to 1})|}{\hat{\tau}(p_{j\to 0})^{1/(1-k)}}\right\},$$
$$I_{m,2} = \mathbb{E}\left\{\sum_{j=1}^{m} \left|\frac{1}{\hat{\tau}(p_{j\to 0})^{1/(1-k)}} - \frac{1}{\hat{\tau}(p_{j\to 1})^{1/(1-k)}}\right|\right\}.$$

Next we derive upper bounds for $I_{m,1}$ and $I_{m,2}$. To deal with $I_{m,1}$, we note that for any $1 \leq i, j \leq m$,

$$\begin{aligned}
|\hat{\pi}(x_i; p_{j\to 0}) - \hat{\pi}(x_i; p_{j\to 1})| &= \left|\left\{\frac{1}{1 + e^{-x_i^{\mathrm{T}}\hat{\beta}(p_{j\to 0})}} \vee \varepsilon_1\right\} \wedge \varepsilon_2 - \left\{\frac{1}{1 + e^{-x_i^{\mathrm{T}}\hat{\beta}(p_{j\to 1})}} \vee \varepsilon_1\right\} \wedge \varepsilon_2\right| \\
&\leq \left|\frac{1}{1 + e^{-x_i^{\mathrm{T}}\hat{\beta}(p_{j\to 0})}} - \frac{1}{1 + e^{-x_i^{\mathrm{T}}\hat{\beta}(p_{j\to 1})}}\right| \\
&\leq |x_i^{\mathrm{T}}\{\hat{\beta}(p_{j\to 0}) - \hat{\beta}(p_{j\to 1})\}|,
\end{aligned}$$

where the first inequality is due to the Lipschitz continuity of the function $f(x) = (x \vee \epsilon_1) \wedge \epsilon_2$, and the last inequality follows from an application of the mean-value theorem to the function $f(x) = (1 + e^{-x})^{-1}$. For the ease of notation, set $\hat{b}(x_i) = [\{1 - \hat{\pi}(x_i)\}/\hat{\pi}(x_i)]^{1/(1-k)}$. As $\varepsilon_1 \leq \hat{\pi} \leq \varepsilon_2$, we have $b_1 \leq \hat{b} \leq b_2$ for some constants b_1 and b_2 with $0 < b_1 \leq b_2$. It is straightforward to see that

$$\begin{aligned}
\frac{|\hat{\pi}(x_j; p_{j\to 0}) - \hat{\pi}(x_j; p_{j\to 1})|}{\hat{\tau}(p_{j\to 0})^{1/(1-k)}} &\leq \frac{|x_j^{\mathrm{T}}\{\hat{\beta}(p_{j\to 0}) - \hat{\beta}(p_{j\to 1})\}|}{\left\{k^{1/(1-k)}(1-\gamma)^{-1}\alpha^{-1}\sum_{i\neq j}\mathbb{I}(p_i > \gamma)\hat{b}(x_i; p_{j\to 0})\right\} \vee \varepsilon^{1/(1-k)}} \\
&\leq \frac{|x_j^{\mathrm{T}}\{\hat{\beta}(p_{j\to 0}) - \hat{\beta}(p_{j\to 1})\}|}{\left\{c\alpha^{-1}\sum_{i\neq j}\mathbb{I}(p_i > \gamma)\right\} \vee \varepsilon^{1/(1-k)}},
\end{aligned}$$

For $I_{m,2}$, we notice that

$$\begin{aligned}
&\left|\frac{1}{\hat{\tau}(p_{j\to 0})^{1/(1-k)}}-\frac{1}{\hat{\tau}(p_{j\to 1})^{1/(1-k)}}\right| \leq \frac{\left|\tilde{\tau}(p_{j\to 1})^{1/(1-k)}-\tilde{\tau}(p_{j\to 0})^{1/(1-k)}\right|}{\{\tilde{\tau}(p_{j\to 0})^{1/(1-k)}\vee \varepsilon^{1/(1-k)}\}\{\tilde{\tau}(p_{j\to 1})^{1/(1-k)}\vee \varepsilon^{1/(1-k)}\}} \\
=&\frac{k^{1/(1-k)}(1-\gamma)^{-1}\alpha^{-1}\left|\sum_{i\neq j}\mathbb{I}(p_i>\gamma)\{\hat{b}(x_i;p_{j\to 1})-\hat{b}(x_i;p_{j\to 0})\}+\hat{b}(x_j;p_{j\to 1})\right|}{\{\tilde{\tau}(p_{j\to 0})^{1/(1-k)}\vee \varepsilon^{1/(1-k)}\}\{\tilde{\tau}(p_{j\to 1})^{1/(1-k)}\vee \varepsilon^{1/(1-k)}\}} \\
\leq&\frac{c\alpha^{-1}\sum_{i\neq j}\mathbb{I}(p_i>\gamma)|x_i^{\mathrm{T}}\{\hat{\beta}(p_{j\to 0})-\hat{\beta}(p_{j\to 1})\}|+c\alpha^{-1}}{\left[\left\{c\alpha^{-1}\sum_{i\neq j}\mathbb{I}(p_i>\gamma)\right\}\vee \varepsilon^{1/(1-k)}\right]^2},
\end{aligned}$$

where we used the fact that $|\hat{b}(x_i;p_{j\to 1})-\hat{b}(x_i;p_{j\to 0})|\leq c|x_i^{\mathrm{T}}\{\hat{\beta}(p_{j\to 0})-\hat{\beta}(p_{j\to 1})\}|$ which follows from the mean-value theorem. Summarizing the above results, we have

$$J_m \leq c(I_{m,1}+I_{m,2}) \leq c(J_{m,1}+J_{m,2}),$$

where

$$\begin{aligned}
J_{m,1} =& \sum_{j=1}^{m}\mathbb{E}\left[\frac{|x_j^{\mathrm{T}}\{\hat{\beta}(p_{j\to 0})-\hat{\beta}(p_{j\to 1})\}|}{\left\{c\alpha^{-1}\sum_{i\neq j}\mathbb{I}(p_i>\gamma)\right\}\vee \varepsilon^{1/(1-k)}}\right], \\
J_{m,2} =& \sum_{j=1}^{m}\mathbb{E}\left(\frac{\alpha^{-1}\sum_{i\neq j}\mathbb{I}(p_i>\gamma)|x_i^{\mathrm{T}}\{\hat{\beta}(p_{j\to 0})-\hat{\beta}(p_{j\to 1})\}|+\alpha^{-1}}{\left[\left\{c\alpha^{-1}\sum_{i\neq j}\mathbb{I}(p_i>\gamma)\right\}\vee \varepsilon^{1/(1-k)}\right]^2}\right).
\end{aligned}$$

□

Proof of Proposition 2. We divide the proof into four steps. (i) Calculate the difference between the two estimating equations (EE) associated with $\hat{\beta}(p_{j\to 1})$ and $\hat{\beta}(p_{j\to 0})$; (ii) Perform Taylor expansions to extract the leading terms in the EEs; (iii) Deduce an expansion for $\hat{\beta}(p_{j\to 0})-\hat{\beta}(p_{j\to 1})$ based on the results in steps (i)–(ii); (iv) Derive the order of the remainder terms involved in the expansion of $\hat{\beta}(p_{j\to 0})-\hat{\beta}(p_{j\to 1})$.

(i) Recall that we have defined the quasi log-likelihood function

$$\sum_{i=1}^{m} \log \left[\pi(x_i)(1-\gamma)^{y_i}\gamma^{1-y_i} + \{1-\pi(x_i)\}(1-\gamma^k)^{y_i}\gamma^{k(1-y_i)} \right], \ \pi(x_i) = (1+e^{-x_i^{\mathrm{T}}\beta})^{-1}.$$

For the purpose of analysis, we use the following notation and expression instead,

$$\sum_{i=1}^{m} \log \left[q_i(\beta)(1-\gamma)^{y_i}\gamma^{1-y_i} + \{1-q_i(\beta)\}(1-\gamma^k)^{y_i}\gamma^{k(1-y_i)} \right], \ q_i(\beta) = (1+e^{-x_i^{\mathrm{T}}\beta})^{-1}.$$

The quasi-MLE $\hat{\beta}$ satisfies the estimating equation

$$\sum_{i=1}^{m} \frac{\left\{(1-\gamma)^{y_i}\gamma^{1-y_i} - (1-\gamma^k)^{y_i}\gamma^{k(1-y_i)}\right\} \nabla q_i(\hat{\beta})}{q_i(\hat{\beta})(1-\gamma)^{y_i}\gamma^{1-y_i} + \{1-q_i(\hat{\beta})\}(1-\gamma^k)^{y_i}\gamma^{k(1-y_i)}} = 0,$$

where $\nabla q_i(\beta) = x_i e^{x_i^{\mathrm{T}}\beta}/(1+e^{x_i^{\mathrm{T}}\beta})^2$. Taking the difference between the estimating equations associated with $\hat{\beta}(p_{j\to 1})$ and $\hat{\beta}(p_{j\to 0})$, we obtain

$$\begin{aligned}
&\sum_{i\neq j} \frac{\left\{(1-\gamma)^{y_i}\gamma^{1-y_i} - (1-\gamma^k)^{y_i}\gamma^{k(1-y_i)}\right\} \nabla q_i\{\hat{\beta}(p_{j\to 1})\}}{q_i\{\hat{\beta}(p_{j\to 1})\}(1-\gamma)^{y_i}\gamma^{1-y_i} + [1-q_i\{\hat{\beta}(p_{j\to 1})\}](1-\gamma^k)^{y_i}\gamma^{k(1-y_i)}} \\
&- \sum_{i\neq j} \frac{\left\{(1-\gamma)^{y_i}\gamma^{1-y_i} - (1-\gamma^k)^{y_i}\gamma^{k(1-y_i)}\right\} \nabla q_i\{\hat{\beta}(p_{j\to 0})\}}{q_i\{\hat{\beta}(p_{j\to 0})\}(1-\gamma)^{y_i}\gamma^{1-y_i} + [1-q_i\{\hat{\beta}(p_{j\to 0})\}](1-\gamma^k)^{y_i}\gamma^{k(1-y_i)}} \\
&+ \frac{(\gamma^k-\gamma)\nabla q_j\{\hat{\beta}(p_{j\to 1})\}}{q_j\{\hat{\beta}(p_{j\to 1})\}(1-\gamma) + [1-q_j\{\hat{\beta}(p_{j\to 1})\}](1-\gamma^k)} - \frac{(\gamma-\gamma^k)\nabla q_j\{\hat{\beta}(p_{j\to 0})\}}{q_j\{\hat{\beta}(p_{j\to 0})\}\gamma + [1-q_j\{\hat{\beta}(p_{j\to 0})\}]\gamma^k} = 0.
\end{aligned}$$

For the ease of notation, let $b_{0i} = (1-\gamma)^{y_i}\gamma^{1-y_i}$ and $b_{1i} = (1-\gamma^k)^{y_i}\gamma^{k(1-y_i)}$. Further define

$$\begin{aligned}
&Q_i\{\hat{\beta}(p_{j\to a})\} = q_i\{\hat{\beta}(p_{j\to a})\}b_{0i} + [1-q_i\{\hat{\beta}(p_{j\to a})\}]b_{1i}, \quad \text{for } a = 0, 1 \text{ and } i \neq j, \\
&Q_{j0}\{\hat{\beta}(p_{j\to 0})\} = q_j\{\hat{\beta}(p_{j\to 0})\}\gamma + [1-q_j\{\hat{\beta}(p_{j\to 0})\}]\gamma^k, \\
&Q_{j1}\{\hat{\beta}(p_{j\to 1})\} = q_j\{\hat{\beta}(p_{j\to 1})\}(1-\gamma) + [1-q_j\{\hat{\beta}(p_{j\to 1})\}](1-\gamma^k).
\end{aligned}$$

Then the above equation can be expressed as

$$\sum_{i\neq j}\frac{(b_{0i}-b_{1i})\left[\nabla q_i\{\hat{\beta}(p_{j\to 1})\}Q_i\{\hat{\beta}(p_{j\to 0})\}-\nabla q_i\{\hat{\beta}(p_{j\to 0})\}Q_i\{\hat{\beta}(p_{j\to 1})\}\right]}{Q_i\{\hat{\beta}(p_{j\to 1})\}Q_i\{\hat{\beta}(p_{j\to 0})\}}+ \\ (\gamma^k-\gamma)\frac{\nabla q_j\{\hat{\beta}(p_{j\to 1})\}Q_{j0}\{\hat{\beta}(p_{j\to 0})\}+\nabla q_j\{\hat{\beta}(p_{j\to 0})\}Q_{j1}\{\hat{\beta}(p_{j\to 1})\}}{Q_{j1}\{\hat{\beta}(p_{j\to 1})\}Q_{j0}\{\hat{\beta}(p_{j\to 0})\}}=0. \tag{A.2}$$

(ii) We analyze the two terms in (A.2). For the first term, we observe that

$$\begin{aligned}
&\nabla q_i\{\hat{\beta}(p_{j\to 1})\}Q_i\{\hat{\beta}(p_{j\to 0})\}-\nabla q_i\{\hat{\beta}(p_{j\to 0})\}Q_i\{\hat{\beta}(p_{j\to 1})\}\\
=&\nabla q_i\{\hat{\beta}(p_{j\to 1})\}Q_i\{\hat{\beta}(p_{j\to 0})\}-\nabla q_i\{\hat{\beta}(p_{j\to 1})\}Q_i\{\hat{\beta}(p_{j\to 1})\}+\nabla q_i\{\hat{\beta}(p_{j\to 1})\}Q_i\{\hat{\beta}(p_{j\to 1})\}\\
&-\nabla q_i\{\hat{\beta}(p_{j\to 0})\}Q_i\{\hat{\beta}(p_{j\to 1})\}\\
=&\nabla q_i\{\hat{\beta}(p_{j\to 1})\}\left[Q_i\{\hat{\beta}(p_{j\to 0})\}-Q_i\{\hat{\beta}(p_{j\to 1})\}\right]-Q_i\{\hat{\beta}(p_{j\to 1})\}\left[\nabla q_i\{\hat{\beta}(p_{j\to 0})\}-\nabla q_i\{\hat{\beta}(p_{j\to 1})\}\right].
\end{aligned}$$

By the Taylor expansion, we have

$$\begin{aligned}
&\nabla q_i\{\hat{\beta}(p_{j\to 1})\}=\nabla q_i(\beta^*)+\nabla^2 q_i(\tilde{\beta}_1)\{\hat{\beta}(p_{j\to 1})-\beta^*\},\\
&Q_i\{\hat{\beta}(p_{j\to 0})\}-Q_i\{\hat{\beta}(p_{j\to 1})\}=(b_{0i}-b_{1i})\left[q_i\{\hat{\beta}(p_{j\to 0})\}-q_i\{\hat{\beta}(p_{j\to 1})\}\right]\\
=&(b_{0i}-b_{1i})\left[\nabla q_i(\beta^*)^{\mathrm{T}}+\left\{\nabla q_i(\tilde{\beta}_2)-\nabla q_i(\beta^*)\right\}^{\mathrm{T}}\right]\{\hat{\beta}(p_{j\to 0})-\hat{\beta}(p_{j\to 1})\}\\
=&(b_{0i}-b_{1i})\left\{\nabla q_i(\beta^*)^{\mathrm{T}}+(\tilde{\beta}_2-\beta^*)^{\mathrm{T}}\nabla^2 q_i(\tilde{\beta}_3)^{\mathrm{T}}\right\}\{\hat{\beta}(p_{j\to 0})-\hat{\beta}(p_{j\to 1})\},
\end{aligned}$$

where $\nabla^2 q_i(\beta)=x_i x_i^{\mathrm{T}}e^{x_i^{\mathrm{T}}\beta}(1-e^{x_i^{\mathrm{T}}\beta})/(1+e^{x_i^{\mathrm{T}}\beta})^3$, and $\tilde{\beta}_1,\tilde{\beta}_2$ and $\tilde{\beta}_3$ are the corresponding intermediate values in the mean value theorem, which may vary with i and j. We suppress the dependence on i and j for notational simplicity. Note that the mean value theorem does not generally hold for vector-valued function. Here we are applying the mean value theorem to the scalar-valued function

$e^{x_i^{\mathrm{T}}\beta}/(1+e^{x_i^{\mathrm{T}}\beta})^2$. Using similar technique, we have

$$\begin{aligned}
&Q_i\{\hat{\beta}(p_{j\to 1})\} = (b_{0i}-b_{1i})q_i\{\hat{\beta}(p_{j\to 1})\} + b_{1i} \\
=&(b_{0i}-b_{1i})q_i(\beta^*) + b_{1i} + (b_{0i}-b_{1i})\nabla q_i(\bar{\beta}_1)^{\mathrm{T}}\{\hat{\beta}(p_{j\to 1}) - \beta^*\} \\
=&Q_i(\beta^*) + (b_{0i}-b_{1i})\nabla q_i(\bar{\beta}_1)^{\mathrm{T}}\{\hat{\beta}(p_{j\to 1}) - \beta^*\}.
\end{aligned}$$

Let $\phi_i(\beta) = e^{x_i^{\mathrm{T}}\beta}(1-e^{x_i^{\mathrm{T}}\beta})/(1+e^{x_i^{\mathrm{T}}\beta})^3$. Then $\nabla^2 q_i(\beta) = \phi_i(\beta)x_i x_i^{\mathrm{T}}$ and $\nabla\phi_i(\beta) = x_i e^{x_i^{\mathrm{T}}\beta}(1 - 4e^{x_i^{\mathrm{T}}\beta} + e^{2x_i^{\mathrm{T}}\beta})(1+e^{x_i^{\mathrm{T}}\beta})^4$. Again by the mean value theorem, we have

$$\begin{aligned}
&\nabla q_i\{\hat{\beta}(p_{j\to 0})\} - \nabla q_i\{\hat{\beta}(p_{j\to 1})\} \\
=&\left[\nabla^2 q_i(\beta^*) + \left\{\nabla^2 q_i(\bar{\beta}_2) - \nabla^2 q_i(\beta^*)\right\}\right]\{\hat{\beta}(p_{j\to 0}) - \hat{\beta}(p_{j\to 1})\} \\
=&\left[\nabla^2 q_i(\beta^*) + \left\{\phi_i(\bar{\beta}_2) - \phi_i(\beta^*)\right\}x_i x_i^{\mathrm{T}}\right]\{\hat{\beta}(p_{j\to 0}) - \hat{\beta}(p_{j\to 1})\} \\
=&\left\{\nabla^2 q_i(\beta^*) + \nabla\phi_i(\bar{\beta}_3)^{\mathrm{T}}(\bar{\beta}_2 - \beta^*)x_i x_i^{\mathrm{T}}\right\}\{\hat{\beta}(p_{j\to 0}) - \hat{\beta}(p_{j\to 1})\},
\end{aligned}$$

where $\bar{\beta}_1, \bar{\beta}_2$ and $\bar{\beta}_3$ are the corresponding intermediate values and dependent on i and j. Using the above expansions, we deduce that

$$\begin{aligned}
&\nabla q_i\{\hat{\beta}(p_{j\to 1})\}\left[Q_i\{\hat{\beta}(p_{j\to 0})\} - Q_i\{\hat{\beta}(p_{j\to 1})\}\right] \\
=&(b_{0i}-b_{1i})\left[\nabla q_i(\beta^*) + \nabla^2 q_i(\tilde{\beta}_1)\{\hat{\beta}(p_{j\to 1}) - \beta^*\}\right]\left\{\nabla q_i(\beta^*)^{\mathrm{T}} + (\tilde{\beta}_2 - \beta^*)^{\mathrm{T}}\nabla^2 q_i(\tilde{\beta}_3)^{\mathrm{T}}\right\} \\
&\{\hat{\beta}(p_{j\to 0}) - \hat{\beta}(p_{j\to 1})\} \\
=&(b_{0i}-b_{1i})\nabla q_i(\beta^*)\nabla q_i(\beta^*)^{\mathrm{T}}\{\hat{\beta}(p_{j\to 0}) - \hat{\beta}(p_{j\to 1})\} \\
&+ (b_{0i}-b_{1i})\Big[\nabla q_i(\beta^*)(\tilde{\beta}_2 - \beta^*)^{\mathrm{T}}\nabla^2 q_i(\tilde{\beta}_3)^{\mathrm{T}} + \nabla^2 q_i(\tilde{\beta}_1)\{\hat{\beta}(p_{j\to 1}) - \beta^*\} \\
&\qquad\qquad \left\{\nabla q_i(\beta^*)^{\mathrm{T}} + (\tilde{\beta}_2 - \beta^*)^{\mathrm{T}}\nabla^2 q_i(\tilde{\beta}_3)^{\mathrm{T}}\right\}\Big]\{\hat{\beta}(p_{j\to 0}) - \hat{\beta}(p_{j\to 1})\} \\
=&(b_{0i}-b_{1i})\nabla q_i(\beta^*)\nabla q_i(\beta^*)^{\mathrm{T}}\{\hat{\beta}(p_{j\to 0}) - \hat{\beta}(p_{j\to 1})\} + R_{ij}^{(1)}\{\hat{\beta}(p_{j\to 0}) - \hat{\beta}(p_{j\to 1})\},
\end{aligned}$$

and

$$
\begin{aligned}
&Q_i\{\hat{\beta}(p_{j\to 1})\}\left[\nabla q_i\{\hat{\beta}(p_{j\to 0})\}-\nabla q_i\{\hat{\beta}(p_{j\to 1})\}\right]\\
=&\left[Q_i(\beta^*)+(b_{0i}-b_{1i})\nabla q_i(\bar{\beta}_1)^{\mathrm{T}}\{\hat{\beta}(p_{j\to 1})-\beta^*\}\right]\left\{\nabla^2 q_i(\beta^*)+\nabla\phi_i(\bar{\beta}_3)^{\mathrm{T}}(\bar{\beta}_2-\beta^*)x_ix_i^{\mathrm{T}}\right\}\\
&\{\hat{\beta}(p_{j\to 0})-\hat{\beta}(p_{j\to 1})\}\\
=&Q_i(\beta^*)\nabla^2 q_i(\beta^*)\{\hat{\beta}(p_{j\to 0})-\hat{\beta}(p_{j\to 1})\}\\
&+\left[Q_i(\beta^*)\nabla\phi_i(\bar{\beta}_3)^{\mathrm{T}}(\bar{\beta}_2-\beta^*)x_ix_i^{\mathrm{T}}+(b_{0i}-b_{1i})\nabla q_i(\bar{\beta}_1)^{\mathrm{T}}\{\hat{\beta}(p_{j\to 1})-\beta^*\}\right.\\
&\qquad\left.\left\{\nabla^2 q_i(\beta^*)+\nabla\phi_i(\bar{\beta}_3)^{\mathrm{T}}(\bar{\beta}_2-\beta^*)x_ix_i^{\mathrm{T}}\right\}\right]\{\hat{\beta}(p_{j\to 0})-\hat{\beta}(p_{j\to 1})\}\\
=&Q_i(\beta^*)\nabla^2 q_i(\beta^*)\{\hat{\beta}(p_{j\to 0})-\hat{\beta}(p_{j\to 1})\}+R_{ij}^{(2)}\{\hat{\beta}(p_{j\to 0})-\hat{\beta}(p_{j\to 1})\},
\end{aligned}
$$

where

$$
\begin{aligned}
R_{ij}^{(1)}=&(b_{0i}-b_{1i})\left[\nabla q_i(\beta^*)(\tilde{\beta}_2-\beta^*)^{\mathrm{T}}\nabla^2 q_i(\tilde{\beta}_3)^{\mathrm{T}}\right.\\
&\left.+\nabla^2 q_i(\tilde{\beta}_1)\{\hat{\beta}(p_{j\to 1})-\beta^*\}\left\{\nabla q_i(\beta^*)^{\mathrm{T}}+(\tilde{\beta}_2-\beta^*)^{\mathrm{T}}\nabla^2 q_i(\tilde{\beta}_3)^{\mathrm{T}}\right\}\right],\\
R_{ij}^{(2)}=&Q_i(\beta^*)\nabla\phi_i(\bar{\beta}_3)^{\mathrm{T}}(\bar{\beta}_2-\beta^*)x_ix_i^{\mathrm{T}}\\
&+(b_{0i}-b_{1i})\nabla q_i(\bar{\beta}_1)^{\mathrm{T}}\{\hat{\beta}(p_{j\to 1})-\beta^*\}\left\{\nabla^2 q_i(\beta^*)+\nabla\phi_i(\bar{\beta}_3)^{\mathrm{T}}(\bar{\beta}_2-\beta^*)x_ix_i^{\mathrm{T}}\right\}.
\end{aligned}
$$

To deal with the second term of (A.2), we observe that

$$
\begin{aligned}
&\nabla q_j\{\hat{\beta}(p_{j\to 1})\}Q_{j0}\{\hat{\beta}(p_{j\to 0})\}\\
=&\left[\nabla q_j(\beta^*)+\nabla^2 q_j(\check{\beta}_1)\{\hat{\beta}(p_{j\to 1})-\beta^*\}\right]\left[Q_{j0}(\beta^*)+(\gamma-\gamma^k)\nabla q_j(\check{\beta}_2)^{\mathrm{T}}\{\hat{\beta}(p_{j\to 0})-\beta^*\}\right]\\
=&\nabla q_j(\beta^*)Q_{j0}(\beta^*)+(\gamma-\gamma^k)\nabla q_j(\beta^*)\nabla q_j(\check{\beta}_2)^{\mathrm{T}}\{\hat{\beta}(p_{j\to 0})-\beta^*\}\\
&+\nabla^2 q_j(\check{\beta}_1)\{\hat{\beta}(p_{j\to 1})-\beta^*\}\left[Q_{j0}(\beta^*)+(\gamma-\gamma^k)\nabla q_j(\check{\beta}_2)^{\mathrm{T}}\{\hat{\beta}(p_{j\to 0})-\beta^*\}\right]\\
=&\nabla q_j(\beta^*)Q_{j0}(\beta^*)+R_j^{(3)},
\end{aligned}
$$

and

$$
\begin{aligned}
&\nabla q_j\{\hat{\beta}(p_{j\to 0})\}Q_{j1}\{\hat{\beta}(p_{j\to 1})\} \\
=&\left[\nabla q_j(\beta^*)+\nabla^2 q_j(\check{\beta}_3)\{\hat{\beta}(p_{j\to 0})-\beta^*\}\right]\left[Q_{j1}(\beta^*)+(\gamma^k-\gamma)\nabla q_j(\check{\beta}_4)^{\mathrm{T}}\{\hat{\beta}(p_{j\to 1})-\beta^*\}\right] \\
=&\nabla q_j(\beta^*)Q_{j1}(\beta^*)+(\gamma^k-\gamma)\nabla q_j(\beta^*)\nabla q_j(\check{\beta}_4)^{\mathrm{T}}\{\hat{\beta}(p_{j\to 1})-\beta^*\} \\
&+\nabla^2 q_j(\check{\beta}_3)\{\hat{\beta}(p_{j\to 0})-\beta^*\}\left[Q_{j1}(\beta^*)+(\gamma^k-\gamma)\nabla q_j(\check{\beta}_4)^{\mathrm{T}}\{\hat{\beta}(p_{j\to 1})-\beta^*\}\right] \\
=&\nabla q_j(\beta^*)Q_{j1}(\beta^*)+R_j^{(4)},
\end{aligned}
$$

where

$$
\begin{aligned}
R_j^{(3)} =&(\gamma-\gamma^k)\nabla q_j(\beta^*)\nabla q_j(\check{\beta}_2)^{\mathrm{T}}\{\hat{\beta}(p_{j\to 0})-\beta^*\} \\
&+\nabla^2 q_j(\check{\beta}_1)\{\hat{\beta}(p_{j\to 1})-\beta^*\}\left[Q_{j0}(\beta^*)+(\gamma-\gamma^k)\nabla q_j(\check{\beta}_2)^{\mathrm{T}}\{\hat{\beta}(p_{j\to 0})-\beta^*\}\right], \\
R_j^{(4)} =&(\gamma^k-\gamma)\nabla q_j(\beta^*)\nabla q_j(\check{\beta}_4)^{\mathrm{T}}\{\hat{\beta}(p_{j\to 1})-\beta^*\} \\
&+\nabla^2 q_j(\check{\beta}_3)\{\hat{\beta}(p_{j\to 0})-\beta^*\}\left[Q_{j1}(\beta^*)+(\gamma^k-\gamma)\nabla q_j(\check{\beta}_4)^{\mathrm{T}}\{\hat{\beta}(p_{j\to 1})-\beta^*\}\right],
\end{aligned}
$$

and $\check{\beta}_1, \check{\beta}_2, \check{\beta}_3, \check{\beta}_4$ are the corresponding intermediate values in the mean value theorem which vary with i and j.

(iii) Let $v^{\otimes 2} = vv^{\mathrm{T}}$ for a vector v. Plugging the equations we obtain in step (ii) into (A.2), we get

$$
\begin{aligned}
&\sum_{i\neq j}\frac{(b_{0i}-b_{1i})\left\{(b_{0i}-b_{1i})\nabla q_i(\beta^*)^{\otimes 2}-Q_i(\beta^*)\nabla^2 q_i(\beta^*)\right\}\left\{\hat{\beta}(p_{j\to 0})-\hat{\beta}(p_{j\to 1})\right\}}{Q_i\{\hat{\beta}(p_{j\to 1})\}Q_i\{\hat{\beta}(p_{j\to 0})\}} \\
&+\sum_{i\neq j}\frac{(b_{0i}-b_{1i})(R_{ij}^{(1)}-R_{ij}^{(2)})\{\hat{\beta}(p_{j\to 0})-\hat{\beta}(p_{j\to 1})\}}{Q_i\{\hat{\beta}(p_{j\to 1})\}Q_i\{\hat{\beta}(p_{j\to 0})\}} \\
&+(\gamma^k-\gamma)\frac{\nabla q_j(\beta^*)Q_{j0}(\beta^*)+\nabla q_j(\beta^*)Q_{j1}(\beta^*)}{Q_{j1}\{\hat{\beta}(p_{j\to 1})\}Q_{j0}\{\hat{\beta}(p_{j\to 0})\}}+(\gamma^k-\gamma)\frac{R_j^{(3)}+R_j^{(4)}}{Q_{j1}\{\hat{\beta}(p_{j\to 1})\}Q_{j0}\{\hat{\beta}(p_{j\to 0})\}}=0.
\end{aligned}
\tag{A.3}
$$

Let

$$
\begin{aligned}
S_j &= \sum_{i \neq j} \frac{(b_{0i} - b_{1i}) \left\{ (b_{0i} - b_{1i}) \nabla q_i(\beta^*)^{\otimes 2} - Q_i(\beta^*) \nabla^2 q_i(\beta^*) \right\}}{Q_i\{\hat{\beta}(p_{j\to 1})\} Q_i\{\hat{\beta}(p_{j\to 0})\}}, \\
\widetilde{S}_j &= \sum_{i \neq j} \frac{(b_{0i} - b_{1i})(R_{ij}^{(1)} - R_{ij}^{(2)})}{Q_i\{\hat{\beta}(p_{j\to 1})\} Q_i\{\hat{\beta}(p_{j\to 0})\}}, \\
U_j &= (\gamma^k - \gamma) \frac{\nabla q_j(\beta^*) Q_{j0}(\beta^*) + \nabla q_j(\beta^*) Q_{j1}(\beta^*)}{Q_{j1}\{\hat{\beta}(p_{j\to 1})\} Q_{j0}\{\hat{\beta}(p_{j\to 0})\}}, \\
\widetilde{U}_j &= (\gamma^k - \gamma) \frac{R_j^{(3)} + R_j^{(4)}}{Q_{j1}\{\hat{\beta}(p_{j\to 1})\} Q_{j0}\{\hat{\beta}(p_{j\to 0})\}}.
\end{aligned}
$$

Then (A.3) can be written compactly as

$$
(S_j + \widetilde{S}_j)\{\hat{\beta}(p_{j\to 0}) - \hat{\beta}(p_{j\to 1})\} + U_j + \widetilde{U}_j = 0.
$$

Further define

$$
\begin{aligned}
S_j^* &= \sum_{i \neq j} \frac{(b_{0i} - b_{1i}) \left\{ (b_{0i} - b_{1i}) \nabla q_i(\beta^*)^{\otimes 2} - Q_i(\beta^*) \nabla^2 q_i(\beta^*) \right\}}{Q_i(\beta^*)^2}, \\
U_j^* &= (\gamma^k - \gamma) \frac{\nabla q_j(\beta^*) Q_{j0}(\beta^*) + \nabla q_j(\beta^*) Q_{j1}(\beta^*)}{Q_{j1}(\beta^*) Q_{j0}(\beta^*)}.
\end{aligned}
$$

Note that

$$
\begin{aligned}
Q_i\{\hat{\beta}(p_{j\to 1})\} &= Q_i(\beta^*) + (b_{0i} - b_{1i}) \nabla q_i(\bar{\beta}_1)^{\mathrm{T}} \{\hat{\beta}(p_{j\to 1}) - \beta^*\}, \\
Q_i\{\hat{\beta}(p_{j\to 0})\} &= Q_i(\beta^*) + (b_{0i} - b_{1i}) \nabla q_i(\bar{\beta}_0)^{\mathrm{T}} \{\hat{\beta}(p_{j\to 0}) - \beta^*\}, \\
Q_{j1}\{\hat{\beta}(p_{j\to 1})\} &= Q_{j1}(\beta^*) + (\gamma^k - \gamma) \nabla q_j(\check{\beta}_4)^{\mathrm{T}} \{\hat{\beta}(p_{j\to 1}) - \beta^*\}, \\
Q_{j0}\{\hat{\beta}(p_{j\to 0})\} &= Q_{j0}(\beta^*) + (\gamma - \gamma^k) \nabla q_j(\check{\beta}_2)^{\mathrm{T}} \{\hat{\beta}(p_{j\to 0}) - \beta^*\},
\end{aligned}
$$

where $\bar{\beta}_0$ is the corresponding intermediate value that depends on i and j, and $\bar{\beta}_1, \check{\beta}_4, \check{\beta}_2$ have been

defined before. Thus we obtain

$$\begin{aligned}
R_{ij}^{(5)} :=& Q_i(\beta^*)^2 - Q_i\{\hat{\beta}(p_{j\to 1})\}Q_i\{\hat{\beta}(p_{j\to 0})\} \\
=& - Q_i(\beta^*)(b_{0i} - b_{1i})\nabla q_i(\bar{\beta}_0)^{\mathrm{T}}\{\hat{\beta}(p_{j\to 0}) - \beta^*\} - Q_i(\beta^*)(b_{0i} - b_{1i})\nabla q_i(\bar{\beta}_1)^{\mathrm{T}}\{\hat{\beta}(p_{j\to 1}) - \beta^*\} \\
& - (b_{0i} - b_{1i})^2\nabla q_i(\bar{\beta}_1)^{\mathrm{T}}\{\hat{\beta}(p_{j\to 1}) - \beta^*\}\nabla q_i(\bar{\beta}_0)^{\mathrm{T}}\{\hat{\beta}(p_{j\to 0}) - \beta^*\},
\end{aligned}$$

and

$$\begin{aligned}
R_{j}^{(6)} :=& Q_{j1}(\beta^*)Q_{j0}(\beta^*) - Q_{j1}\{\hat{\beta}(p_{j\to 1})\}Q_{j0}\{\hat{\beta}(p_{j\to 0})\} \\
=& - Q_{j1}(\beta^*)(\gamma - \gamma^k)\nabla q_j(\check{\beta}_2)^{\mathrm{T}}\{\hat{\beta}(p_{j\to 0}) - \beta^*\} + Q_{j0}(\beta^*)(\gamma - \gamma^k)\nabla q_j(\check{\beta}_4)^{\mathrm{T}}\{\hat{\beta}(p_{j\to 1}) - \beta^*\} \\
& + (\gamma - \gamma^k)^2\nabla q_j(\check{\beta}_4)^{\mathrm{T}}\{\hat{\beta}(p_{j\to 1}) - \beta^*\}\nabla q_j(\check{\beta}_2)^{\mathrm{T}}\{\hat{\beta}(p_{j\to 0}) - \beta^*\}.
\end{aligned}$$

It implies that

$$\begin{aligned}
S_j - S_j^* &= \sum_{i\neq j} \frac{(b_{0i} - b_{1i})\left\{(b_{0i} - b_{1i})\nabla q_i(\beta^*)^{\otimes 2} - Q_i(\beta^*)\nabla^2 q_i(\beta^*)\right\} R_{ij}^{(5)}}{Q_i\{\hat{\beta}(p_{j\to 1})\}Q_i\{\hat{\beta}(p_{j\to 0})\}Q_i(\beta^*)^2}, \\
U_j - U_j^* &= (\gamma^k - \gamma)\frac{\nabla q_j(\beta^*)Q_{j0}(\beta^*) + \nabla q_j(\beta^*)Q_{j1}(\beta^*)}{Q_{j1}\{\hat{\beta}(p_{j\to 1})\}Q_{j0}\{\hat{\beta}(p_{j\to 0})\}Q_{j1}(\beta^*)Q_{j0}(\beta^*)} R_j^{(6)}.
\end{aligned}$$

Combining the above arguments, we obtain

$$(S_j^* + \Delta_j)\{\hat{\beta}(p_{j\to 0}) - \hat{\beta}(p_{j\to 1})\} + U_j^* + \Pi_j = 0,$$

where $\Delta_j = S_j - S_j^* + \widetilde{S}_j$ and $\Pi_j = U_j - U_j^* + \widetilde{U}_j$, and Δ_j, Π_j are smaller order terms.

(iv) Recall that $q_i(\beta) = (1 + e^{-x_i^{\mathrm{T}}\beta})^{-1}$, $b_{0i} = (1-\gamma)^{y_i}\gamma^{1-y_i}$, $b_{1i} = (1-\gamma^k)^{y_i}\gamma^{k(1-y_i)}$ and

$Q_i(\beta) = q_i(\beta)b_{0i} + \{1 - q_i(\beta)\}b_{1i}$. We have uniformly over i, j and $\beta \in \mathcal{B}$,

$$
\begin{aligned}
&|b_{0i} - b_{1i}| = \gamma^k - \gamma, \\
&\min\{1 - \gamma^k, \gamma\} \le Q_i(\beta) \le \max\{1 - \gamma, \gamma^k\}, \\
&\gamma \le Q_{j0}(\beta) = q_j(\beta)\gamma + \{1 - q_j(\beta)\}\gamma^k \le \gamma^k, \\
&1 - \gamma^k \le Q_{j1}(\beta) = q_j(\beta)(1 - \gamma) + \{1 - q_j(\beta)\}(1 - \gamma^k) \le 1 - \gamma,
\end{aligned}
$$

and

$$
\begin{aligned}
\|\nabla q_i(\beta)\| &= \left\| \frac{x_i e^{x_i^{\mathrm{T}}\beta}}{(1 + e^{x_i^{\mathrm{T}}\beta})^2} \right\| \le c\|x_i\|, \\
\|\nabla^2 q_i(\beta)\| &= \left\| \frac{x_i x_i^{\mathrm{T}} e^{x_i^{\mathrm{T}}\beta}(1 - e^{x_i^{\mathrm{T}}\beta})}{(1 + e^{x_i^{\mathrm{T}}\beta})^3} \right\| \le c\|x_i\|^2, \\
\|\nabla \phi_i(\beta)\| &= \left\| \frac{x_i e^{x_i^{\mathrm{T}}\beta}(1 - 4e^{x_i^{\mathrm{T}}\beta} + e^{2x_i^{\mathrm{T}}\beta})}{(1 + e^{x_i^{\mathrm{T}}\beta})^4} \right\| \le c\|x_i\|.
\end{aligned}
$$

Then we have

$$
\|S_j - S_j^*\| \le \sum_{i \ne j} \left\| \frac{(b_{0i} - b_{1i})\left\{(b_{0i} - b_{1i})\nabla q_i(\beta^*)^{\otimes 2} - Q_i(\beta^*)\nabla^2 q_i(\beta^*)\right\} R_{ij}^{(5)}}{Q_i\{\hat{\beta}(p_{j\to 1})\}Q_i\{\hat{\beta}(p_{j\to 0})\}Q_i(\beta^*)^2} \right\| \le c \sum_{i \ne j} \|x_i\|^2 \cdot |R_{ij}^{(5)}|,
$$

and

$$
\|\widetilde{S}_j\| \le \sum_{i \ne j} \left\| \frac{(b_{0i} - b_{1i})(R_{ij}^{(1)} - R_{ij}^{(2)})}{Q_i\{\hat{\beta}(p_{j\to 1})\}Q_i\{\hat{\beta}(p_{j\to 0})\}} \right\| \le c \sum_{i \ne j} \left(\|R_{ij}^{(1)}\| + \|R_{ij}^{(2)}\| \right),
$$

where

$$
\begin{aligned}
&|R_{ij}^{(5)}| \le c\|x_i\| \left\{ \|\hat{\beta}(p_{j\to 1}) - \beta^*\| + \|\hat{\beta}(p_{j\to 0}) - \beta^*\| \right\} + c\|x_i\|^2 \|\hat{\beta}(p_{j\to 1}) - \beta^*\| \|\hat{\beta}(p_{j\to 0}) - \beta^*\|, \\
&\|R_{ij}^{(1)}\| \le c\|x_i\|^3 \left\{ \|\tilde{\beta}_2 - \beta^*\| + \|\hat{\beta}(p_{j\to 1}) - \beta^*\| \right\} + c\|x_i\|^4 \|\tilde{\beta}_2 - \beta^*\| \|\hat{\beta}(p_{j\to 1}) - \beta^*\|, \\
&\|R_{ij}^{(2)}\| \le c\|x_i\|^3 \left\{ \|\bar{\beta}_2 - \beta^*\| + \|\hat{\beta}(p_{j\to 1}) - \beta^*\| \right\} + c\|x_i\|^4 \|\bar{\beta}_2 - \beta^*\| \|\hat{\beta}(p_{j\to 1}) - \beta^*\|.
\end{aligned}
$$

Similarly, we have

$$\|U_j - U_j^*\| \leq c\|x_j\|\|R_j^{(6)}\| \quad \text{and} \quad \|\widetilde{U}_j\| \leq c\left(\|R_j^{(3)}\| + \|R_j^{(4)}\|\right),$$

where

$$\|R_j^{(6)}\| \leq c\|x_j\|\left\{\|\hat{\beta}(p_{j\to 1}) - \beta^*\| + \|\hat{\beta}(p_{j\to 0}) - \beta^*\|\right\} + c\|x_j\|^2\|\hat{\beta}(p_{j\to 1}) - \beta^*\|\|\hat{\beta}(p_{j\to 0}) - \beta^*\|,$$
$$\|R_j^{(3)}\| \leq c\|x_j\|^2\left\{\|\hat{\beta}(p_{j\to 1}) - \beta^*\| + \|\hat{\beta}(p_{j\to 0}) - \beta^*\|\right\} + c\|x_j\|^3\|\hat{\beta}(p_{j\to 1}) - \beta^*\|\|\hat{\beta}(p_{j\to 0}) - \beta^*\|,$$
$$\|R_j^{(4)}\| \leq c\|x_j\|^2\left\{\|\hat{\beta}(p_{j\to 1}) - \beta^*\| + \|\hat{\beta}(p_{j\to 0}) - \beta^*\|\right\} + c\|x_j\|^3\|\hat{\beta}(p_{j\to 1}) - \beta^*\|\|\hat{\beta}(p_{j\to 0}) - \beta^*\|.$$

As we assume that $\sup_{1\leq i\leq m}\mathbb{E}(\|x_i\|^8) < \infty$, then by Kolmogorov's strong law of large numbers, we know that $\sup_{1\leq j\leq m}\sum_{i\neq j}\|x_i\|^3 = O_{\mathbb{P}}(m)$ and $\sup_{1\leq j\leq m}\sum_{i\neq j}\|x_i\|^4 = O_{\mathbb{P}}(m)$. Combining the above inequalities with the result from Lemma 2 that $\sup_{1\leq j\leq m}|\hat{\beta}(p_{j\to a}) - \beta^*| = o_{\mathbb{P}}(1)$, we deduce that

$$S_j^* = \sum_{i\neq j}\frac{(b_{0i} - b_{1i})\left\{(b_{0i} - b_{1i})\nabla q_i(\beta^*)^{\otimes 2} - Q_i(\beta^*)\nabla^2 q_i(\beta^*)\right\}}{Q_i(\beta^*)^2} = -\sum_{i\neq j}\nabla^2 l(\beta^*; z_i),$$
$$\sup_{1\leq j\leq m}\|U_j^*\| = \sup_{1\leq j\leq m}\left\|(\gamma^k - \gamma)\frac{\nabla q_j(\beta^*)Q_{j0}(\beta^*) + \nabla q_j(\beta^*)Q_{j1}(\beta^*)}{Q_{j1}(\beta^*)Q_{j0}(\beta^*)}\right\| \leq c\sup_{1\leq j\leq m}\|x_j\| = O_{\mathbb{P}}(1), \tag{A.4}$$

and

$$\begin{aligned}\sup_{1\le j\le m}\|\Delta_j\| \le& \sup_{1\le j\le m}\Big(\|S_j - S_j^*\| + \|\widetilde{S}_j\|\Big) \le c \sup_{1\le j\le m}\sum_{i\neq j}\Big(\|x_i\|^2\cdot|R_{ij}^{(5)}| + \|R_{ij}^{(1)}\| + \|R_{ij}^{(2)}\|\Big)\\ \le& c\sup_{1\le j\le m}\Big\{\|\hat\beta(p_{j\to1}) - \beta^*\| + \|\hat\beta(p_{j\to0}) - \beta^*\|\Big\}\sum_{i\neq j}\|x_i\|^3\\ &+ c\sup_{1\le j\le m}\|\hat\beta(p_{j\to1}) - \beta^*\|\|\hat\beta(p_{j\to0}) - \beta^*\|\sum_{i\neq j}\|x_i\|^4\\ =& o_{\mathbb{P}}(m),\end{aligned} \tag{A.5}$$

$$\begin{aligned}\sup_{1\le j\le m}\|\Pi_j\| \le& \sup_{1\le j\le m}\Big(\|U_j - U_j^*\| + \|\widetilde{U}_j\|\Big) \le c \sup_{1\le j\le m}\Big(\|x_j\|\|R_j^{(6)}\| + \|R_j^{(3)}\| + \|R_j^{(4)}\|\Big)\\ \le& c\sup_{1\le j\le m}\Big\{\|\hat\beta(p_{j\to1}) - \beta^*\| + \|\hat\beta(p_{j\to0}) - \beta^*\|\Big\}\|x_j\|^2\\ &+ c\sup_{1\le j\le m}\|\hat\beta(p_{j\to1}) - \beta^*\|\|\hat\beta(p_{j\to0}) - \beta^*\|\|x_j\|^3\\ =& o_{\mathbb{P}}(1).\end{aligned} \tag{A.6}$$

□

A.4 Other intermediate results

Lemma 3. *For a sequence of independent random variables* $\{W_i\}_{i=1}^m$*, if* $\sup_{1\le i\le m}\mathbb{E}(|W_i|^{q+\epsilon}) < \infty$ *for some* $q \ge 1$ *and any* $\epsilon > 0$*, then we have*

$$\frac{1}{m}\sup_{1\le i\le m}\mathbb{E}\left\{|W_i|^{u+1}\mathbb{I}(|W_i|\le m)\right\} \to 0,$$

for any $0 < u \le q$.

Proof. Since $\sup_{1\le i\le m}\mathbb{E}(|W_i|^{q+\epsilon}) < \infty$ implies $\sup_{1\le i\le m}\mathbb{E}(|W_i|^{u+\epsilon}) < \infty$ for any $u < q$, we only need to show

$$\frac{1}{m}\sup_{1\le i\le m}\mathbb{E}\left\{|W_i|^{q+1}\mathbb{I}(|W_i|\le m)\right\} \to 0.$$

Let $F_i(w)$ be the distribution function of W_i. It shows that

$$\begin{aligned}
&\mathbb{E}\left\{|W_i|^{q+1}\mathbb{I}(|W_i|\le m)\right\} = \int_{|w|\le m} |w|^{q+1}\mathrm{d}F_i(w)\\
=&(q+1)\int_{|w|\le m}\int_0^{|w|} s^q\mathrm{d}s\ \mathrm{d}F_i(w) \overset{\text{Fubini}}{=} (q+1)\int_0^m \int_{s<|w|\le m} \mathrm{d}F_i(w)\ s^q\mathrm{d}s\\
=&(q+1)\int_0^m \left\{\mathbb{P}\left(|W_i|>s\right)-\mathbb{P}\left(|W_i|>m\right)\right\} s^q\mathrm{d}s\\
\le&(q+1)\int_0^m \mathbb{P}\left(|W_i|>s\right) s^q\mathrm{d}s \le (q+1)\int_0^m \mathbb{E}\left(\frac{|W_i|^{q+\epsilon}}{s^{q+\epsilon}}\right) s^q\mathrm{d}s\\
=&(q+1)\mathbb{E}(|W_i|^{q+\epsilon})\frac{m^{1-\epsilon}}{1-\epsilon},
\end{aligned}$$

which directly implies the desired result. □

Lemma 4. *Consider a sequence of independent random variables* $\{W_i\}_{i=1}^m$ *with* $\mathbb{E}(W_i)=0$ *and* $\sup_{1\le i\le m}\mathbb{E}(|W_i|^{q+\epsilon})<\infty$ *for some* $q\ge 2$ *and any* $\epsilon>0$*. Then for every* $t>0$*, we have*

$$\mathbb{P}\left(\left|\sum_{i=1}^m W_i\right|>mt\right)=o(m^{1-q}).$$

Furthermore, we have

$$\mathbb{P}\left(\sup_{1\le j\le m}\left|\sum_{i\ne j} W_i\right|>mt\right)=o(m^{1-q}).$$

If W_i*'s are not necessarily mean-zero, we get* $\sup_{1\le j\le m}\sum_{i\ne j}W_i = O_{\mathbb{P}}(m)$.

Remark 4. *As seen from the proof, we can replace the condition that* $\sup_{1\le i\le m}\mathbb{E}(|W_i|^{q+\epsilon})<\infty$ *for some* $q\ge 2$ *and any* $\epsilon>0$ *in Lemma 4 by a weaker condition that* $\sup_{1\le i\le m}\mathbb{E}(|W_i|^{q})<\infty$ *for some* $q\ge 2$ *and* $\{|W_i|^q\}_{i=1}^m$ *are uniformly integrable.*

Proof. Let $W_{m,i}=W_i\mathbb{I}(|W_i|\le m)$ and $W'_{m,i}=W_{m,i}-\mathbb{E}(W_{m,i})$. Further define $T_m=\sum_{i=1}^m W_i$,

$\widehat{T}_m = \sum_{i=1}^m W_{m,i}$ and $T'_m = \sum_{i=1}^m W'_{m,i}$. Note that

$$
\begin{aligned}
&m^{q-1}\mathbb{P}\left(|T_m| > mt\right) = m^{q-1}\mathbb{P}\left(|T_m - \widehat{T}_m + \widehat{T}_m - T'_m + T'_m| > mt\right) \\
\leq &m^{q-1}\left\{\mathbb{P}\left(|T_m - \widehat{T}_m| > mt/3\right) + \mathbb{P}\left(|\widehat{T}_m - T'_m| > mt/3\right) + \mathbb{P}\left(|T'_m| > mt/3\right)\right\}.
\end{aligned}
$$

We show the first term in the above inequality converges to 0 by proving $\mathbb{P}(T_m \neq \widehat{T}_m) = o(m^{1-q})$. To see this, note that

$$
\begin{aligned}
&m^{q-1}\mathbb{P}\left(T_m \neq \widehat{T}_m\right) \leq m^{q-1}\mathbb{P}\left\{\bigcup_{i=1}^m (W_i \neq W_{m,i})\right\} \\
\leq &m^{q-1}\sum_{i=1}^m \mathbb{P}\left(W_i \neq W_{m,i}\right) = m^{q-1}\sum_{i=1}^m \mathbb{P}\left(|W_i| > m\right) \\
\leq &m^{q-1}\sum_{i=1}^m \mathbb{E}\left(\frac{|W_i|^{q+\epsilon}}{m^{q+\epsilon}}\right) \leq \frac{m \sup_{1\leq i\leq m}\mathbb{E}(|W_i|^{q+\epsilon})}{m^{1+\epsilon}} \to 0.
\end{aligned}
$$

To prove $m^{q-1}\mathbb{P}(|\widehat{T}_m - T'_m| > mt/3) \to 0$, we note that

$$
\begin{aligned}
&\sup_{1\leq i\leq m}|\mathbb{E}(W_{m,i})| = \sup_{1\leq i\leq m}|\mathbb{E}\left\{W_i\mathbb{I}(|W_i| \leq m)\right\}| = \sup_{1\leq i\leq m}|\mathbb{E}\left\{W_i\mathbb{I}(|W_i| > m)\right\}| \\
\leq &\sup_{1\leq i\leq m}\mathbb{E}\left\{\frac{|W_i|^{1+\epsilon}}{m^\epsilon}\mathbb{I}(|W_i| > m)\right\} \leq \frac{\sup_{1\leq i\leq m}\mathbb{E}(|W_i|^{1+\epsilon})}{m^\epsilon} \to 0,
\end{aligned}
$$

and

$$
|\widehat{T}_m - T'_m| = \left|\sum_{i=1}^m \mathbb{E}(W_{m,i})\right| \leq m \sup_{1\leq i\leq m}|\mathbb{E}(W_{m,i})|.
$$

Hence $\mathbb{P}(|\widehat{T}_m - T'_m| > mt/3) = 0$ as long as m is large enough. Therefore, to show $\mathbb{P}\left(|T_m| > mt\right) =$

$o(m^{1-q})$, we only need to prove $m^{q-1}\mathbb{P}\left(|T'_m| > mt\right) \to 0$. Note that

$$\begin{aligned} & m^{q-1}\mathbb{P}\left(|T'_m| > mt\right) \leq m^{q-1}\frac{\mathbb{E}(|T'_m|^{2q})}{m^{2q}t^{2q}} \\ \leq & \frac{c}{m^{q+1}t^{2q}}\left[\sum_{i=1}^{m}\mathbb{E}(|W'_{m,i}|^{2q}) + \left\{\sum_{i=1}^{m}\mathbb{E}(|W'_{m,i}|^{2})\right\}^{q}\right], \end{aligned}$$

where the last inequality follows from Rosenthal's inequality. For the first term, we have

$$\begin{aligned} & \frac{c}{m^{q+1}t^{2q}}\sum_{i=1}^{m}\mathbb{E}(|W'_{m,i}|^{2q}) \leq \frac{2^{q-1}c}{m^{2}t^{2q}}\sum_{i=1}^{m}\mathbb{E}(|W'_{m,i}|^{q+1}) \\ \leq & \frac{2^{q-1}c}{m^{2}t^{2q}}\sum_{i=1}^{m}\mathbb{E}\left[\{|W_{m,i}| + |\mathbb{E}(W_{m,i})|\}^{q+1}\right] \to 0, \end{aligned}$$

where we have used the result of Lemma 3 and the fact that $\sup_{1\leq i\leq m}|\mathbb{E}(W_{m,i})| \to 0$. For the second term, we deduce that

$$\begin{aligned} & \frac{c}{m^{q+1}t^{2q}}\left\{\sum_{i=1}^{m}\mathbb{E}(|W'_{m,i}|^{2})\right\}^{q} \leq \frac{c}{m^{q+1}t^{2q}}\left\{\sum_{i=1}^{m}\mathbb{E}(|W_{m,i}|^{2})\right\}^{q} \\ \leq & \frac{c}{m^{q+1}t^{2q}}\left\{m\sup_{1\leq i\leq m}\mathbb{E}(|W_i|^{2})\right\}^{q} \to 0. \end{aligned}$$

Thus we have proved that $\mathbb{P}\left(|T_m| > mt\right) = o(m^{1-q})$. Furthermore, we have

$$\begin{aligned} \mathbb{P}\left(\sup_{1\leq j\leq m}\left|\sum_{i\neq j}W_i\right| > mt\right) \leq & \mathbb{P}\left(|T_m| > mt/2\right) + \mathbb{P}\left(\sup_{1\leq j\leq m}|W_j| > mt/2\right) \\ \leq & o(m^{1-q}) + \sum_{i=1}^{m}\frac{\mathbb{E}(|W_i|^{q})}{(mt/2)^{q}} = o(m^{1-q}), \end{aligned}$$

which indicates that $\sup_{1\leq j\leq m}\sum_{i\neq j}W_i = o_{\mathbb{P}}(m)$. If W_i's are not necessarily mean-zero, then

$$\begin{aligned} & \left|\sup_{1\leq j\leq m}\sum_{i\neq j}W_i\right| = \left|\sup_{1\leq j\leq m}\sum_{i\neq j}\{W_i - \mathbb{E}(W_i) + \mathbb{E}(W_i)\}\right| \\ \leq & \left|\sup_{1\leq j\leq m}\sum_{i\neq j}\{W_i - \mathbb{E}(W_i)\}\right| + \left|\sup_{1\leq j\leq m}\sum_{i\neq j}\mathbb{E}(W_i)\right| \leq o_{\mathbb{P}}(m) + \sum_{i=1}^{m}\mathbb{E}(|W_i|) = O_{\mathbb{P}}(m). \end{aligned}$$

□

Proposition 3. *Assume that* $\sup_{1\le i\le m}\mathbb{E}(\|x_i\|^{q'+\epsilon})<\infty$ *for some* q' *and any* $\epsilon>0$*. Then we have*

$$\begin{aligned}
&\sup_{1\le j\le m}\mathbb{P}\left\{\left\|\frac{S_j^*}{m}-\mathbb{E}\left(\frac{S_j^*}{m}\right)\right\|>t\right\}=o(m^{1-q}),\quad \textit{if } q'=2q,\\
&\sup_{1\le j\le m}\mathbb{P}\left\{\left|\frac{\sum_{i\neq j}\|x_i\|^3}{m}-\mathbb{E}\left(\frac{\sum_{i\neq j}\|x_i\|^3}{m}\right)\right|>t\right\}=o(m^{1-q}),\quad \textit{if } q'=3q,\\
&\sup_{1\le j\le m}\mathbb{P}\left\{\left|\frac{\sum_{i\neq j}\|x_i\|^4}{m}-\mathbb{E}\left(\frac{\sum_{i\neq j}\|x_i\|^4}{m}\right)\right|>t\right\}=o(m^{1-q}),\quad \textit{if } q'=4q,
\end{aligned}$$

where $q\ge 2$*.*

Proof. Let $\|A\|_F$ be Frobenius norm of a matrix A. Recall that $S_j^*=-\sum_{i\neq j}\nabla^2 l(\beta^*;z_i)=\sum_{i\neq j}h(\beta^*;z_i)x_ix_i^{\mathrm{T}}$ for some function h, where $h(\beta;z)$ is uniformly bounded over β and z . For any $t>0$,

$$\begin{aligned}
&\mathbb{P}\left\{\left\|\frac{S_j^*}{m}-\mathbb{E}\left(\frac{S_j^*}{m}\right)\right\|>t\right\}\le\mathbb{P}\left\{\left\|\frac{S_j^*}{m}-\mathbb{E}\left(\frac{S_j^*}{m}\right)\right\|_F>t\right\}\\
\le&\sum_{u=1}^d\sum_{v=1}^d\mathbb{P}\left\{\left|\frac{S_j^*(u,v)}{m}-\mathbb{E}\left(\frac{S_j^*(u,v)}{m}\right)\right|^2>\frac{t^2}{d^2}\right\}\\
=&\sum_{u=1}^d\sum_{v=1}^d\mathbb{P}\left\{\left|\frac{S_j^*(u,v)}{m}-\mathbb{E}\left(\frac{S_j^*(u,v)}{m}\right)\right|>\frac{t}{d}\right\}\\
=&\sum_{u=1}^d\sum_{v=1}^d\mathbb{P}\left[\left|\frac{1}{m}\sum_{i\neq j}h(\beta^*;z_i)x_i(u)x_i(v)-\frac{1}{m}\sum_{i\neq j}\mathbb{E}\left\{h(\beta^*;z_i)x_i(u)x_i(v)\right\}\right|>\frac{t}{d}\right],
\end{aligned}$$

where $S_j^*(u,v)$ is the (u,v)th element of the matrix S_j^*. For $q\ge 2$ and any $\epsilon>0$, by Hölder inequality, we have

$$\begin{aligned}
\sup_{1\le i\le m}\mathbb{E}\left\{|h(\beta^*;z_i)x_i(u)x_i(v)|^{q+\epsilon}\right\}\le&c\sup_{1\le i\le m}\mathbb{E}\left\{|x_i(u)|^{2(q+\epsilon)}\right\}^{\frac{1}{2}}\mathbb{E}\left\{|x_i(v)|^{2(q+\epsilon)}\right\}^{\frac{1}{2}}\\
\le&c\sup_{1\le i\le m}\mathbb{E}\left\{\|x_i\|^{2(q+\epsilon)}\right\}.
\end{aligned}$$

Then proof is completed by applying the result of Lemma 4. □

Lemma 5. *If Assumption 2 holds and* $\sup_{1\leq i\leq m}\mathbb{E}(\|x_i\|^2)<\infty$*, then*

$$\mathbb{E}\left[\sup_{\beta\in\mathcal{B}}|\mathbb{P}_m l(\beta)-\mathbb{E}\left\{\mathbb{P}_m l(\beta)\right\}|\right]=O(m^{-\frac{1}{2}}).$$

Proof. Let e_i be i.i.d Rademacher variables. By symmetrization argument, we have

$$\mathbb{E}\left[\sup_{\beta\in\mathcal{B}}|\mathbb{P}_m l(\beta)-\mathbb{E}\left\{\mathbb{P}_m l(\beta)\right\}|\right]\leq\frac{2}{\sqrt{m}}\mathbb{E}\left[\mathbb{E}\left\{\sup_{\beta\in\mathcal{B}}\left|\frac{1}{\sqrt{m}}\sum_{i=1}^{m}e_i l(\beta;z_i)\right|\mid z_1,...,z_m\right\}\right].$$

Define $\mathcal{E}_{m,\beta}=\sum_{i=1}^{m}e_i l(\beta;z_i)/\sqrt{m}$. Then

$$\begin{aligned}
&\mathbb{E}\left[\exp\{\lambda(\mathcal{E}_{m,\beta_1}-\mathcal{E}_{m,\beta_2})\}\mid z_1,...,z_m\right]=\prod_{i=1}^{m}\mathbb{E}\left(\exp\left[\frac{\lambda}{\sqrt{m}}e_i\left\{l(\beta_1;z_i)-l(\beta_2;z_i)\right\}\right]\mid z_1,...,z_m\right)\\
\leq&\prod_{i=1}^{m}\exp\left[\frac{\lambda^2}{2m}\left\{l(\beta_1;z_i)-l(\beta_2;z_i)\right\}^2\right]=\exp\left[\frac{\lambda^2}{2}\frac{1}{m}\sum_{i=1}^{m}\left\{l(\beta_1;z_i)-l(\beta_2;z_i)\right\}^2\right]\\
\leq&\exp\left(\frac{\lambda^2}{2}\frac{1}{m}\sum_{i=1}^{m}c\|x_i\|^2\|\beta_1-\beta_2\|^2\right)=\exp\left(\frac{\lambda^2}{2}\|\beta_1-\beta_2\|^2\rho_m^2\right),
\end{aligned}$$

where $\rho_m^2=\sum_{i=1}^{m}c\|x_i\|^2/m$. Define

$$\begin{aligned}
N(\mathcal{B},\|\cdot\|,\epsilon)=\inf\Big\{&N:\text{there exists a set }\{\beta_i\}_{i=1}^{N},\\
&\text{such that for any }\beta\in\mathcal{B},\ \text{there exists an }i,\ \text{s.t. }\|\beta-\beta_i\|\leq\epsilon\Big\}
\end{aligned}$$

and $\text{diam}(\mathcal{B})=\sup\{\|\beta_1-\beta_2\|:\beta_1,\beta_2\in\mathcal{B}\}$. By Dudley's entropy integral, we have

$$\mathbb{E}\left(\sup_{\beta\in\mathcal{B}}|\mathcal{E}_{m,\beta}|\mid z_1,...,z_m\right)\leq 4\sqrt{2}\int_0^{\frac{\text{diam}(\mathcal{B})\rho_m}{2}}\sqrt{\log\left\{N\left(\mathcal{B},\|\cdot\|,\frac{\epsilon}{\rho_m}\right)\right\}}d\epsilon,$$

Set $u=2\epsilon/\{\text{diam}(\mathcal{B})\rho_m\}$ and note that $\log N(\mathcal{B},\|\cdot\|,\epsilon)\leq d\log\{1+2\text{diam}(\mathcal{B})/\epsilon\}$. We deduce

that

$$\mathbb{E}\left[\sup_{\beta\in\mathcal{B}}|\mathbb{P}_m l(\beta)-\mathbb{E}\left\{\mathbb{P}_m l(\beta)\right\}|\right]\leq\frac{8\sqrt{2}}{\sqrt{m}}\mathbb{E}\left[\int_0^{\frac{\text{diam}(\mathcal{B})\rho_m}{2}}\sqrt{\log\left\{N\left(\mathcal{B},\|\cdot\|,\frac{\epsilon}{\rho_m}\right)\right\}}d\epsilon\right]$$
$$=\frac{8\sqrt{2}}{\sqrt{m}}\mathbb{E}\left[\int_0^1\sqrt{\log\left\{N\left(\mathcal{B},\|\cdot\|,\frac{\text{diam}(\mathcal{B})u}{2}\right)\right\}}\frac{\text{diam}(\mathcal{B})\rho_m}{2}du\right]$$
$$\leq\frac{4\sqrt{2}}{\sqrt{m}}\text{diam}(\mathcal{B})\mathbb{E}\left\{\rho_m\int_0^1\sqrt{d\log\left(1+\frac{4}{u}\right)}du\right\}=cm^{-\frac{1}{2}}\mathbb{E}(\rho_m)=O(m^{-\frac{1}{2}}).$$

□

Lemma 6. *For two functions f and g defined on the same space $\mathcal{W}$, we have*

$$\left|\sup_{w\in\mathcal{W}}f(w)-\sup_{w\in\mathcal{W}}g(w)\right|\leq\sup_{w\in\mathcal{W}}|f(w)-g(w)|.$$

Proof. Note that

$$\sup_{w\in\mathcal{W}}f(w)-\sup_{w\in\mathcal{W}}g(w)=\sup_{w\in\mathcal{W}}\inf_{w'\in\mathcal{W}}\{f(w)-g(w')\}$$
$$\leq\sup_{w\in\mathcal{W}}\{f(w)-g(w)\}\leq\sup_{w\in\mathcal{W}}|f(w)-g(w)|,$$

and similarly,

$$\sup_{w\in\mathcal{W}}g(w)-\sup_{w\in\mathcal{W}}f(w)\leq\sup_{w\in\mathcal{W}}|f(w)-g(w)|,$$

which completes the proof. □

Proposition 4. *Suppose the following conditions are satisfied:*

(i) Assumptions 2–4 hold;

(ii) we have $\sup_{1\leq i\leq m}\mathbb{E}(\|x_i\|^2)<\infty$*;*

(iii) for some $\nu>0$*, we have* $\sup_{\beta\in\mathcal{B}}|\mathbb{E}\left\{\mathbb{P}_m l(\beta)\right\}-\mathcal{L}(\beta)|=O(m^{-\nu})$*;*

(iv) the function $\mathcal{L}(\beta)$ *is twice continuously differentiable;*

(v) the global maximizerβ^* is not on the boundary of $\mathcal{B}$; and

(vi) for some $c > 0$, we have $\nabla^2 \mathcal{L}(\beta^*) \preceq -cI$, where I is the identity matrix.

Then for $t = O(m^{-\omega})$ with $0 < \omega < (\nu/2) \wedge (1/4)$, we have for $a = 0, 1$,

$$\mathbb{P}\left\{ \sup_{1 \le j \le m} \|\hat{\beta}(p_{j\to a}) - \beta^*\| > t \right\} \le \exp[-c\{t^4 + o(t^4)\}m].$$

Proof. Under Assumption 4 and Conditions (iv)–(vi), we know that there exists δ such that for all $\|\beta - \beta^*\| \le \delta$, we have $\bigtriangledown^2 \mathcal{L}(\beta) \preceq -cI$ for some constant $c > 0$. Under Condition (v) and by the Taylor expansion, we have

$$\begin{aligned}
\mathcal{L}(\beta) =& \mathcal{L}(\beta^*) + (\beta - \beta^*)^{\mathrm{T}} \bigtriangledown^2 \mathcal{L}(\tilde{\beta})(\beta - \beta^*)/2 \\
\le& \mathcal{L}(\beta^*) - c\|\beta - \beta^*\|^2.
\end{aligned}$$

Then for small enough t with $t \le \delta$, we have

$$\begin{aligned}
\mathcal{L}(\beta^*) - \sup_{\beta:\|\beta-\beta^*\|>t} \mathcal{L}(\beta) =& \mathcal{L}(\beta^*) - \max\left\{ \sup_{\beta:\|\beta-\beta^*\|\ge\delta} \mathcal{L}(\beta), \sup_{\beta:t<\|\beta-\beta^*\|<\delta} \mathcal{L}(\beta) \right\} \\
\ge& \mathcal{L}(\beta^*) - \max\left\{ \mathcal{L}(\beta^*) - c, \mathcal{L}(\beta^*) - ct^2 \right\} \\
\ge& \min\{c, ct^2\} = ct^2.
\end{aligned}$$

For any $\beta \in \mathcal{B}$ and $z_1, z_2 \in \mathbb{R}^d \times \{0, 1\}$, $|l(\beta; z_1) - l(\beta; z_2)| \le L$. Applying the result of Lemma

6, we have

$$
\begin{aligned}
&\left| \sup_{\beta\in\mathcal{B}} \left| \frac{1}{m} \left\{ \sum_{i\neq j} l(\beta; z_i) + l(\beta; z_j) \right\} - \mathbb{E}\left\{ \mathbb{P}_m l(\beta) \right\} \right| \right. \\
&\left. - \sup_{\beta\in\mathcal{B}} \left| \frac{1}{m} \left\{ \sum_{i\neq j} l(\beta; z_i) + l(\beta; z'_j) \right\} - \mathbb{E}\left\{ \mathbb{P}_m l(\beta) \right\} \right| \right| \\
\leq &\sup_{\beta\in\mathcal{B}} \left| \left| \frac{1}{m} \left\{ \sum_{i\neq j} l(\beta; z_i) + l(\beta; z_j) \right\} - \mathbb{E}\left\{ \mathbb{P}_m l(\beta) \right\} \right| - \left| \frac{1}{m} \left\{ \sum_{i\neq j} l(\beta; z_i) + l(\beta; z'_j) \right\} - \mathbb{E}\left\{ \mathbb{P}_m l(\beta) \right\} \right| \right| \\
\leq &\sup_{\beta\in\mathcal{B}} \left| \frac{l(\beta; z_j)}{m} - \frac{l(\beta; z'_j)}{m} \right| \leq \frac{L}{m},
\end{aligned}
$$

which means that $\sup_{\beta\in\mathcal{B}} |\mathbb{P}_m l(\beta) - \mathbb{E}\{\mathbb{P}_m l(\beta)\}|$ is L/m-bounded difference function. Note that

$$
\begin{aligned}
&\mathbb{P}(\|\hat{\beta} - \beta^*\| > t) \\
\leq &\mathbb{P}\left\{ \sup_{\beta:\|\beta-\beta^*\|>t} \mathbb{P}_m l(\beta) > \mathbb{P}_m l(\beta^*) \right\} \\
\leq &\mathbb{P}\left(\sup_{\beta:\|\beta-\beta^*\|>t} \left[\mathbb{P}_m l(\beta) - \mathbb{E}\left\{ \mathbb{P}_m l(\beta) \right\} \right] + \sup_{\beta:\|\beta-\beta^*\|>t} \mathbb{E}\left\{ \mathbb{P}_m l(\beta) \right\} \right. \\
&\qquad \left. > \mathbb{P}_m l(\beta^*) - \mathbb{E}\left\{ \mathbb{P}_m l(\beta^*) \right\} + \mathbb{E}\left\{ \mathbb{P}_m l(\beta^*) \right\} \right) \\
= &\mathbb{P}\left(\sup_{\beta:\|\beta-\beta^*\|>t} \left[\mathbb{P}_m l(\beta) - \mathbb{E}\left\{ \mathbb{P}_m l(\beta) \right\} \right] - \left[\mathbb{P}_m l(\beta^*) - \mathbb{E}\left\{ \mathbb{P}_m l(\beta^*) \right\} \right] \right. \\
&\qquad \left. > \mathbb{E}\left\{ \mathbb{P}_m l(\beta^*) \right\} - \sup_{\beta:\|\beta-\beta^*\|>t} \mathbb{E}\left\{ \mathbb{P}_m l(\beta) \right\} \right) \\
\leq &\mathbb{P}\left[2 \sup_{\beta\in\mathcal{B}} |\mathbb{P}_m l(\beta) - \mathbb{E}\left\{ \mathbb{P}_m l(\beta) \right\}| > \mathbb{E}\left\{ \mathbb{P}_m l(\beta^*) \right\} - \sup_{\beta:\|\beta-\beta^*\|>t} \mathbb{E}\left\{ \mathbb{P}_m l(\beta) \right\} \right],
\end{aligned}
$$

and

$$
\begin{aligned}
&\mathbb{E}\left\{\mathbb{P}_m l(\beta^*)\right\} - \sup_{\beta:\|\beta-\beta^*\|>t} \mathbb{E}\left\{\mathbb{P}_m l(\beta)\right\} \\
=&\mathbb{E}\left\{\mathbb{P}_m l(\beta^*)\right\} - \mathcal{L}(\beta^*) + \mathcal{L}(\beta^*) - \sup_{\beta:\|\beta-\beta^*\|>t} \mathcal{L}(\beta) + \sup_{\beta:\|\beta-\beta^*\|>t} \mathcal{L}(\beta) - \sup_{\beta:\|\beta-\beta^*\|>t} \mathbb{E}\left\{\mathbb{P}_m l(\beta)\right\} \\
\geq& -\left|\mathbb{E}\left\{\mathbb{P}_m l(\beta^*)\right\} - \mathcal{L}(\beta^*)\right| + \mathcal{L}(\beta^*) - \sup_{\beta:\|\beta-\beta^*\|>t} \mathcal{L}(\beta) - \sup_{\beta:\|\beta-\beta^*\|>t} \left|\mathbb{E}\left\{\mathbb{P}_m l(\beta)\right\} - \mathcal{L}(\beta)\right| \\
\geq& \mathcal{L}(\beta^*) - \sup_{\beta:\|\beta-\beta^*\|>t} \mathcal{L}(\beta) - 2\sup_{\beta\in\mathcal{B}} \left|\mathbb{E}\left\{\mathbb{P}_m l(\beta)\right\} - \mathcal{L}(\beta)\right| \\
\geq& ct^2 - 2\sup_{\beta\in\mathcal{B}} \left|\mathbb{E}\left\{\mathbb{P}_m l(\beta)\right\} - \mathcal{L}(\beta)\right|,
\end{aligned}
$$

where we have applied the result of Lemma 6 in the first inequality. We deduce that

$$
\begin{aligned}
&\mathbb{P}(\|\hat{\beta} - \beta^*\| > t) \\
\leq& \mathbb{P}\left[\sup_{\beta\in\mathcal{B}} \left|\mathbb{P}_m l(\beta) - \mathbb{E}\left\{\mathbb{P}_m l(\beta)\right\}\right| > ct^2 - \sup_{\beta\in\mathcal{B}} \left|\mathbb{E}\left\{\mathbb{P}_m l(\beta)\right\} - \mathcal{L}(\beta)\right|\right] \\
=& \mathbb{P}\Bigg(\sup_{\beta\in\mathcal{B}} \left|\mathbb{P}_m l(\beta) - \mathbb{E}\left\{\mathbb{P}_m l(\beta)\right\}\right| - \mathbb{E}\left[\sup_{\beta\in\mathcal{B}} \left|\mathbb{P}_m l(\beta) - \mathbb{E}\left\{\mathbb{P}_m l(\beta)\right\}\right|\right] \\
&\qquad > ct^2 - \sup_{\beta\in\mathcal{B}} \left|\mathbb{E}\left\{\mathbb{P}_m l(\beta)\right\} - \mathcal{L}(\beta)\right| - \mathbb{E}\left[\sup_{\beta\in\mathcal{B}} \left|\mathbb{P}_m l(\beta) - \mathbb{E}\left\{\mathbb{P}_m l(\beta)\right\}\right|\right]\Bigg) \\
\leq& \exp\left[-2\left\{ct^2 + O(m^{-\nu}) + O(m^{-\frac{1}{2}})\right\}^2 m/L^2\right] = \exp[-c\{t^4 + o(t^4)\}m],
\end{aligned}
$$

where we have used the Condition (iii) that $\sup_{\beta\in\mathcal{B}} |\mathbb{E}\{\mathbb{P}_m l(\beta)\} - \mathcal{L}(\beta)| = O(m^{-\nu})$, the result of Lemma 5, the condition that $t = O(m^{-\omega})$ with $0 < \omega < (\nu/2) \wedge (1/4)$, and the McDiarmid's

inequality. Recall that $\sup_{1\le j\le m}\sup_{\beta\in\mathcal{B}}|\mathbb{P}_m^{j\to a}l(\beta)-\mathbb{P}_m l(\beta)|\le L/m$. Then we have

$$
\begin{aligned}
&\mathbb{P}\{\sup_{1\le j\le m}\|\hat{\beta}(p_{j\to a})-\beta^*\|>t\}\\
\le&\mathbb{P}\left[\bigcup_{1\le j\le m}\left\{\sup_{\beta:\|\beta-\beta^*\|>t}\mathbb{P}_m^{j\to a}l(\beta)>\mathbb{P}_m^{j\to a}l(\beta^*)\right\}\right]\\
\le&\mathbb{P}\left(\bigcup_{1\le j\le m}\left[\sup_{\beta\in\mathcal{B}}\left|\mathbb{P}_m^{j\to a}l(\beta)-\mathbb{E}\left\{\mathbb{P}_m^{j\to a}l(\beta)\right\}\right|>ct^2-\sup_{\beta\in\mathcal{B}}\left|\mathbb{E}\left\{\mathbb{P}_m^{j\to a}l(\beta)\right\}-\mathcal{L}(\beta)\right|\right]\right)\\
=&\mathbb{P}\Bigg(\bigcup_{1\le j\le m}\Bigg[\sup_{\beta\in\mathcal{B}}\left|\mathbb{P}_m^{j\to a}l(\beta)-\mathbb{P}_m l(\beta)+\mathbb{P}_m l(\beta)-\mathbb{E}\left\{\mathbb{P}_m l(\beta)\right\}+\mathbb{E}\left\{\mathbb{P}_m l(\beta)\right\}-\mathbb{E}\left\{\mathbb{P}_m^{j\to a}l(\beta)\right\}\right|\\
&\qquad>ct^2-\sup_{\beta\in\mathcal{B}}\left|\mathbb{E}\left\{\mathbb{P}_m^{j\to a}l(\beta)\right\}-\mathbb{E}\left\{\mathbb{P}_m l(\beta)\right\}+\mathbb{E}\left\{\mathbb{P}_m l(\beta)\right\}-\mathcal{L}(\beta)\right|\Bigg]\Bigg)\\
\le&\mathbb{P}\left(\bigcup_{1\le j\le m}\left[\sup_{\beta\in\mathcal{B}}\left|\mathbb{P}_m l(\beta)-\mathbb{E}\left\{\mathbb{P}_m l(\beta)\right\}\right|+\frac{2L}{m}>ct^2-\sup_{\beta\in\mathcal{B}}\left|\mathbb{E}\left\{\mathbb{P}_m l(\beta)\right\}-\mathcal{L}(\beta)\right|-\frac{L}{m}\right]\right)\\
=&\mathbb{P}\Bigg(\sup_{\beta\in\mathcal{B}}\left|\mathbb{P}_m l(\beta)-\mathbb{E}\left\{\mathbb{P}_m l(\beta)\right\}\right|-\mathbb{E}\left[\sup_{\beta\in\mathcal{B}}\left|\mathbb{P}_m l(\beta)-\mathbb{E}\left\{\mathbb{P}_m l(\beta)\right\}\right|\right]\\
&\qquad>ct^2-\sup_{\beta\in\mathcal{B}}\left|\mathbb{E}\left\{\mathbb{P}_m l(\beta)\right\}-\mathcal{L}(\beta)\right|-\frac{3L}{m}-\mathbb{E}\left[\sup_{\beta\in\mathcal{B}}\left|\mathbb{P}_m l(\beta)-\mathbb{E}\left\{\mathbb{P}_m l(\beta)\right\}\right|\right]\Bigg)\\
\le&\exp\left[-2\left\{ct^2+O(m^{-\nu})+O(m^{-1})+O(m^{-\frac{1}{2}})\right\}^2 m/L^2\right]=\exp[-c\{t^4+o(t^4)\}m].
\end{aligned}
$$

□

Lemma 7. *Denote by $B(m,p)$ the binomial distribution with m Bernoulli trials and success probability p. Consider two sequences of independent Bernoulli random variables $\{V_i\}_{i=1}^m$ and $\{U_i\}_{i=1}^m$, where $V_i\sim B(1,p_i)$ independently and $U_i\sim^{i.i.d}B(1,p)$ with $p_i\ge p$ for $i=1,...,m$. Let $W_1=\sum_{i=1}^m V_i$ and $W_2=\sum_{i=1}^m U_i$. Suppose f is non-decreasing and W_1 and W_2 belong to the domain of f almost surely. Then we have*

$$\mathbb{E}\left\{f(W_1)\right\}\ge\mathbb{E}\left\{f(W_2)\right\}.$$

Proof. Suppose there are n p_i's such that $p_i\neq p$. Without loss of generality, we assume $p_i>p$ for

$i = 1, ..., n$ and $p_i = p$ for $i = n+1, ..., m$. Then the conclusion is obviously true if $n = 0$. We use the induction argument. Suppose the conclusion is true if $n = s$. Consider the case $n = s+1$. Let $T = \sum_{i=1}^{s} \mathrm{B}(1, p_i) + \mathrm{B}(m-s-1, p)$, where $\mathrm{B}(1, p_i)$'s and $\mathrm{B}(m-s-1, p)$ are independent with each other. We note that

$$
\begin{aligned}
&\mathbb{E}\left\{f(W_1)\right\} - \mathbb{E}\left\{f(W_2)\right\} = \mathbb{E}\left\{f\left(\sum_{i=1}^{m} V_i\right)\right\} - \mathbb{E}\left\{f\left(\sum_{i=1}^{m} U_i\right)\right\} \\
=&\mathbb{E}\left[f\left\{\sum_{i=1}^{s} \mathrm{B}(1, p_i) + \mathrm{B}(1, p_{s+1}) + \mathrm{B}(m-s-1, p)\right\}\right] \\
&- \mathbb{E}\left[f\left\{\sum_{i=1}^{s} \mathrm{B}(1, p_i) + \mathrm{B}(1, p) + \mathrm{B}(m-s-1, p)\right\}\right] \\
&+ \mathbb{E}\left[f\left\{\sum_{i=1}^{s} \mathrm{B}(1, p_i) + \mathrm{B}(1, p) + \mathrm{B}(m-s-1, p)\right\}\right] - \mathbb{E}\left[f\left\{\mathrm{B}(m, p)\right\}\right] \\
=&p_{s+1}\mathbb{E}\left\{f(T+1)\right\} + (1-p_{s+1})\mathbb{E}\left\{f(T)\right\} - p\mathbb{E}\left\{f(T+1)\right\} - (1-p)\mathbb{E}\left\{f(T)\right\} \\
&+ \mathbb{E}\left[f\left\{\sum_{i=1}^{s} \mathrm{B}(1, p_i) + \mathrm{B}(1, p) + \mathrm{B}(m-s-1, p)\right\}\right] - \mathbb{E}\left[f\left\{\mathrm{B}(m, p)\right\}\right] \\
=&\left(p_{s+1} - p\right)\left[\mathbb{E}\left\{f(T+1)\right\} - \mathbb{E}\left\{f(T)\right\}\right] \\
&+ \mathbb{E}\left[f\left\{\sum_{i=1}^{s} \mathrm{B}(1, p_i) + \mathrm{B}(m-s, p)\right\}\right] - \mathbb{E}\left[f\left\{\mathrm{B}(m, p)\right\}\right] \geq 0,
\end{aligned}
$$

where the first term in the last equation is greater or equal to zero as f is non-decreasing and $p_{s+1} > p$, and the second term is greater or equal to zero by the induction hypothesis. □

Lemma 8. *For a matrix A with $\|A\| < \infty$, let $\sigma_{\min}(A) = \inf_{\|w\|=1} \|Aw\|$. For two matrices $A, B \in \mathbb{R}^{n_1 \times n_2}$ and any $\epsilon > 0$, there exists δ such that $|\sigma_{\min}(A) - \sigma_{\min}(B)| \leq \epsilon$ as long as $\|A - B\| \leq \delta$.*

Proof. Let $A = U\Sigma V^{\mathrm{T}}$ be the singular value decomposition of the matrix A. Then

$$
\inf_{\|w\|=1} \|Aw\| = \inf_{\|w\|=1} \|U\Sigma V^{\mathrm{T}} w\| = \inf_{\|Vw\|=1} \|U\Sigma w\| = \inf_{\|w\|=1} \|\Sigma w\| = \sigma_{\min}(A).
$$

Define the function $A(w) = \|Aw\|$, which is continuous. This can be easily proved by noting that

$\big|\|Aw_1\| - \|Aw_2\|\big| \le \|A\|\|w_1 - w_2\|$. Thus $\inf_{\|w\|=1} \|Aw\| = \min_{\|w\|=1} \|Aw\|$. Let $\sigma_{\min}(A) = a$ and $\sigma_{\min}(B) = b$. Further set $w_a = \arg\min_{\|w\|=1} \|Aw\|$ and $w_b = \arg\min_{\|w\|=1} \|Bw\|$. For any $\epsilon > 0$ and $\|A - B\| \le \epsilon$, we have

$$a \le \|Aw_b\| = \|(A - B + B)w_b\| \le \|A - B\|\|w_b\| + \|Bw_b\| \le \epsilon + b,$$

and similarly $b \le \epsilon + a$, which leads to $|a - b| \le \epsilon$. □

A.5 Proof of Theorem 1

Proof. By Proposition 1 and the Cauchy-Schwarz inequality, we have

$$\begin{aligned}
J_{m,1} &= \sum_{j=1}^{m} \mathbb{E}\left[\frac{|x_j^{\mathrm{T}}\{\hat{\beta}(p_{j\to 0}) - \hat{\beta}(p_{j\to 1})\}|}{\left\{c\alpha^{-1}\sum_{i\neq j}\mathbb{I}(p_i > \gamma)\right\} \vee \varepsilon^{1/(1-k)}}\right] \\
&\le \sum_{j=1}^{m}\left(\mathbb{E}\left[\left|x_j^{\mathrm{T}}\{\hat{\beta}(p_{j\to 0}) - \hat{\beta}(p_{j\to 1})\}\right|^2\right]\right)^{1/2}\left\{\mathbb{E}\left(\left[\left\{c\alpha^{-1}\sum_{i\neq j}\mathbb{I}(p_i > \gamma)\right\} \vee \varepsilon^{1/(1-k)}\right]^{-2}\right)\right\}^{1/2} \\
&\le \sum_{j=1}^{m}\left\{\mathbb{E}(\|x_j\|^4)\right\}^{\frac{1}{4}}\left[\mathbb{E}\left\{\left\|\hat{\beta}(p_{j\to 0}) - \hat{\beta}(p_{j\to 1})\right\|^4\right\}\right]^{\frac{1}{4}} \\
&\qquad \left\{\mathbb{E}\left(\left[\left\{c\alpha^{-1}\sum_{i\neq j}\mathbb{I}(p_i > \gamma)\right\} \vee \varepsilon^{1/(1-k)}\right]^{-2}\right)\right\}^{\frac{1}{2}},
\end{aligned}$$

and

$$
\begin{aligned}
J_{m,2} =& \sum_{j=1}^{m} \mathbb{E}\left(\frac{\alpha^{-1} \sum_{i \neq j} \mathbb{I}(p_i > \gamma) |x_i^{\mathrm{T}} \{\hat{\beta}(p_{j\to 0}) - \hat{\beta}(p_{j\to 1})\}| + \alpha^{-1}}{\left[\left\{ c\alpha^{-1} \sum_{i \neq j} \mathbb{I}(p_i > \gamma) \right\} \vee \varepsilon^{1/(1-k)} \right]^2} \right) \\
\leq & \alpha^{-1} \sum_{j=1}^{m} \left\{ \mathbb{E}\left(\left[\sum_{i \neq j} \mathbb{I}(p_i > \gamma) \left| x_i^{\mathrm{T}} \{\hat{\beta}(p_{j\to 0}) - \hat{\beta}(p_{j\to 1})\} \right| \right]^2 \right) \right\}^{1/2} \\
& \qquad \left\{ \mathbb{E}\left(\left[\left\{ c\alpha^{-1} \sum_{i \neq j} \mathbb{I}(p_i > \gamma) \right\} \vee \varepsilon^{1/(1-k)} \right]^{-4} \right) \right\}^{1/2} \\
& + \alpha^{-1} \sum_{j=1}^{m} \mathbb{E}\left(\left[\left\{ c\alpha^{-1} \sum_{i \neq j} \mathbb{I}(p_i > \gamma) \right\} \vee \varepsilon^{1/(1-k)} \right]^{-2} \right) \\
\leq & \alpha^{-1} \sum_{j=1}^{m} m \left(\mathbb{E}\left[\left\{ \frac{1}{m} \sum_{i \neq j} \mathbb{I}(p_i > \gamma) \|x_i\| \right\}^4 \right] \right)^{1/4} \left[\mathbb{E}\left\{ \left\| \hat{\beta}(p_{j\to 0}) - \hat{\beta}(p_{j\to 1}) \right\|^4 \right\} \right]^{1/4} \\
& \qquad \left\{ \mathbb{E}\left(\left[\left\{ c\alpha^{-1} \sum_{i \neq j} \mathbb{I}(p_i > \gamma) \right\} \vee \varepsilon^{1/(1-k)} \right]^{-4} \right) \right\}^{1/2} \\
& + \alpha^{-1} \sum_{j=1}^{m} \mathbb{E}\left(\left[\left\{ c\alpha^{-1} \sum_{i \neq j} \mathbb{I}(p_i > \gamma) \right\} \vee \varepsilon^{1/(1-k)} \right]^{-2} \right) \\
\leq & \alpha^{-1} \sum_{j=1}^{m} m \left\{ \frac{1}{m} \sum_{i=1}^{m} \mathbb{E}(\|x_i\|^4) \right\}^{1/4} \left[\mathbb{E}\left\{ \left\| \hat{\beta}(p_{j\to 0}) - \hat{\beta}(p_{j\to 1}) \right\|^4 \right\} \right]^{1/4} \\
& \qquad \left\{ \mathbb{E}\left(\left[\left\{ c\alpha^{-1} \sum_{i \neq j} \mathbb{I}(p_i > \gamma) \right\} \vee \varepsilon^{1/(1-k)} \right]^{-4} \right) \right\}^{1/2} \\
& + \alpha^{-1} \sum_{j=1}^{m} \mathbb{E}\left(\left[\left\{ c\alpha^{-1} \sum_{i \neq j} \mathbb{I}(p_i > \gamma) \right\} \vee \varepsilon^{1/(1-k)} \right]^{-2} \right).
\end{aligned}
$$

To get the last inequality, we note that for a sequence of random variables $\{W_i\}_{i=1}^m$ and $N \geq 1$,

$$
\mathbb{E}\left\{ \left(\frac{1}{m} \sum_{i=1}^{m} \|W_i\| \right)^N \right\} \leq \mathbb{E}\left(\frac{1}{m} \sum_{i=1}^{m} \|W_i\|^N \right) = \frac{1}{m} \sum_{i=1}^{m} \mathbb{E}\left(\|W_i\|^N \right)
$$

by Jensen's inequality. Note that

$$\left[\left\{c\alpha^{-1}\sum_{i\neq j}\mathbb{I}(p_i>\gamma)\right\}\vee\varepsilon^{1/(1-k)}\right]^{-N}\leq\left[\left\{c\alpha^{-1}\sum_{i\in\mathcal{M}_0,i\neq j}\mathbb{I}(p_i>\gamma)\right\}\vee\varepsilon^{1/(1-k)}\right]^{-N}$$
$$\leq\left[\left\{c\alpha^{-1}\sum_{i,j\in\mathcal{M}_0,i\neq j}\mathbb{I}(p_i>\gamma)\right\}\vee\varepsilon^{1/(1-k)}\right]^{-N}.$$

Under Assumption 1, we have $\mathbb{P}(p_i>\gamma)\geq 1-\gamma$ for $i\in\mathcal{M}_0$. Consider m_0-1 independent random variables u_i's which follow uniform distribution on $[0,1]$. Set $\varepsilon^{1/(1-k)}\leq c\alpha^{-1}$, then $\{c\alpha^{-1}\sum_{i=1}^{m_0-1}\mathbb{I}(u_i>\gamma)\geq\varepsilon^{1/(1-k)}\}=\{\sum_{i=1}^{m_0-1}\mathbb{I}(u_i>\gamma)\geq 1\}$. Let $\mu=1-\gamma$. Then by the result of Lemma 7, for any positive integer N, we have

$$\sup_{1\leq j\leq m}\mathbb{E}\left(\left[\left\{c\alpha^{-1}\sum_{i\neq j}\mathbb{I}(p_i>\gamma)\right\}\vee\varepsilon^{1/(1-k)}\right]^{-N}\right)\leq\mathbb{E}\left(\left[\left\{c\alpha^{-1}\sum_{i=1}^{m_0-1}\mathbb{I}(u_i>\gamma)\right\}\vee\varepsilon^{1/(1-k)}\right]^{-N}\right)$$
$$=(1-\mu)^{m_0-1}\varepsilon^{-N/(1-k)}+c\alpha^N\sum_{i=1}^{m_0-1}\binom{m_0-1}{i}\mu^i(1-\mu)^{m_0-1-i}i^{-N}.$$

We notice that

$$\begin{aligned}\sum_{i=1}^{m_0-1}\binom{m_0-1}{i}\mu^i(1-\mu)^{m_0-1-i}i^{-N}&=\sum_{j=0}^{m_0-2}\binom{m_0-1}{j+1}\mu^{j+1}(1-\mu)^{m_0-1-(j+1)}(j+1)^{-N}\\&=\sum_{j=0}^{m_0-2}\binom{m_0-2}{j}\frac{m_0-1}{j+1}\mu^{j+1}(1-\mu)^{m_0-2-j}(j+1)^{-N}\\&=(m_0-1)\mu\sum_{j=0}^{m_0-2}\binom{m_0-2}{j}\mu^j(1-\mu)^{m_0-2-j}(j+1)^{-(N+1)}\\&=(m_0-1)\mu\mathbb{E}\left\{(W+1)^{-(N+1)}\right\}=O(m_0^{-N}),\end{aligned}$$

where $W\sim\mathrm{B}(m_0-2,\mu)$ and we have used the result from Cribari-Neto et al. (2000, A note on inverse moments of binomial variates). As $(1-\mu)^{m_0-1}=o(\alpha^N m_0^{-N})$ and $m_0=cm$ from

Condition (viii), it follows that

$$\sup_{1\le j\le m}\mathbb{E}\left(\left[\left\{c\alpha^{-1}\sum_{i\neq j}\mathbb{I}(p_i>\gamma)\right\}\vee\varepsilon^{1/(1-k)}\right]^{-N}\right)=O(\alpha^N m_0^{-N})=O(\alpha^N m^{-N}).$$

Since $\mathcal{B}$ is compact, $\left\|\hat{\beta}(p_{j\to a})-\beta^*\right\|\le c$ for $a=0,1$. Thus we get

$$\begin{aligned}
&\mathbb{E}\left\{\left\|\hat{\beta}(p_{j\to 0})-\hat{\beta}(p_{j\to 1})\right\|^N\right\}\\
=&\mathbb{E}\left[\left\|\hat{\beta}(p_{j\to 0})-\hat{\beta}(p_{j\to 1})\right\|^N\mathbb{I}\left\{\left\|\hat{\beta}(p_{j\to 0})-\hat{\beta}(p_{j\to 1})\right\|\le K/m\right\}\right]\\
&+\mathbb{E}\left[\left\|\hat{\beta}(p_{j\to 0})-\hat{\beta}(p_{j\to 1})\right\|^N\mathbb{I}\left\{\left\|\hat{\beta}(p_{j\to 0})-\hat{\beta}(p_{j\to 1})\right\|> K/m\right\}\right]\\
\le&\left(Km^{-1}\right)^N+\mathbb{E}\left[\left\|\hat{\beta}(p_{j\to 0})-\hat{\beta}(p_{j\to 1})\right\|^N\mathbb{I}\left\{\left\|\hat{\beta}(p_{j\to 0})-\hat{\beta}(p_{j\to 1})\right\|> K/m\right\}\right]\\
\le&\left(Km^{-1}\right)^N+c\mathbb{P}\left\{\left\|\hat{\beta}(p_{j\to 0})-\hat{\beta}(p_{j\to 1})\right\|> K/m\right\}.
\end{aligned}$$

Recall that $S_j^*=-\sum_{i\neq j}\nabla^2 l(\beta^*;z_i)=\sum_{i\neq j}h(\beta^*;z_i)x_ix_i^{\mathrm{T}}$ with $h(\beta;z)$ being uniformly bounded over β and z. Under Condition (vii) , we have $\sigma_{\min}[-\mathbb{E}\{\sum_{i=1}^m\nabla^2 l(\beta^*;z_i)/m\}]>c$ as $m\to\infty$. Then we have

$$\inf_{1\le j\le m}\sigma_{\min}\left\{\mathbb{E}\left(\frac{S_j^*}{m}\right)\right\}=\inf_{1\le j\le m}\sigma_{\min}\left[\mathbb{E}\left\{\frac{-\sum_{i=1}^m\nabla^2 l(\beta^*;z_i)}{m}+\frac{h(\beta^*;z_j)x_jx_j^{\mathrm{T}}}{m}\right\}\right]>c$$

as $m\to\infty$, where we have used Condition (ii) and Lemma 8. Let $\{\lambda_i\}_{i=1}^4$ be four positive numbers such that $\lambda_1=o(1)$, $\lambda_2=O(m^{-\omega})$ with $0<\omega<1/4$, $\lambda_3=o(1)$ and $\lambda_4=o(1)$. If $\|S_j^*/m-\mathbb{E}(S_j^*/m)\|\le\lambda_1$, $\|\hat{\beta}(p_{j\to a})-\beta^*\|\le\lambda_2$ for $a=0,1$, $|\sum_{i\neq j}\|x_i\|^3/m-\mathbb{E}(\sum_{i\neq j}\|x_i\|^3/m)|\le\lambda_3$ and $|\sum_{i\neq j}\|x_i\|^4/m-\mathbb{E}(\sum_{i\neq j}\|x_i\|^4/m)|\le\lambda_4$ for any $j=1,...,m$, then by (A.5) and Condition (ii), we have

$$\sup_{1\le j\le m}\left\|\frac{S_j^*+\Delta_j}{m}-\mathbb{E}\left(\frac{S_j^*}{m}\right)\right\|\le c\left(\lambda_1+\lambda_2+\lambda_2^2\right),$$

which leads to that $\sup_{1\le j\le m}\|\{(S_j^*+\Delta_j)/m\}^{-1}\| = \sup_{1\le j\le m}[\sigma_{\min}\{(S_j^*+\Delta_j)/m\}]^{-1} < c$ as $m\to\infty$ by Lemma 8. And by (A.4) and (A.6), for $j=1,...,m$, we have

$$\left\|U_j^*+\Pi_j\right\| \le c(\|x_j\|+\lambda_2\|x_j\|^2+\lambda_2^2\|x_j\|^3).$$

Applying the result from Proposition 2, we have

$$\begin{aligned}
&\sup_{1\le j\le m}\mathbb{P}\left\{\left\|\hat\beta(p_{j\to 0})-\hat\beta(p_{j\to 1})\right\| > K/m\right\}\\
=&\sup_{1\le j\le m}\mathbb{P}\left\{\left\|(S_j^*+\Delta_j)^{-1}(U_j^*+\Pi_j)\right\| > K/m\right\}\\
\le&\sup_{1\le j\le m}\Bigg[\mathbb{P}\Bigg\{\left\|(S_j^*+\Delta_j)^{-1}(U_j^*+\Pi_j)\right\| > K/m, \left\|\frac{S_j^*}{m}-\mathbb{E}\left(\frac{S_j^*}{m}\right)\right\|\le\lambda_1, \|\hat\beta(p_{j\to a})-\beta^*\|\le\lambda_2,\\
&\qquad\left|\frac{\sum_{i\neq j}\|x_i\|^3}{m}-\mathbb{E}\left(\frac{\sum_{i\neq j}\|x_i\|^3}{m}\right)\right|\le\lambda_3, \left|\frac{\sum_{i\neq j}\|x_i\|^4}{m}-\mathbb{E}\left(\frac{\sum_{i\neq j}\|x_i\|^4}{m}\right)\right|\le\lambda_4\Bigg\}\\
&\quad+\mathbb{P}\left\{\left\|\frac{S_j^*}{m}-\mathbb{E}\left(\frac{S_j^*}{m}\right)\right\|>\lambda_1\right\}+\mathbb{P}\left\{\|\hat\beta(p_{j\to a})-\beta^*\|>\lambda_2\right\}\\
&\quad+\mathbb{P}\left\{\left|\frac{\sum_{i\neq j}\|x_i\|^3}{m}-\mathbb{E}\left(\frac{\sum_{i\neq j}\|x_i\|^3}{m}\right)\right|>\lambda_3\right\}\\
&\quad+\mathbb{P}\left\{\left|\frac{\sum_{i\neq j}\|x_i\|^4}{m}-\mathbb{E}\left(\frac{\sum_{i\neq j}\|x_i\|^4}{m}\right)\right|>\lambda_4\right\}\Bigg]\\
\le&\sup_{1\le j\le m}\Bigg[\mathbb{P}\left(\|x_j\|+\lambda_2\|x_j\|^2+\lambda_2^2\|x_j\|^3>cK\right)+\mathbb{P}\left\{\left\|\frac{S_j^*}{m}-\mathbb{E}\left(\frac{S_j^*}{m}\right)\right\|>\lambda_1\right\}\\
&\quad+\mathbb{P}\left\{\|\hat\beta(p_{j\to a})-\beta^*\|>\lambda_2\right\}+\mathbb{P}\left\{\left|\frac{\sum_{i\neq j}\|x_i\|^3}{m}-\mathbb{E}\left(\frac{\sum_{i\neq j}\|x_i\|^3}{m}\right)\right|>\lambda_3\right\}\\
&\quad+\mathbb{P}\left\{\left|\frac{\sum_{i\neq j}\|x_i\|^4}{m}-\mathbb{E}\left(\frac{\sum_{i\neq j}\|x_i\|^4}{m}\right)\right|>\lambda_4\right\}\Bigg].
\end{aligned}$$

Thus we conclude that

$$\begin{aligned}
&\sup_{1\le j\le m} \mathbb{E}\left\{\left\|\hat{\beta}(p_{j\to 0})-\hat{\beta}(p_{j\to 1})\right\|^4\right\} \\
&\le \sup_{1\le j\le m}\Bigg[c\left(Km^{-1}\right)^4 + P\left(\|x_j\|+\lambda_2\|x_j\|^2+\lambda_2^2\|x_j\|^3 > cK\right) \\
&\qquad + \mathbb{P}\left\{\left\|\frac{S_j^*}{m}-\mathbb{E}\left(\frac{S_j^*}{m}\right)\right\|>\lambda_1\right\} + \mathbb{P}\left\{\|\hat{\beta}(p_{j\to a})-\beta^*\|>\lambda_2\right\} \\
&\qquad + \mathbb{P}\left\{\left|\frac{\sum_{i\neq j}\|x_i\|^3}{m}-\mathbb{E}\left(\frac{\sum_{i\neq j}\|x_i\|^3}{m}\right)\right|>\lambda_3\right\} \\
&\qquad + \mathbb{P}\left\{\left|\frac{\sum_{i\neq j}\|x_i\|^4}{m}-\mathbb{E}\left(\frac{\sum_{i\neq j}\|x_i\|^4}{m}\right)\right|>\lambda_4\right\}\Bigg].
\end{aligned}$$

As seen from above, there are six terms to be considered. From the result of Proposition 4, we know that $\mathbb{P}\{\sup_j \|\hat{\beta}(p_{j\to a})-\beta^*\|>\lambda_2\} \le \exp[-c\{\lambda_2^4+o(\lambda_2^4)\}m]$, which implies that the convergence rate of $\mathbb{P}\{\|\hat{\beta}(p_{j\to 0})-\hat{\beta}(p_{j\to 1})\|>K/m\}$ is not determined by the term $\mathbb{P}\{\|\hat{\beta}(p_{j\to a})-\beta^*\|>\lambda_2\}$. We thus focus on the other five terms. Let $K=m^\kappa$ with $0<\kappa<1$. Applying the result of Proposition 3, we have

$$\begin{aligned}
\sup_{1\le j\le m}\Bigg[&\mathbb{P}\left\{\left\|\frac{S_j^*}{m}-\mathbb{E}\left(\frac{S_j^*}{m}\right)\right\|>\lambda_1\right\} + \mathbb{P}\left\{\left|\frac{\sum_{i\neq j}\|x_i\|^3}{m}-\mathbb{E}\left(\frac{\sum_{i\neq j}\|x_i\|^3}{m}\right)\right|>\lambda_3\right\} \\
&+ \mathbb{P}\left\{\left|\frac{\sum_{i\neq j}\|x_i\|^4}{m}-\mathbb{E}\left(\frac{\sum_{i\neq j}\|x_i\|^4}{m}\right)\right|>\lambda_4\right\}\Bigg] = o(m^{1-q}).
\end{aligned}$$

Note that

$$
\begin{aligned}
&\sup_{1\le j\le m}\left\{c\left(Km^{-1}\right)^4+\mathbb{P}\left(\|x_j\|+\lambda_2\|x_j\|^2+\lambda_2^2\|x_j\|^3>cK\right)+o(m^{1-q})\right\}\\
\le&\sup_{1\le j\le m}\left\{c\left(Km^{-1}\right)^4+c\mathbb{E}\left(\|x_j\|^{4q}\right)K^{-4q}+c\mathbb{E}\left(\|x_j\|^{4q}\right)(\lambda_2K^{-1})^{2q}\right.\\
&\qquad\left.+c\mathbb{E}\left(\|x_j\|^{4q}\right)\left(\lambda_2^2K^{-1}\right)^{\frac{4q}{3}}+o(m^{1-q})\right\}\\
\le&c\left\{\left(Km^{-1}\right)^4+K^{-4q}+\left(\lambda_2K^{-1}\right)^{2q}+\left(\lambda_2^2K^{-1}\right)^{\frac{4q}{3}}\right\}+o(m^{1-q})\\
=&O\left(m^{4(\kappa-1)}+m^{-4\kappa q}+m^{-2\omega q-2\kappa q}+m^{-\frac{8}{3}\omega q-\frac{4}{3}\kappa q}\right)+o(m^{1-q}),
\end{aligned}
\tag{A.7}
$$

where $0<\kappa<1$ and $0<\omega<1/4$. Let

$$
\eta(\kappa,\omega,q)=\max\left\{v_1=4(\kappa-1),v_2=-4\kappa q,v_3=-2\omega q-2\kappa q,v_4=-\frac{8}{3}\omega q-\frac{4}{3}\kappa q\right\}.
$$

Finding the order of (A.7) is equivalent to solving the following problem

$$
\min_{0<\kappa<1,0<\omega<1/4}\eta(\kappa,\omega,q),\quad q\ge 2. \tag{A.8}
$$

We notice that the three lines v_2,v_3,v_4 intersect at point $(\omega,-4\omega q)$ for any ω and q, and lines v_1,v_2 intersect at point $(1/(1+q),-4q/(1+q))$. Observe that $\eta(\kappa,\omega_2,q)\le\eta(\kappa,\omega_1,q)$ if $\omega_2\ge\omega_1$ for any κ and q. Thus we let $\omega=1/4-\epsilon$, where ϵ is an arbitrarily small positive number. If $2\le q\le 3$, then $1/(1+q)>\omega$ and hence the solution to (A.8) is obtained when $v_1=v_4$. If $q>3$, then $1/(1+q)<\omega$ as ϵ can be arbitrarily small, and hence the solution is obtained when $v_1=v_2$. The idea is illustrated in Figure A.3, where we set $\omega=1/4-0.001$. Therefore, for $2\le q\le 3$, the solution to (A.8) is obtained when $4(\kappa-1)=-8\omega q/3-4\kappa q/3$. In this case, $\kappa=(3-2\omega q)/(3+q)$ and $4(\kappa-1)=-4(2\omega+1)q/(3+q)$. Thus we have

$$
\sup_{1\le j\le m}\mathbb{E}\left\{\left\|\hat{\beta}(p_{j\to 0})-\hat{\beta}(p_{j\to 1})\right\|^4\right\}\le\max\left\{O\left(m^{\frac{-4(2\omega+1)q}{3+q}}\right),o\left(m^{1-q}\right)\right\}=o(m^{1-q}).
$$

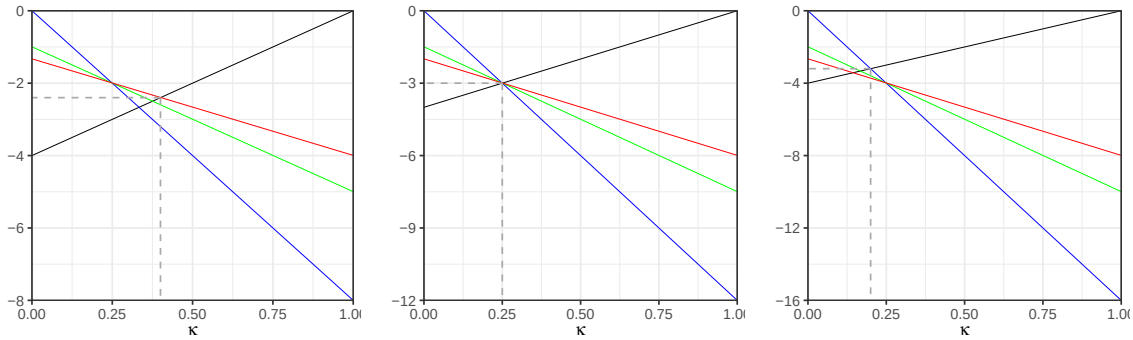

Figure A.3: Illustration of the linear programming problem (A.8) with $\omega = 1/4 - 0.001$. The black, blue, green and red lines represent v_1, v_2, v_3 and v_4 in (A.8) respectively. From left to right, the three panels correspond to $q = 2, 3, 4$ respectively.

For $q > 3$, the solution is obtained when $4(\kappa - 1) = -4\kappa q$. In this case, $\kappa = 1/(1+q)$ and $4(\kappa - 1) = -4q/(1+q)$. Hence we get

$$\sup_{1\le j\le m} \mathbb{E}\left\{\left\|\hat{\beta}(p_{j\to 0}) - \hat{\beta}(p_{j\to 1})\right\|^4\right\} \le \max\left\{O\left(m^{\frac{-4q}{1+q}}\right), o\left(m^{1-q}\right)\right\}$$
$$= \begin{cases} o(m^{1-q}), & \text{if } 3 < q \le 2+\sqrt{5}, \\ O\left(m^{\frac{-4q}{1+q}}\right), & \text{if } q > 2+\sqrt{5}. \end{cases}$$

Summarizing the above results, we have

$$\begin{aligned} J_{m,1} \le & \sum_{j=1}^{m} \left\{\mathbb{E}\left(\|x_j\|^4\right)\right\}^{\frac{1}{4}} \left[\mathbb{E}\left\{\left\|\hat{\beta}(p_{j\to 0}) - \hat{\beta}(p_{j\to 1})\right\|^4\right\}\right]^{\frac{1}{4}} \\ & \left\{\mathbb{E}\left(\left[\left\{\alpha^{-1}\sum_{i\ne j}\mathbb{I}(p_i > \gamma)\right\} \vee \varepsilon^{1/(1-k)}\right]^{-2}\right)\right\}^{\frac{1}{2}} \\ \le & \sum_{j=1}^{m} \left\{\mathbb{E}\left(\|x_j\|^4\right)\right\}^{\frac{1}{4}} \left[\mathbb{E}\left\{\left\|\hat{\beta}(p_{j\to 0}) - \hat{\beta}(p_{j\to 1})\right\|^4\right\}\right]^{\frac{1}{4}} O(\alpha m^{-1}) \\ \le & \left[\sup_{1\le j\le m} \mathbb{E}\left\{\left\|\hat{\beta}(p_{j\to 0}) - \hat{\beta}(p_{j\to 1})\right\|^4\right\}\right]^{\frac{1}{4}} O(\alpha), \end{aligned}$$

and

$$
\begin{aligned}
J_{m,2} \leq & \alpha^{-1} \sum_{j=1}^{m} m \left\{ \frac{1}{m} \sum_{i=1}^{m} \mathbb{E}\left(\|x_i\|^4 \right) \right\}^{1/4} \left[\mathbb{E}\left\{ \left\| \hat{\beta}(p_{j\to 0}) - \hat{\beta}(p_{j\to 1}) \right\|^4 \right\} \right]^{1/4} \\
& \left\{ \mathbb{E}\left(\left[\left\{ c\alpha^{-1} \sum_{i\neq j} \mathbb{I}(p_i > \gamma) \right\} \vee \varepsilon^{1/(1-k)} \right]^{-4} \right) \right\}^{1/2} \\
& + \alpha^{-1} \sum_{j=1}^{m} \mathbb{E}\left(\left[\left\{ c\alpha^{-1} \sum_{i\neq j} \mathbb{I}(p_i > \gamma) \right\} \vee \varepsilon^{1/(1-k)} \right]^{-2} \right) \\
\leq & \alpha^{-1} \sum_{j=1}^{m} m \left[\mathbb{E}\left\{ \left\| \hat{\beta}(p_{j\to 0}) - \hat{\beta}(p_{j\to 1}) \right\|^4 \right\} \right]^{\frac{1}{4}} O(\alpha^2 m^{-2}) + \alpha^{-1} \sum_{j=1}^{m} O(\alpha^2 m^{-2}) \\
\leq & \left[\sup_{1\leq j\leq m} \mathbb{E}\left\{ \left\| \hat{\beta}(p_{j\to 0}) - \hat{\beta}(p_{j\to 1}) \right\|^4 \right\} \right]^{\frac{1}{4}} O(\alpha) + O(\alpha m^{-1}),
\end{aligned}
$$

where we have used Condition (ii) to obtain that $\sup_{1\leq i\leq m} \mathbb{E}(\|x_i\|^4) < \infty$. Finally, we obtain

$$
\text{FWER} \leq J_m + \alpha = \begin{cases} o(\alpha m^{\frac{1-q}{4}}) + \alpha, & \text{if } 2 \leq q \leq 2+\sqrt{5}, \\ O(\alpha m^{\frac{-q}{1+q}}) + \alpha, & \text{if } q > 2+\sqrt{5}. \end{cases}
$$

□

A.6 Additional simulation results

Figures A.4–A.6 show the FWER control across different target levels. Figures A.7–A.11 present the results of Setups S1–S2.

A.7 Addition result for Application to GWAS of UK Biobank data Section

We present the numbers of rejections before clumping mentioned in Section 2.5 of the main text.

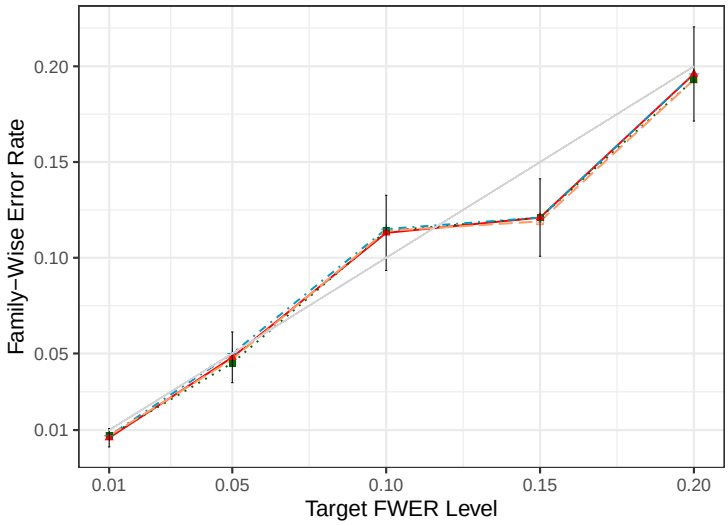

Figure A.4: FWER control at various target levels (0.01 - 0.20) under the complete null (no signal was simulated). Family-wise error rates were averaged over 1,000 simulation runs. The solid red, dotted green, dot-dashed blue and long-dashed orange lines represent CAMT.fwer, IHW- Bonferroni, weighted Bonferroni and Holm's step-down methods respectively. The gray diagonal line represents the target FWER levels and the error bars represent the 95% CIs of the method CAMT.fwer.

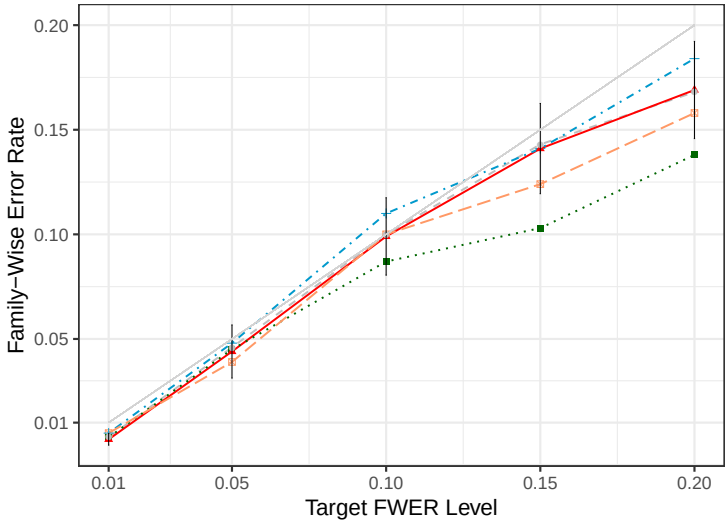

Figure A.5: FWER control at various target levels (0.01 - 0.20) under Setup S0 with moderate signal density, signal strength and covariate informativeness. Family-wise error rates were averaged over 1,000 simulation runs. The solid red, dotted green, dot-dashed blue and long-dashed orange lines represent CAMT.fwer, IHW- Bonferroni, weighted Bonferroni and Holm's step-down methods respectively. The gray diagonal line represents the target FWER levels and the error bars represent the 95% CIs of the method CAMT.fwer.

Table A.1: Significant SNPs detected at the FWER level of 0.05. Improve=(CAMT.fwer − Holm)/Holm $\times$ 100%.

Traits	Holm	IHW	weighted Bonferroni	CAMT.fwer	Improve
Balding Type I	28,752	28,752	29,021	30,441	5.9%
BMI	54,965	54,965	60,171	64,057	16.5%
Heel T Score	108,112	108,112	113,962	117,136	8.3%
Height	256,353	256,051	273,020	278,034	8.5%
Waist-hip Ratio	35,984	35,983	37,720	39,625	10.1%
Eosinophil Count	66,384	66,384	70,495	71,623	7.9%
Mean Corpular Hemoglobin	92,048	92,048	95,790	96,142	4.4%
Red Blood Cell Count	70,919	70,919	74,565	78,061	10.1%
Red Blood Cell Distribution Width	69,583	69,583	73,162	74,427	7.0%
White Blood Cell Count	55,881	55,881	62,483	65,453	17.1%
Auto Immune Traits	7,571	7,571	7,774	7,336	−3.1%
Cardiovascular Diseases	12,531	12,531	13,776	14,859	18.6%
Eczema	13,099	13,099	13,513	14,683	12.1%
Hypothyroidism	12,681	12,681	13,043	14,651	15.5%
Respiratory and Ear-nose-throat Diseases	7,588	7,588	7,750	8,709	14.8%
Type 2 Diabetes	2,459	2,459	2,524	2,684	9.2%
Age at Menarche	25,549	25,549	26,519	27,391	7.2%
Age at Menopause	6,109	6,109	6,211	8,675	42.0%
FEV1-FVC Ratio	50,529	50,529	55,659	58,503	15.8%
Forced Vital Capacity (FVC)	33,549	33,549	36,674	38,985	16.2%
Hair Color	57,608	57,608	58,326	60,391	4.8%
Morning Person	8,154	8,154	8,681	9,559	17.2%
Neuroticism	5,513	6,186	6,073	6,955	26.2%
Smoking Status	6,297	6,623	6,857	8,016	27.3%
Sunburn Occasion	10,076	10,076	10,150	11,000	9.2%
Systolic Blood Pressure	46,063	46,063	51,157	54,749	18.9%
Years of Education	13,927	13,927	15,632	16,933	21.6%

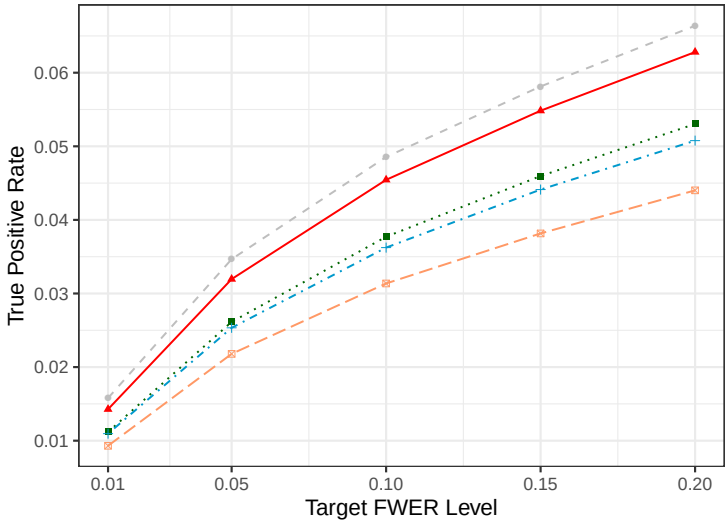

Figure A.6: FWER control at various target levels (0.01 - 0.20) under Setup S0 with moderate signal density, signal strength and covariate informativeness. True positive rates were averaged over 1,000 simulation runs. The dashed gray, solid red, dotted green, dot-dashed blue and long-dashed orange lines represent the oracle, CAMT.fwer, IHW- Bonferroni, weighted Bonferroni and Holm's step-down methods respectively.

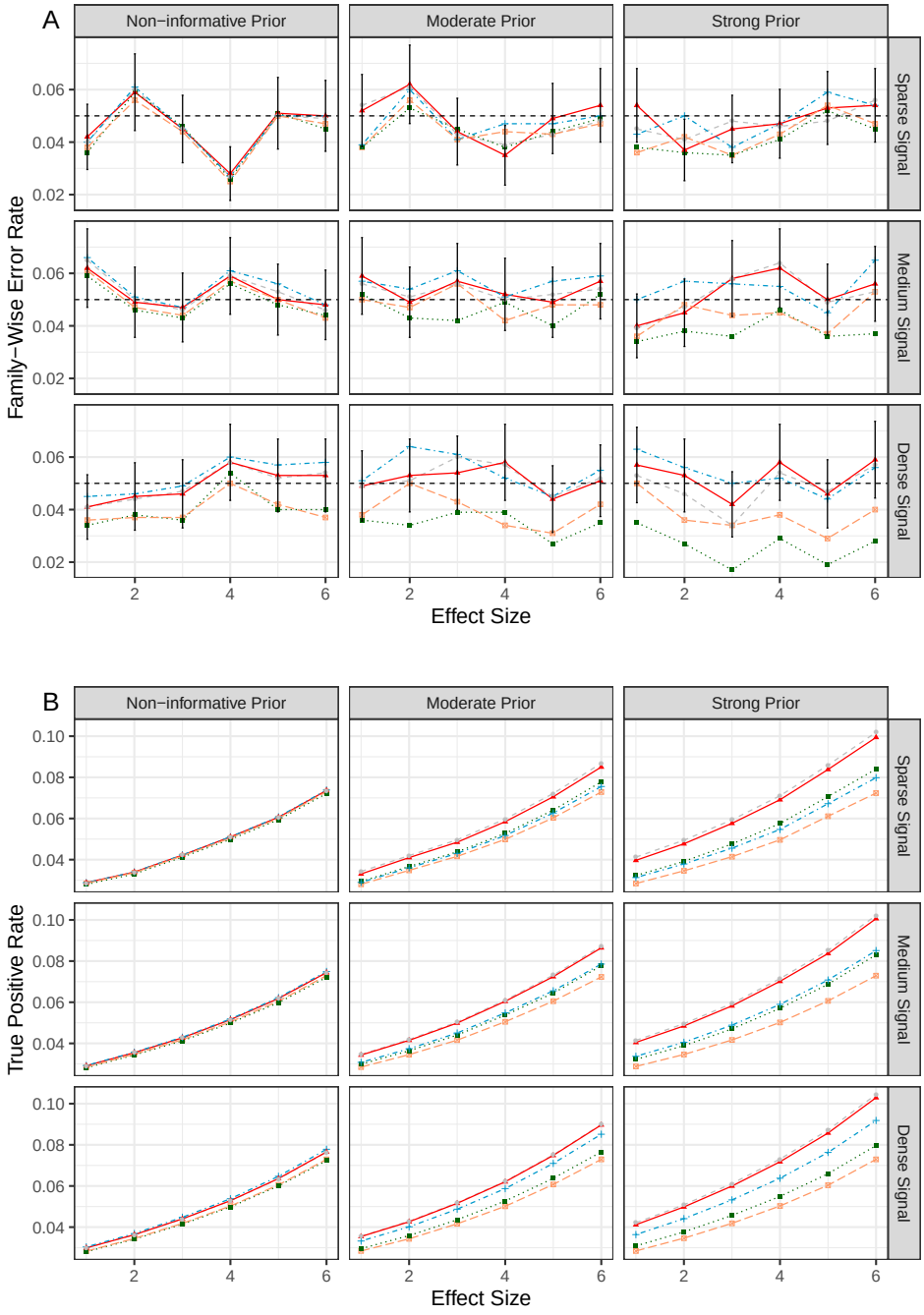

Figure A.7: Performance comparison under additional f_1 distribution (S1). Family-wise error rates (A) and true positive rates (B) were averaged over 1000 simulation runs. The dashed gray, solid red, dotted green, dot-dashed blue and long-dashed orange lines represent the oracle, CAMT.fwer, IHW- Bonferroni, weighted Bonferroni and Holm's step-down methods respectively. The error bars (A) represent the 95% CIs of the method CAMT.fwer and the dashed horizontal line indicates the target FWER level of 0.05.

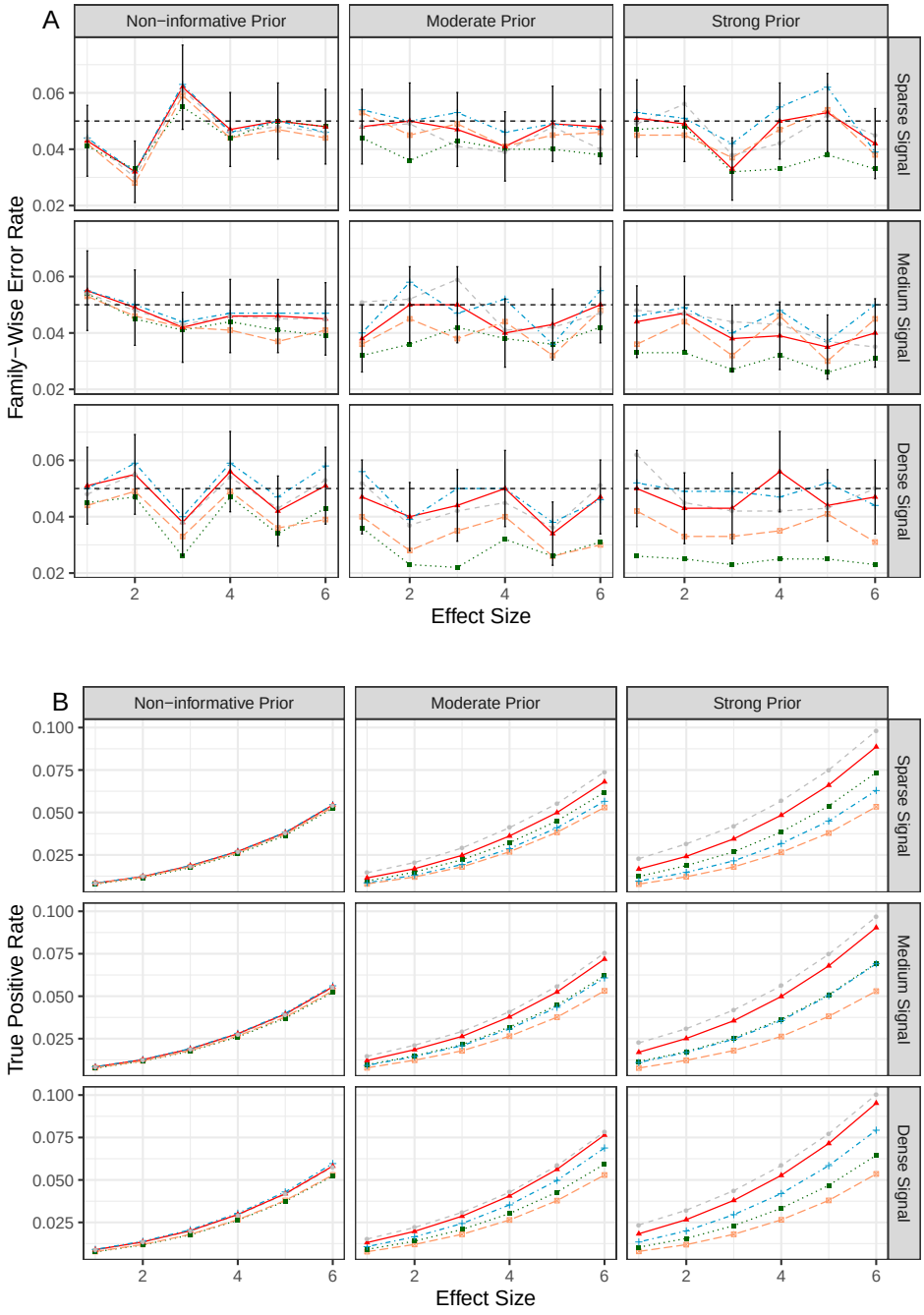

Figure A.8: Performance comparison under correlated hypotheses (S2.1). Family-wise error rates (A) and true positive rates (B) were averaged over 1000 simulation runs. The dashed gray, solid red, dotted green, dot-dashed blue and long-dashed orange lines represent the oracle, CAMT.fwer, IHW- Bonferroni, weighted Bonferroni and Holm's step-down methods respectively. The error bars (A) represent the 95% CIs of the method CAMT.fwer and the dashed horizontal line indicates the target FWER level of 0.05.

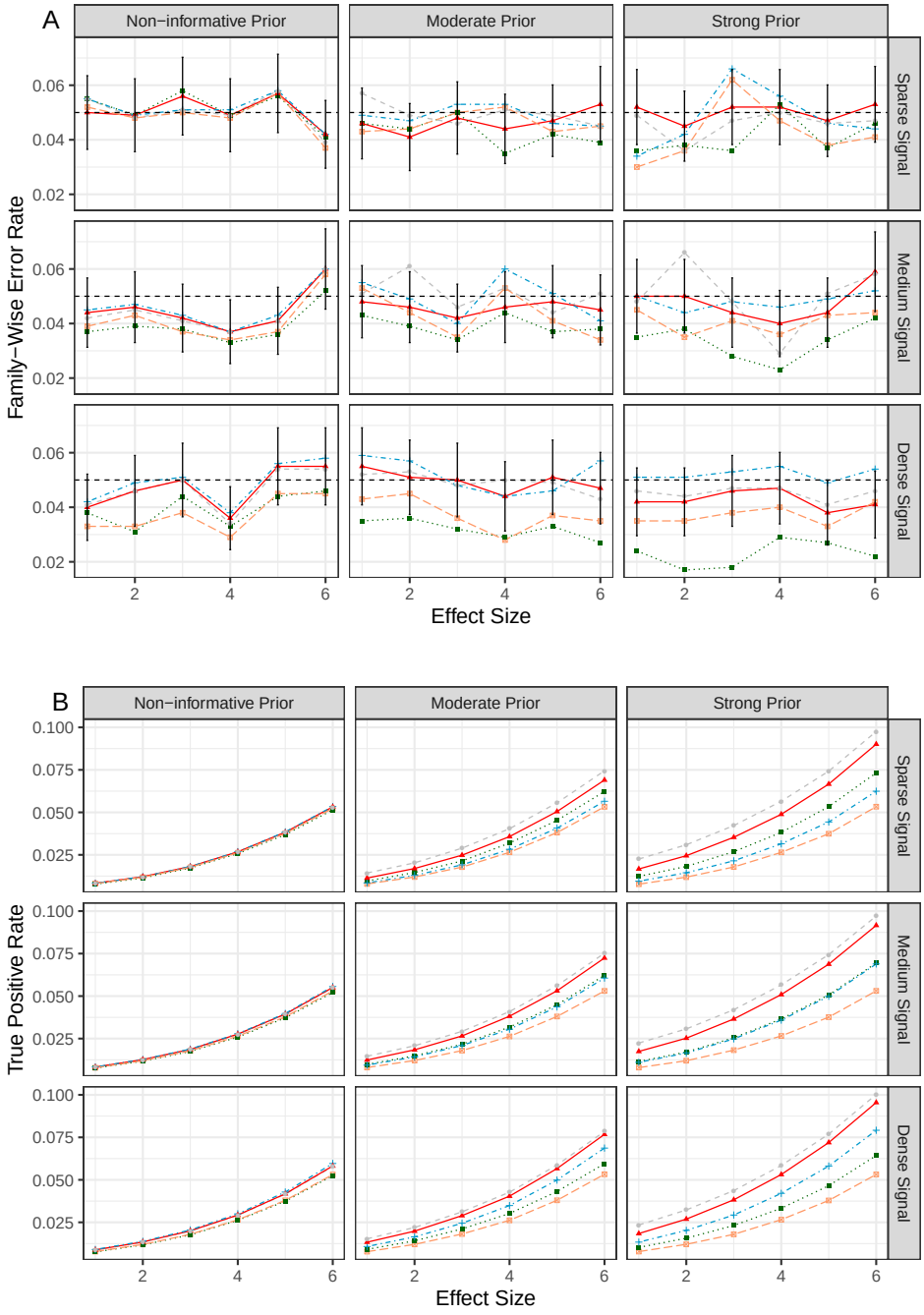

Figure A.9: Performance comparison under correlated hypotheses (S2.2). Family-wise error rates (A) and true positive rates (B) were averaged over 1000 simulation runs. The dashed gray, solid red, dotted green, dot-dashed blue and long-dashed orange lines represent the oracle, CAMT.fwer, IHW- Bonferroni, weighted Bonferroni and Holm's step-down methods respectively. The error bars (A) represent the 95% CIs of the method CAMT.fwer and the dashed horizontal line indicates the target FWER level of 0.05.

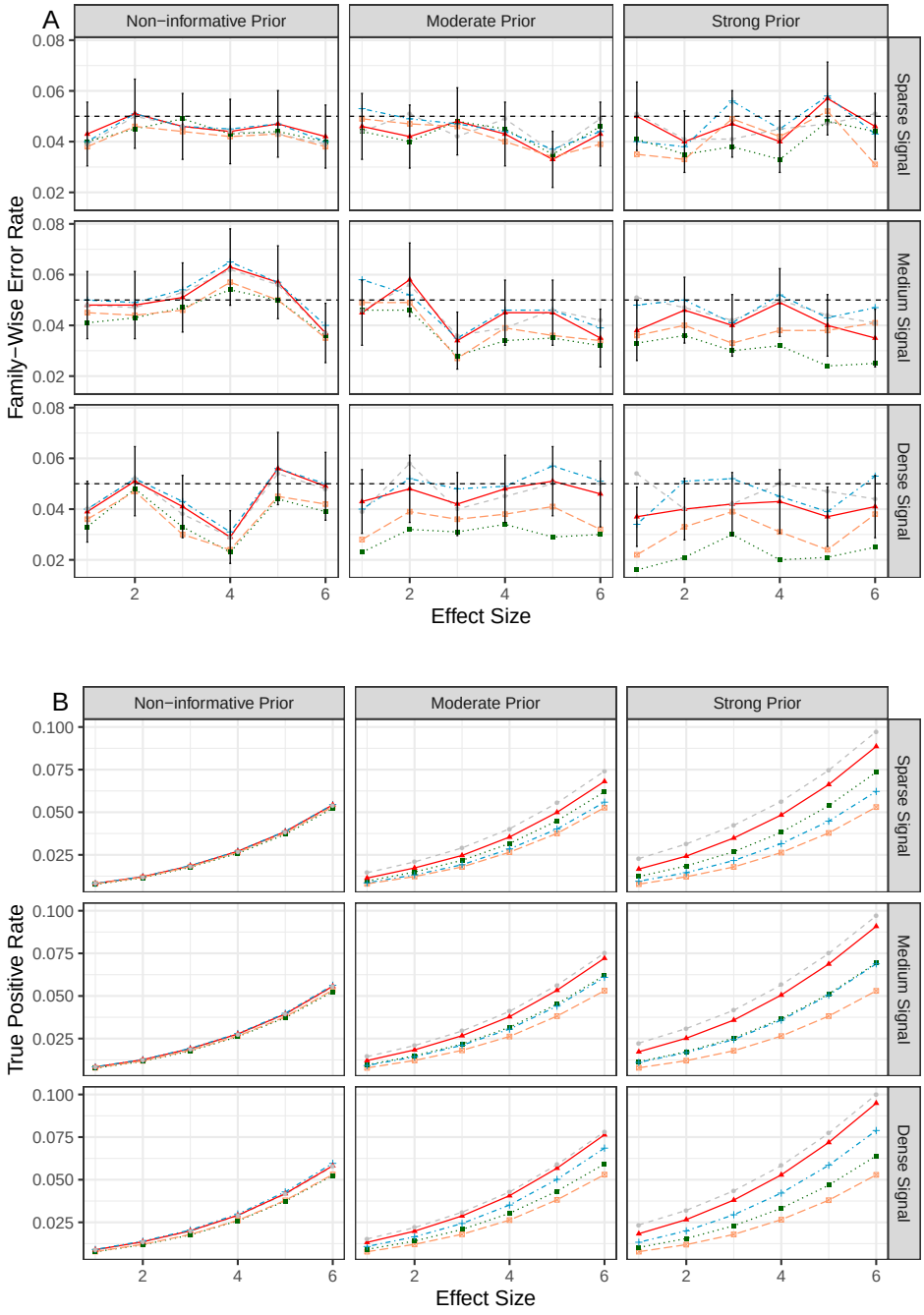

Figure A.10: Performance comparison under correlated hypotheses (S2.3). Family-wise error rates (A) and true positive rates (B) were averaged over 1000 simulation runs. The dashed gray, solid red, dotted green, dot-dashed blue and long-dashed orange lines represent the oracle, CAMT.fwer, IHW- Bonferroni, weighted Bonferroni and Holm's step-down methods respectively. The error bars (A) represent the 95% CIs of the method CAMT.fwer and the dashed horizontal line indicates the target FWER level of 0.05.

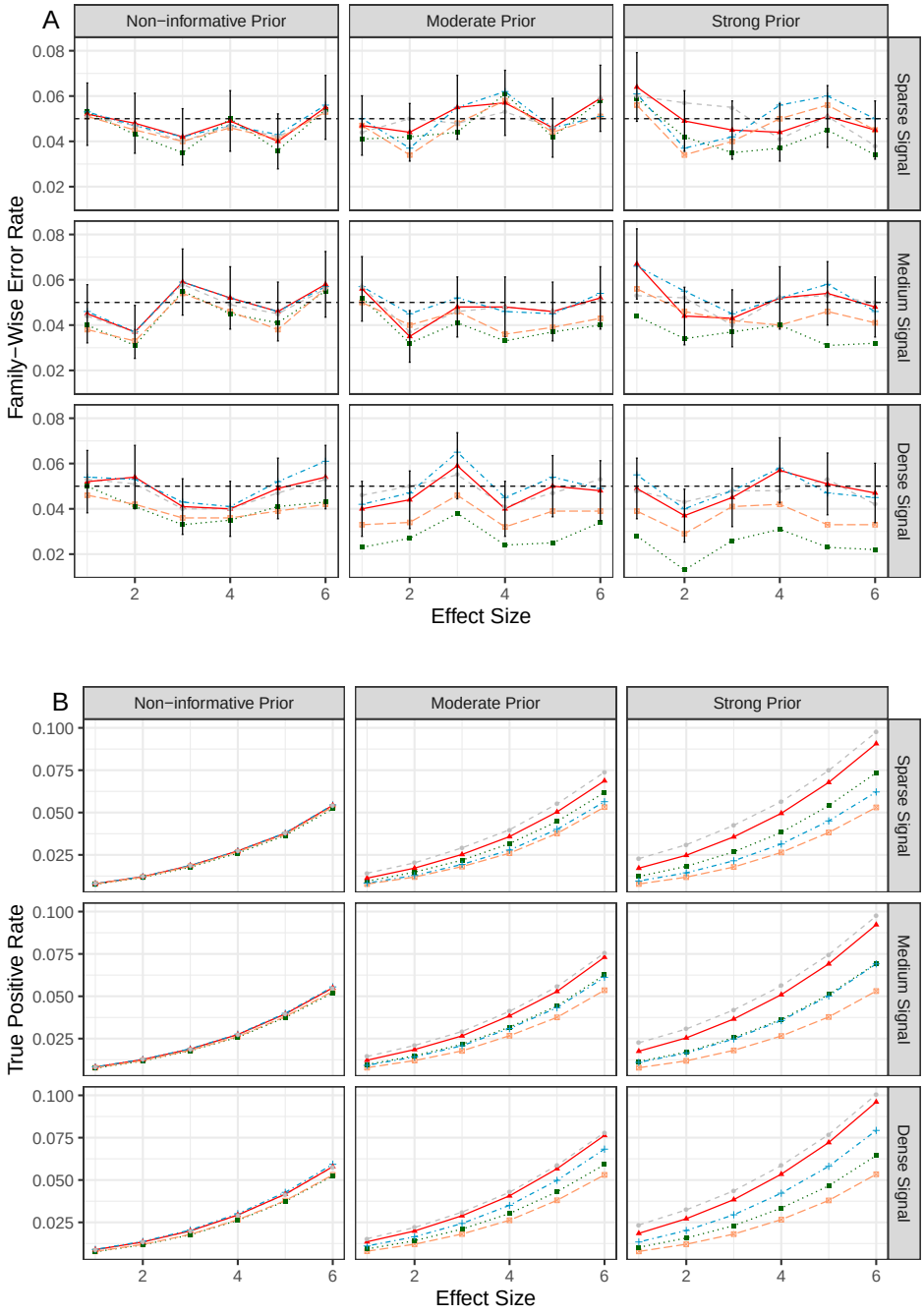

Figure A.11: Performance comparison under correlated hypotheses (S2.4). Family-wise error rates (A) and true positive rates (B) were averaged over 1000 simulation runs. The dashed gray, solid red, dotted green, dot-dashed blue and long-dashed orange lines represent the oracle, CAMT.fwer, IHW- Bonferroni, weighted Bonferroni and Holm's step-down methods respectively. The error bars (A) represent the 95% CIs of the method CAMT.fwer and the dashed horizontal line indicates the target FWER level of 0.05.

APPENDIX B

APPENDIX FOR CHAPTER 3

B.1 Normalization approaches

Table B.1: Some robust normalization methods.

Method	Description
Trimmed mean of M-values (TMM, Robinson and Oshlack, 2010)	TMM (in log scale) is the weighted mean of the log-ratios between the relative abundances and a referenced relative abundance after excluding the most abundant taxa and the taxa with the largest log-fold changes.
DESeq normalization (RLE, Anders and Huber, 2010)	In RLE, the normalizing factor is the median of the ratios between the counts and the geometric mean of the counts of all samples.
Cumulative-sum scaling (CSS, Paulson et al., 2013)	In CSS, counts are divided by the cumulative sum of counts, up to a quantile determined using a data-driven approach.
Geometric mean of pairwise ratios (GMPR, Chen et al., 2018)	GMPR is the geometric mean of the medians of the ratios between the pairs of counts of two samples, which reverses the order of the two steps in the RLE.

B.2 Technical details

In the following, we use $F_X(\cdot)$ to denote the cumulative distribution function of a random variable X. Denote by $o_{\mathbb{P}_m}$ ($O_{\mathbb{P}_m}$), $o_{\mathbb{P}_n}$ ($O_{\mathbb{P}_n}$) and $o_{\mathbb{P}}$ ($O_{\mathbb{P}}$) the corresponding rates of convergence as $m \to \infty$, $n \to \infty$ and $m, n \to \infty$ simultaneously, respectively. We first introduce some useful

lemmas before proving Theorem 2.

Lemma 9. *Under Condition (i) in Theorem 2, we have*

$$|\hat{\rho} - \rho| = o_{\mathbb{P}_n}(1).$$

Lemma 10. *Under Conditions (i),(ii),(iii),(v) and (ix) in Theorem 2, we have*

$$\max_i |\hat{\sigma}_i^2 - \sigma_i^2| = o_{\mathbb{P}}(1).$$

Lemma 11. *Under Conditions (i)–(viii) in Theorem 2, we have*

$$\sqrt{n}(\tilde{\alpha} - \bar{\alpha}) = o_{\mathbb{P}}(1).$$

Lemma 12. *Suppose Conditions (i)–(ix) in Theorem 2 are satisfied. Let m_0 be the number of true null hypotheses and*

$$\begin{aligned}
V_{m,n}(t) &= \sum_{i:\alpha_i=0} \mathbb{I}\left(|\sqrt{n}\hat{\alpha}_i|/\sqrt{\hat{\rho}\hat{\sigma}_i^2} > t\right), \\
S_{m,n}(t) &= \sum_{i=1}^{m} \mathbb{I}\left(|\sqrt{n}\hat{\alpha}_i|/\sqrt{\hat{\rho}\hat{\sigma}_i^2} > t\right), \\
S_{\infty,n}(t) &= \mathbb{P}\left(\left|\mathcal{E} + \sqrt{n}\alpha_i/\sqrt{\rho\sigma_i^2}\right| > t\right).
\end{aligned}$$

Then for any $0 < t_0 < \infty$,

$$\begin{aligned}
\sup_{0<t<t_0} \left|m^{-1}S_{m,n}(t) - S_{\infty,n}(t)\right| &= o_{\mathbb{P}}(1), \\
\sup_{0<t<t_0} \left|m_0^{-1}V_{m,n}(t) - 2F_{n-d-2}(-t)\right| &= o_{\mathbb{P}}(1).
\end{aligned}$$

Proof of Lemma 9. From Condition (i), we know that each element of $\mathbb{E}(\mathbf{z}_s\mathbf{z}_s^\top)$ is finite and $\det\{\mathbb{E}(\mathbf{z}_s\mathbf{z}_s^\top)\} > C$. We have $\hat{\rho} = \det(\hat{\mathbf{B}})/\det(\hat{\mathbf{A}})$ and $\rho = \det(\mathbf{B})/\det(\mathbf{A})$, where $\mathbf{A} = \mathbb{E}(\mathbf{z}_s\mathbf{z}_s^\top)$,

$\hat{\mathbf{A}} = n^{-1}\sum_{s=1}^{n}\mathbf{z}_s\mathbf{z}_s^\top$, and $\mathbf{B}$ and $\hat{\mathbf{B}}$ are the principal submatrices obtained by deleting the first row and first column of $\mathbf{A}$ and $\hat{\mathbf{A}}$ respectively. Thus we have that $|\det(\hat{\mathbf{B}}) - \det(\mathbf{B})| = o_{\mathbb{P}}(1)$ and $|\det(\hat{\mathbf{A}}) - \det(\mathbf{A})| = o_{\mathbb{P}}(1)$ using the law of large numbers. The Slutsky's theorem thus implies that $|\hat{\rho} - \rho| = o_{\mathbb{P}_n}(1)$. □

Proof of Lemma 10. Throughout the proof, we shall assume that $\varepsilon_{is}/\sigma_i$ is C-sub-Gaussian, which is indeed weaker than Condition (iii). For any $\lambda > 0$, we have

$$\begin{aligned}
&\mathbb{E}[e^{\lambda\varepsilon_{is}} \mid \sigma_i] = \mathbb{E}\left[e^{\lambda\sigma_i(\varepsilon_{is}/\sigma_i)} \mid \sigma_i\right] \le e^{\lambda^2\sigma_i^2C^2/2},\\
&\mathbb{E}[e^{\lambda\bar{\varepsilon}_{is}} \mid \{\sigma_i\}] = \mathbb{E}\left[e^{\lambda\left\{(m-1)m^{-1}\varepsilon_{is} - m^{-1}\sum_{j\neq i}\varepsilon_{js}\right\}} \mid \{\sigma_i\}\right] \le e^{\lambda^2(\max_i\sigma_i^2)C^2/2}.
\end{aligned}$$

Thus $\bar{\varepsilon}_{is}$ conditional on $\{\sigma_i\}$ is sub-Gaussian by Condition (ii). Let $\bar{\boldsymbol{\theta}}_i = (\bar{\alpha}_i, \bar{\boldsymbol{\beta}}_i^\top)^\top$ and $\tilde{\boldsymbol{\theta}}_i = (\tilde{\alpha}_i, \tilde{\boldsymbol{\beta}}_i^\top)^\top$. Note that

$$\begin{aligned}
\tilde{\boldsymbol{\theta}}_i =& \bar{\boldsymbol{\theta}}_i + \left(\sum_{s=1}^{n}\mathbf{z}_s\mathbf{z}_s^\top\right)^{-1}\left(\sum_{s=1}^{n}\mathbf{z}_s\bar{\varepsilon}_{is}\right),\\
\hat{\sigma}_i^2 =& \frac{1}{n-d-2}\sum_{s=1}^{n}\left(W_{is} - \mathbf{z}_s^\top\tilde{\boldsymbol{\theta}}_i\right)^2 = \frac{1}{n-d-2}\sum_{s=1}^{n}\left(W_{is} - \mathbf{z}_s^\top\bar{\boldsymbol{\theta}}_i + \mathbf{z}_s^\top\bar{\boldsymbol{\theta}}_i - \mathbf{z}_s^\top\tilde{\boldsymbol{\theta}}_i\right)^2\\
=& \frac{1}{n-d-2}\sum_{s=1}^{n}\bar{\varepsilon}_{is}^2 + \frac{2}{n-d-2}(\bar{\boldsymbol{\theta}}_i - \tilde{\boldsymbol{\theta}}_i)^\top\sum_{s=1}^{n}\mathbf{z}_s\bar{\varepsilon}_{is} + \frac{1}{n-d-2}(\bar{\boldsymbol{\theta}}_i - \tilde{\boldsymbol{\theta}}_i)^\top\left(\sum_{s=1}^{n}\mathbf{z}_s\mathbf{z}_s^\top\right)(\bar{\boldsymbol{\theta}}_i - \tilde{\boldsymbol{\theta}}_i)\\
=& \frac{1}{n-d-2}\sum_{s=1}^{n}\bar{\varepsilon}_{is}^2 - \frac{1}{n-d-2}\left(\sum_{s=1}^{n}\mathbf{z}_s\bar{\varepsilon}_{is}\right)^\top\left(\sum_{s=1}^{n}\mathbf{z}_s\mathbf{z}_s^\top\right)^{-1}\left(\sum_{s=1}^{n}\mathbf{z}_s\bar{\varepsilon}_{is}\right),
\end{aligned}$$

and for any $\delta > 0$,

$$\begin{aligned}
\mathbb{P}\left(\left|\hat{\sigma}_i^2 - \bar{\sigma}_i^2\right| > \delta\right) \le& \mathbb{P}\left(\left|\frac{1}{n-d-2}\sum_{s=1}^{n}\bar{\varepsilon}_{is}^2 - \bar{\sigma}_i^2\right| > \frac{\delta}{2}\right)\\
&+ \mathbb{P}\left\{\left(\sum_{s=1}^{n}\mathbf{z}_s\bar{\varepsilon}_{is}\right)^\top\left(\sum_{s=1}^{n}\mathbf{z}_s\mathbf{z}_s^\top\right)^{-1}\left(\sum_{s=1}^{n}\mathbf{z}_s\bar{\varepsilon}_{is}\right) > \frac{(n-d-2)\delta}{2}\right\}.
\end{aligned}$$

For the first term, we have

$$\mathbb{P}\left(\left|\frac{1}{n-d-2}\sum_{s=1}^{n}\bar{\varepsilon}_{is}^2-\bar{\sigma}_i^2\right|>\frac{\delta}{2}\right)\leq\mathbb{P}\left\{\left|\frac{1}{n}\sum_{s=1}^{n}\bar{\varepsilon}_{is}^2-\bar{\sigma}_i^2\right|>\frac{(n-d-2)\delta}{4n}\right\}+\mathbb{P}\left(\frac{d+2}{n-d-2}\bar{\sigma}_i^2>\frac{\delta}{4}\right).$$

For the second term, we deduce that

$$\begin{aligned}&\mathbb{P}\left\{\left(\sum_{s=1}^{n}\mathbf{z}_s\bar{\varepsilon}_{is}\right)^\top\left(\sum_{s=1}^{n}\mathbf{z}_s\mathbf{z}_s^\top\right)^{-1}\left(\sum_{s=1}^{n}\mathbf{z}_s\bar{\varepsilon}_{is}\right)>\frac{(n-d-2)\delta}{2}\right\}\\
\leq&\mathbb{P}\left\{\left(\frac{1}{n}\sum_{s=1}^{n}\mathbf{z}_s\bar{\varepsilon}_{is}\right)^\top\left(\frac{1}{n}\sum_{s=1}^{n}\mathbf{z}_s\mathbf{z}_s^\top\right)^{-1}\left(\frac{1}{n}\sum_{s=1}^{n}\mathbf{z}_s\bar{\varepsilon}_{is}\right)>\frac{(n-d-2)\delta}{2n},\right.\\
&\left.\left\|\frac{1}{n}\sum_{s=1}^{n}\mathbf{z}_s\mathbf{z}_s^\top-\mathbb{E}(\mathbf{z}_s\mathbf{z}_s^\top)\right\|\leq\delta_1\right\}+\mathbb{P}\left\{\left\|\frac{1}{n}\sum_{s=1}^{n}\mathbf{z}_s\mathbf{z}_s^\top-\mathbb{E}(\mathbf{z}_s\mathbf{z}_s^\top)\right\|>\delta_1\right\}\\
\leq&\mathbb{P}\left\{\left\|\frac{1}{n}\sum_{s=1}^{n}\mathbf{z}_s\bar{\varepsilon}_{is}\right\|>\sqrt{\frac{C(n-d-2)\delta}{n}}\right\}+\mathbb{P}\left\{\left\|\frac{1}{n}\sum_{s=1}^{n}\mathbf{z}_s\mathbf{z}_s^\top-\mathbb{E}(\mathbf{z}_s\mathbf{z}_s^\top)\right\|>\delta_1\right\},\end{aligned}$$

with $\delta_1>0$ being a small enough constant. Here we have used the condition $\sigma_{\min}\{\mathbb{E}(\mathbf{z}_s\mathbf{z}_s^\top)\}>C$ and Lemma S8 of Zhou et al. (2020, Covariate Adaptive Family-wise Error Rate Control for Genome-Wide Association Studies) to get the last inequality. We conclude that $|\hat{\sigma}_i^2-\bar{\sigma}_i^2|$ has an exponential tail of the order $O(e^{-C_1 n})$ by using the Chernoff technique and the fact that the product of two sub-Gaussian variables is sub-exponential (Vershynin, 2018, High-dimensional probability: An introduction with applications in data science). Thus by the union bound and Condition (ix), we have $\max_i|\hat{\sigma}_i^2-\bar{\sigma}_i^2|=o_{\mathbb{P}}(1)$. Observing that

$$|\bar{\sigma}_i^2-\sigma_i^2|=\left|\frac{1}{m}\left\{(m-2)\sigma_i^2+m^{-1}\sum_{i=1}^{m}\sigma_i^2\right\}-\sigma_i^2\right|=\left|\frac{-2}{m}\sigma_i^2-\frac{1}{m^2}\sum_{i=1}^{m}\sigma_i^2\right|=o_{\mathbb{P}_m}(1),$$

we obtain the desired result that $\max_i|\hat{\sigma}_i^2-\sigma_i^2|=o_{\mathbb{P}}(1)$. □

Proof of Lemma 11. We have

$$\sqrt{n}\tilde{\alpha}_i = \sqrt{n}\bar{\alpha}_i + \sqrt{n}\hat{\boldsymbol{\eta}}^\top n^{-1}\sum_{s=1}^{n}\mathbf{z}_s\bar{\varepsilon}_{is} = \sqrt{n}\alpha_i - \sqrt{n}\bar{\alpha} + U_i - U,$$

where

$$U_i = \hat{\boldsymbol{\eta}}^\top\frac{1}{\sqrt{n}}\sum_{s=1}^{n}\mathbf{z}_s\varepsilon_{is}, \quad U = \hat{\boldsymbol{\eta}}^\top\frac{1}{\sqrt{n}}\sum_{s=1}^{n}\mathbf{z}_s\left(\frac{1}{m}\sum_{i=1}^{m}\varepsilon_{is}\right),$$

and $\hat{\boldsymbol{\eta}}$ is the first row of $(n^{-1}\sum_{s=1}^{n}\mathbf{z}_s\mathbf{z}_s^\top)^{-1}$. We first prove that $U = o_{\mathbb{P}}(1)$. Using similar arguments as in the proof of Lemma 9, we have $|\hat{\boldsymbol{\eta}} - \boldsymbol{\eta}| = o_{\mathbb{P}_n}(1)$, where $\boldsymbol{\eta}$ is the first row of $\{\mathbb{E}(\mathbf{z}_s\mathbf{z}_s^\top)\}^{-1}$. Under Conditions (i), (iii), and (v), $\mathbf{z}_s(\sum_{i=1}^{m}\varepsilon_{is})/\sqrt{m}$ are conditionally i.i.d. given $\sigma_1, \ldots, \sigma_m$. Thus,

$$\mathbb{E}\left\{\mathbf{z}_s\left(\frac{1}{\sqrt{m}}\sum_{i=1}^{m}\varepsilon_{is}\right) \;\middle|\; \sigma_1, ..., \sigma_m\right\} = 0,$$
$$\mathbb{E}\left\{(\mathbf{z}_s \odot \mathbf{z}_s)\left(\frac{1}{\sqrt{m}}\sum_{i=1}^{m}\varepsilon_{is}\right)^2 \;\middle|\; \sigma_1, \ldots, \sigma_m\right\} = \frac{\mathbb{E}(\mathbf{z}_s \odot \mathbf{z}_s)}{m}\sum_{i=1}^{m}\sigma_i^2,$$

where $\odot$ denotes the Hadamard product (element-wise product). The above implies that

$$\frac{1}{\sqrt{n}}\sum_{s=1}^{n}\mathbf{z}_s\left(\frac{1}{\sqrt{m}}\sum_{i=1}^{m}\varepsilon_{is}\right) = O_{\mathbb{P}_n}(1)$$

whenever $\sum_{i=1}^{m}\sigma_i^2/m < \infty$. Using Conditions (ii), we have $\mathbb{P}(\sum_{i=1}^{m}\sigma_i^2/m < \infty) = 1$. Thus $U = O_{\mathbb{P}}(m^{-1/2})$. Recall that

$$\widehat{\text{mode}}(\{X_i\}_{i=1}^m) = \arg\max_{x\in\mathbb{R}}\frac{1}{mh}\sum_{i=1}^{m}K\left(\frac{x - X_i}{h}\right).$$

It is not hard to see that $\widehat{\text{mode}}(\{X_i + a\}_{i=1}^m) = \widehat{\text{mode}}(\{X_i\}_{i=1}^m) + a$, for any a, which may be related

to m but is independent of i. Then we have

$$\widehat{\text{mode}}(\{\sqrt{n}\tilde{\alpha}_i\}_{i=1}^m) = \widehat{\text{mode}}(\{\sqrt{n}\alpha_i - \sqrt{n}\bar{\alpha} + U_i - U\}_{i=1}^m) = \widehat{\text{mode}}(\{\sqrt{n}\alpha_i + U_i\}_{i=1}^m) - \sqrt{n}\bar{\alpha} - U.$$

Therefore, we only need to show that $\tilde{M} := \widehat{\text{mode}}(\{\sqrt{n}\alpha_i + U_i\}_{i=1}^m) = o_{\mathbb{P}}(1)$. To this end, let

$$f_{m,h}(x) = \frac{1}{mh}\sum_{i=1}^{m} K\left(\frac{x - (\sqrt{n}\alpha_i + U_i)}{h}\right).$$

Given Condition (vi), we have that for large enough n,

$$\begin{aligned}
&|f_n(\tilde{M};\rho) - f_n(0;\rho)| \le |f_n(\tilde{M};\rho) - f_{m,h}(\tilde{M})| + |f_{m,h}(\tilde{M}) - f_n(0;\rho)| \\
=&|f_n(\tilde{M};\rho) - f_{m,h}(\tilde{M})| + \left|\sup_{x\in\mathbb{R}} f_{m,h}(x) - \sup_{x\in\mathbb{R}} f_n(x;\rho)\right| \le 2\sup_{x\in\mathbb{R}} |f_{m,h}(x) - f_n(x;\rho)|,
\end{aligned}$$

and then it boils down to show that

$$\sup_{x\in\mathbb{R}} |f_{m,h}(x) - f_n(x;\rho)| = o_{\mathbb{P}}(1).$$

We first note that

$$f_n(x;a) = \int\int \frac{1}{\sqrt{a}u}\phi\left(\frac{x-v}{\sqrt{a}u}\right) dF_{\sigma_i}(u) dF_{\sqrt{n}\alpha_i}(v)$$

for any $a > 0$, where $\phi(\cdot)$ denotes the density function of the standard normal distribution. Thus $f_n(x;a)$ is uniformly continuous and bounded uniformly over n and $a > C$. In other words, for any $\epsilon > 0$, there exists a $\delta > 0$ such that $\sup_{n,a>C,|x_1-x_2|<\delta} |f_n(x_1;a) - f_n(x_2;a)| < \epsilon$ and $\sup_{n,a>C,x\in\mathbb{R}} f_n(x;a) < \infty$. Besides, $\sup_{n,x\in\mathbb{R}} |f_n(x;\hat{\rho}) - f_n(x;\rho)|$ can be made arbitrarily small

as long as $|\hat{\rho} - \rho|$ is small enough and $\rho > C > 0$. Thus we have

$$\begin{aligned}
&\mathbb{P}\left\{\sup_{x\in\mathbb{R}} |f_{m,h}(x) - f_n(x;\rho)| > \delta\right\} \\
\leq &\mathbb{P}\left\{\sup_{x\in\mathbb{R}} |f_{m,h}(x) - f_n(x;\rho)| > \delta, |\hat{\rho} - \rho| \leq \delta_1\right\} + \mathbb{P}\left(|\hat{\rho} - \rho| > \delta_1\right) \\
\leq &\mathbb{P}\left\{\sup_{x\in\mathbb{R}} |f_{m,h}(x) - f_n(x;\hat{\rho})| > \delta/2, |\hat{\rho} - \rho| \leq \delta_1\right\} + \mathbb{P}\left(|\hat{\rho} - \rho| > \delta_1\right) \\
= &\int_{|u-\rho|\leq\delta_1} \mathbb{P}\left\{\sup_{x\in\mathbb{R}} |f_{m,h}(x) - f_n(x;\hat{\rho})| > \delta/2 \mid \hat{\rho} = u\right\} dF_{\hat{\rho}}(u) + \mathbb{P}\left(|\hat{\rho} - \rho| > \delta_1\right)
\end{aligned}$$

for any $\delta > 0$ and small enough $\delta_1 > 0$. Because $|\hat{\rho} - \rho| = o_{\mathbb{P}_n}(1)$ as shown in Lemma 9, our goal narrows down to proving that for any $\delta > 0$ and $\epsilon > 0$, there exists a $\xi > 0$ such that for large enough m,

$$\sup_{n,|\hat{\rho}-\rho|\leq\xi} \mathbb{P}\left\{\sup_{x\in\mathbb{R}} |f_{m,h}(x) - f_n(x;\hat{\rho})| > \delta \mid \hat{\rho}\right\} < \epsilon,$$

or sufficiently,

$$\begin{aligned}
&\sup_{n,|\hat{\rho}-\rho|\leq\xi,x\in\mathbb{R}} |\mathbb{E}\{f_{m,h}(x) \mid \hat{\rho}\} - f_n(x;\hat{\rho})| < \epsilon, \\
&\sup_{n,|\hat{\rho}-\rho|\leq\xi} \mathbb{E}\left[\sup_{x\in\mathbb{R}} |f_{m,h}(x) - \mathbb{E}\{f_{m,h}(x) \mid \hat{\rho}\}|^2 \mid \hat{\rho}\right] < \epsilon.
\end{aligned}$$

Let ξ and $\nu > 0$ be small enough constants. Observe that

$$
\begin{aligned}
&\sup_{n,|\hat{\rho}-\rho|\leq\xi,x\in\mathbb{R}} |\mathbb{E}\{f_{m,h}(x) \mid \hat{\rho}\} - f_n(x;\hat{\rho})| \\
&= \sup_{n,|\hat{\rho}-\rho|\leq\xi,x\in\mathbb{R}} \left| \int_{-\infty}^{\infty} \frac{1}{h} K\left(\frac{x-y}{h}\right) f_n(y;\hat{\rho}) dy - f_n(x;\hat{\rho}) \right| \\
&= \sup_{n,|\hat{\rho}-\rho|\leq\xi,x\in\mathbb{R}} \left| \int_{-\infty}^{\infty} \frac{1}{h} K\left(\frac{y}{h}\right) \{f_n(x-y;\hat{\rho}) - f_n(x;\hat{\rho})\} dy \right| \\
&= \sup_{n,|\hat{\rho}-\rho|\leq\xi,x\in\mathbb{R}} \left| \int_{|y|\leq\nu} \frac{1}{h} K\left(\frac{y}{h}\right) \{f_n(x-y;\hat{\rho}) - f_n(x;\hat{\rho})\} dy \right| \\
&\quad + \sup_{n,|\hat{\rho}-\rho|\leq\xi,x\in\mathbb{R}} \left| \int_{|y|>\nu} \frac{1}{h} K\left(\frac{y}{h}\right) \{f_n(x-y;\hat{\rho}) - f_n(x;\hat{\rho})\} dy \right| \\
&\leq \sup_{n,|\hat{\rho}-\rho|\leq\xi,x\in\mathbb{R},|y|\leq\nu} |f_n(x-y;\hat{\rho}) - f_n(x;\hat{\rho})| \int_{|u|\leq\nu/h} K(u) du \\
&\quad + \sup_{n,|\hat{\rho}-\rho|\leq\xi,x\in\mathbb{R}} f_n(x;\hat{\rho}) \int_{|u|>\nu/h} K(u) du < \epsilon,
\end{aligned}
$$

where we have used the condition that $\int_{-\infty}^{\infty} K(y)dy = 1$ to get the second equality, and we also used the result that $f_n(x;a)$ is uniformly continuous and bounded uniformly over n in the above derivations. Note that U_i's have the same distribution as $\sqrt{\hat{\rho}}\varepsilon_{is}$ and are independent given $\hat{\rho}$. Let $X_i = \sqrt{n}\alpha_i + U_i$. Define

$$
\varphi_m(u) = m^{-1} \sum_{i=1}^{m} e^{\imath u X_i}.
$$

By the inverse Fourier transformation, we have

$$
K(y) = (2\pi)^{-1} \int_{-\infty}^{\infty} k(u) e^{\imath u y} du.
$$

Plugging this expression into the definition of $f_{m,h}$, we have

$$\begin{aligned} f_{m,h}(x) =& \frac{1}{mh}\sum_{i=1}^{m} K\left(\frac{x-X_i}{h}\right) = (2\pi mh)^{-1}\sum_{i=1}^{m}\int_{-\infty}^{\infty} k(u)e^{\imath u\frac{x-X_i}{h}}du \\ =& (2\pi m)^{-1}\sum_{i=1}^{m}\int_{-\infty}^{\infty} k(hu)e^{\imath u(x-X_i)}du = (2\pi)^{-1}\int_{-\infty}^{\infty} e^{-\imath ux}k(hu)\varphi_m(u)du, \end{aligned}$$

where the last equality follows as $k(u)$ is even. Using this result, we obtain

$$\sup_{x\in\mathbb{R}}|f_{m,h}(x) - \mathbb{E}\{f_{m,h}(x) \mid \hat{\rho}\}| \leq (2\pi)^{-1}\int_{-\infty}^{\infty}|k(hu)||\varphi_m(u) - \mathbb{E}\{\varphi_m(u) \mid \hat{\rho}\}|du.$$

Thus we have

$$\begin{aligned} &\sup_{n,|\hat{\rho}-\rho|\leq\xi}\mathbb{E}\left[\sup_{x\in\mathbb{R}}|f_{m,h}(x) - \mathbb{E}\{f_{m,h}(x) \mid \hat{\rho}\}|^2 \mid \hat{\rho}\right] \\ \leq& \sup_{n,|\hat{\rho}-\rho|\leq\xi}\mathbb{E}\left(\left[(2\pi)^{-1}\int_{-\infty}^{\infty}|k(hu)||\varphi_m(u) - \mathbb{E}\{\varphi_m(u) \mid \hat{\rho}\}|du\right]^2 \mid \hat{\rho}\right) \\ \leq& \sup_{n,|\hat{\rho}-\rho|\leq\xi}(2\pi)^{-2}\int_{-\infty}^{\infty}|k(hu)|du\int_{-\infty}^{\infty}|k(hu)|\mathbb{E}\left[|\varphi_m(u) - \mathbb{E}\{\varphi_m(u) \mid \hat{\rho}\}|^2 \mid \hat{\rho}\right]du \\ =& \sup_{n,|\hat{\rho}-\rho|\leq\xi}(2\pi)^{-2}m^{-1}\int_{-\infty}^{\infty}|k(hu)|du\int_{-\infty}^{\infty}|k(hu)|\mathbb{E}\left[|e^{\imath uX_i} - \mathbb{E}\{e^{\imath uX_i} \mid \hat{\rho}\}|^2 \mid \hat{\rho}\right]du \\ \leq& \pi^{-2}m^{-1}h^{-2}\left\{\int_{-\infty}^{\infty}|k(u)|du\right\}^2 \to 0 \end{aligned}$$

as a result of Conditions (vii) and (viii), which completes the proof. □

Proof of Lemma 12. Let

$$S_{m,n}^{-}(t) = \sum_{i=1}^{m}\mathbb{I}\left(\sqrt{n}\hat{\alpha}_i/\sqrt{\hat{\rho}\hat{\sigma}_i^2} < -t\right).$$

The goal is to show

$$\sup_{0<t<t_0}\left|\frac{1}{m}S_{m,n}^{-}(t) - \mathbb{P}\left(\mathcal{E} + \sqrt{n}\alpha_i/\sqrt{\rho\sigma_i^2} < -t\right)\right| = o_{\mathbb{P}}(1).$$

Recall in the proof of Lemma 11, we have

$$\sqrt{n}\hat{\alpha}_i = \sqrt{n}(\tilde{\alpha}_i + \tilde{\alpha}) = \sqrt{n}\alpha_i + \sqrt{n}(\tilde{\alpha} - \bar{\alpha}) + U_i - U,$$

where $U_i/\sqrt{\hat{\rho}\sigma_i^2} \sim^{\text{i.i.d.}} N(0,1)$, $U = o_{\mathbb{P}}(1)$ and $\sqrt{n}(\tilde{\alpha} - \bar{\alpha}) = o_{\mathbb{P}}(1)$. Then

$$\frac{1}{m}S^-_{m,n}(t) = \frac{1}{m}\sum_{i=1}^{m}\mathbb{I}\left\{\frac{U_i}{\sqrt{\hat{\rho}\sigma_i^2}} + \frac{\alpha_i}{\sqrt{\hat{\rho}\sigma_i^2/n}} < -t\frac{\hat{\sigma}_i}{\sigma_i} + \frac{U - \sqrt{n}(\tilde{\alpha} - \bar{\alpha})}{\sqrt{\hat{\rho}\sigma_i^2}}\right\},$$

and

$$\begin{aligned}
&\mathbb{P}\left\{\sup_{0<t<t_0}\left|\frac{1}{m}S^-_{m,n}(t) - \mathbb{P}\left(\mathcal{E} + \alpha_i/\sqrt{\rho\sigma_i^2/n} < -t\right)\right| > \delta\right\} \\
\leq&\mathbb{P}\Bigg[\sup_{0<t<t_0}\Bigg|\frac{1}{m}\sum_{i=1}^{m}\mathbb{I}\left\{\frac{U_i}{\sqrt{\hat{\rho}\sigma_i^2}} + \frac{\alpha_i}{\sqrt{\hat{\rho}\sigma_i^2/n}} < -t\frac{\hat{\sigma}_i}{\sigma_i} + \frac{U - \sqrt{n}(\tilde{\alpha} - \bar{\alpha})}{\sqrt{\hat{\rho}\sigma_i^2}}\right\} \\
&\qquad - \mathbb{P}\left(\mathcal{E} + \alpha_i/\sqrt{\rho\sigma_i^2/n} < -t\right)\Bigg| > \delta, \\
&\qquad \sup_i\left|\frac{\hat{\sigma}_i}{\sigma_i} - 1\right| \leq \delta_1, \sup_i\left|\frac{U - \sqrt{n}(\tilde{\alpha} - \bar{\alpha})}{\sqrt{\hat{\rho}\sigma_i^2}}\right| \leq \delta_2\Bigg] \\
&+ \mathbb{P}\left(\sup_i\left|\frac{\hat{\sigma}_i}{\sigma_i} - 1\right| > \delta_1\right) + \mathbb{P}\left\{\sup_i\left|\frac{U - \sqrt{n}(\tilde{\alpha} - \bar{\alpha})}{\sqrt{\hat{\rho}\sigma_i^2}}\right| > \delta_2\right\} \\
\leq&\mathbb{P}\left\{\sup_{0<t<t_0}\left|\frac{1}{m}\sum_{i=1}^{m}\mathbb{I}\left(\frac{U_i}{\sqrt{\hat{\rho}\sigma_i^2}} + \frac{\alpha_i}{\sqrt{\hat{\rho}\sigma_i^2/n}} < -t - t\delta_1 - \delta_2\right) - \mathbb{P}\left(\mathcal{E} + \frac{\alpha_i}{\sqrt{\rho\sigma_i^2/n}} < -t\right)\right| > \delta\right\} \\
&+ \mathbb{P}\left\{\sup_{0<t<t_0}\left|\frac{1}{m}\sum_{i=1}^{m}\mathbb{I}\left(\frac{U_i}{\sqrt{\hat{\rho}\sigma_i^2}} + \frac{\alpha_i}{\sqrt{\hat{\rho}\sigma_i^2/n}} < -t + t\delta_1 + \delta_2\right) - \mathbb{P}\left(\mathcal{E} + \frac{\alpha_i}{\sqrt{\rho\sigma_i^2/n}} < -t\right)\right| > \delta\right\} \\
&+ o(1)
\end{aligned}$$

for any positive constants δ, δ_1 and δ_2, where in the last step, we have used the fact that $\rho > C$, $\sigma_i > C$ and the results from Lemmas 9–11. Thus we only need to show that for any $\delta > 0$ and

$\epsilon > 0$, there exist $\xi > 0$, $\delta_1 \neq 0$ and $\delta_2 \neq 0$ such that for large enough m,

$$\sup_{n,|\hat{\rho}-\rho|<\xi} \mathbb{P}\Bigg\{ \sup_{0<t<t_0} \Bigg| \frac{1}{m}\sum_{i=1}^{m} \mathbb{I}\left(\frac{U_i}{\sqrt{\hat{\rho}\sigma_i^2}} + \frac{\alpha_i}{\sqrt{\hat{\rho}\sigma_i^2/n}} < -t + t\delta_1 + \delta_2 \right) - \mathbb{P}\left(\mathcal{E} + \frac{\alpha_i}{\sqrt{\rho\sigma_i^2/n}} < -t \right) \Bigg| > \delta \;\Bigg|\; \hat{\rho} \Bigg\} < \epsilon,$$

or sufficiently,

$$\begin{aligned}
&\sup_{n,|\hat{\rho}-\rho|<\xi} \mathbb{P}\Bigg\{ \sup_{0<t<t_0} \Bigg| \frac{1}{m}\sum_{i=1}^{m} \mathbb{I}\left(\frac{U_i}{\sqrt{\hat{\rho}\sigma_i^2}} + \frac{\alpha_i}{\sqrt{\hat{\rho}\sigma_i^2/n}} < -t + t\delta_1 + \delta_2 \right) \\
&\qquad - \mathbb{P}\left(\mathcal{E} + \frac{\alpha_i}{\sqrt{\hat{\rho}\sigma_i^2/n}} < -t + t\delta_1 + \delta_2 \;\middle|\; \hat{\rho} \right) \Bigg| > \delta \;\Bigg|\; \hat{\rho} \Bigg\} < \epsilon, \\
&\sup_{n,|\hat{\rho}-\rho|<\xi,0<t<t_0} \left| \mathbb{P}\left(\mathcal{E} + \frac{\alpha_i}{\sqrt{\hat{\rho}\sigma_i^2/n}} < -t + t\delta_1 + \delta_2 \;\middle|\; \hat{\rho} \right) - \mathbb{P}\left(\mathcal{E} + \frac{\alpha_i}{\sqrt{\hat{\rho}\sigma_i^2/n}} < -t \;\middle|\; \hat{\rho} \right) \right| < \epsilon, \\
&\sup_{n,|\hat{\rho}-\rho|<\xi,0<t<t_0} \left| \mathbb{P}\left(\mathcal{E} + \frac{\alpha_i}{\sqrt{\hat{\rho}\sigma_i^2/n}} < -t \;\middle|\; \hat{\rho} \right) - \mathbb{P}\left(\mathcal{E} + \frac{\alpha_i}{\sqrt{\rho\sigma_i^2/n}} < -t \right) \right| < \epsilon,
\end{aligned}$$

where the first result holds due to the Glivenko–Cantelli theorem (Corollary 4.15, Wainwright, 2019, High-dimensional statistics: A non-asymptotic viewpoint). We note that the cumulative distribution function of $\mathcal{E} + \alpha_i/\sqrt{a\sigma_i^2/n}$ for any $a > 0$, denoted by $G_n(\cdot; a)$, can be expressed as

$$G_n(x;a) = \int_{-\infty}^{\infty} \Phi\left(x-u\right) dF_{\alpha_i/\sqrt{a\sigma_i^2/n}}(u) = \int_{-\infty}^{\infty} \Phi\left(x - \sqrt{\frac{\rho}{a}}u\right) dF_{\alpha_i/\sqrt{\rho\sigma_i^2/n}}(u),$$

where $\Phi(\cdot)$ represents the cumulative distribution function of the standard normal distribution. Thus $G_n(x;a)$ is uniformly continuous uniformly over n and $a > 0$. In other words, for any $\epsilon > 0$, there exists a $\delta > 0$ such that $\sup_{n,a>0,|x_1-x_2|<\delta} |G_n(x_1;a) - G_n(x_2;a)| < \epsilon$, which verifies the second result. In addition, $\sup_{n,|\hat{\rho}-\rho|<\xi,|x|<t_0} |G_n(x;\hat{\rho}) - G_n(x;\rho)|$ can be made arbitrarily small as long as ξ is small enough, which confirms the third result. □

Proof of Theorem 2. Observe that

$$\left|\widehat{\mathrm{FDP}}(t) - \frac{2F_{n-d-2}(-t)}{S_{\infty,n}(t)}\right| = \left|2F_{n-d-2}(-t)\left\{\frac{1}{S_{m,n}(t)/m} - \frac{1}{S_{\infty,n}(t)}\right\}\right|.$$

Combing with Lemma 12 and Condition (x), we deduce that there exists some t_0 such that $t^* < t_0$ for large enough n, and

$$\begin{aligned}
&\sup_{0<t<t_0}\left|\frac{V_{m,n}(t)}{1\vee S_{m,n}(t)} - \frac{m_0}{m}\frac{2F_{n-d-2}(-t)}{S_{\infty,n}(t)}\right| \\
=&\sup_{0<t<t_0}\left|\frac{V_{m,n}(t)}{1\vee S_{m,n}(t)} - \frac{2F_{n-d-2}(-t)}{\{1\vee S_{m,n}(t)\}/m_0} + \frac{2F_{n-d-2}(-t)}{\{1\vee S_{m,n}(t)\}/m_0} - \frac{m_0}{m}\frac{2F_{n-d-2}(-t)}{S_{\infty,n}(t)}\right| \\
\le&\sup_{0<t<t_0}\left|\frac{m_0^{-1}V_{m,n}(t) - 2F_{n-d-2}(-t)}{\{1\vee S_{m,n}(t)\}/m_0}\right| + \sup_{0<t<t_0}\left|\frac{2m_0F_{n-d-2}(-t)}{m}\left[\frac{1}{\{1\vee S_{m,n}(t)\}/m} - \frac{1}{S_{\infty,n}(t)}\right]\right| \\
=&o_{\mathbb{P}}(1),
\end{aligned}$$

and

$$\sup_{0<t<t_0}\left|\widehat{\mathrm{FDP}}(t) - \frac{2F_{n-d-2}(-t)}{S_{\infty,n}(t)}\right| = \sup_{0<t<t_0}\left|2F_{n-d-2}(-t)\left\{\frac{1}{S_{m,n}(t)/m} - \frac{1}{S_{\infty,n}(t)}\right\}\right| = o_{\mathbb{P}}(1).$$

Therefore, we have

$$\begin{aligned}
\frac{V_{m,n}(t^*)}{1\vee S_{m,n}(t^*)} \le& \frac{V_{m,n}(t^*)}{1\vee S_{m,n}(t^*)} - \frac{m_0}{m}\frac{2F_{n-d-2}(-t^*)}{S_{\infty,n}(t^*)} + \frac{2F_{n-d-2}(-t^*)}{S_{\infty,n}(t^*)} - \widehat{\mathrm{FDP}}(t^*) + \widehat{\mathrm{FDP}}(t^*) \\
\le& q + o_{\mathbb{P}}(1).
\end{aligned}$$

The conclusion follows by using Lemma 8.3 of Cao et al. (2020, Optimal false discovery rate control for large scale multiple testing with auxiliary information). □

B.3 Additional simulation results

Figures B.1 and B.2 compare the proposed method LinDA with different zero-handling approaches under settings S6C0 and S0C0. Figure B.3 shows the results of methods DESeq2, EdgeR

and MetagenomeSeq-2 under setting S0C0. Figure B.11 compares the ANCOM-BC disabling and enabling zero treatment for setting S6C0. Figures B.4–B.10 and B.12–B.13 show the results of settings S0C1, S0C2, S1C0, S2C0, S4C0, S5C0, S6C0, and S7.1C0 and S7.2C0 respectively. Figure B.14 shows the results under S0C0 with stronger compositional effects.

B.4 Additional results of real data applications

Figures B.15–B.18 show the effect size plots and volcano plots for the four datasets (CDI, IBD, RA and SMOKE) respectively.

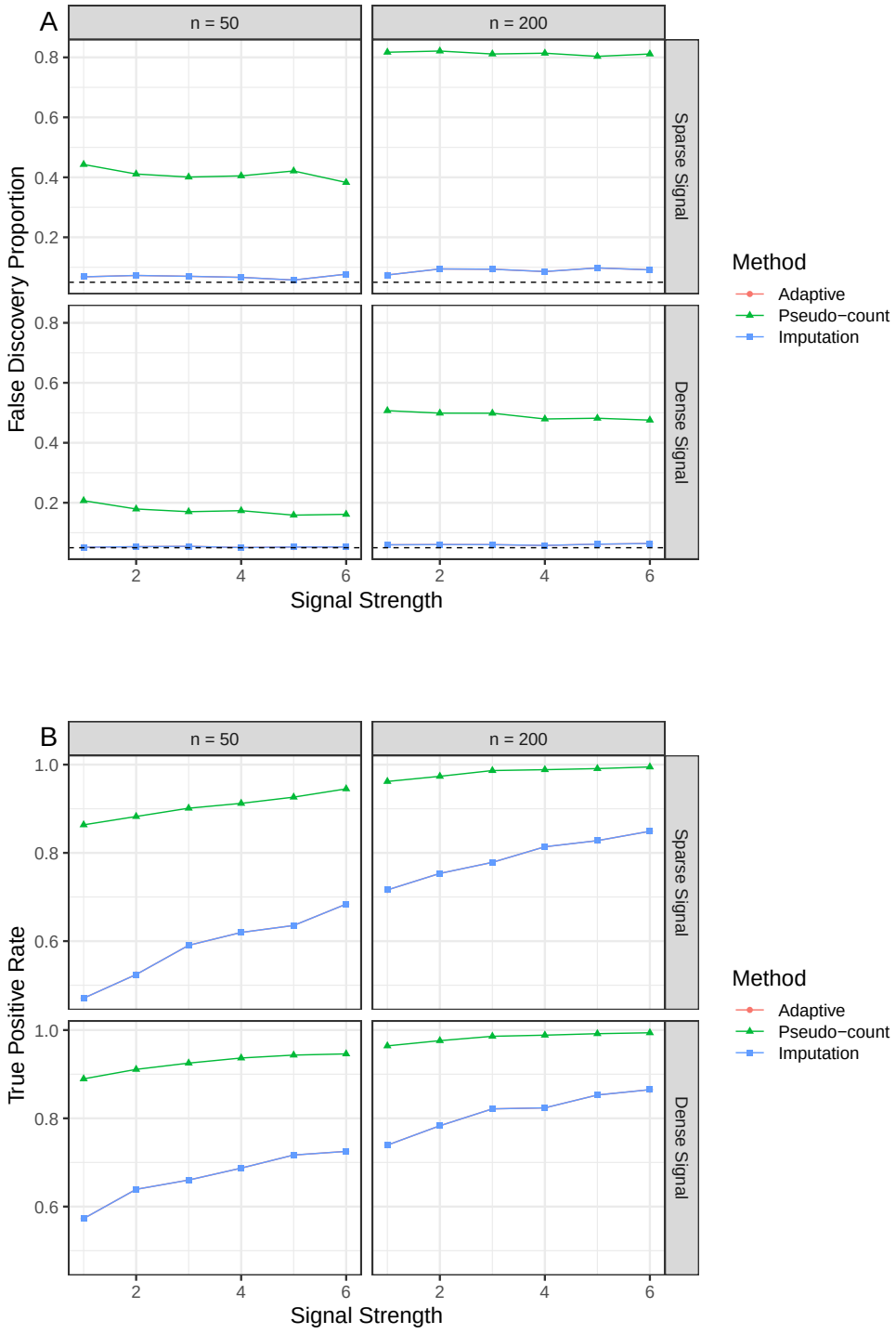

Figure B.1: Performance of LinDA with different zero-handling approaches (S6C0, 10-fold difference in library size). False discovery proportions (A) and true positive rates (B) were averaged over 100 simulation runs. The dashed horizontal line (A) indicates the target FDR level of 0.05.

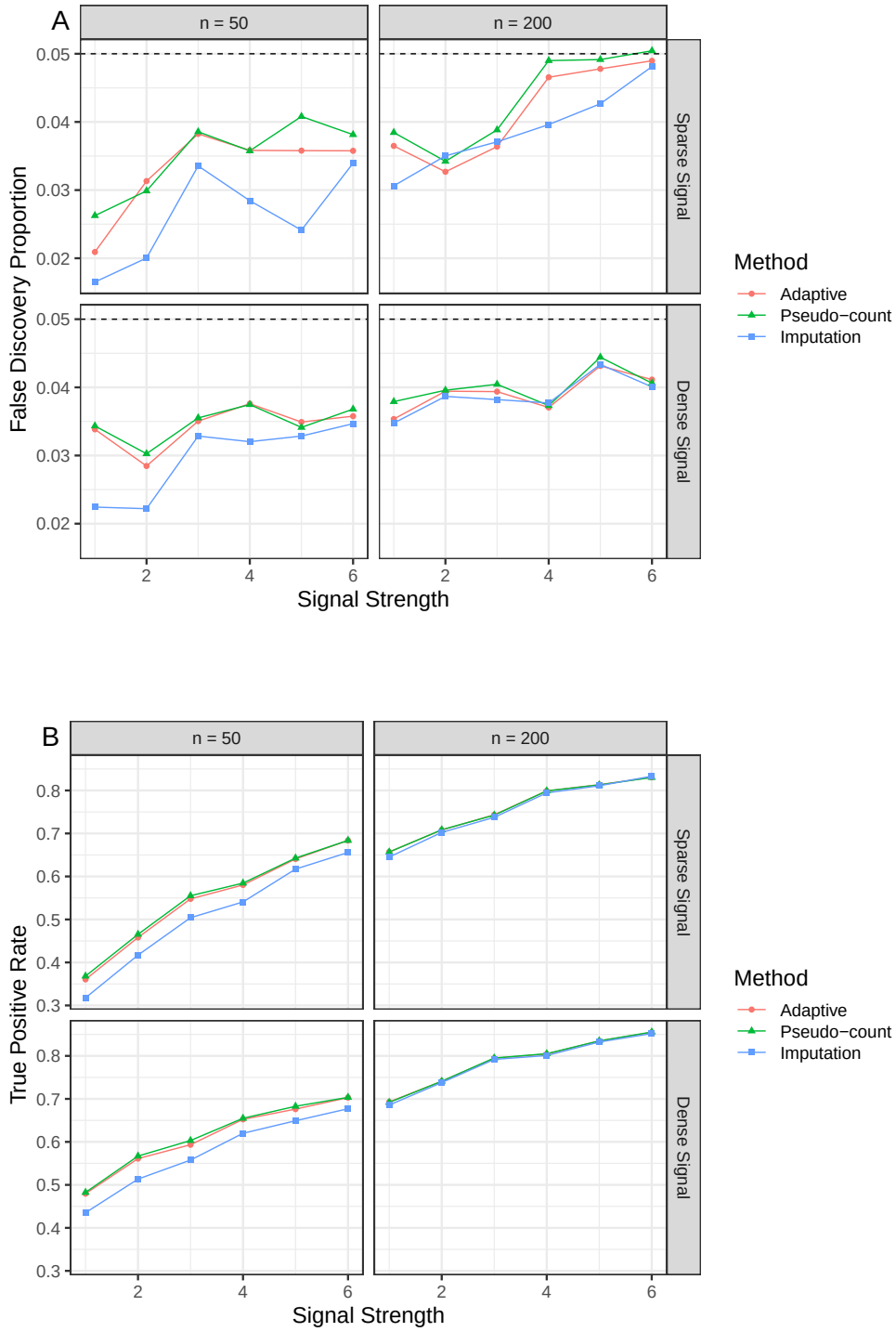

Figure B.2: Performance of LinDA with different zero-handling approaches (S0C0, log normal distribution for absolute abundances with a binary covariate). False discovery proportions (A) and true positive rates (B) were averaged over 100 simulation runs. The dashed horizontal line (A) indicates the target FDR level of 0.05.

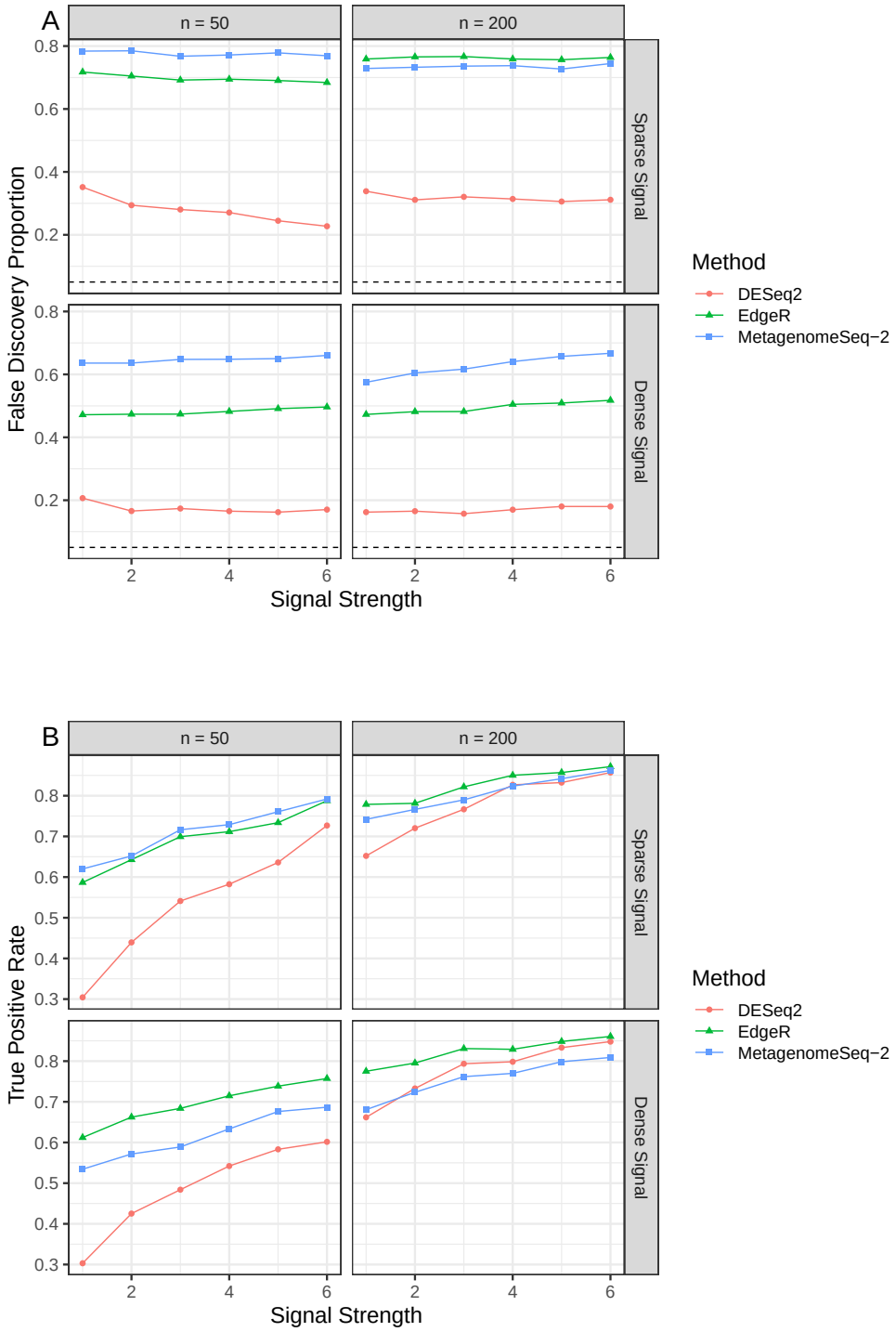

Figure B.3: Performance of DESeq2, EdgeR and MetagenomeSeq-2 (S0C0, log normal distribution for absolute abundances with a binary covariate). False discovery proportions (A) and true positive rates (B) were averaged over 100 simulation runs. The dashed horizontal line (A) indicates the target FDR level of 0.05.

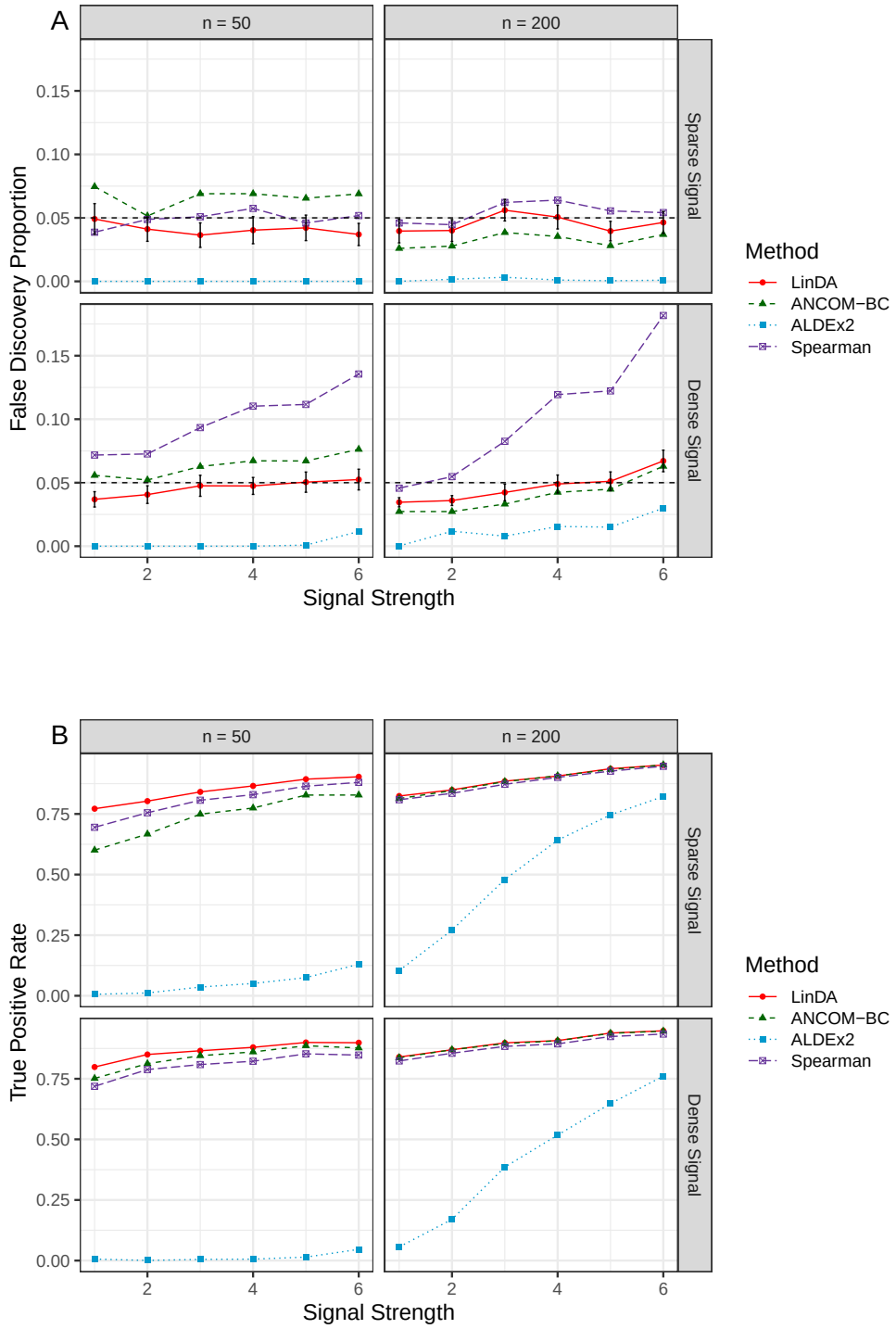

Figure B.4: Performance comparison (S0C1, log normal distribution for absolute abundances with a continuous covariate). False discovery proportions (A) and true positive rates (B) were averaged over 100 simulation runs. Error bars (A) represent the 95% CIs of the method LinDA and the dashed horizontal line indicates the target FDR level of 0.05.

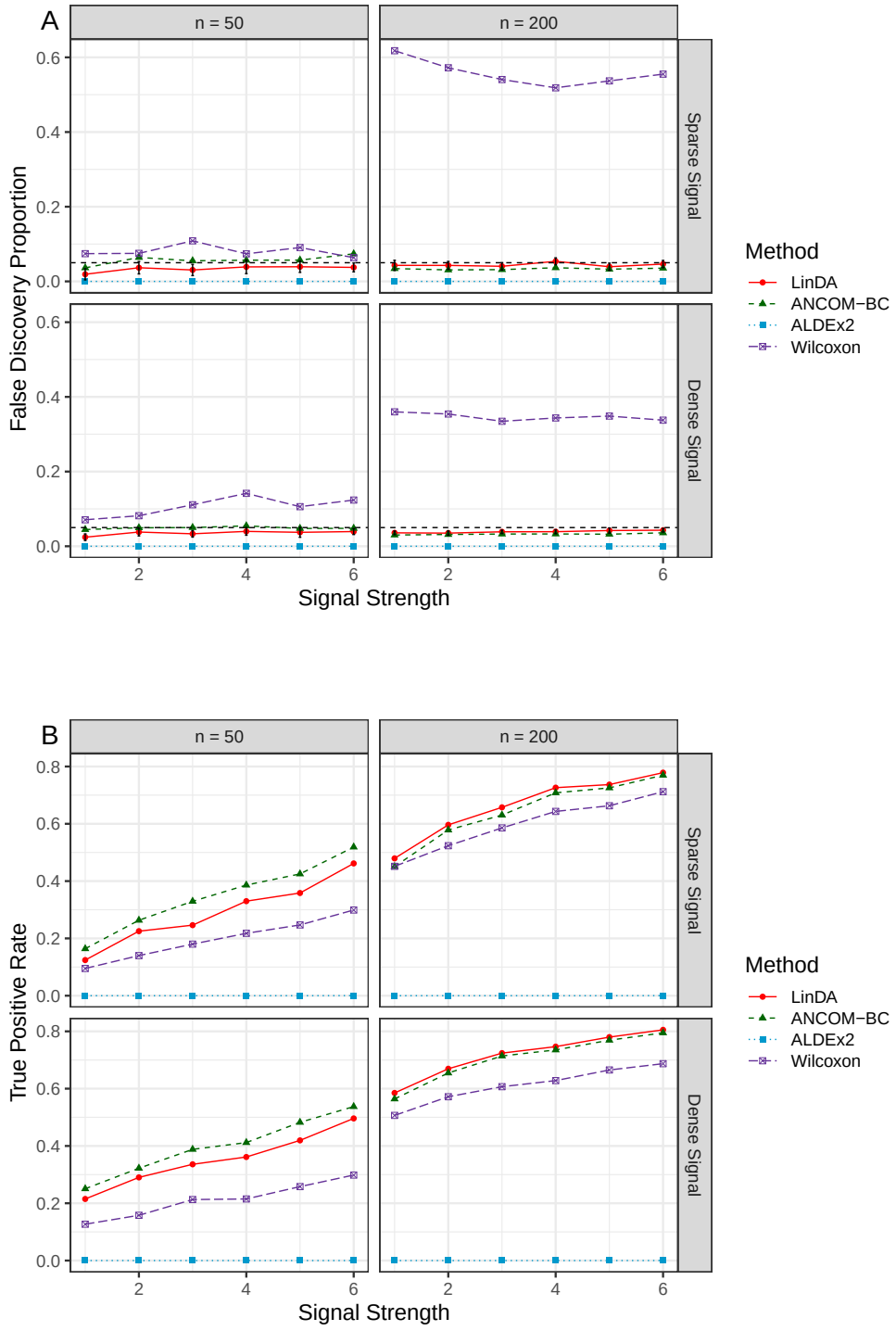

Figure B.5: Performance comparison (S0C2, log normal distribution for absolute abundances with a binary variable of interest and two confounders). False discovery proportions (A) and true positive rates (B) were averaged over 100 simulation runs. Error bars (A) represent the 95% CIs of the method LinDA and the dashed horizontal line indicates the target FDR level of 0.05.

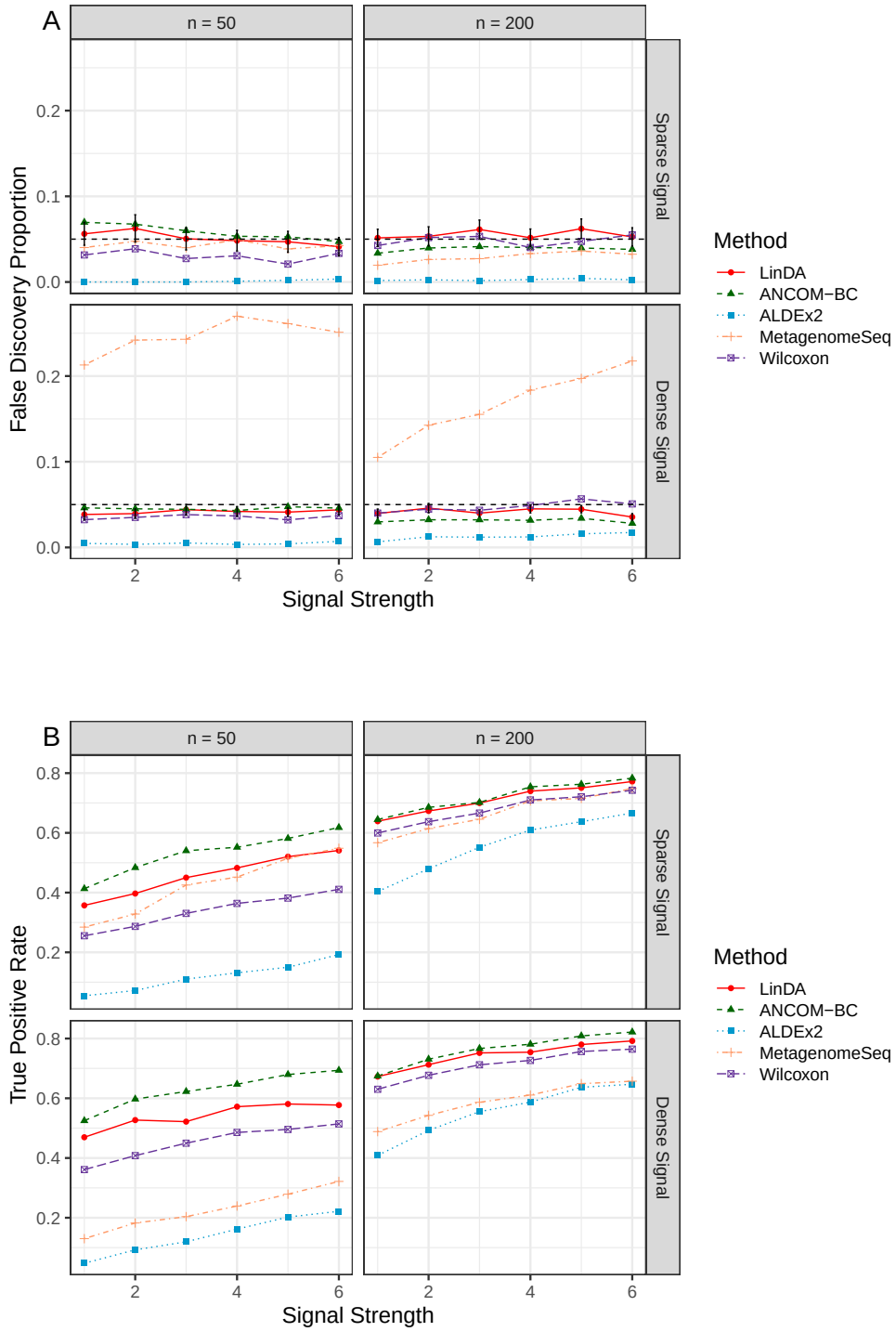

Figure B.6: Performance comparison (S1C0, zero inflated absolute abundances). False discovery proportions (A) and true positive rates (B) were averaged over 100 simulation runs. Error bars (A) represent the 95% CIs of the method LinDA and the dashed horizontal line indicates the target FDR level of 0.05.

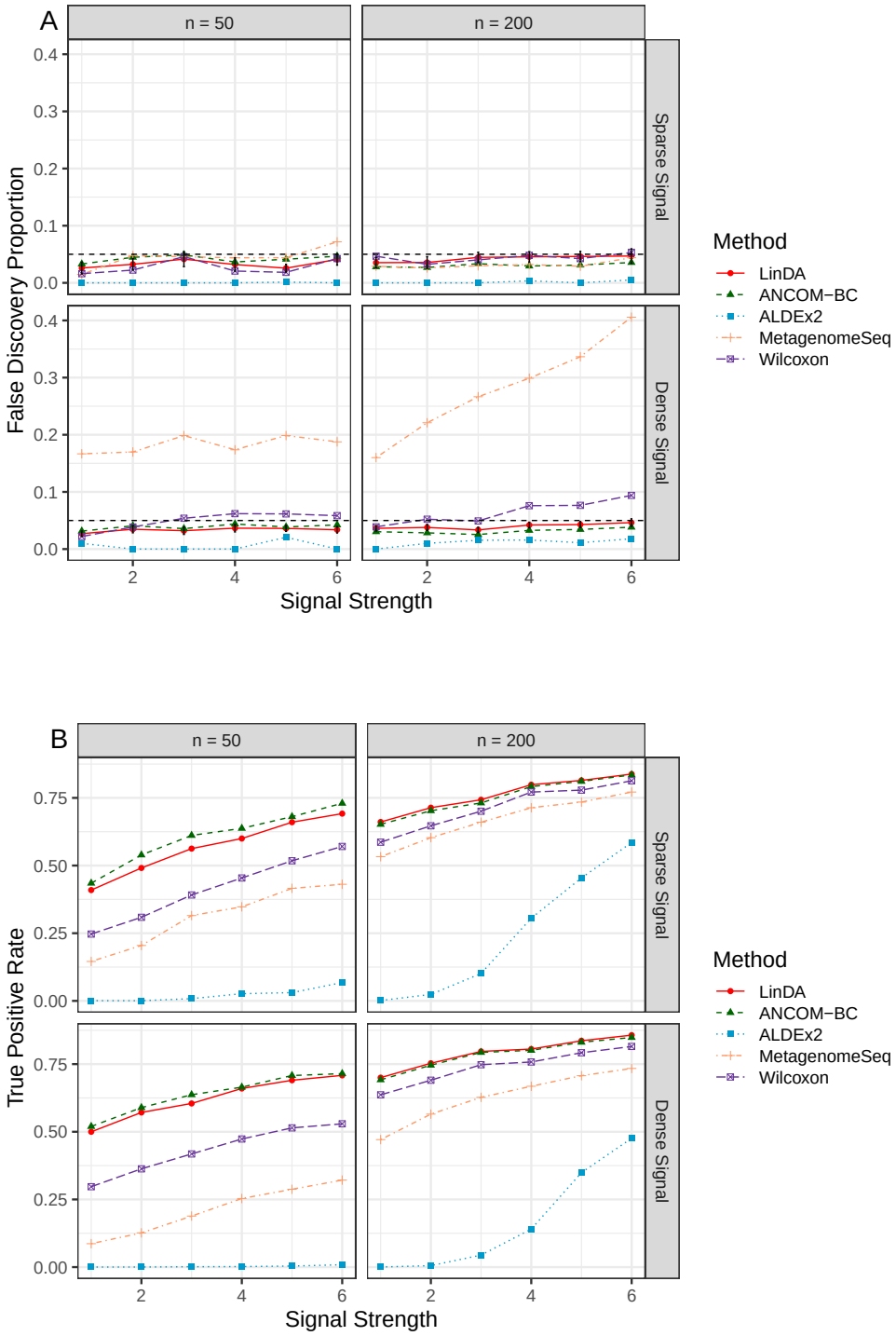

Figure B.7: Performance comparison (S2C0, correlated absolute abundances). False discovery proportions (A) and true positive rates (B) were averaged over 100 simulation runs. Error bars (A) represent the 95% CIs of the method LinDA and the dashed horizontal line indicates the target FDR level of 0.05.

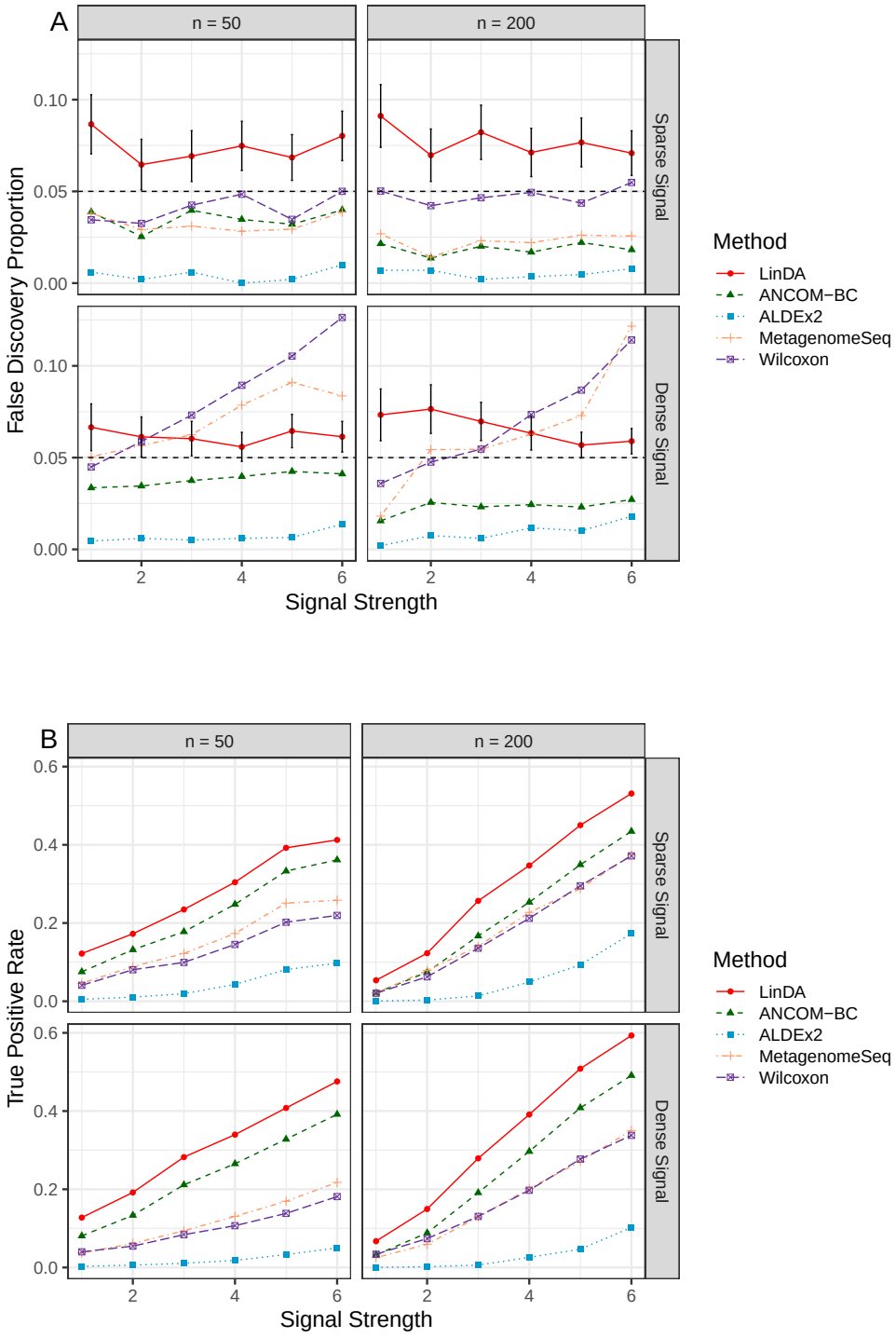

Figure B.8: Performance comparison (S4C0, smaller m). False discovery proportions (A) and true positive rates (B) were averaged over 1000 simulation runs. Error bars (A) represent the 95% CIs of the method LinDA and the dashed horizontal line indicates the target FDR level of 0.05.

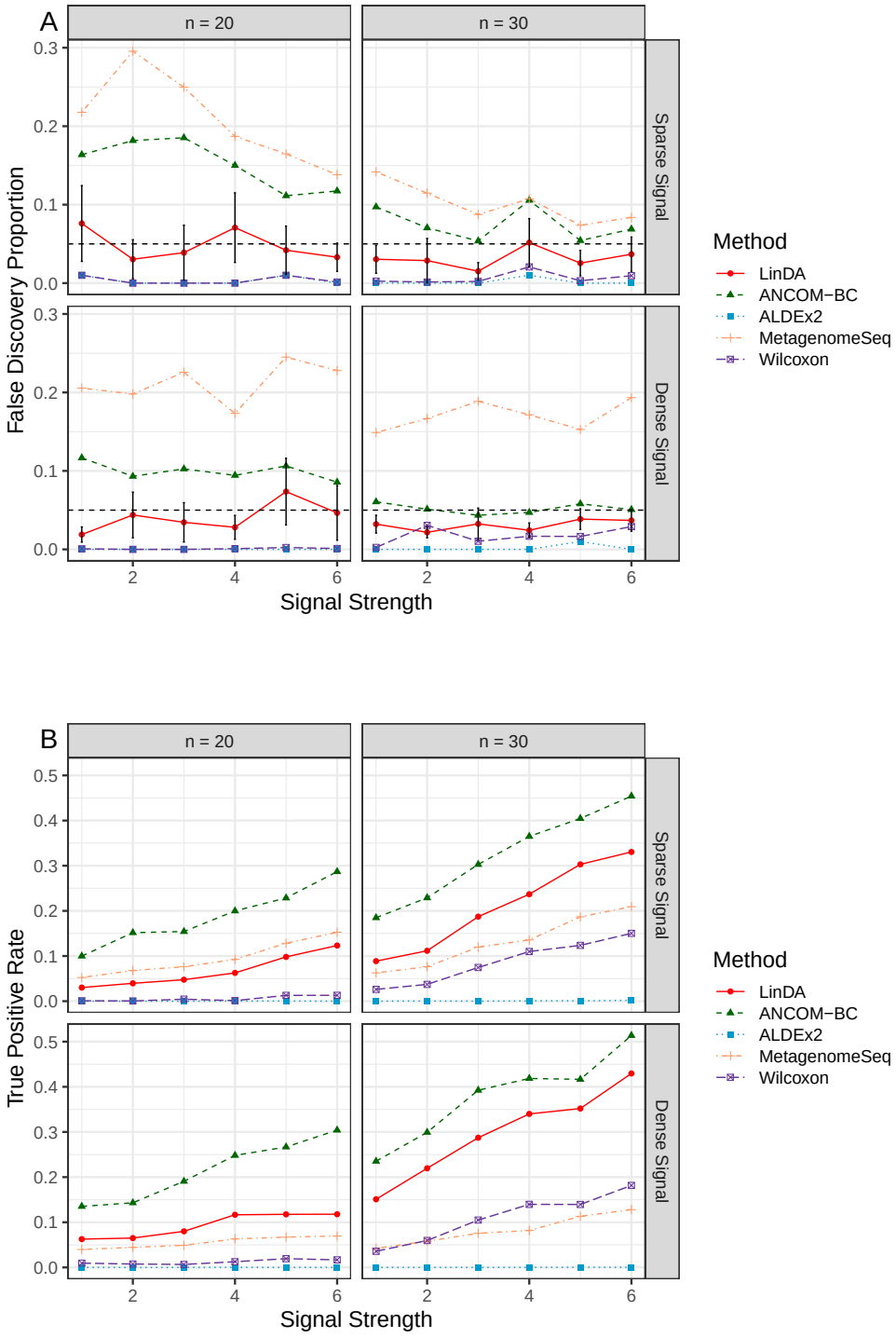

Figure B.9: Performance comparison (S5C0, smaller n). False discovery proportions (A) and true positive rates (B) were averaged over 100 simulation runs. Error bars (A) represent the 95% CIs of the method LinDA and the dashed horizontal line indicates the target FDR level of 0.05.

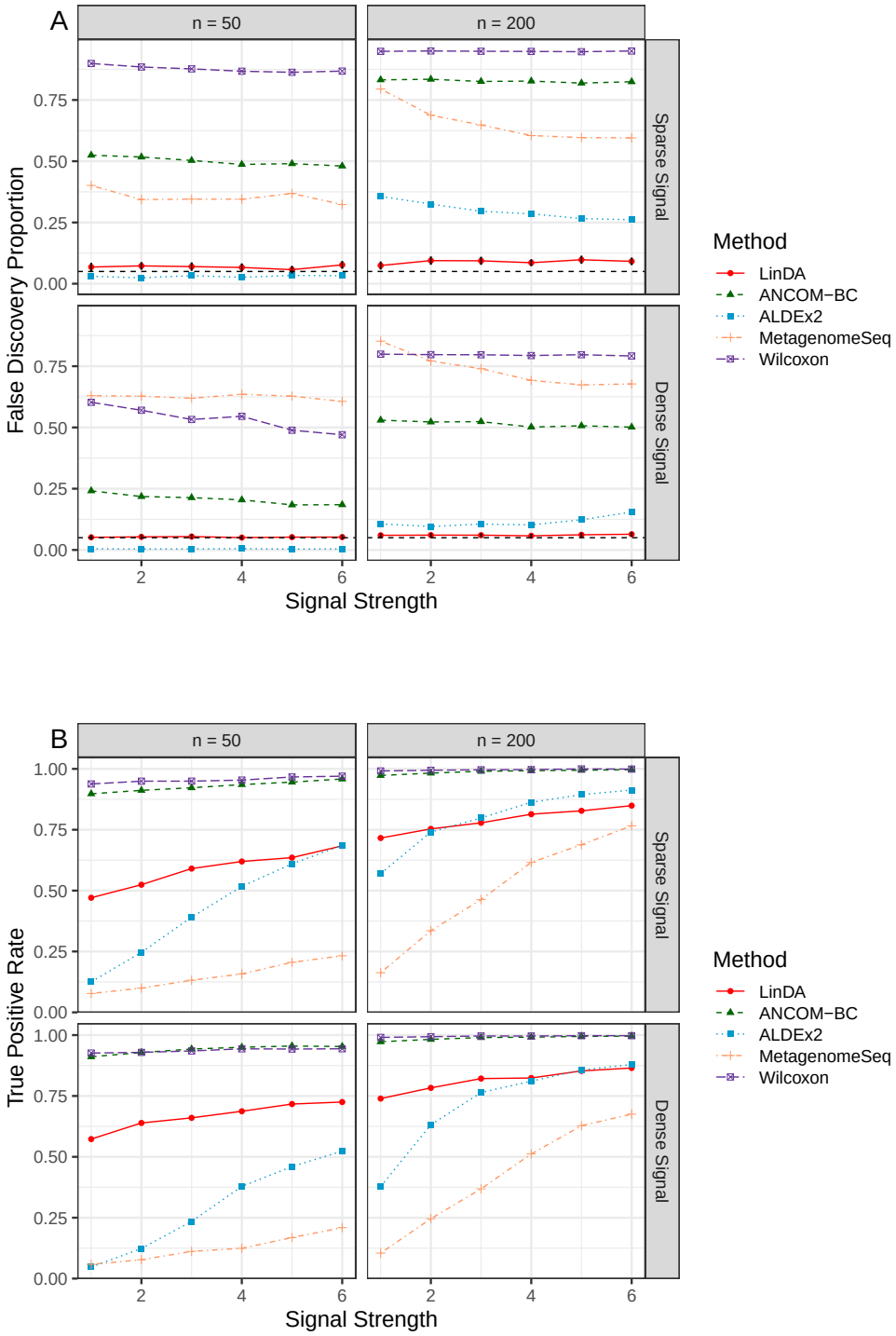

Figure B.10: Performance comparison (S6C0, 10-fold difference in library size). False discovery proportions (A) and true positive rates (B) were averaged over 100 simulation runs. Error bars (A) represent the 95% CIs of the method LinDA and the dashed horizontal line indicates the target FDR level of 0.05.

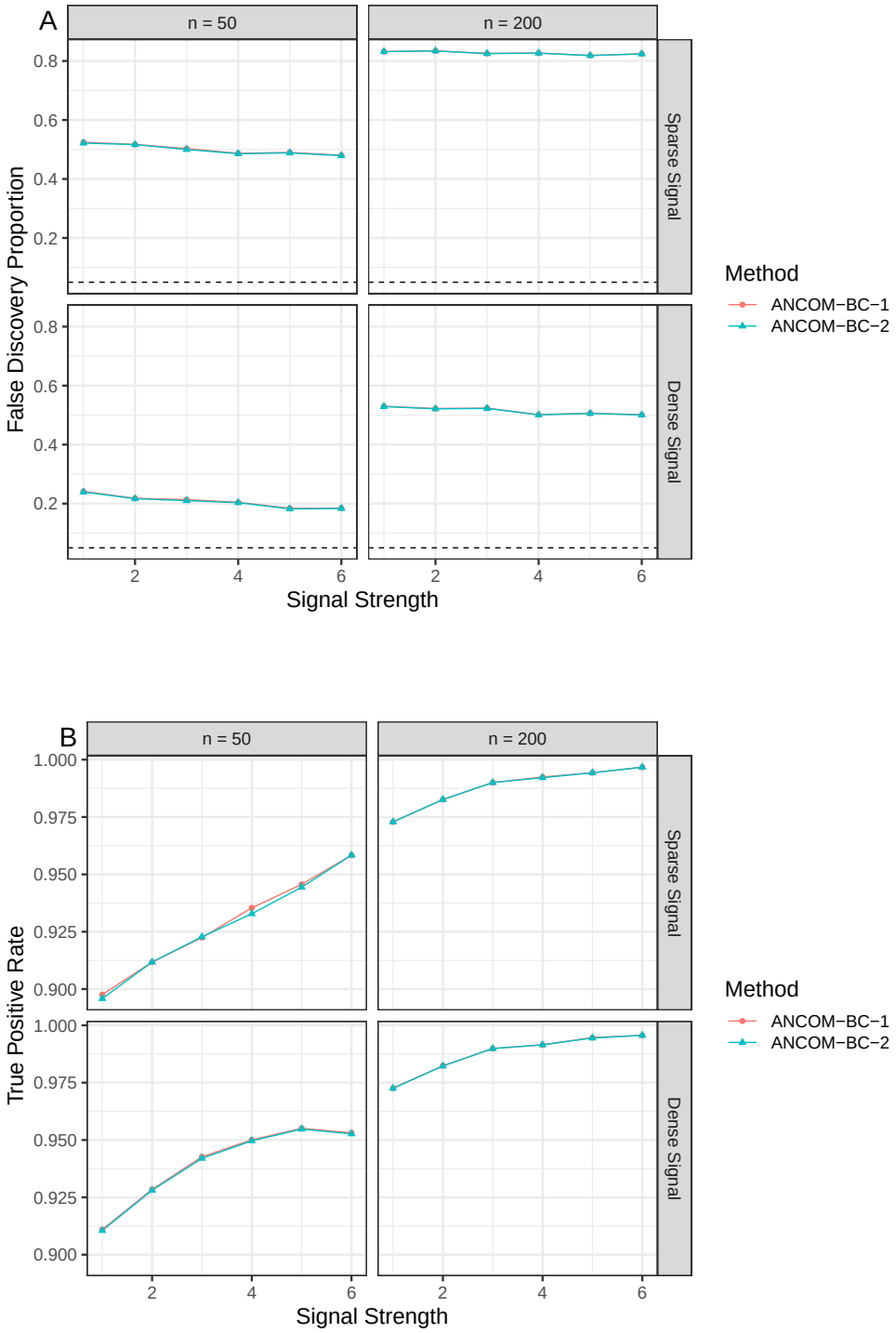

Figure B.11: Performance of ANCOM-BC disabling (ANCOM-BC-1) and enabling (ANCOM-BC-2) zero treatment (S6C0, 10-fold difference in library size). False discovery proportions (A) and true positive rates (B) were averaged over 100 simulation runs. The dashed horizontal line (A) indicates the target FDR level of 0.05.

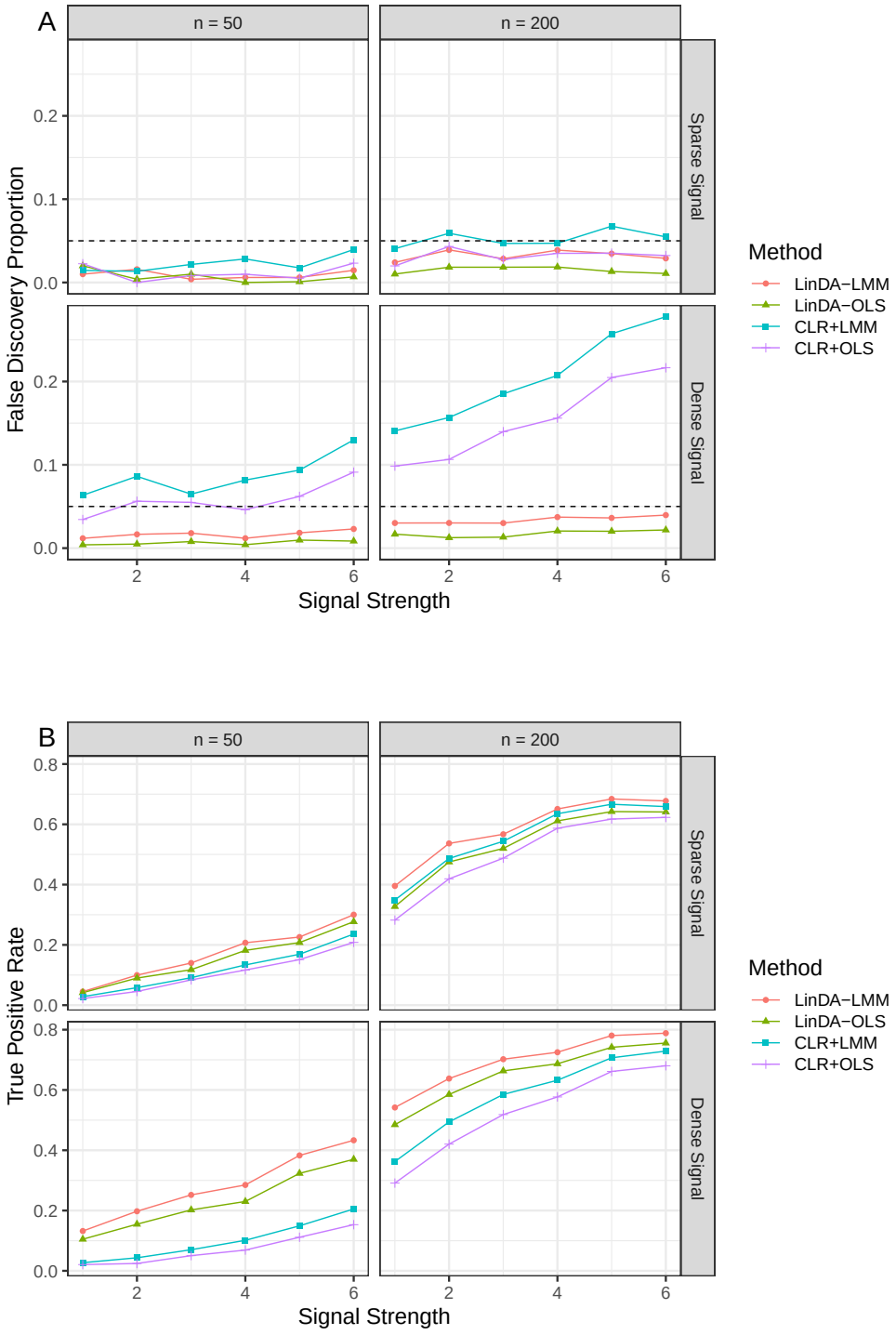

Figure B.12: Performance comparison (S7.1C0, pre-treatment and post-treatment comparison). False discovery proportions (A) and true positive rates (B) were averaged over 100 simulation runs. The dashed horizontal line (A) indicates the target FDR level of 0.05.

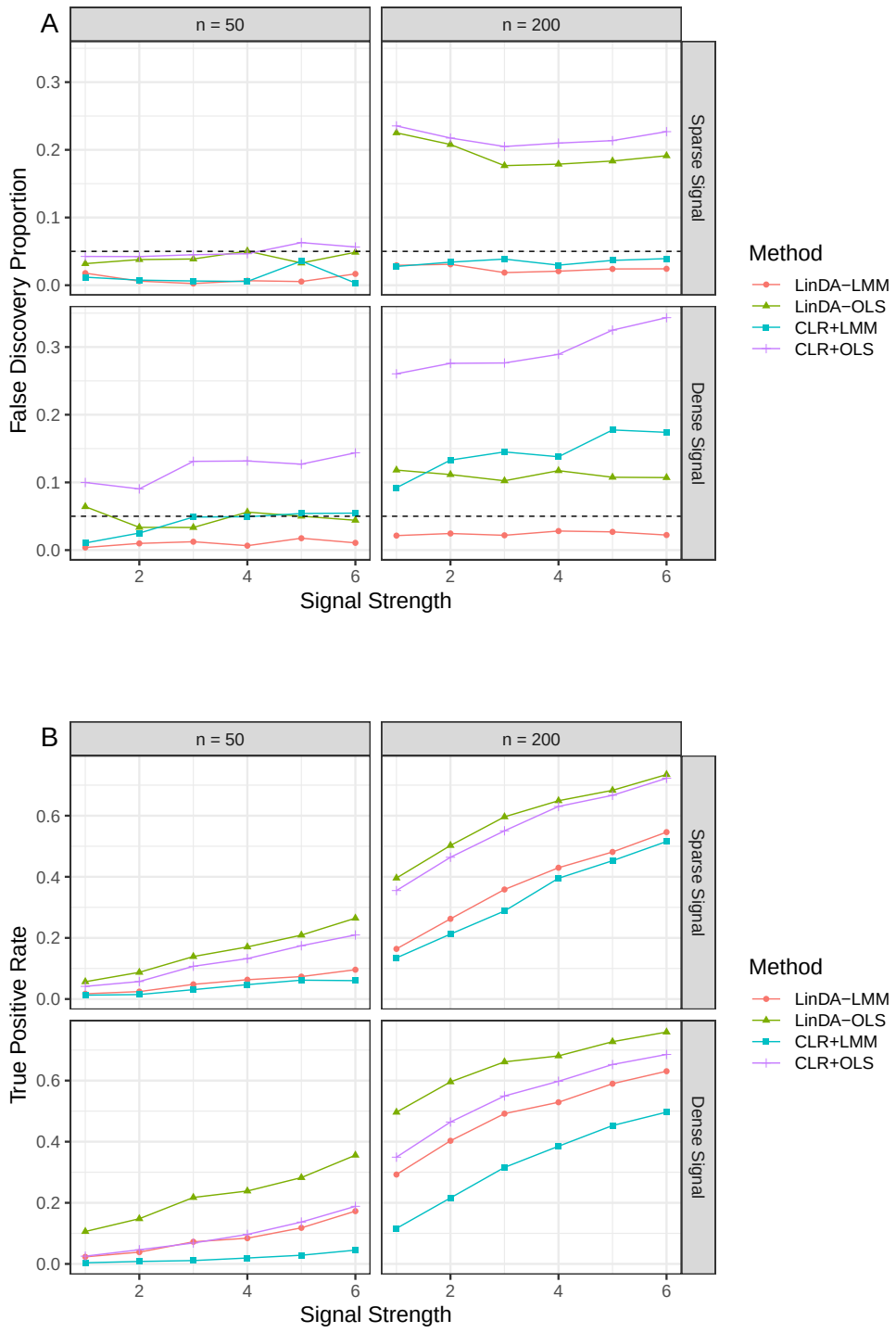

Figure B.13: Performance comparison (S7.2C0, replicate sampling). False discovery proportions (A) and true positive rates (B) were averaged over 100 simulation runs. The dashed horizontal line (A) indicates the target FDR level of 0.05.

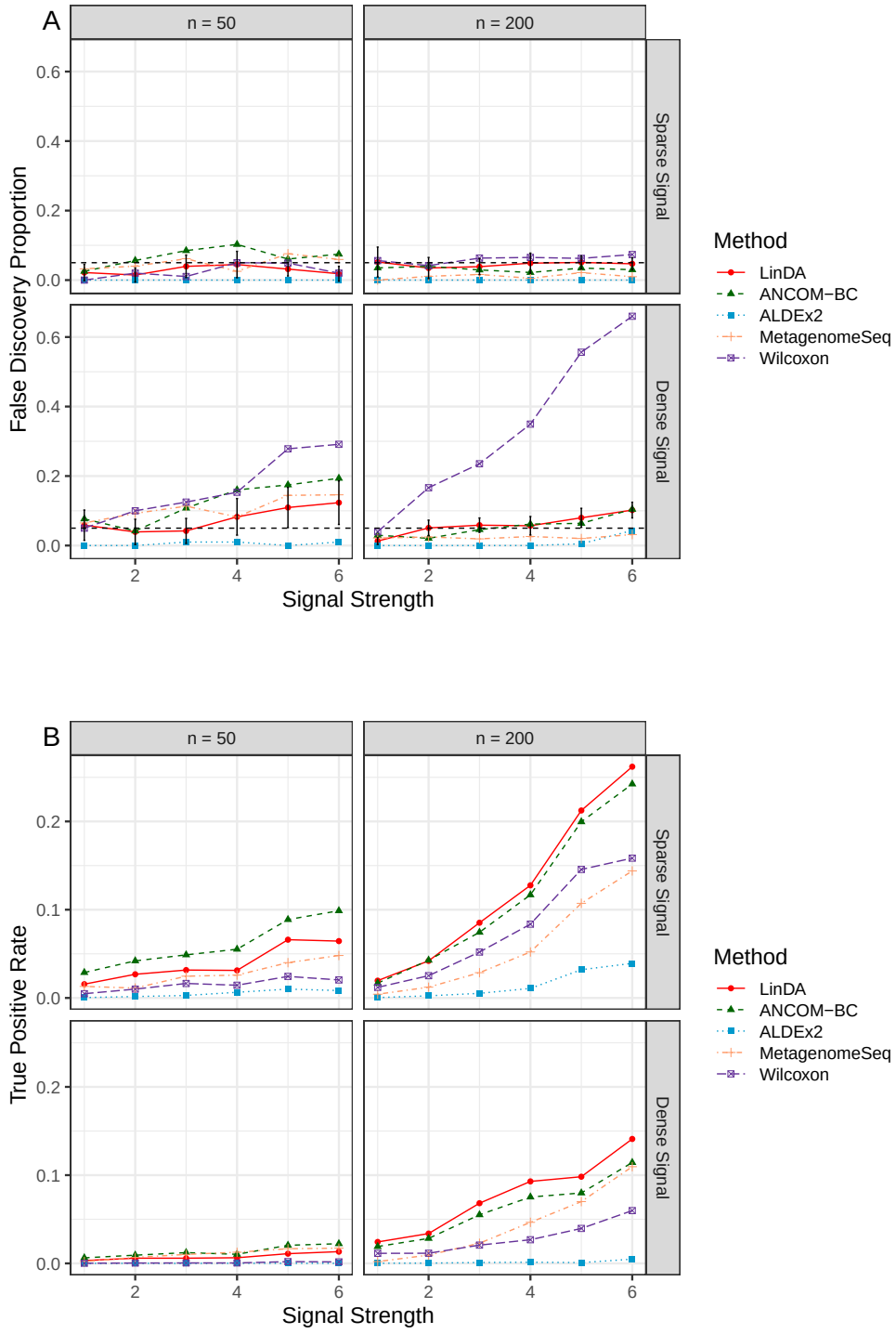

Figure B.14: Performance comparison (S0C0 with strong compositional effects). False discovery proportions (A) and true positive rates (B) were averaged over 100 simulation runs. Error bars (A) represent the 95% CIs of the method LinDA and the dashed horizontal line indicates the target FDR level of 0.05.

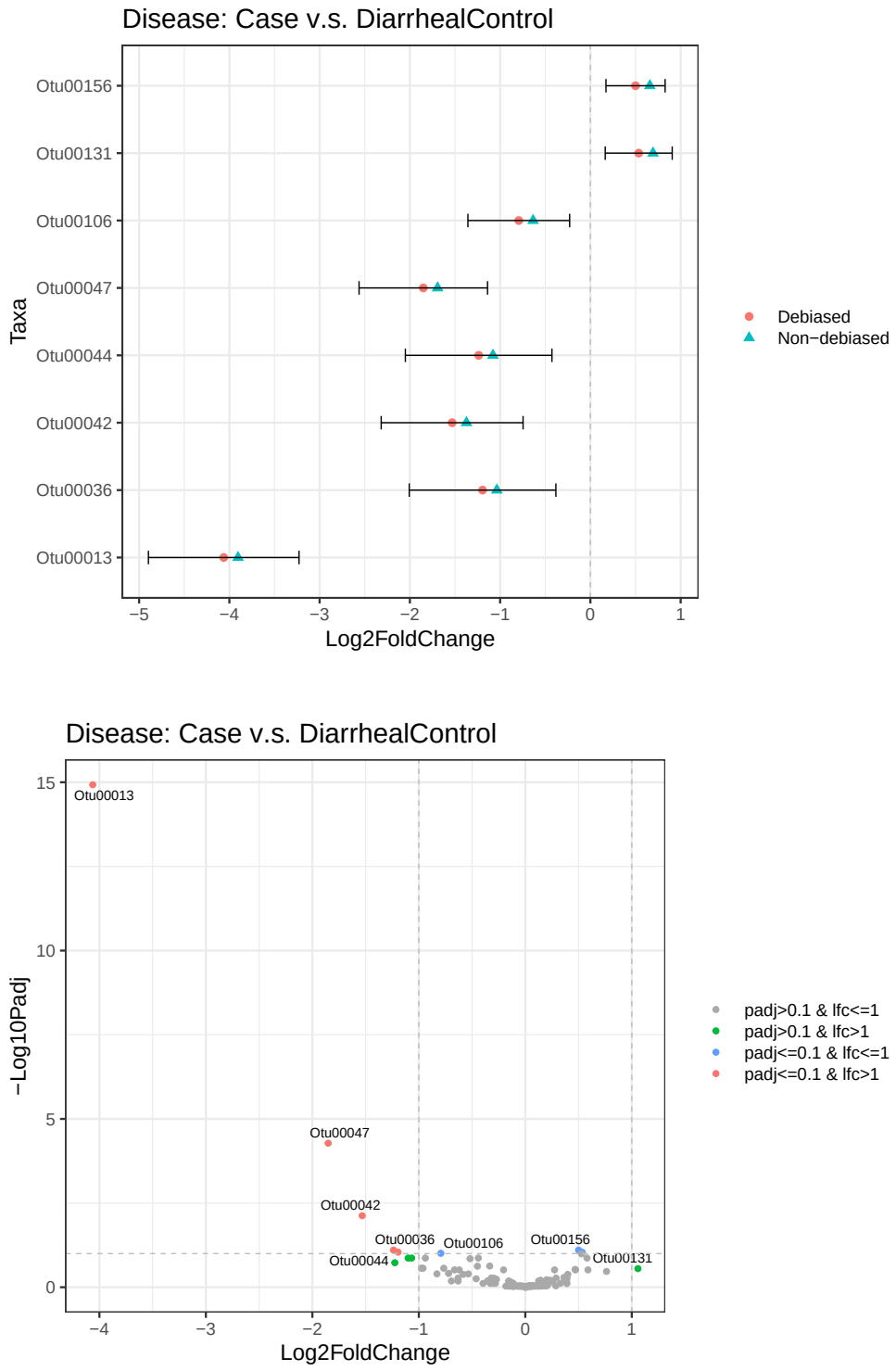

Figure B.15: Effect size plot and volcano plot for CDI dataset. The “Debiased" points represent the bias-corrected regression coefficients, and “Non-debiased" points represent the original (biased) regression coefficients. The error bars represent the 95% CIs of the “Debiased" points.

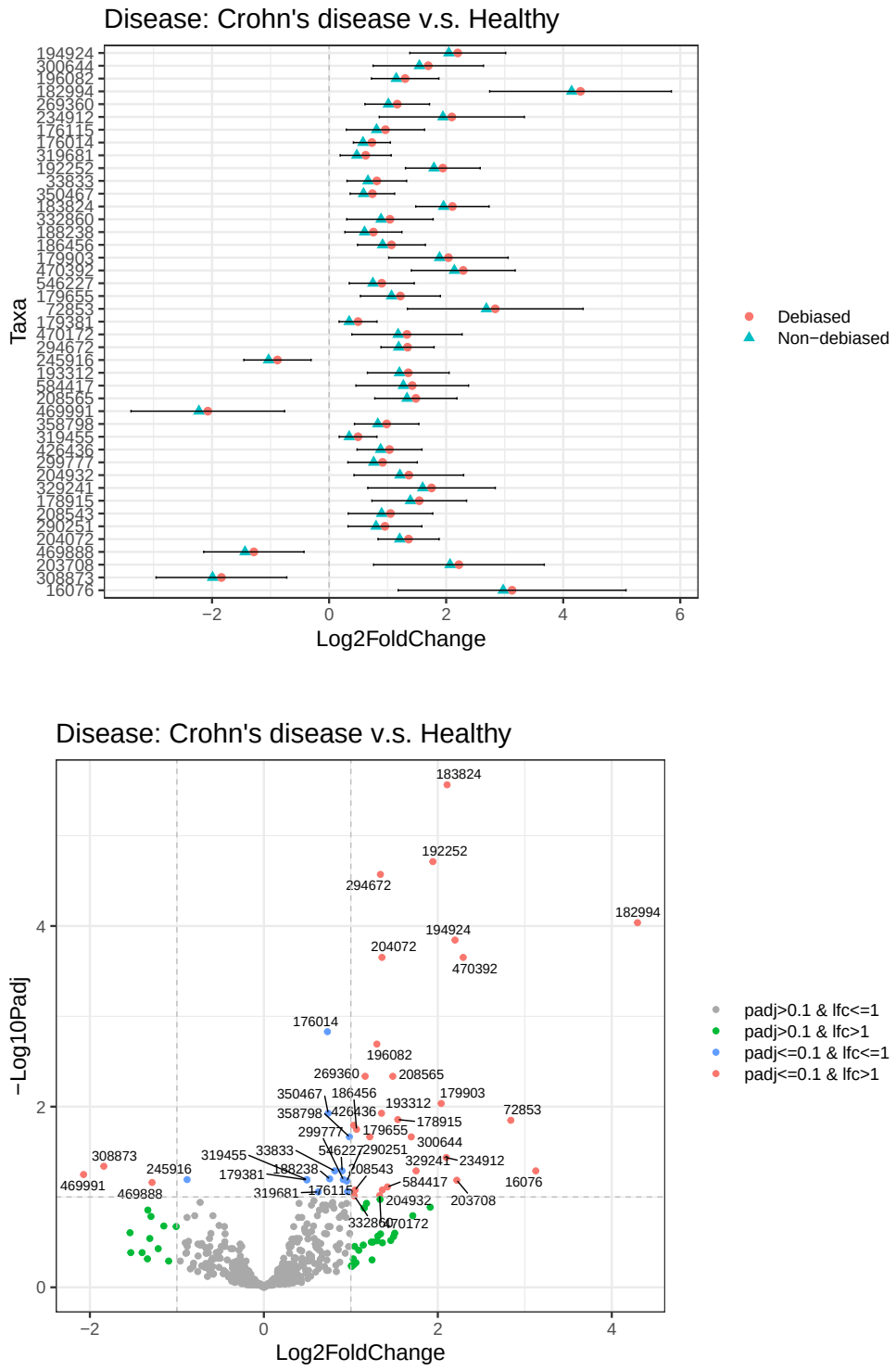

Figure B.16: Effect size plot and volcano plot for IBD dataset. The “Debiased" points represent the bias-corrected regression coefficients, and “Non-debiased" points represent the original (biased) regression coefficients. The error bars represent the 95% CIs of the “Debiased" points.

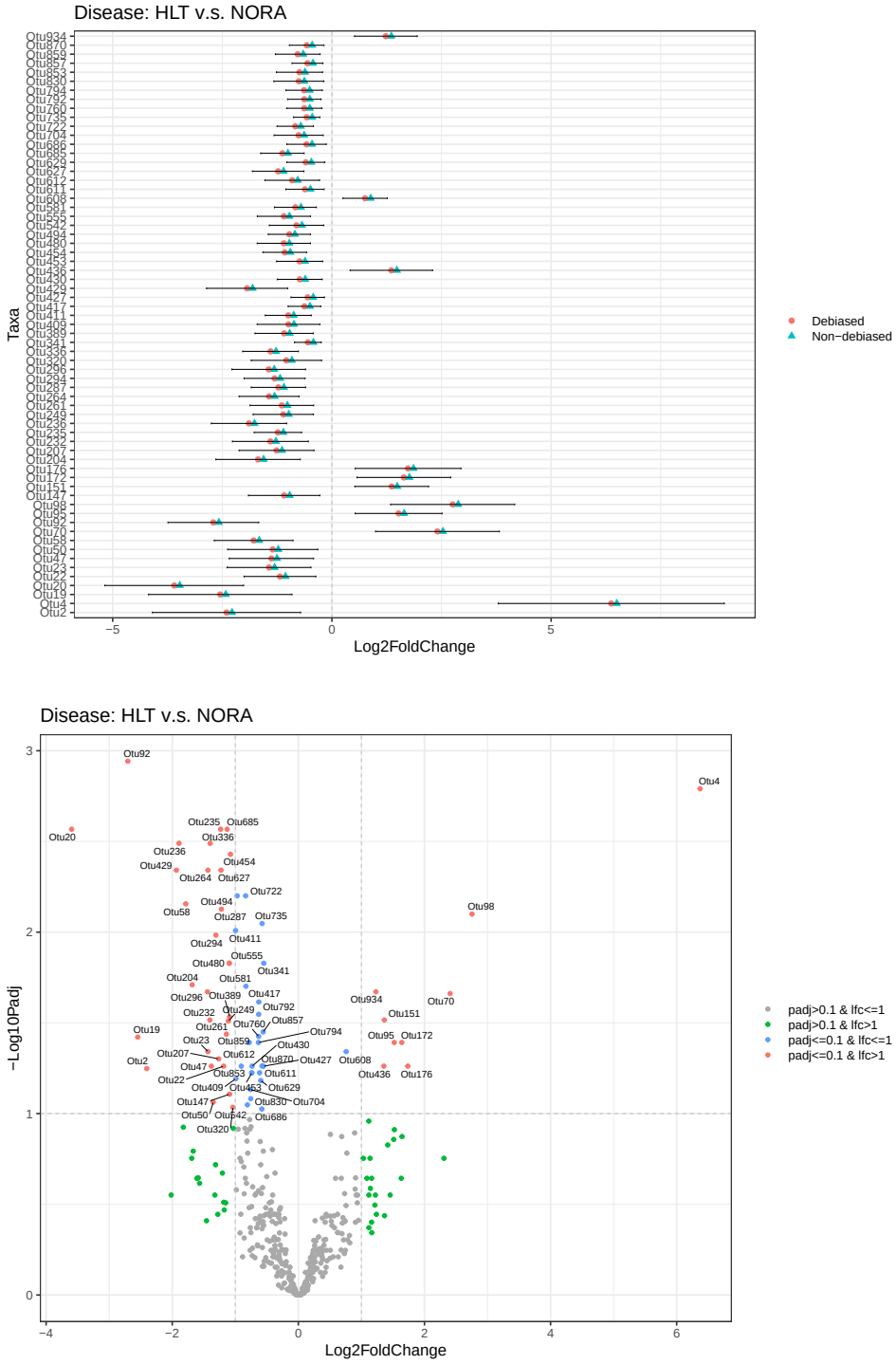

Figure B.17: Effect size plot and volcano plot for RA dataset. The “Debiased" points represent the bias-corrected regression coefficients, and “Non-debiased" points represent the original (biased) regression coefficients. The error bars represent the 95% CIs of the “Debiased" points.

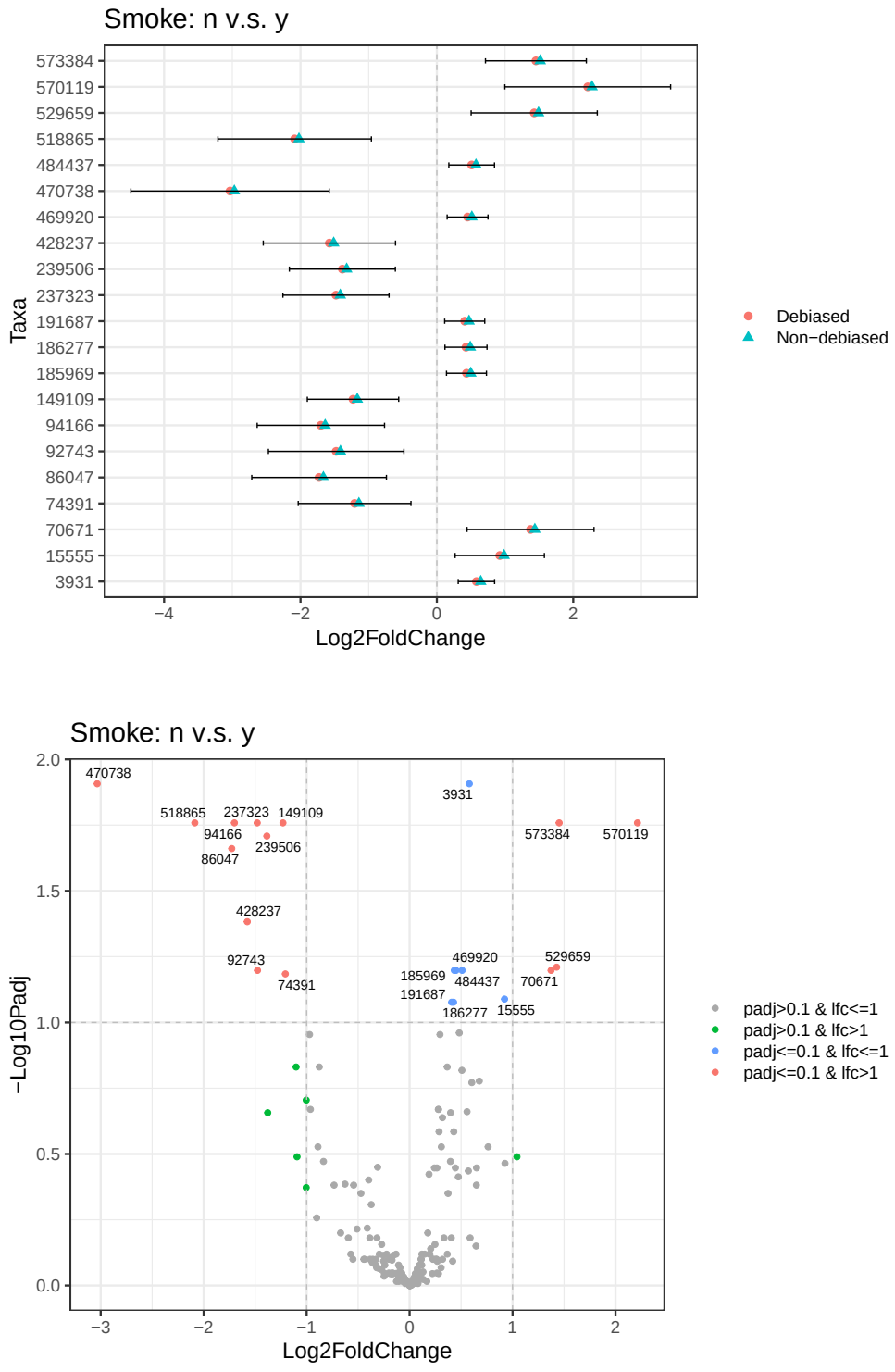

Figure B.18: Effect size plot and volcano plot for SMOKE dataset. The “Debiased" points represent the bias-corrected regression coefficients, and “Non-debiased" points represent the original (biased) regression coefficients. The error bars represent the 95% CIs of the “Debiased" points.